The Effects of Surface Modification on the Osseointegration of Titanium Dental Implants

A thesis submitted in fulfilment of the requirements of the degree of

Doctor of Philosophy

Cardiff University

May 2010

John Samuel Lawrence Colombo BSc (Hons)

Tissue Engineering and Reparative Dentistry,

School of Dentistry,

Cardiff University

ProQuest LLC
789 East Eisenhower Parkway
P.O. Box 1346
Ann Arbor, MI 48106-1346

Acknowledgements

Firstly, I would like to extend my thanks to my supervisors, Dr Rachel J. Waddington, Dr Alastair J. Sloan and Professor StJohn Crean for facilitating this project and taking me on as their PhD student, in addition to all of the assistance they have provided me with at various times. I would like to especially thank Rachel who, as my primary supervisor, has read this entire thesis more than once (!) in much less polished forms, and is directly responsible for a nearly infinite number of useful suggestions and refinements. Further, this project would not have been possible at all without the generous financial support of General Implant Forum & Training (GIFT), and so Dr. Stewart Harding, GIFT's director, has my particular thanks.

This thesis would be substantially lighter without the invaluable assistance of the collaborators who contributed to it. I would therefore like to thank Mr Adam Dowling and Dr Garry Fleming at Trinity College, Dublin for their help with the profilometry, Dr Albert Carley in the School of Chemistry for his help with the XPS, and Dr Daigo Sakai and Professor Joji Okazaki at the Osaka Dental University in Japan, without whom the *in vivo* work presented herein would not have been possible.

I have also had the benefit of excellent technical guidance from Mr Martin Langley, who has always been available for questions, comments and other, more generalised harassment and Mrs Katherine Allsopp, whose instructions have without any doubt saved me from being dismembered by a microtome. For general moral support, I have to thank my fellow students in the MTG, who are both individually and collectively brilliant.

My thanks also extend to my parents, who have always supported me and whose guidance has no doubt led me to this point, and to my family in both its American and French divisions. Finally, I have to acknowledge all of the support that my wife Cécile has given me over the course of my PhD, and to thank her for everything, which is scarcely possible to do in such a limited space as I have here.

Summary

Titanium dental implants have become an integral part of modern dentistry. Implant surfaces may be modified in a number of ways which influence the rate of implant osseointegration. It is therefore desirable to characterise a surface with characteristics which are optimal for osseointegration.

Three commercially available surfaces: machined (M), grit blasted and acid etched (GB) and TCP coated (TCP), were characterised in terms of surface topography, chemistry and hydrophobicity. Osseointegrative potential was evaluated either (1) *in vitro*, by characterising the attachment, morphology and cellular behaviour of bone marrow stromal cells (BMSCs) cultured on the titanium surfaces or (2) using an *in vivo* model whereby aspects of the process of osseointegration were monitored over time following placement of implants into excised incisor sockets of rat mandibles. Additionally this *in vivo* model was used to compare the bone repair process in both normal and GK rats, which represent a model of type II diabetes mellitus (DM).

In vitro, BMSCs cultured in osteogenic media on M appeared more rounded, while they were more elongated on GB and TCP. BMSCs attached to all surfaces and produced matrix material. The matrix formed appeared as a thin layer covering M, while matrix was thicker on the GB and TCP surfaces, infilling topographical features. Surface modification appeared to have little effect on the osteogenic activity of BMSCs. However, titanium was found to suppress differentiation down the adipogenic pathway and expression of IL-1β compared to plastic. Surface modification appeared to have little effect on osteoblast activity or osseointegration, although roughened surfaces may provide better mechanical interlocking with bone. *In vivo*, no differences in the progression of osseointegration around any of the modified surfaces were observed. In DM, osteoblast activity was altered and bone healing was delayed. There is therefore clearly scope to investigate surface modifications such as biomimetic coatings for use in compromised clinical situations.

Abbreviations

°C	Degrees Celsius
µl	Micro Litre
µm	Micro Metre
AGE	Advanced Glycation End Product
AP	Alkaline Phosphatase
AR	Alizarin Red
BCA	Bicinchoninic Acid
Bis-Tris	Bis (2-hydroxyethyl)-Amino-Tris(Hydroxymethyl)-Methane
BMD	Bone Mass Density
BMP	Bone Morphogenic Protein
BMSC	Bone Marrow Stromal Cell
BSA	Bovine Seru m Albumin
BSP	Bone Sialoprotein
cDNA	Complimentary Deoxyribonucleic Acid
CO_2	Carbon Dioxide
Col I	Type I Collagen
Col III	Type III Collagen
CSF-1	Colony Stimulating Factor 1
DAB	3,3'-Diaminobenzidine
DM	Diabetes Mellitus
EDTA	Ethylenediaminetetraacetic Acid
ELISA	Enzyme-Linked Immunosorbent Assay
eV	Electronvolt
FCS	Foetal Calf Serum
FGF	Fibroblast Growth Factor
g	Gravitation Acceleration
GAPDH	Glyceraldehyde 3-Phosphate Dehydrogenase
GK	Goto-Kakizaki
GT	Granulation Tissue
H&E	Haematoxylin and Eosin
H_2SO_4	Sulphuric Acid

HCl	**Hydrochloric Acid**
HF	**Hydrofluoric Acid**
HNO_3	**Nitric Acid**
HRP	**Horse Radish Peroxidase**
Hs	**Hours**
IGF	**Insulin-Like Growth Factor**
IgG	**Immunoglobulin-G**
IgM	**Immunoglobulin-M**
IL	**Interleukin**
IMS	**Industrial Methylated Spirit**
LPS	**Lipopolysaccharide**
Min	**Minute**
Ml	**Millilitre**
Mm	**Millimetre**
mRNA	**Messenger Ribonucleic Acid**
MSC	**Mesenchymal Stem Cell**
NF-κβ	**Nuclear Factor κβ**
Nm	**Nanometre**
OC	**Osteocalcin**
ON	**Osteonectin**
OP	**Osteopontin**
OPG	**Osteoprotegerin**
PCNA	**Proliferating Cell Nuclear Antigen**
PDGF	**Platelet Derived Growth Factor**
Pparγ	**Peroxisome Proliferator-Activated Receptor γ**
R_a	**Average Roughness**
RAGE	**Receptor for Advanced Glycation End Products**
RANK	**Receptor Activator of Nuclear Factor κβ**
RANKL	**Receptor Activator of Nuclear Factor κβ Ligand**
ROS	**Reactive Oxygen Species**
RT	**Reverse Transcription**
RT-PCR	**Reverse Transcription-Polymerase Chain Reaction**
SDS	**Sodium Dodecyl Sulfate**

SEM	**Scanning Electron Microscopy**
SMAD	**SMA and MAD Related Protein**
TBE	**Tris/Borate/EDTA**
TBS	**Tris-Buffered Solution**
TCP	**Tri-Calcium Phosphate**
TGFβ	**Transforming Growth Factor β**
TNAP	**Tissue-Nonspecific Alkaline Phosphatase**
TNF	**Tumour Necrosis Factor**
TNFα	**Tumour Necrosis Factor α**
UV	**Ultra-Violet**
VEGF	**Vascular Endothelial Growth Factor**
XPS	**X-Ray Photoelectron Spectroscopy**
α-MEM	**α-Minimum Essential Media**

Contents

Chapter 1: Introduction

1.1 Introduction

Titanium dental implants have established themselves as a critically important part of modern dentistry, with an estimated one million implantations performed annually (Le Guéhennec et al. 2007). The advent of what can effectively be described as a 'screw in tooth' has opened a broad range of new treatment options to dentists confronted by tooth loss. Consequently, implants can be employed to act as stable anchors to which artificial crowns can be affixed as replacement teeth, or can be used to stabilize a denture, providing a full or partially edentulous individual with a new, well anchored replacement dentition (Davies 2003; Ellingsen et al. 2006; Le Guéhennec et al. 2007). The use of titanium prosthetics, when successful, can result in dental restorations which closely approximate the look and feel of the original teeth, which is beneficial to the patients from both aesthetic and oral health perspectives.

The success or failure of titanium implants is directly related to how quickly and completely the surrounding tissues attach to the implant, integrating it, a process known as osseointegration. Osseointegration can be defined as the attachment of bone directly to the surface of the implant, anchoring and integrating it into the surrounding tissues (Ellingsen et al. 2006; Le Guéhennec et al. 2007; Puleo and Thomas 2006). Briefly, this occurs through the infiltration, proliferation and differentiation of mesenchymal stem cells into osteogenic cells on the surface of an implant (Davies 2003; Ellingsen et al. 2006; Le Guéhennec et al. 2007). These cells secrete the components of a collagenous extracellular matrix which mineralises (Davies 2003; Ellingsen et al. 2006). This newly formed mineralised tissue is then remodelled, resulting in the formation of mature bone around the implant, which secures it to the surrounding bone (Davies 2003; Ellingsen et al. 2006). The stability given to the implant as a result of this process is a critical determinate of the long term success of dental

implants, due to the relatively intense loading they are subjected to in routine use.

Titanium is generally considered to be an excellent material for dental implants and is in widespread use clinically (Ellingsen et al. 2006; Le Guéhennec et al. 2007; Puleo and Thomas 2006). Titanium surfaces can and have been widely modified in attempt to improve their osseointegrative potential. Surface characteristics of titanium implants, particularly their topography and chemical properties, play a major role in the interactions between the implant surface and the tissue around the implant site and thus influence the extent and rate of osseointegration (Ellingsen et al. 2006; Joos et al. 2006; Hata et al. 2007; Tsukimura et al. 2008; Shibli et al. 2007; Sul et al. 2006; Zhao et al. 2005).

Ultimately, the clinical 'holy grail' of implantology is the design of titanium implants which osseointegrate quickly and efficiently with a minimal number of additional procedures required to ensure long term success of the implant (Davies 2003). In practice, this would mean that a patient could have an implant capped with an artificial tooth immediately placed after only one clinical procedure, significantly reducing chair-time and thereby reducing the currently substantial cost of dental implants. In addition, there are certain patient groups, for example those with Diabetes Mellitus (DM), severe periodontitis or osteoporosis which have a significantly reduced capability for osseointegration (Lerner 2006; Taubman and Kawai 2001; Valero et al. 2007). These are public health concerns which will only become more prevalent due to an aging population in the UK (Lerner 2006; Valero et al. 2007). Titanium surfaces which improve the chances of efficient osseointegration would widen the access of implants to these potentially large patient groups, allowing them to benefit significantly.

This thesis will take a systematic approach to analyzing the effects of modified titanium surfaces on the process of osseointegration, using both *in vitro* and *in vivo* models. By investigating the interactions of cells and tissues with well characterised titanium surfaces, individual surface modifications favourable

to osseointegration will be identified. Additionally, the *in vivo* model system will be employed to investigate the effects of Type II DM on osseointegration, which will allow the effects of a disease state with direct implications for the process of bone formation to be examined. Improving the understanding of how the process of osseointegration is influenced by alterations in the surface characteristics of titanium implants will hopefully contribute to improvements in implant design, ultimately producing implants which will osseointegrate quickly and efficiently in both routine use and in more challenging clinical situations.

1.2 Organization of Bone

In order to understand the wider interactions between bone and titanium implants, it is crucial to understand the basic composition of bone and its influence on the process of osseointegration. Ostensibly, the main functions of bone are to provide a rigid structure for the support of the body and to provide points of attachment for muscles and tendons, although it also has a myriad of other roles such as providing a reservoir for minerals and the production of many humoral cell types (Waugh and Grant 2002). Constituently, the components of bone tissue may be broadly divided into two major categories which together facilitate the function of the tissue: cellular and acellular. Bone contains various cell types which carry out a wide range of functions, from the anabolic osteoblasts and catabolic osteoclasts to pluripotent progenitor cells which are ultimately capable of developing into a number of different cell types. Essentially, the cellular component of bone forms the living part of the tissue and is responsible for maintaining the tissue structure and function in addition to providing physiological connections with other tissues (Waugh and Grant 2002). The acellular component of bone is the mineralised tissue, formed from the deposition of minerals onto an organic matrix secreted by cells of an osteoblastic lineage (Waugh and Grant 2002).

The mineralised matrix of bone provides the structural properties of the tissue and acts as the mineral reservoir of the body where ions critical to a variety

of functions can be stored and accessed as needed. Understanding the way in which the mineralised matrix is formed, shaped and maintained by the cellular component is central to the topic of osseointegration. The extracellular matrix of bone is comprised of around 90% type I collagen, with the remainder comprised of a variety of non-collagenous proteins like osteopontin, osteocalcin, osteonectin and bone sialoprotein to name several examples (Hughes et al. 2006; Nanci 1999; Waugh and Grant 2002). Type I collagen is the primary secretory product of osteoblasts and forms the framework for the mineralised matrix, providing much of the strength and flexibility of bone tissue. The non-collagenous proteins combine with type I collagen, forming a matrix which is a favourable environment for the collection of calcium and phosphate ions. These ions mineralise this protein matrix formed in a manner which forms a regular crystal structure, hydroxyapatite, ultimately resulting in an organic framework produced by cells overlaid with a mineralised deposit which provides many of the overall structural properties of bone (MacDonald and Gowen 1993; Nanci 1999; Ng et al. 1997; Roberts and Hartsfield 2004).

There are several different types of bone, depending on the conditions under which is synthesized and its level of maturity. Woven bone consists of a web-like arrangement of intertwined and mineralised collagen fibres, oriented in many different directions and can be laid down quickly, although due to its irregular structure, woven bone is not an optimal for structural strength (Davies 2003; Nanci 1999; Waugh and Grant 2002). In general, woven bone is typical of the initial period of fracture repair, when bone must be synthesized rapidly in order to fill the defect resulting from an injury. This is a similar situation to the creation of a socket for the placement of an implant, which occurs in some cases via tooth extraction and in others by surgical means (Davies 2003; Ellingsen et al. 2006; Le Guéhennec et al. 2007; Nanci 1999; Puleo and Thomas 2006). After the rapid deposition and mineralization of woven bone, it is gradually remodelled into lamellar bone, characterised by layered sheets of collagen fibres, which run parallel to one another (Nanci 1999). This arrangement is much stronger than woven bone due to its more regular structure and can be considered as 'mature' bone which provides the greatest level of structural strength. Finally, cancellous

bone is very low density bone generally found in the marrow cavities and is characterised by trabeculae separated by marrow spaces (Ng et al. 1997). The outer layer of cancellous bone is where progenitor or stem cells, ultimately responsible for the formation of cells in both mesenchymal and hematopoietic lineages, reside. Cancellous bone also has a very high surface to volume ratio and therefore lends itself to easy storage and release of calcium and phosphate ions (Ng et al. 1997). Although cancellous bone is a key component of bone physiology, it does not have a direct structural role.

1.3 Cellular Components of Bone, Their Function and Their Role in Bone Formation and Remodelling

The cellular component of bone is comprised of those cells mainly responsible for the maintenance of the mineralised tissue and those cells which contribute to formation of humoral cells. Within the marrow space is the hemopoietic stem cell niche, containing progenitor cells which produce erythrocytes, leukocytes and osteoclasts (Kartsogiannis and Ng 2004; Taichman 2005). Also present within the marrow space and in the periosteum are mesenchymal stem or progenitor cells from which are derived many connective tissue cells including adipocytes, fibroblasts, chondrocytes, osteoblasts and osteocytes (Kartsogiannis and Ng 2004; Taichman 2005). Bone formation results from the coordinated action of osteoblasts, which synthesize new bone matrix and osteoclasts, which strategically break down bone matrix. This interaction largely determines bone morphology and serves to remodel matrix from its initially deposited form into a more mature form (Boyle et al. 2003; Hughes et al. 2006; Kartsogiannis and Ng 2004; Katagiri and Takahashi 2002). Osteocytes, meanwhile, provide communication and coordination between the two interrelated processes (Franz-Odendaal et al. 2006).

1.3.1 Osteoblasts

The first phase of bone repair is one of recruitment, migration and proliferation. Osteoblasts arise from mesenchymal stem cells which are recruited from connective tissues to the surface of a bone (Owen 1967) and are also present in the bone marrow (Friedenstein 1976). Mesenchymal stem cells are undifferentiated, self renewing cells that have the potential to differentiate into diverse connective tissue cell types, including chondrocytes, myocytes, adipocytes, fibroblasts and osteoblasts (Beyer Nardi and da Silva Meirelles 2006). They arise from the embryonic mesenchyme, and are ultimately responsible for the formation of the connective tissues of the mammalian body (Beyer Nardi and da Silva Meirelles 2006). While they are commonly found in the bone marrow, it is currently unclear if they occupy a physical location, or 'niche', or if they are simply distributed in a decentralised way around the bone marrow (Beyer Nardi and da Silva Meirelles 2006; Stewart et al. 1999). Although there are currently no definitive cell markers which are specific for mesenchymal stem cells, Stro-1, a cell surface protein with an unknown function, is thought to be associated with the early phases of osteoblast differentiation and is currently used as a marker to indicated the presence of osteoblast progenitor cells (Stewart et al. 1999).

Mesenchymal stem cell recruitment is mediated by a wide variety of chemotactic signals, and results in mesenchymal cells migrating from the periosteum and bone marrow to a site of bone repair (Davies 1996; Hughes et al. 2006; Kartsogiannis and Ng 2004; Katagiri and Takahashi 2002; MacDonald and Gowen 1993; Ng et al. 1997). Upon arrival at this site, the mesenchymal cells begin a series of proliferative cycles, which serve to increase their number (Hughes et al. 1995; Katagiri and Takahashi 2002). Subsequently, they begin to progress down the osteoblast lineage under the direction of a complex signalling cascade and become osteoblast progenitor cells, an immature cell-type with a high proliferative potential firmly committed to the osteoblast differentiation pathway (Chaudhary et al. 2004; Hughes et al. 2006; Katagiri and Takahashi 2002). Osteoblast progenitor cells undergo a number of proliferation and

differentiation cycles before becoming pre-osteoblasts. Pre-osteoblasts have the cuboidal shape characteristic of mature osteoblasts and begin to express a number of markers associated with osteoblasts, for example Osteopontin (OP), Osteocalcin (OC), Osteonectin (ON), Bone Sialoprotein (BSP), Type I&III Collagen, and Alkaline Phosphatase (AP), although they retain their ability to proliferate (Katagiri and Takahashi 2002; Mackie 2003). Ultimately, pre-osteoblasts mature into post mitotic osteoblasts, which represent the pinnacle of bone forming capability. A diagram from the review by Hughes and colleagues (2006) shows the simplified osteoblast differentiation pathway, including some of the growth factors which are known to act on mesenchymal stem cells to initiate osteoblast differentiation, although due to its complexity, current understanding of the process is far from complete (Figure 1.1).

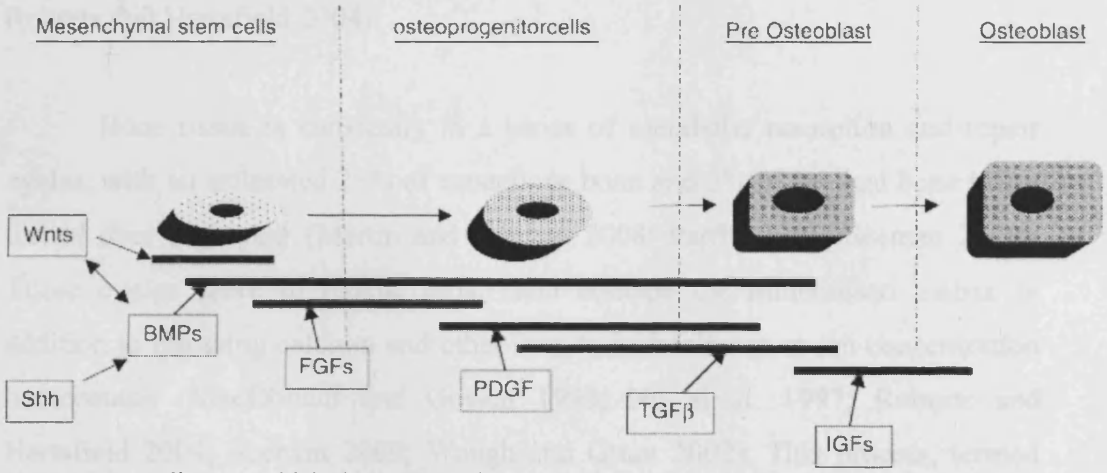

Figure 1.1: A diagram which shows the main stages of the osteoblast lineage and where various growth factors are thought to exert their primary effects. BMP, bone morphogenetic protein; IGF, insulin-like growth factor; FGF, fibroblast growth factor; PDGF, platelet-derived growth factor; Shh, Sonic hedgehog; TGF-β, transforming growth factor-β; Wnts, a group of >15 related extracellular signalling molecules (Taken from Hughes et al, 2006).

Upon reaching the final stages of their differentiation pathway, osteoblasts begin to synthesize and secrete non-collagenous proteins, which have a variety of functions, including the induction of mineralisation, and type I collagen from their apical membranes, which together form an extracellular matrix (Davies 1996, 2003; MacDonald and Gowen 1993; Ng et al. 1997; Robling et al. 2006). This matrix is referred to as the osteoid prior to mineralization and forms a template for the formation of bone. Osteoblasts also secrete a number of osteogenic growth factors into the osteoid, sequestering them. When bone resorption occurs, these growth factors are released creating a feedback mechanism which balances bone resorption with bone formation (MacDonald and Gowen 1993; Ng et al. 1997; Roberts and Hartsfield 2004). The osteoid then undergoes mineralisation, which subsequently forms the mineralised extracellular matrix of bone tissue (MacDonald and Gowen 1993; Ng et al. 1997; Roberts and Hartsfield 2004).

Bone tissue is constantly in a series of metabolic resorption and repair cycles, with an estimated 25% of cancellous bone and 3% of cortical bone being turned over each year (Martin and Seeman 2008; Parfitt 1994; Seeman 2009). These cycles serve to renew, repair and reshape the mineralised matrix in addition to releasing calcium and other ions to maintain serum ion concentration homeostasis (MacDonald and Gowen 1993; Ng et al. 1997; Roberts and Hartsfield 2004; Seeman 2009; Waugh and Grant 2002). This process, termed remodelling, is critical in the repair of bone and comprises the final stage of bone formation. Bone remodelling is necessary for biomechanical adaptation, which allows bone tissue to be strengthened in response to increases in mechanical load. Remodelling is the means by which sections of mineralised matrix, which suffer damage while in routine use, are renewed with fresh depositions. It is also the means by which woven bone is laid down rapidly in response to bone injury is converted into stronger, mature cortical bone. Finally, bone remodelling moulds the matrix secreted by osteoblasts into the correct anatomical shape to form bones, specifically in foetal development (Roberts and Hartsfield 2004; Waugh and Grant 2002). In order to facilitate this process, osteoblasts must work

directly in concert with their osteoclast counterparts in order to ensure that bone is laid down, strategically resorbed and synthesized again in the correct location and format.

1.3.2 Osteoclasts

Osteoclasts are large, multinucleated cells which are specialized to resorb the mineralised matrix of bone by adhering tightly to the bone surface via the apical membrane and secreting protons and osteolytic enzymes, forming a structure known as a resorption pit (Boyle et al. 2003; Chambers 2000; Katagiri and Takahashi 2002; Kollet et al. 2007). In contrast to osteoblasts and osteocytes, they are descended from hemopoietic progenitor cells found in the bone marrow. Monocyte precursor cells are recruited from either the bone marrow or possibly from the circulation, to the surface of the bone where they differentiate into mature osteoclasts, capable of bone resorption on an impressive scale (Boyle et al. 2003; Chambers 2000; Katagiri and Takahashi 2002; Kollet et al. 2007). The process of osteoclast differentiation is tightly regulated both directly and indirectly by a number of local and systemic factors including hormones, growth factors, inflammatory cytokines and other signalling molecules (Figure 1.2) (Calvi et al. 2003; Kollet et al. 2007; Takahashi et al. 1988).

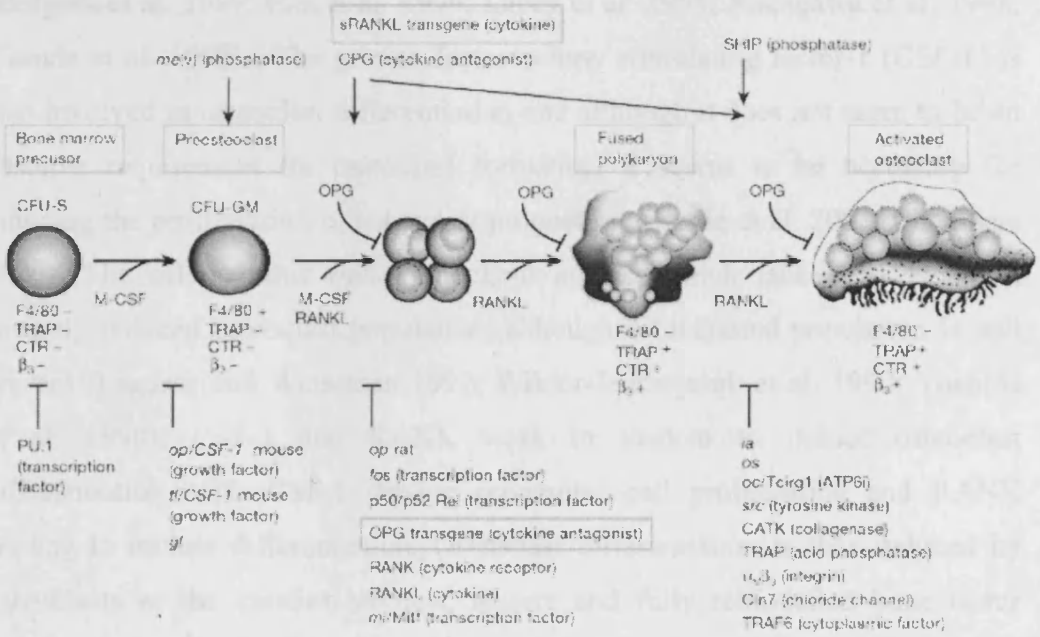

Figure 1.2: The osteoclast differentiation pathway, from bone marrow precursor cells to mature, active osteoclasts. (Boyle et al. 2003)

Local signalling molecules produced by osteoblasts play a central role in regulating the process of osteoclast differentiation. It has long been known that stromal cells contain factors which are necessary for osteoclast formation *in vivo*. Takahashi and colleagues (1988) observed osteoclast formation in mouse bone marrow stromal cell cultures upon exposure to parathyroid hormone and, interestingly, that they tended to form around clusters of osteoblasts, implicating these cells in locally mediating a systemic differentiation signal. The specific signalling molecule expressed by osteoblasts which is directly responsible for the regulation of osteoclast differentiation is the tumour necrosis factor (TNF) related type II transmembrane protein receptor activator of nuclear factor κ β ligand (RANKL) (Hsu et al. 1999; Yasuda et al. 1998). RANKL acts through the receptor activator of nuclear factor κ β (RANK), which is expressed by hemopoietic monocyte precursor cells, initiating a complex intracellular signalling cascade which ultimately results in the phenotypic changes associated with the osteoclast lineage (Burgess et al. 1999; Hsu et al. 1999; Nakagawa et al. 1998). RANK expression has been repeatedly shown to be required for the formation of osteoclasts in variety of studies in both *in vivo* and *in vitro* models (Burgess et al. 1999; Hsu et al. 1999; Lacey et al. 1998; Nakagawa et al. 1998; Yasuda et al. 1998). The growth factor colony stimulating factor-1 (CSF-1) is also involved in osteoclast differentiation and although it does not seem to be an absolute requirement for osteoclast formation, it seems to be necessary for inducing the proliferation of osteoclast progenitors (Boyle et al. 2003; Chambers 2000). The osteopetrotic *op/op* knockout mouse, which lacks CSF-1, has a severely reduced osteoclast population, although a functional population is still present (Lagasse and Weissman 1997; Wiktor-Jedrzejczak et al. 1990; Yoshida et al. 1990). CSF-1 and RANK work in tandem to induce osteoclast differentiation, with CSF-1 driving progenitor cell proliferation and RANK serving to initiate differentiation. Osteoclast differentiation is thus induced by osteoblasts as the creation of new, mature and fully remodelled bone tissue requires the actions of both osteoblasts to synthesize new bone matrix and osteoclasts to shape and renew that bone matrix, allowing it to reach the required final structure.

Due to the severity of the pathologies which result from the unregulated resorption of bone, it is fortunate that the differentiation of osteoclasts is tightly regulated. Osteoprotegerin (OPG) is an extracellular signalling peptide in the TNF (Tumour Necrosis Factor) receptor superfamily and has been shown to induce marked osteopetrosis when over-expressed in transgenic mice and when applied to rats (Simonet et al. 1997; Yasuda et al. 1998). OPG blocks the formation of osteoclasts by acting as a decoy receptor for RANKL, preventing its binding to RANK, thereby inhibiting osteoclast differentiation and leading to osteoclast apoptosis (Schoppet et al. 2002; Simonet et al. 1997; Udagawa et al. 2000). Osteoblasts secrete OPG in response to various osteogenic signals, curtailing bone resorption as required by the physiological situation (Schoppet et al. 2002; Udagawa et al. 2000). The activation and inhibition of osteoclast differentiation is therefore regulated by the receptor RANK, via its interactions with either RANKL or OPG produced by osteoblasts. Osteoblasts are in turn induced to express OPG by both systemic osteogenic signals and by local growth factors sequestered in the matrix by osteoblasts and released via osteoclast resorption. This results in a return to new bone formation after a period of resorption, completing a remodelling cycle and creating a complex physiological feedback system which balances bone resorption with formation.

Bone remodelling therefore, is the net result of initial deposition of osteoid by osteoblasts, its subsequent mineralization and the remodelling of the newly formed bone by osteoclasts. The resorption of the quickly synthesized woven bone results in increased osteoblast activity via the action of sequestered osteogenic growth factors released by either bone injury or osteoclast resorption, which culminate in the formation of the stronger cortical bone. Localized groups of osteoblasts and osteoclasts which coordinate their activities are referred to as bone multi-cellular units. This creates a system whereby woven bone can be laid down initially and rapidly by osteoblasts, creating a temporary structure which can then be resorbed incrementally by osteoblasts, and then reformed into a stronger, more permanent structure. Osteocytes play a role in modulating this

system, serving to coordinate the activities of osteoblasts and osteoclasts, and providing a link to mechanical stimuli applied to the bone tissue.

1.3.3 Osteocytes

Osteoblasts have a lifespan of around 3 months, after which they undergo apoptosis, become inactive bone lining cells or become embedded in the secreted matrix where they differentiate into osteocytes (Bonewald 2007). Osteocytes are terminally differentiated, non-secretory cells responsible for overall control of bone maintenance and communication with surrounding tissues (Franz-Odendaal et al. 2006; Owen 1967). They are the most numerous cells found in bone tissue, comprising around 95% of the total and are 10 times more prevalent than osteoblasts (Franz-Odendaal et al. 2006). It is not currently clear what specific events lead to certain osteoblasts being selected for terminal differentiation to osteocytes and effectively becoming encased in newly formed bone, although it is probably influenced by a variety of factors, for example cell position and the presence of local cellular signalling (Bonewald 2007; Franz-Odendaal et al. 2006; Manolagas 2000). Osteoblasts fated to become osteocytes, once embedded in the matrix, cease all secretory activity and undergo a series of radical phenotypic changes, including a loss of cell body size and a reduction in secretory organelles, for example Golgi bodies and endoplasmic reticula. Most notably however, osteocytes develop a web of dendritic extensions into the surrounding extracellular matrix which extend along the bone canaliculi, minute channels running through the compact bone tissue, connecting osteocytes to each other and to osteoblast and osteoclasts (Burger et al. 2003; Franz-Odendaal et al. 2006; Manolagas 2000; Palumbo et al. 1990).

The dendritic extensions formed by osteocytes are central to their function, as they are the avenues of communication by which osteocytes exert overall regulation of bone mass. Osteocytes act as mechanoreceptor cells which detect changes in loading and bone micro-damage, and subsequently transmit signals for resorption or bone formation to the appropriate cell type, i.e.

osteoblasts or osteoclasts (Burger et al. 2003; Manolagas 2000; Rodan 1997). It is thought that osteocytes detect changes in mechanical loading through sensitivity to alterations in sheer stress caused by the passage of bone interstitial fluid. As mechanical load is applied to or removed from bone, it causes alterations in the flow of interstitial fluid, which leads to deformation of osteocytes within their lacunae and mechanical signal transduction (Bonewald 2007; Weinbaum et al. 1994). It is also a possibility that mechanical forces applied to the matrix surrounding osteocytes may directly cause deformation of either osteocyte cell bodies or their dendritic extensions, resulting in signal transduction (Bonewald 2006; Nicolella et al. 2006). Osteocytes are thought to communicate with and influence the activity of both osteoblasts and osteoclasts via gap junctions formed at the end of their dendritic extensions (Bonewald 2007). Supernatants from osteocyte cell line cultures have been reported to increase the expression of AP and OC in mouse bone marrow stromal cell cultures, suggesting that osteocytes may play a direct role in stimulating osteoblast differentiation (Heino et al. 2004). Osteocytes have also been shown to stimulate osteoclast formation in response to bone micro-damage (Heino et al. 2009), and osteocyte death has been shown increase osteoclast activity *in vitro* (Gu et al. 2005).

Physiologically, it is well known that bone mass density (BMD) decreases due to an increase in resorption when bones are not mechanically loaded (Turner et al. 1995; Van der Meulen et al. 1995; Van der Wiel et al. 1995) and that the mechanical loading of bone increases bone formation (Bourrin et al. 1995; Hillam and Skerry 1995). Osteoclasts have been shown to resorb mechanically inactive bone with the application mechanical stimulation having the opposite effect (Gross and Rubin 1995). There is some evidence to indicate that osteocytes are responsible for inducing these changes in activity in response to stress, for example increased levels of osteocyte apoptosis is linked to increased bone fragility, presumably due to the loss of central control over bone formation and resorption, and thus tissue renewal (Tomkinson et al. 1997; Weinstein et al. 1998). As they may have a role in increasing the amount of bone tissue under a mechanical load, such as those seen by dental implants in routine

use, osteocytes may a key player in the osseointegration of implants, but the process by which they transduce mechanical signals is not currently well understood.

1.4 Control of the Synthetic Activity of Osteoblasts

As mentioned previously, the differentiation of osteoblasts, and by extension bone formation, is controlled by a plethora of systemic signals, which act through a number of local signalling molecules and growth factors. These all act synergistically to produce mature osteoblasts from the early progenitor cells which migrate to the site of bone formation. The interactions between all of these factors are highly complex and many different molecules have been implicated in the process of osteoblast differentiation. It simplifies the situation to consider each factor and its individual role in the osteoblast lineage, but it must be remembered that *in vivo,* they act in concert. It may be somewhat erroneous to attribute functions such as the induction of proliferation or the phenotypic changes associated with a particular phase of the osteoblast differentiation pathway to the action of a single signal working individually; the reality is that osteoblast differentiation is the product of a 'cocktail' of factors each impacting the functions of the others.

From the standpoint of titanium dental implants and the process of osseointegration, the osteoblast differentiation factors described here serve as useful markers for different stages of the osteoblast differentiation pathway. By visualizing and confirming the presence of these molecules, the presence of cells in the osteoblast lineage around a site of interest can be confirmed and their stage of differentiation identified. This makes understanding the role of these factors critically important to the study of osseointegration, as they provide a window into the cellular processes underway during interactions with a given titanium surface.

1.4.1 Bone Morphogenetic Proteins

Bone morphogenetic proteins (BMPs) are generally considered a principle factor for inducing osteoblast differentiation, although it is clear that they act synergistically with other growth factors (Canalis and Gabbitas 1994; Centrella et al. 1992). Members of the transforming growth factor β (TGFβ) superfamily, BMPs were discovered as the result of a study by Urist and colleagues (1971) where decalcified bone matrix explants in muscle induced ectopic bone formation. BMPs act through serine/threonine kinase receptors at the cell surface and initiate complex intracellular signalling cascades resulting in a wide range of effects on the transcriptional and translation activity of the cell (Yamaguchi et al. 2000). There are type I and II BMP receptors and the activation of both receptor types is required for signal transduction, which is mainly carried out by the SMADs (Derynck et al. 2001; Heldin et al. 1997; Massague et al. 2005). SMADs are a group of intracellular signalling proteins which modulate the activity of all of the members of the TGFβ superfamily members. There are currently eight SMADs. SMADs 1, 2, 3, 5 and 8 transduce signals from membrane receptors, SMAD 4 acts as a co-factor to the signalling SMADs and SMADs 6 and 7 act as inhibitors to the other SMADs (Massague et al. 2005). SMADs 1, 5, and 8 are the primary substrates for the BMP receptor (Massague et al. 2005).

Osteoblasts produce BMPs and sequester them in the bone matrix, to be released during periods of bone resorption, providing a physiological feedback response in order to maintain bone mass homeostasis (Mackie 2003). Genes for more than 20 different BMPs have been identified in vertebrates, several of which have been shown to independently induce ectopic bone formation, an ability unique among growth factors, and it is often claimed that they are the most important growth factor for initiating osteoblast differentiation (Katagiri and Takahashi 2002; Miyazono et al. 2005). There has been much evidence reported in the literature of BMPs being directly connected to skeletal formation and therefore osteoblast differentiation. BMP-2, BMP-4, BMP-6 have been reported to increase the formation of bone nodules in rat calvarial cell cultures,

implicating these proteins in the recruitment of progenitor cells to the osteoblast lineage (Hughes et al. 1995). Similarly, BMP-2 has been shown to induce osteoblast formation in several pluripotent cell lines (Katagiri et al. 1990; Rosen et al. 1994; Yamaguchi et al. 1991). When treated with BMP-7, mesenchymal stem cells have been shown to differentiate into osteoblasts (Gerstenfeld et al. 2002). Transfection with an adenovirus containing a BMP-7 cDNA construct has also been shown to induce an osteogenic response under both *in vitro* and *in vivo* models (Franceschi et al. 2000). Knockout mice for BMP-5, BMP-7 and BMP-11 demonstrate localized skeletal abnormalities, indicating different positional roles for the various BMPs, in addition to other defects like abnormal kidney and eye development (Kingsley et al. 1992; Luo et al. 1995; McPherron et al. 1999). Many other BMP knockouts are not viable due to catastrophic disruption of their skeletal development, as is the case with both BMP-2 and BMP-4 knockout mice (Yamaguchi et al. 2000). BMPs are generally thought to act via a cascade of transcription factors, most notably Runx-2, reported to be the major driver of osteoblast differentiation (Ducy et al. 1997; Katagiri and Takahashi 2002; Yamaguchi et al. 2000). The extracellular signalling molecules Wnts and sonic hedgehog have been implicated in the regulation of BMP activity in osteoblasts (Baron et al. 2006; Kawai and Sugiura 2001). At the cellular level, BMPs are an indicator that there are cells present which are in the later stages of osteoblast development, especially if mature osteoblast markers such as osteopontin and osteocalcin are concurrently expressed.

1.4.2 Wnts

A group of over 19 different extracellular glycoprotein signalling molecules known as Wnts has been implicated in the initial recruitment of mesenchymal stem cells into the osteoblast lineage (Westendorf et al. 2004). Wnts bind to the extracellular receptor fizzled and to the co-receptors LRP5/6, whereupon they initiate a complex cascade of intracellular signalling events involving β-catenin (termed the canonical pathway) and other β-catenin independent pathways (non-canonical) (Westendorf et al. 2004). Wnt signalling

seems to be involved in the early stages of osteoblast differentiation, as Wnt addition to precursor cell cultures induced alkaline phosphatase expression, an early marker of osteoblast differentiation present at the osteoprogenitor cell stage, but did not induce the osteocalcin or type one collagen production, which is generally associated with pre-osteoblasts and mature osteoblasts (Rawadi et al. 2003). The Wnt-β-catenin signalling pathway has been shown to be required for skeletogenesis, and acts specifically by promoting osteoblast differentiation at the expense of chondrocyte differentiation (Day et al. 2005). In the absence of this signalling pathway mesenchymal progenitor cells turn into chondrocytes (Hill et al. 2005). It has also been reported that over-expression of Wnts in a transgenic mouse model results in high bone mass and increased expression of both Runx-2 and osteocalcin, suggesting Wnt signalling is involved in regulating the differentiation of osteoblasts (Gaur et al. 2005). It has also been proposed that Wnt signalling is the one of the key mechanisms by which osteocytes regulate osteoblast activity, linking it to the osteogenic response stimulated by bone loading (Bonewald and Johnson 2008). Currently, the interaction of Wnts and other osteogenic factors is not completely understood. BMP-2 for example has been variously reported to both induce (Bain et al. 2003) and to be induced by (Winkler et al. 2005) the actions of Wnts. It appears that the regulatory actions of the Wnts are related to those of the BMPs, although the exact nature of this interaction is not currently clear.

1.4.3 Sonic Hedgehog

Sonic hedgehog is a polypeptide signalling molecule which acts through the cell surface receptor 'patched' and are involved in the regulation of BMP action (Hughes et al. 2006). *In vitro,* sonic hedgehog induces osteoblast formation in osteoblast and fibroblast cell lines, in addition to causing ectopic bone formation in mice by inducing BMP (Kinto et al. 1997; Yuasa et al. 2002). It has also been reported that sonic hedgehog enhances the induction of osteoblast differentiation by BMP-2 *in vitro* and inhibits adipocyte formation (Spinella-Jaegle et al. 2001). The actions of sonic hedgehog have been shown to

be upstream of the BMPs; Kawai and Sugiura (2001) have demonstrated that the sonic hedgehog mediators, Gli proteins, directly enhance the expression of BMP-4 and BMP-7 when transfected into a COS-7 cell model. Like the Wnts, the presence of sonic hedgehog around an implant site may be a good indication that cells have migrated to the area and entered the osteoblasts differentiation pathway via the actions of BMPs.

1.4.4 Transforming Growth Factor β

Transforming growth factor β (TGFβ) belong to the same superfamily of proteins as the BMPs and also play a major role in osteoblast differentiation. TGFβ, specifically TGFβ1, is found in many tissues of the body, but is particularly prevalent in bone tissue and platelets (Hughes et al. 2006; Janssens et al. 2005). Like the BMPs, TGFβs act through serine/threonine kinase receptors, which in turn transduce signals into the cell via the SMADs (Heldin et al. 1997; Janssens et al. 2005). SMADs 2 and 3 are the primary substrates for the TGFβ receptors (Massague et al. 2005). In addition TGFβ1 is known to signal through MAP Kinase pathways and thus also has SMAD-independent activity (Janssens et al. 2005; Miyazono et al. 2007). It has been shown *in vitro* that TGFβ1 reduces the expression of both Runx-2 and osteocalcin, which is reversed by treatment with TGFβ1 receptor blockers (Alliston et al. 2001; Maeda et al. 2004). This rules out their participation in the later stages of osteoblast differentiation, but there have been many descriptions of their mitogenic properties and stimulation of matrix synthesis earlier in the pathway. It has long been known that TGFβ1 increases the proliferation rate of osteoblasts *in vitro* in addition to increasing the levels of type I collagen synthesis, indicating its importance in bone matrix production (Centrella et al. 1992; Centrella et al. 1986). Essentially this has the effect of producing a large pool of matrix producing cells ready to be moved on into the later stages of osteoblast development by other growth factors such as the BMPs (Centrella et al. 1992; Hughes et al. 2006; Janssens et al. 2005). TGFβ1 has a complex and synergistic relationship with the BMPs in producing mature osteoblasts that is currently not fully understood, but it seems

that TGFβ1 effectively increase osteoprogenitor cell numbers which the BMPs then induce into the later stages of the osteoblast lineage while simultaneously suppressing the inhibitory effects of TGFβ1 on differentiation. As a marker of cell activity, the presence of TGFβ1 around an implant site would be a strong indicator of osseointegrative activity.

1.4.5 Fibroblast Growth Factors

The fibroblast growth factors (FGFs) are another family of signalling polypeptides implicated in the osteoblast differentiation pathway which act through tyrosine kinase receptors (Duchesne et al. 2006). FGFs have long been implicated in the development of osteoblasts, particularly in the early stages of differentiation, although the extent of their role in the osteoblast differentiation pathway is not completely clear. FGF-2 knockout mice show decreased bone mass compared to normal mice (Naganawa et al. 2006). Naganawa and colleagues (2006) also demonstrated that cultures of bone marrow stromal cells from these mice appear to have lower expression levels of Runx-2 and decreased bone nodule formation. Determining the exact function of FGFs in osteoblast differentiation has proved more problematic however, although they seem to be mainly involved in inducing proliferation at the osteoprogenitor stage as opposed to driving differentiation. Canalis and colleagues (1988) demonstrated that basic FGF, when applied to rat calvarial cells, stimulated the proliferation of type I collagen producing cells (i.e. osteoblasts), while simultaneously and directly decreasing type I collagen synthesis. Interestingly, it has also been reported that FGFs, when applied to immature human calvarial cell cultures, increases the rate of proliferation but decreases the expression of mature osteoblast cell markers (Debiais et al. 1998). FGF-2 increases proliferation in immature osteoblasts from both rat calvarial cell culture and the OB1 osteoblast cell line, while it induces apoptosis in more mature osteoblasts from those sources (Mansukhani et al. 2000). Transgenic mice over-expressing FGF-2 have an increased level of apoptosis in their calvariae (Mansukhani et al. 2000). Taken together, these paradoxical effects seem to suggest that the function of FGFs is differentiation phase dependent; FGFs drive the proliferation of cells in the osteoprogenitor

phase of osteoblast development, while they seem to obstruct and actively prohibit their differentiation. While there is ample evidence that FGFs drive osteoprogenitor cell proliferation, their involvement in cell differentiation and the mechanisms by which this is regulated remain to be elucidated. The presence of FGF alone around an implant site may not be a useful indicator of osseointegration as it is also expressed at an early, pre-commitment stage in the osteoblast lineage, and could, depending on local conditions, stimulate the development of fibroblasts among other connective tissue cells.

1.4.6 Platelet Derived Growth Factor

As the name suggests, platelet derived growth factor (PDGF) is released by platelets when they are ruptured, but can also be found in a variety of tissue types. PDGF is composed of two polypeptide chains and acts through an 'a' receptor and a 'b' receptor (D'Andrea et al. 2009). PDGF has many functions and has been reported to induce osteoblast proliferation in primary human osteoblast cell cultures but decreases differentiation in a similar fashion to FGFs (Kirn and Valentini 1997). It has been demonstrated that PDGF inhibits osteoblast differentiation; Yu et al (1997) report that PDGF decreases the expression of alkaline phosphatase, osteocalcin and type I collagen in addition to inhibiting the formation of mineralised nodules *in vitro*. PDGF has been shown to induce the migration of osteoblasts in rat calvarial cell cultures and is a major chemotactic factor for many other connective tissue cell types (Hughes et al. 1992), which is not surprising given that it is one of the first factors released around a wound site where cell migration is the first step to healing. The regulatory mechanisms which control PDGF production by osteoblasts are not fully understood; Rydziel and colleagues (1992; 1994) have reported that transforming growth factor β1 is capable of inducing PDGF production, although they have subsequently reported that PDGF is capable of autoinduction. The overall functions of PDGF, as it relates to osteoblast differentiation, appear to be the stimulation of osteoprogenitor cell proliferation in a manner akin to FGFs and the recruitment of osteoprogenitor cells to wound sites in order to initiate repair. This last

function is particularly interesting as the first step towards the osseointegration of a titanium implant is to recruit osteoprogenitor cells to the implant site, so PDGF may be therapeutically relevant. Clinically for example, Bio-Oss™ and other artificial bone matrices are commonly mixed with blood before being used to fill a defect, in an attempt to impregnate them with PDGF amongst other factors thereby stimulating the recruitment and differentiation of osteoblast progenitor cells. Accordingly their presence at an implant site indicates early migration and proliferation, but would not be a useful indicator of osseointegration as it would be expressed at a wound site regardless of *de novo* bone synthesis occurring due to the disruption of platelets.

1.4.7 Insulin-Like Growth Factors

The insulin-like growth factors (IGFs) are systemic signalling peptides released by growth hormone acting on target cells in various tissues, including osteoblasts, depending on local conditions. There are two types of IGF, IGF-I and IGF-II, both of which display bone specific activity (Rosen et al. 1997). IGFs actually bind to a variety of receptors *in vivo*, including specific IGF receptors and insulin receptors. Due to the wide variety of systemic activity which the IGFs carry out, it has been difficult to localize specific effects to bone (Delafontaine et al. 2004; Hughes et al. 2006). IGFs have been reported to have synergistic effects with several other growth factors implicated in the osteoblast differentiation pathway. Treatment with BMP-2 substantially increases the expression of IGFI and IGFII in foetal rat calvarial cell cultures (Canalis and Gabbitas 1994). Okazaki and colleagues (1995) have reported that TGFβ1 increases the expression of IGF I and II in human osteoblast cell cultures, while it has also been reported in Gangji et al (1998) that TGFβ1, along with FGF-2 and PDGF suppresses the expression of IGF II across several *in vitro* models. Although the ways in which IGF is modulated by other growth factors in bone is currently unclear, it is associated with the later stages of osteoblast differentiation, specifically the final maturation from pre-osteoblast to osteoblasts. BMPs may induce the IGFs, which seem to be suppressed by many

of the growth factors involved in the early stages of osteoblast differentiation, in order to begin the final phase of maturation before they reach the mature osteoblast phenotype. Although known to be involved with osteoblast differentiation, the specific actions of IGFs on bone as a tissue remain fairly enigmatic and due to their ubiquity, they may not in themselves be specific markers of osseointegration.

1.4.8 Major Transcription Factors in Osteoblast Differentiation

Growth factors exert transcriptional regulation through a wide range of molecules, initiating a wide range of intracellular signalling cascades which result in shifting progenitor cells away from certain differentiation pathways, for example the adipocyte or chondrocyte lineages, and towards the osteoblast differentiation pathway. Some of these signalling pathways are known, for example, BMP-2 has been reported to up-regulate the transcription factor TAZ, associated with the differentiation of mesenchymal stem cells into fully committed osteoprogenitor cells. Hong and colleagues (2005) have reported that in cell line, mouse embryonic fibroblast and primary mesenchymal cell model systems, the presence of BMP-2 upregulates TAZ expression, which in turn initiates the formation of osteoblasts and the suppression of adipocyte formation.

Runx-2 is a transcription factor that is reported to be the 'switch' responsible for moving osteoprogenitor cells to the pre-osteoblast phenotype. It has been shown to be up-regulated by both TAZ and thus is downstream of BMP signalling (Ducy et al. 1997; Gersbach et al. 2004; Hong et al. 2005). Wnt signalling has also been shown to directly upregulate Rux-2 via the β Catenin pathway (Gaur et al. 2005). Transfection of a fibroblast cell line with Runx-2 cDNA induces expression of the osteoblast cell marker alkaline phosphatase (Harada et al. 1999). Similarly, transfection of a primary mouse myocyte cultures with Runx-2 cDNA results in the suppression of myogenesis and the expression of a variety of osteoblast markers (Gersbach et al. 2004). Komori and colleagues (1997) have also reported that Runx-2 expression is an absolute requirement for

bone formation, as Runx-2 knockout mice fail to develop either osteoblasts or a skeletal system.

The transcription factor Msx-2 has also been reported to be induced by BMP-2 in primary aortic myofibroblasts, resulting in differentiation into the osteoblast phenotype via the induction of osterix, a transcription factor which, like Runx-2, is an absolute requirement for osteoblast development (Cheng et al. 2003). Osterix was identified by Nakashima and colleagues (2002) in cultured osteoblast cells and subsequently they managed to create a knockout mouse which failed to develop a skeleton. Interestingly, Runx-2 is still expressed in these mice although osterix is not expressed in the Runx-2 knockout mouse, suggesting that osterix is activated downstream of Runx-2 (Nakashima et al. 2002). BMP-2 and IGF have been reported to synergistically act to increase osterix expression, moving osteoblasts into late stage differentiation (Celil and Campbell 2005). There are many other transcription factors involved in intracellular signalling which synergistically act to induce the differentiation of osteoblasts from mesenchymal stem cells, each being modulated by the combined effects of the growth factors previously described. Although the net result of bone formation is relatively well understood, it is clear that the majority of the fine detail regarding signalling and modulation remains obscure in its complexity.

The growth and transcription factors described here as being involved in the osteoblast differentiation pathway do not comprise an exhaustive list and there are no doubt many other factors involved in the process at both direct and regulatory levels. There is a significant amount of work implicating the signalling molecules described here in the osteoblast differentiation pathways however, even if the nature of their involvement is not totally understood. As they are established indicators of osteoblast development and in many cases are detectable qualitatively and quantitatively by various techniques, they provide the components from which a picture of cellular activity can be built when examining an implant site. Data collected from these markers could indicate the

presence, quantity, and developmental phase of cells in the osteoblast lineage and how these factors are altered under various conditions.

1.5 Proteins Expressed During the Osteogenic Pathway

The protein products induced by the transcription and growth factors responsible for driving osteoblast differentiation can also represent important markers when considering the cellular events around a site of bone formation. Table 1.1 gives some of the many cellular markers and secretory products induced during different phases during osteoblast differentiation. Although the specific function of many proteins expressed by osteoblasts is unknown, they have been associated with particular phases in the osteoblast lineage and can therefore be visualized to give an indication of the osteogenic situation around a site of interest.

Differentiation Stage	**Mesenchymal Stem Cells**	**Osteoprogenitor Cells**	**Pre-osteoblasts**	**Osteoblasts**
Markers Expressed	-Stro-1 (early progenitor cell marker) -Capable of collagen type I, II, III synthesis	-Stro-1 -Alkaline Phosphatase -Capable of collagen type I, II, III synthesis	-Alkaline Phosphatase -Stro-1 not expressed -Bone Sialoprotein -Parathyroid hormone related protein receptor -Only capable of collagen type I synthesis	-Alkaline Phosphatase -Stro-1 not expressed -Bone Sialoprotein -Parathyroid hormone related protein receptor -Only capable of collagen type I synthesis -Osteopontin -Osteocalcin -Osteonectin

Table 1.1: A table giving some of the markers of each phase in the osteoblast differentiation pathway. Compiled from (Hughes et al. 2006; Katagiri and Takahashi 2002).

1.5.1 Type I Collagen

Type I collagen is the primary secretary product of osteoblasts and by far the main component of the osteoid matrix. It constitutes approximately 90% of the bone matrix proteins produced by osteoblasts (Buckwalter et al. 1995; Kalfas 2001). Type III collagen is also a major component of bone tissue, but is typically found in initially deposited woven bone (Kalfas 2001). Type I collagen has a unique triple helical structure, with the three helices intertwining to form fibrils (Allori et al. 2008). These fibrils are then bundled together in larger fibres, an arrangement which is directly related to the structural properties of type I collagen and forms a framework for mineral deposition (Allori et al. 2008). As fibres of type I collagen are laid down, the gap zones formed between each triple helical subunit serve as nucleation sites for mineral deposition, resulting in a highly organised mineralised structure (Allori et al. 2008; Buckwalter et al. 1995). The process of mineralisation is not directly facilitated by type I collagen, but it interacts with the other non-collagenous bone matrix proteins which act as nucleators, providing the scaffold for the formation of mineralised bone tissue (Boskey 1992). Type I collagen may also directly regulate cellular activity in relation to bone repair. It has been shown induce osteoblast differentiation via interaction with α_2 integrin (Xiao et al. 1998), and has been shown to be involved in the recruitment of osteoblast progenitor cells (Malone et al. 1982). Due to its central role in both the structural and cellular functions of bone, type I collagen is of critical importance in the process of osseointegration. Its expression around an implant site would be a clear indicator of osteoblast activity and therefore suggestive of osseointegrative activity.

1.5.2 Osteocalcin

Osteocalcin (OC) is a non-collagenous matrix protein which is generally held to be bone-specific due to its exclusive synthesis by osteoblasts, and is the most abundant non-collagenous protein in bone (Boivin et al. 1990; Ducy et al.

1996; Weinreb et al. 1990). Normally, osteocalcin is tightly bound to the hydroxyapatite of the mineralised bone matrix due to the post-translational carboxylation of glutamic acid residues, which favour calcium binding (Hoang et al. 2003; Poser and Price 1979). Therefore, osteocalcin is primarily incorporated into the bone matrix, although the detection of osteocalcin in the plasma is used as an indicator of bone turnover in osteoporosis (Lateef et al. 2009). Interestingly, osteocalcin knockout mice have no initial skeletal defects and express normal levels of all other bone matrix non-collagenous proteins, but over time show increased bone formation rate and a higher overall BMD, indicating a currently undefined regulatory role in skeletal development (Ducy et al. 1996). Osteocalcin has also been reported to be involved in the recruitment of both osteoblast and osteoclast progenitors, indicating that it may have a role in the regulation of bone formation (Lucas et al. 1988; Malone et al. 1982). Although the exact function of osteocalcin is unknown, it is exclusively expressed in bone tissue by osteoblasts and is therefore a useful marker of osteoblast activity. Around an implant site, its presence would be strongly indicative of osseointegrative activity.

1.5.3 Osteopontin

Osteopontin (OP) is a non-collagenous matrix protein which serves as an early marker for osteoblast activity. It contains the cell adhesion amino acid sequence Gly-Asp-Ser, and has been found to act as a cell attachment protein (Oldberg et al. 1986; Sodek et al. 2000; Somerman et al. 1988; Young et al. 1992). Like osteocalcin, it contains post-translational carboxylated glutamic acid residues, which enable calcium binding and resulting in an affinity to hydroxyapatite (Giachelli and Steitz 2000). Osteopontin has also been shown to bind both type I collagen and osteocalcin, which leads to its sequestration in the matrix and suggests a possible role in maintaining the structure of bone as a tissue (Giachelli and Steitz 2000). Expression of osteopontin is seen in bone tissue, particularly woven bone, where it has been detected in the cytoplasm of both osteoblast precursor cells and mature osteoblasts (Mark et al. 1987; Young et al. 1992). It is not exclusive to bone tissue however, and has also been

localized in the proximal convoluted tubule of the kidney and also sensory epithelia of the ear (Young et al. 1992). There is also a possibility that osteopontin is involved in the mediation of the inflammatory process, as it been shown to act as a chemo-attractant and anti-apoptotic signal for macrophages, neutrophils, T-cells, fibroblasts and endothelial cells as well as osteoblast progenitors (Ashkar et al. 2000; Denhardt et al. 2001; Giachelli and Steitz 2000; O'Regan et al. 1999; Wang and Denhardt 2008). Osteopontin knock out mice display normal skeletal development, but have abnormal osteoclast function and are resistant to ovariectomy-induced bone resorption (Rittling et al. 1998; Yoshitake et al. 1999), indicating that it may also have a role in regulating osteoclast function. Osteopontin is a useful indicator of the process of bone formation around titanium implant sites, as its expression may be indicative of osteoblast progenitor attachment and differentiation into osteoblasts. Although it is not specific to bone, its expression alongside other bone markers in a bone healing context is indicative of osseointegrative activity.

1.5.4 Bone Sialoprotein

Bone sialoprotein (BSP) is a non-collagenous matrix protein expressed by mature osteoblasts at a late stage in their differentiation and, like osteopontin, it contains the Gly-Asp-Ser cell adhesion sequence, despite having a markedly different structure (Oldberg et al. 1988; Young et al. 1992). BSP binds to type I collagen and a variety of other matrix proteins including various matrix metalloproteinases and integrins (Fisher et al. 2001; Wuttke et al. 2001) and has been shown to directly promote hydroxyapatite nucleation (Baht et al. 2008), suggesting a role in initiating the mineralisation of the osteoid matrix. Osteoclasts have also been reported to express BSP and it is a possibility that it, like many of the non-collagenous bone matrix proteins, plays either an indirect or a direct role in regulating bone resorption (Wuttke et al. 2001; Young et al. 1992). Indeed, BSP has been associated with areas in which bone has been recently formed or remodelled (Hultenby et al. 1994). BSP knockout mice are smaller than normal counterparts and have under-mineralised skeletons (Malaval et al. 2008) and display impaired bone defect repair (Luc et al. 2009), indicating that BSP has important roles in bone formation and healing. Although the exact mechanisms by which BSP functions enigmatic, it is most probably directly involved in the formation and mineralisation of bone. As it is widely expressed by osteoblasts, particularly in areas of new bone formation, it is a useful indicator of osseointegrative activity.

1.5.5 Osteonectin

Osteonectin is a calcium binding glycoprotein expressed by many different cell types, including osteoblasts. It is thought to be involved in the formation of mineralised tissues by regulating the deposition and assembly of other osteoid matrix proteins (Brekken and Sage 2001; Lane and Sage 1994). The expression of osteonectin is primarily associated with tissues undergoing remodelling or healing (Brekken and Sage 2001; Lane and Sage 1994). Although

its specific role in bone formation is not fully understood, osteonectin does not appear to support cell attachment and inhibits cell spreading (Sage and Bornstein 1991), and has also been shown to inhibit cellular proliferation and mineralisation *in vitro* (Brekken and Sage 2001; Kelm et al. 1994). Osteonectin knock-out mice display impaired bone formation and osteopenia, and have decreased numbers of both osteoblasts and osteoclasts (Delany et al. 2000). Stromal cells from these osteonectin knock-out mice display decreased osteoblast differentiation *in vitro* (Delany et al. 2003). It therefore appears that osteonectin has a role in the maintenance of bone tissue and in driving osteoblast differentiation, although not necessarily in osteoid mineralisation. Due to its association with healing tissues, particularly bone, and its involvement in regulating osteoblast differentiation, its presence around an implant site would be indicative of bone healing.

1.5.6 Alkaline Phosphatase

Alkaline Phosphatase is an enzyme which is widely expressed in various tissues around the body. There are four different isoforms of alkaline phosphatase, however the one associated with bone is the tissue non-specific alkaline phosphatase (TNAP), although it is expressed ubiquitously (Moss 1992; Young et al. 1992). This alkaline phosphatase has long been associated with bone formation, and is directly involved in the mineralisation of the osteoid matrix by removing pyrophosphates which inhibit hydroxyapatite formation (Whyte 1994). It is known to be expressed on the surface of both osteoblasts and osteoblast progenitor cells and is therefore commonly used as an indicator of osteoblast differentiation and activity (Katagiri and Takahashi 2002; Sharp and Magnusson 2008). The ubiquity of alkaline phosphatase makes it fairly non-specific as an indicator of bone formation despite its wide acceptance as a marker. Its expression alongside other markers of osteoblast activity would however, serve as an indicator of osseointegrative activity around an implant site.

1.6 The Process of Osseointegration of Titanium Dental Implants

The insertion of a dental implant into bone tissue results in an injury and therefore the process of osseointegration is also one of bone healing. Bone healing involves a complex cascade of events and is comprised of several stages (Davies 2003). Initially inflammation results from the injury and the subsequently both immune and mesenchymal progenitor cells infiltrate the site. These cells then undergo cycles of proliferation and differentiation, transforming the initial haematoma into more stable, vascularised granulation tissue. As the mesenchymal cells differentiate into osteoblasts, they begin to synthesize the osteoid matrix, which is composed of both type I and type III collagen and the various non-collagenous proteins. Together, the components of the osteoid form a matrix which then undergoes mineralisation as woven bone and is subsequently remodelled to form lamellar bone. An understanding of the bone repair process after implant placement is central to the study of the osseointegration of titanium implants, as it is during this process which the level of bone apposition to the implant surface is determined.

1.6.1 Initial Inflammatory Response

One of the first events after the placement of an implant which has a major influence on the subsequent rate of osseointegration is the resolution of the initial inflammatory response. This response is modulated by a cascade of signalling molecules released from cells in the damaged tissue and ruptured platelets, including many of the growth factors described (Bolander 1992; Einhorn 1998). Inflammatory cytokines implicated in the early inflammatory process and also in the regulation of osteoblast differentiation and function include interleukin (IL)-1, IL-6 and tumour necrosis factor (TNF) α (Bertolini et al. 1986; Einhorn et al. 1995). While the inflammatory response is necessary to initiate the process of bone repair, it is critical that it is quickly resolved as many of the inflammatory cytokines released have a deleterious effect on osseointegration (Davies, 2003; Hughes et al. 2006). Sustained inflammation

around an implant site can therefore ultimately lead to implant failure (Davies 2003). Implants modified in such a way as to improve the rate of bone synthesis in apposition to the implant surface can minimise the risk of sustained local inflammation (Le Guéhennec et al. 2007).

1.6.1.1 IL-1

IL-1 has two subtypes, IL-1α and IL-1β, which both act through the same receptor and appear to have similar biological activities (Hughes et al. 2006). A variety of functions have been attributed to IL-1, some of which are apparently contradictory. In different instances, IL-1 has been reported to inhibit osteoblast proliferation yet increase bone formation and also to enhance osteoblast proliferation but decrease bone formation (Ellies and Aubin 1990; Hanazawa et al. 1986; Rickard et al. 1993). IL-1 has also been shown to induce the synthesis of many other inflammatory cytokines and mediators, including IL-6, TNFα, prostaglandin E_2, and nitric oxide (Hughes et al. 1999; Hukkanen et al. 1995; Ishimi et al. 1990; Wei et al. 2005). IL-1 also induces bone resorption *in vitro,* although whether this is a direct action of IL-1 or an indirect effect through the induction of a variety of other cytokines is unknown (Lorenzo et al. 1987).

1.6.1.2 IL-6

Osteoblasts and stromal cells are the main source of IL-6 in bone (Holt et al. 1996). IL-6 forms a complex with a soluble form of its receptor, termed sIL-6R, which has been shown to decrease the proliferation of osteoprogenitor cells and drive osteoblast differentiation (Bellido et al. 1997). In addition to the direct action of IL-6 on osteoblasts, via an intracellular signalling cascade mediated by the IL-6/sIL6R complex receptor subunit gp130, IL-6 has been shown to induce the expression of IGFs and BMPs which are potent drivers of osteoblast differentiation (Franchimont et al. 1997; Yeh et al. 2002). IL-6 therefore appears to be an important step in initiating additional osteoblast differentiation, and thereby bone formation, in the aftermath of injury to bone tissue.

1.6.1.3 TNFα

TNFα is a cytokine well known to be involved in the inflammatory response, and has been clearly shown to increase the rate bone resorption by the induction of osteoclast formation and to decrease bone formation through the inhibition of osteoblast differentiation, proliferation and secretory activity (Bertolini et al. 1986; Nanes 2003). The main producers of TNFα are the T-cells of the acquired immune system, which produce it response to IL-1 secretion by osteoblasts (Nanes 2003). TNFα is a major repressor of osteoblast activity at a number of levels and, as such, is a key mediator of the deleterious effects of inflammation on osseointegration.

The cumulative result of sustained secretion of inflammatory cytokines and mediators, not withstanding their ability to concurrently mediate certain osteogenic effects, is osteoclast activation and bone resorption (Hofbauer et al. 1999; O'Brien et al. 2000; Wei et al. 2005).

1.6.2 Resolution of Inflammation

The inflammatory response is necessary for initiating wound healing and the elimination of infectious agents. If it is not contained and arrested promptly however, it can seriously hamper successful osseointegration by promoting the destruction of tissues adjacent to the implant site while simultaneously preventing bone repair.

Inflammation is generally resolved by a number of signalling molecules which suppress the infiltration and activation of inflammatory cells present at the site of injury. These include the glucocorticoids which decrease the infiltration of immune cells, the production of prostaglandins and a number of other well characterised anti-inflammatory actions (Adcock 2000; Lawrence et al. 2002). TGFβ1 has been shown to have a role in the resolution of inflammation by down-

regulating macrophage production of various inflammatory cytokines, including IL-1β, via Smad 3 activity (Werner et al. 2000). There are a number of anti-inflammatory cytokines which have roles in suppressing immune cell inflammatory activity, a prominent example being IL-10. IL-10 is primarily produced by monocytes and has been shown inhibit the synthesis of a variety of inflammatory cytokines by leukocytes, including TNFα and IL-1β (Cassatella et al. 1993; de Vries 1995). A variety of lipid signalling molecules, for example lipoxins, are also thought to have a variety of anti-inflammatory functions including reducing the infiltration of neutrophils and eosinophils (Lawrence et al. 2002; Maddox et al. 1998; Soyombo et al. 1994). The relatively short half life of inflammatory cytokines means that switching off the cells which produce them quickly results in their clearance from the site of injury, thus resolving the inflammation (Lawrence et al. 2002).

In addition to suppressing the cells that produce inflammatory mediators, inflammatory mediators themselves are directly antagonized through the synthesis of anti-inflammatory molecules such as the soluble TNF receptor, which acts as a decoy for TNFα (Olsson et al. 1993) and IL-1 receptor antagonist, which occupies the IL-1 receptor without activating it (Dinarello 2000). When these molecules act in concert with the suppression of immune cell activity, it leads to a rapid containment and resolution of inflammation, which is necessary for the progression of bone healing to occur.

1.6.3 Initiation of Bone Repair around the Implant Site

The disruption of tissue and the subsequent degranulation of platelets which occurs during the placement of an implant also results in the formation of a fibrin clot around the site which adheres to the implant surface (Davies 2003; Einhorn 1998). During the initial injury and inflammatory response a wide range of chemical signals are released, initiating a whirlwind of growth factors, inflammatory mediators and cell chemotactic factors, major examples being PDGF and TGFβ. These factors stimulate the infiltration of the fibrin clot

surrounding the implant site by many different cell types, including various immune cell types and mesenchymal progenitor cells which ultimately differentiate into a variety of cell types including fibroblasts, chondrocytes and osteoblasts (Davies 2003; Einhorn 1998). Invasion by these cell types and their subsequent activity results in the initial fibrin clot resolving into a more stable fibrous connective tissue composed of type III collagen secreted by fibroblasts (Davies 2003; Einhorn 1998). This fibrous or granulation tissue is rapidly vascularised through the actions of angiogenic growth factors such as vascular endothelial growth factor (VEGF) in order to supply the repair site with a ready blood supply, which is absolutely required to support and sustain the healing process (Davies 2003; Einhorn 1998). Although VEGF does not directly stimulate bone formation, it has been shown to be required for normal bone healing in mice (Street et al. 2002). Additionally, endothelial cells produce BMP-2 in response to VEGF (Bouletreau et al. 2002), indicating that the process of angiogenesis is directly linked to the initiation of bone healing.

Osteoblast progenitor cell migration to the site of the implant is stimulated by various growth factors, for example PDGF. As these cells reach the implant site, they adhere to either the bone tissue surrounding the site or move through the granulation tissue and onto the surface of the implant (Davies 2003; Einhorn 1998). Upon reaching the final stage of differentiation, osteoblasts begin to rapidly synthesize osteoid matrix around the implant. Eventually, this process results in a layer of osteoblasts attached to bone tissue surrounding the implant site laying down osteoid, referred to as distance osteogenesis, and a layer of osteoblasts attached to the implant surface synthesizing osteoid matrix directly at the implant surface, or contact osteogenesis. Both distance and contact osteogenesis occur simultaneously, steadily replacing the granulation tissue from both 'sides' with osteoid matrix, which then becomes mineralised, creating woven bone around the implant and initially stabilizing it (Davies 2003; Einhorn 1998). Woven bone is then remodelled incrementally into stronger lamellar bone by the combined action of osteoblasts and osteoclasts, resulting in the osseointegration of the titanium implant. Titanium surfaces which maximize

contact osteogenesis are clearly favourable as bone formation directly around the implant provides rapid stability and enhanced chances of osseointegration.

1.7 Titanium Surface Modifications and their Impact on Osseointegration

Although other materials have been put forward for use implant design, it is generally accepted that titanium is a highly effective material from which to make dental implants, due to several highly beneficial properties. Firstly, titanium and its alloys are highly resistant to corrosion. Corrosion is a major problem with other types of material in dental implants, as it can erode the mechanical strength of implants over time, leading ultimately to implant failure (Lacefield 1999). Titanium is also, critically, a structurally robust material, which is essential for implants to withstand the loading placed on them in the course of normal use, for example during mastication (Lacefield 1999; Le Guéhennec et al. 2007). The immunologically inert nature of titanium is also highly beneficial, as there are minimal complications with hypersensitivity reactions to implants, which can be problematic with other materials like nickel or cobalt (Rushing et al. 2007). Finally, both the surface chemistry and topography of titanium can be easily modified in a variety of ways to enhance its level of interaction with surrounding tissues, increasing contact osteogenesis and thus osseointegration (Ellingsen et al. 2006).

It has long been thought that the modification of titanium implant surfaces to optimize conditions for rapid osseointegration, which is critical for the long term clinical success of a dental implant (Albrektsson et al. 1981; Ellingsen et al. 2006; Le Guéhennec et al. 2007; Puleo and Thomas 2006). Increasing the osseointegrative potential through the modification of titanium surfaces is a key focus of this thesis.

1.7.1 General Principles of Implant Design

There are several general characteristics of implants which are currently thought to enhance to potential for osseointegration to occur and minimize the

chances of eventual failure. Titanium implants are usually made from titanium alloys, grade 5 titanium, consisting of titanium, aluminium, vanadium, iron, and oxygen, being a prime example. Titanium alloys are stronger and less prone to fatigue than pure titanium, and are therefore commonly used in dental implant design (Steinemann 1998). Alterations to the surface chemistry of the implant influence the level of interaction with surrounding tissues. Hydrophilic surfaces have also been reported to be more likely to experience tissue attachment then hydrophobic ones (Buser et al. 2004; Zhao et al. 2005), although there are also contradictory findings (Carlsson et al. 1989; Wennerberg et al. 1991). A key principle in the general design of titanium implants however, is that roughened surfaces have a greater osseointegrative potential than smooth, machined surfaces.

1.7.2 Rough versus Smooth Surfaces

It is a generally held and very widely supported principle that implants which have a roughened surface are much more likely to rapidly osseointegrate than implants with a smooth machined surface, with the optimal roughness being in the range of 1-10μM (Abrahamsson et al. 2004; Buser et al. 1998; Le Guéhennec et al. 2007; Shibli et al. 2007; Trisi et al. 2003; Wennerberg et al. 1995; Wennerberg et al. 1996b; Wennerberg et al. 1998; Zechner et al. 2004). This may be due to implants with smooth surfaces being more susceptible to fibrous encapsulation than implants with roughened surfaces (Abron et al. 2001; Ellingsen et al. 2006; Ronold and Ellingsen 2002).

Fibrous encapsulation is the formation of a poorly vascularised collagenous capsule around the implant, which results in the failure of osseointegration (Ellingsen et al. 2006). There are a number of factors which can cause fibrous encapsulation, including a sustained inflammatory response, lack of vascularisation at the implant site and low levels of osteoblast migration or attachment to the implant surface (Ellingsen et al. 2006; Kyriakides et al. 2001; Le Guéhennec et al. 2007; Shibli et al. 2007). The ultimate result of fibrous

encapsulation is that tissue does not attach directly to the implant surface, leaving a space between the fibrous capsule and implant which fills with fluid. This fluid-filled space provides an ideal environment for bacterial infiltration and a subsequent infection which leads to bone resorption via a sustained inflammatory response (Ellingsen et al. 2006; Kyriakides et al. 2001; Le Guéhennec et al. 2007). Fibrous encapsulation may occur with less frequency around roughened implants due to the increased adherence of the initial fibrin clot to the implant surface, increased osteoblast progenitor migration and vascularisation or through increased rates of contact osteogenesis enhancing implant stability (Davies 2003; Ellingsen et al. 2006; Shibli et al. 2007). Roughened surfaces also have a thicker titanium oxide layer, which is a reactive layer of surface particles thought to have a dynamic effect on surrounding tissues, encouraging attachment (Ellingsen et al. 2006; Mustafa et al. 2001; Sul et al. 2006; Zhao et al. 2005)

There is a broad consensus that rough implant surfaces have superior osseointegrative potential than smooth implant surfaces. There are however, a broad range of methods to create roughened titanium surfaces, and there has been much discussion in the literature about which of these methods creates surfaces optimized for osseointegration (Bagno and Di Bello 2004).

1.7.2.1 Grit Blasted Surfaces

Grit blasting is one of the most common methods by which titanium dental implants are roughened. They are manufactured by bombarding implants with particles composed of a variety of substances, for example alumina (Al_2O_3), titanium oxide, and calcium phosphates such as hydroxyapatite (Davies 2003; Ellingsen et al. 2006; Le Guéhennec et al. 2007). It is interesting to note that residual alumina from the blasting process may have a deleterious effect on osseointegration and may increase the chances of implant corrosion (Aparicio et al. 2003). The use of hydroxyapatite to roughen implant surfaces has been reported to result in similar rates of bone apposition around implants as other

techniques, but hydroxyapatite has the advantage of being resorbable *in situ* (Mueller et al. 2003).

In vitro studies have suggested that grit blasted titanium surfaces encourage osteoblast differentiation and, by extension, osseointegration. Cells from both osteoblast cell lines and primary mandibular bone from various species grown on grit blasted titanium surfaces have been reported increase expression of osteoblast specific mRNA and proteins as well as increased mineralization compared to cell grown on smooth surfaces (Marinucci et al. 2006; Martin et al. 1995; Mustafa et al. 2001; Schneider et al. 2003). These results have been corroborated in a number of *in vivo* studies which reported that implants with grit blasted surfaces have superior bone to implant contact compared to machined implants with smooth surfaces in rabbits, with corresponding increases in the torsional strength of the implants (Gotfredsen et al. 1995; Wennerberg et al. 1996a; Wennerberg et al. 1996b; Wennerberg et al. 1996c). Similarly, grit blasted microimplants in humans have been shown to shown increase bone apposition compared to smooth machined edges (Ivanoff et al. 2001). Grit blasting has been shown in a number of both *in vitro* and *in vivo* studies to increase the amount of bone apposition around titanium dental implants.

1.7.2.2 Acid Etched Surfaces

Another titanium implant surface treatment which has been reported to increase the chances of osseointegration is acid etching. The process of acid etching involves the submersion of implants in a strong acid such as HCl, H_2SO_4, HNO_3 and HF, which creates a topography that is moderately roughened (Le Guéhennec et al. 2007). Acid etching is often used in conjunction with grit blasting in implant manufacture. Cells from osteoblast cell lines cultured on acid etched surfaces express higher levels of alkaline phosphatase than cells cultured on smooth surfaces (Martin et al. 1995). *In vivo*, acid etched surfaces improve bone apposition rates compared to implants with smooth and plasma sprayed

surfaces (Cho and Park 2003; Cochran et al. 1998). Various clinical studies have shown acid etched implants to be successful in humans, with radiological evidence suggesting improved bone apposition rates compared to machined implants (Trisi et al. 2003; Zechner et al. 2004). The use of strong acids in the manufacture of these implants has however, led to some concerns over structural integrity. Exposure to these acids has been shown to cause hydrogen embrittlement of titanium, which can causes micro cracks on the surface, potentially undermining the structural integrity of the implant, and leading ultimately to implant failure (Yokoyama et al. 2002). Nevertheless, acid etched implants have a proven clinical track record and are still currently in use.

1.7.2.3 Calcium Phosphate Coated Surfaces

Tri-calcium phosphate (TCP) coatings have also been widely applied to titanium surfaces, with the intention of encouraging more rapid attachment of bone (de Groot et al. 1998; Lacefield 1999; Le Guéhennec et al. 2007). It is thought that presence of calcium phosphate enhances the attachment of the coating to the surrounding bone due to its chemical similarity to hydroxyapatite (Daculsi et al. 2003; de Groot et al. 1998). TCP coating a titanium surface also increases its surface roughness and it is therefore thought that it encourages the deposition osteoid matrix in apposition to implants by promoting osteoblast progenitor attachment and differentiation (Daculsi et al. 2003; de Groot et al. 1998). TCP coated implants have been reported to undergo more rapid osseointegration in goat femurs (Barrère et al. 2003), although it has been reported that there is no clinical advantage to using them (Morris et al. 2000). *In vitro*, osteoblast-like cells have been reported to adhere preferentially to titanium surfaces with a calcium phosphate coating compared to plastic or smooth titanium (Le Guehennec et al. 2008). Osteoblast-like cells have also been reported to have higher levels of alkaline phosphatase expression on TCP coated titanium surfaces compared to machined controls (Bigi et al. 2005; Montanaro et al. 2002). A possible disadvantage to this type of surface modification is that coating may detach from the implant surface once implanted, decreasing direct

bone-implant contact over time, although there has so far been is little evidence of this occurring (Daculsi et al. 2003; de Groot et al. 1998).

In summary, there are a number of ways in which dental implants can be modified in order to increase their chances of osseointegration. Although there are studies comparing the efficacy of these various techniques, it has proven difficult to determine an optimum surface topography due the wide variety of different surface modifications in existence (Bagno and Di Bello 2004; Cooper 2000).

1.8 Placement of Implants into Compromised Patients

In practice, dental implants currently have a very high clinical success rate, approaching 95% at 5 years post insertion (Lazzara et al. 1996; Le Guéhennec et al. 2007). This high success rate is at least partially due to the fact that candidates for implants are chosen according to highly selective criteria, which may exclude many individuals for whom implants would normally be clinically contraindicated. Ideal candidates have large amounts of healthy mandibular and maxillary bone, which is well supplied by the vasculature. This can severely limit the number of patients who can actually benefit from implants, particularly from groups which demonstrate the largest clinical need for implants. Periodontitis for example, causes tooth loss through bone resorption around the tooth as the result of a sustained inflammatory response to bacterial invasion (Lerner 2006; Taubman and Kawai 2001). Patients with osteoporosis are similarly unlikely to meet the criteria for treatment. Individuals with low levels of maxillary and mandibular bone and are correspondingly poor candidates for treatment with dental implants, despite the fact that they would benefit from it as they have an elevated risk of tooth loss.

1.8.1 Diabetes Mellitus

Diabetes Mellitus is a metabolic disease characterised by chronic hyperglycaemia. It is estimated that DM will affect 220 million individual worldwide by 2010, making it a significant and expanding public health concern (Zimmet et al. 2003). DM results from either a lack of insulin production, as in type I DM, or in the desensitisation of cells to insulin, as in type II DM (Graves et al. 2006; Zimmet et al. 2003). In the context of dental implants, DM has been shown to hamper both bone formation and osseointegration leading to a generally poorer outcome for diabetic individuals (Morris et al. 2000; Valero et al. 2007). Indeed, diabetes is normally a contraindication for dental implants, denying a potentially large patient group the chance to benefit from treatment (Morris et al. 2000; Valero et al. 2007). This is particularly unfortunate for DM patients, as they have a high clinical need for dental implants. Due to their chronic hyperglycaemia, diabetic individuals have an increased risk of severe periodontitis and therefore tooth loss (Loe 1993).

Delayed healing is probably the root cause of increased implant failure in DM, as slower attachment of tissue to the implant surface allows a greater chance for bacterial infiltration, infection and sustained inflammation leading to implant failure (Valero et al. 2007). In the literature, delayed bone healing has been extensively associated with DM. It has been repeatedly demonstrated that diabetic rats have impaired rates of bone formation around titanium implants compared to normal controls in models of both type I (Fiorellini et al. 1999; McCracken et al. 2006; Nevins et al. 1998; Shyng et al. 2006) and type II (Hasegawa et al. 2008; He et al. 2004) DM. Furthermore, this delay in bone healing has been shown to be reversible by treatment with insulin (Fiorellini et al. 1999; Kwon et al. 2005; Siqueira et al. 2003). These findings suggest that the delayed bone formation in DM is a direct result of the hyperglycaemia associated with the disease. Indeed, diabetic pathologies are thought to be the direct result of raised intracellular glucose levels, where sustained systemic hyperglycaemia results in cells losing the ability to regulate their internal glucose levels (Heilig et

al. 1995; Kaiser et al. 1993). Hyperglycaemia, therefore, has a broad range of complex effects relating to bone healing and interferes with cellular processes at a number of different levels.

One of the main systemic effects of DM is a deleterious effect on angiogenesis, which has clear implications for diabetic bone healing (Martin et al. 2003; Valero et al. 2007). In order for rapid and complete bone healing to occur, the injury site must be well vascularised to allow for the transit of a wide array of cell types and growth factors which are critical for stimulating of the bone repair process in addition to providing metabolic support to the site (Davies 2003; Martin et al. 2003). Hyperglycaemic conditions have been shown to impair angiogenesis, indicating that it is probably the central cause of the relatively poor vascularisation associated with DM (Kim et al. 2002; Larger et al. 2004; Martin et al. 2003). A lower level of vascularisation around an implant site is likely to be a significant contributing factor to a delay in bone healing.

It has been demonstrated that the inflammatory response is altered in DM, which is another systemic effect of the disease likely to contribute to a delay in bone healing. Diabetic mice have been shown to have a greater rates of both osteoblast and fibroblast apoptosis in response to bacterial challenge, possibly indicating a reduced capacity to respond to and resolve infection (He et al. 2004; Liu et al. 2004). TNFα expression has been reported to be prolonged in wounds on diabetic mice after bacterial challenge (Naguib et al. 2003). It has also been reported that diabetic rats have a prolonged inflammatory response, enhanced bone resorption and inhibited bone formation (Liu et al. 2006). DM therefore appears to inhibit the immune response to infectious agents in addition to the resolution of the inflammatory process, both of which directly contribute to an impaired bone healing response.

Hyperglycaemia also directly interferes with cellular metabolism and has been shown to directly inhibit osteoblast differentiation and function. Rat mesenchymal progenitor cells have increased rates of apoptosis in response to elevated glucose levels, indicating that the pool of cells from which osteoblasts

arise may be suppressed in DM (Stolzing et al. 2006). Osteoblasts cultured in hyperglycaemic conditions have a decreased capacity to produce mineralised bone nodules (Balint et al. 2001), and hyperglycaemia has been reported to decrease the expression of type I collagen, osteocalcin and Runx-2 in diabetic mice (Lu et al. 2003). Likewise, rat bone marrow stromal cells cultured under hyperglycaemic conditions show decreased rates of proliferation, decreased expression of alkaline phosphatase and type I collagen, and decreased mineralised nodule formation (Gopalakrishnan et al. 2006). Although there is not currently a unified understanding of the cellular processes affected by DM, the formation of advanced glycation end products and the generation of reactive oxygen species are thought be important mechanisms in the impairment of bone healing.

Advanced glycation end products (AGEs) result from sugars which have been nonenzymatically reduced by the amino groups of proteins and subsequently irreversibly cross-link, forming molecules which accumulate in various tissue around the body (Brownlee et al. 1988). They are particularly prevalent in diabetic individuals due to routine hyperglycaemia and can build up to substantial levels, particularly in the absence of treatment with insulin (Brownlee et al. 1988; Valero et al. 2007). AGEs have been shown to induce apoptosis in human mesenchymal progenitor cells and also to inhibit their differentiation of into osteoblasts (Kume et al. 2005). Using a fracturing healing model in diabetic and normal mice, Santana and colleagues (2003) demonstrated that the accumulation of AGEs leads to decreased osteoblast function and differentiation and also significantly alters osteoblast response to parathyroid hormone. AGEs exert their anti-osteogenic effects through a specific receptor for advanced glycation end products or RAGE, a transmembrane receptor in the immunoglobulin superfamily (Bucciarelli et al. 2002; Neeper et al. 1992). It has been shown that increased osteoblast apoptosis in the presence of AGEs is directly caused by RAGE activation (Alikhani et al. 2007). The accumulation of AGEs in bone tissues is therefore likely to be one of the primary underlying causes of the deleterious effects of DM on osteoblast function and, by extension, bone formation.

Reactive oxygen species (ROS) are also thought to play a key role in the cellular pathologies associated with DM. ROS are generated when the increased intracellular glucose levels resulting from systemic hyperglycaemia lead to increased numbers glucose molecules being oxidised by the tricarboxylic acid cycle in the cellular mitochondria, generating a large number of electrons to be transported through electron transport chain, causing in effect a saturation of the chain (Brownlee 2005). As electrons accumulate in the mitochondria, coenzyme Q donates them to oxygen atoms, resulting in oxygen free radicals or superoxides (Brownlee 2005). Increased production of ROS in cells results in the condition known as oxidative stress, which causes a variety of changes within the cell, including the activation of the transcription factor NF-κβ (Hoogeboom and Burgering 2009). Oxidative stress and the subsequent activation of NF-κβ have been associated with a variety of effects, including the inhibition of osteoblast differentiation *in vitro* (Almeida et al. 2007; Bai et al. 2004; Mody et al. 2001). NF-kappaβ also induces a number of inflammatory cytokines, including IL-1β and TNFα (Baeuerle and Henkel 1994) Therefore, increased numbers of ROS may directly contribute to decreased bone formation and increased production of inflammatory mediators. Increased ROS production has also been shown to damage endothelial cells by inhibiting normal GAPDH activity, and is therefore linked to the impairment of angiogenesis which directly contributes to the impaired bone healing (Du et al. 2003). Effectively, ROS are a cellular mechanism which may heavily contribute to the impairment of bone healing observed in DM.

Diabetic patients can attempt to manage their glucose levels through insulin therapy (type I DM) or through dietary regulation (type II DM). They can therefore, in theory, successfully receive implants. The fact remains however that the failure rate for implants is still significantly higher in diabetic individuals, possibly due to the unpredictable nature of their control over blood glucose levels, particularly in type II DM (Valero et al. 2007). Although the exact mechanisms by which osseointegration is delayed in DM are not totally understood, it has been associated with both a diminished capacity for

angiogenesis, possibly resulting in poor vascularisation of the implant site, and an impaired ability to resolve both infection and inflammation. Due to the high cost of the implant procedures, individuals with DM rarely receive implants, despite being a patient group with an increased need for dental implant treatment. Therefore, investigation of the exact effects of DM on osseointegration is of interest, as it may provide information which will be useful in implant design, possibly allowing more of these patients to benefit from treatment with dental implants.

1.8.2 Other Challenging Clinical Conditions

Unsurprisingly, individuals with osteoporosis may have higher rates of implant failure than normal, although comprehensive clinical data is lacking, probably because of the expense of implants is prohibitive in cases which may have complicating conditions (Mombelli and Cionca 2006). The osseointegration of implants with various surface treatments has been shown to be significantly decreased in osteoporotic models of sheep (Borsari et al. 2007a; Borsari et al. 2007b). There have been clinical reports of implants being successfully placed and retained in patients with osteoporosis and that implants can be successfully placed even in severely atrophied mandibles, although it is not possible to draw definitive conclusions as substantial clinical studies have not been performed (Friberg et al. 2001; Friberg et al. 2000; Mombelli and Cionca 2006). In theory, immuno-compromised individuals would also have a higher risk of implant failure, due to their increased chances of infection at the implant site, although there have not been any significant clinical studies to indicate this.

By better understanding the ways in which systemic conditions influence the process of osteogenesis and by extension osseointegration, advances can be made which place dental implants within the reach of individuals who would otherwise not be able to benefit from them. The utility of future research into the osseointegration of titanium implants is not improvement of an already excellent

routine clinical outcome, but rather the expansion of access in cases where implants are generally unavailable.

1.9 Aims

The overall aim of this thesis is to investigate the ways in which modified titanium surfaces influence the osseointegration of titanium dental implants. To this end, three commercially available modified titanium surfaces will be systematically characterised in terms of their topography, surface chemistry and hydrophobicity, variations in all of which are known to influence osseointegrative potential. The influence of these surfaces on the process of osseointegration will be investigated using both an *in vitro* and an *in vivo* model. Titanium implant osseointegration will also be investigated in the context of type II DM using a variation of the *in vivo* model system.

Osteoblasts are central to the investigation of the influence of modified titanium surfaces on osseointegration, as they are the cells which directly drive bone formation. The impairment of bone formation healing in DM is also mediated in a large part through osteoblast dysfunction. Osteoblasts also play a central regulatory role in bone tissue as a whole, both through their eventual differentiation into osteocytes and their involvement in regulating bone resorption through the control of osteoclast differentiation. Therefore, bone marrow derived mesenchymal progenitor cells cultured on modified titanium surfaces will be used to model the effects of surface modification on osteoblasts *in vitro*. In addition to investigating differences in the morphology and adherence of these cells on the different experimental titanium surfaces, the mRNA expression of a variety of osteoblast and bone specific markers will be examined in order to evaluate the influence of surface modification on the process of osteoblast differentiation. Inflammatory cytokine and growth factor mRNA expression profiles will also be compared across the different experimental titanium surfaces, as both of these have obvious implications for both osteoblast differentiation and the process of osseointegration. Expression of RANKL and

OPG mRNA will be examined in bone marrow derived osteoblast progenitors cultured on each of the experimental surfaces, in order to investigate the potential role of modified surfaces in the regulation of bone resorption. The protein composition of extracellular matrices produced by osteoblast progenitors cultured on the different experimental surfaces will also be examined, as this may have an impact on the ultimate rate of osseointegration.

Modelling the effects of modified titanium surfaces on osteoblast cellular behaviour will give an insight into which surface modifications stimulate osteoblasts to more rapidly synthesize bone in apposition to implant surfaces. By characterising the implant surfaces, specific parameters which affect this process can be identified. Also, by examining those factors which impair the process of bone repair, such as increased production of inflammatory cytokines or signals for bone resorption, potentially counter-productive effects of surface modification will be identified. The information generated by this model could therefore be directly applied to improve implant design and manufacture, hopefully improving patient outcomes, even in difficult clinical situations or disease states such as DM or osteoporosis.

It would be fallacious, however, to assume that osteoblasts are the only cells involved in the osseointegration of dental implants, as this process takes place in a tissue with a variety of cell types which interact in complex ways. Therefore an *in vivo* rat model of bone healing will be used in order to examine the interactions between bone tissue and implants with characterised experimental surfaces. Differences in the progression of bone healing around different implant sites over time will be investigated using histological methods, and immunolocalisation of bone markers will be used to gauge the corresponding activity of surrounding cells.

In addition, this model will also be used to investigate the osseointegration of dental implants in type II DM, a relatively common clinical condition with direct implications for dental implant treatment. This will provide an excellent opportunity to investigate the temporal effects of this disease on

bone as a living tissue, and will also provide direct information about alterations in cellular activity, such as the expression of bone markers, inflammatory cytokines and growth factors pertinent to bone formation. Investigating the specific effects of type II DM on the process of implant osseointegration may ultimately provide information which will improve the outcome of dental implant treatments in diabetic individuals.

The data presented in this thesis will be directly applicable to the design and manufacture of titanium dental implants. Any specific influences of surface modification on the differentiation of osteoblasts, bone formation, the inflammatory response and bone resorption will hopefully be elucidated and described. If surfaces which are optimal for rapid osseointegration can be identified, it would increase the applicability of implants in difficult clinical situations, increasing the level of access for patients who have a number of relatively common diseases. Additionally rapidly integrating implants would allow for one-stage implants, which would reduce the overall chair-time currently necessary for treatment, effectively reducing the cost of dental implants. Essentially, this would serve to broaden access to a treatment regime which has been consistently proven to be highly effective in improving the quality of life and overall oral health for a vast number of individuals. This project therefore has a high degree of relevance to not only bone biology, but also the practice of modern dentistry, the wider public health, and commercial and social medicine interests.

Chapter 2: Characterisation of Modified Titanium Surfaces

2.1 Introduction

The surfaces of titanium dental implants are frequently modified in an attempt to enhance their potential for osseointegration. Clinically, implants with surfaces which rapidly and efficiently osseointegrate bring a lower risk of complications and therefore a better outcome for patients (Davies 2003), resulting in a large amount of interest in defining the ideal implant surface. Many investigations into the osseointegrative potential of various modified surfaces have been carried out in both *in vitro* (Annunziata et al. 2008; Le Guehennec et al. 2008; Marinucci et al. 2006; Martin et al. 1996; Postiglione et al. 2003; Qu et al. 2007; Tsukimura et al. 2008) and *in vivo* (Bernd et al. 2008; Buser et al. 2004; Cho and Park 2003; Cochran et al. 1998; Franchi et al. 2007; Schwarz et al. 2007) model systems. These surface modifications generally consist of alterations in surface topography, which may also lead to alterations in the surface chemistry (Tsukimura et al. 2008; Zhao et al. 2005). The ultimate goal of any modification of titanium implant surfaces is to create an environment which is optimally suited for the adhesion, differentiation and osteogenic activity of osteoblasts.

Surface topography can be altered in a number of ways. For example, a surface can be made smooth through machining, which results in a generally more uniform and flat surface. It can also be roughed through a variety of methods, which result in a more varied surface populated by peaks and valleys. In the literature, it is often stated that rougher surfaces are superior in dental implants, as a roughened surface enhances cell attachment, stimulates osteoblast differentiation, and increases the amount of bone apposition to dental implants (Cooper et al. 1999; Masaki et al. 2005; Mustafa et al. 2001). The exact mechanisms for the increased affinity of osteoblasts and roughened titanium surfaces are currently unclear, but are probably multi-factorial and may include increased interaction with the initial fibrin clot, increased surface energy and

hydrophilicity, and provision of an optimal scaffold for the initial deposition and organisation of bone proteins (Bagno and Di Bello 2004; Deligianni et al. 2001; Le Guéhennec et al. 2007; Zhao et al. 2005) .

As noted previously, it is virtually impossible to alter the topography of a titanium surface without also altering its physiochemical properties in some way. For example, grit blasting, etching with an acid or the application of a biomimetic coating to a titanium surface would result in both changes to the topography and the surface chemistry. Consequently, the interaction between cells and titanium surfaces is also influenced by the surface chemistry of those surfaces, specifically in terms of the elemental composition of the surface, formation of a titanium oxide layer, surface energy and hydrophobicity (Buser et al. 2004; Schwarz et al. 2009; Tsukimura et al. 2008; Zhao et al. 2005). Titanium surfaces spontaneously form an oxide layer in both atmospheric and aqueous environments (Tengvall and Lundstrom 1992; Tsukimura et al. 2008; Zhao et al. 2005). This oxide layer increases both the surface energy and hydrophilicity of titanium, which has been shown to increase the absorption of serum proteins and enhance osteoblast cell attachment and activity (Tsukimura et al. 2008; Zhao et al. 2005). When placed in contact with physiologically relevant fluids, oxide layers on titanium surfaces have also been shown to play a role in the induction of hydroxyapatite formation, indicating an important role in the process of osseointegration (Li et al. 1994; Zhao et al. 2005). Various surface modifications, for example acid etching or grit blasting alter the thickness of this oxide layer, thus affecting the interaction of cells with the surface (Tengvall and Lundstrom 1992; Tsukimura et al. 2008; Zhao et al. 2005).

There is an extensive range of techniques which have been used to alter the surface characteristics of titanium (Annunziata et al. 2008; Bagno and Di Bello 2004; Bernd et al. 2008; Buser et al. 2004; Cho and Park 2003; Cochran et al. 2002; Cochran et al. 1998; Mueller et al. 2003). Unfortunately, with this nearly infinite range of possibilities for surface alteration, it remains unclear which factors constitute optimal conditions for osseointegration, despite many studies into the area, as each study is almost invariably carried out under a

different set of conditions with regard to both surface type and model system, making direct comparison difficult (Bagno and Di Bello 2004; Le Guéhennec et al. 2007). It is therefore difficult to determine with certainty which roughened surface is the 'ideally roughened' surface, in terms of osteoblast interaction under either *in vitro* or *in vivo* conditions.

Within this study, three differently modified commercially available titanium surfaces representing a range of surface types were examined for their effects on the process of osteoblast like cell differentiation, adhesion and activity. A machined surface provided a relatively smooth and homogenous environment, while an alumina grit blasted and hydrofluoric acid etched surface provided a rougher heterogeneous one. The third surface was also grit blasted and acid etched, but was then coated with a layer of tri-calcium phosphate, providing a surface with possible bioactivity. Due to the difficulties presented by the wide range of possible surface modifications and the subsequent difficulty comparing surface properties and drawing conclusions over their impact on the process of osseointegration, it is clearly important that these surfaces be thoroughly analyzed in terms of their surface topography, surface chemistry and hydrophobicity. This will enable correlations to be drawn between surface characteristics and the impact these have in both *in vitro* and *in vivo* models of osseointegration. In addition, bone marrow stromal cells extracted from rat femurs will be cultured on the surface to demonstrate that all surfaces are capable of supporting progenitor cells attachment.

2.2 Materials and Methods

2.2.1Manufacture and Surface Treatment of Titanium Discs

Titanium discs were prepared and supplied by Osteo-Ti (Guernsey). A brief description of their preparation was provided by the company, although a more detailed description was unavailable. The discs with a diameter of 1.5 cm were manufactured from grade 5 titanium bar stock (Titanium International Ltd, Birmingham, UK) by a combined lathe and mill machine (Star CNC Machine Tool Corp., New York, USA) in a one step process using Vasomill 10 vegetable based metal working oil (Blaser Swisslube, Switzerland). All discs were cleaned and passivated in 17.5% nitric acid. Machined surfaces were then polished. Both the surfaces to be grit blasted/acid etched and TCP coated surfaces were blasted with alumina grit and then etched in 2% hydrofluoric acid and 17.5% nitric acid for 30 seconds. TCP coated surfaces were then thermally coated with a TCP coating 75-100μm thick. All discs were UV treated for the purposes of sterilisation.

The titanium discs were delivered in two separate batches over the course of this project. Therefore both the first and second batches were both investigated and characterised in terms of their surface characteristics. As some differences were found between the two sets of discs, particularly in terms of their surface topography, it is important to note that the first batch of discs were used for the work presented in this chapter, while the work in all following chapters of this thesis was carried out using discs from the second batch.

2.2.2 Characterisation of Titanium Surfaces

2.2.2.1 Scanning Electron Microscopy (SEM)

Samples were mounted on stubs using double sided adhesive tape before being sputter coated with a thin 7-10nm layer of gold using an EMScope SC 5000 Sputter Coater (Thermo Electron Company, Berkshire, UK). Subsequently, images were captured using an EBT1 scanning electron microscope (SEMTech Ltd, Derbyshire, UK). All images were taken from random sites on each sample in order to visualize the general topographical features of each titanium surface.

2.2.2.2 Profilometry

The surface roughness of the three titanium surfaces was measured using a Precision Talysurf C LI 2000 profilometer (Taylor Hobson, Leicester, UK) running in contact mode. To measure the topography of a surface, the Talysurf passes a diamond edged stylus with a diameter of 2μm over a designated sample area on a surface. As it passes over the topographical features of a surface, the stylus is displaced and moves up or down. This movement creates a series of traces, from which the average roughness, or R_a, of the surface was calculated by the Talymap software package (Taylor Hobson). R_a is defined as the arithmetic mean deviation from a line representing a totally flat surface plane. The Talysurf is capable of measuring very small head displacements, with resolutions of up to 0.1μm possible.

The sample area was designated as a 2mm by 2mm square section of each disc, which the stylus passed over 1001 times, at a velocity of 14mm/min, with a distance of 2μm between each pass. These individual traces were compiled and the average deviation in microns from a zero point was calculated as the R_a value. A three dimensional image of the sample area was generated by the

Talymap software package based on a compilation of all 1001 traces. All samples were run in triplicate, with R_a values averaged and the standard error of the mean calculated using Minitab statistical software (Minitab Inc., Coventry, UK).

2.2.2.3 X-Ray-Photoelectron Spectroscopy (XPS)

In order to analyse the specific elemental composition of the titanium surfaces X-Ray Photoelectron Spectroscopy (XPS) was used. XPS works on the principle that electrons in the atoms of different elements have different binding energies and therefore, when excited by bombardment with X-rays, are released with varying levels of kinetic energy, depending on which type of atom they are contained in. In order to detect the elemental composition of a given sample, the surface is bombarded with x-rays of a known intensity, causing electrons to be freed from the atoms present on the surface of the sample. The number and kinetic energy of the electrons released from the surface are measured, which produces a series of peaks used to determine which elements are present in the first 10nm of the surface and in what relative quantity, with accuracy possible into the parts per thousand range. XPS is capable of detecting elements with an atomic number 3 or greater.

Titanium discs were mounted using double sided adhesive tape and scanned using a Kratos Axis Ultra DLD Spectrometer (Kratos Analytical Ltd, Manchester, UK) which has a monochromatic AlK_α X-Ray source (75-150W). Survey XPS scans, which give a broad view of the elements present on a surface, were acquired at an analyser pass energy of 160eV, while more detailed scans were made with an analyser pass energy of 40eV.

2.2.2.4 Contact Angle Analysis

The hydrophobicity of each titanium surface was analysed using dynamic contact angle analysis. To generate the dynamic contract angle, a sample is submerged and withdrawn in liquid, commonly water, by a force transducer at a constant speed. By measuring the force on the transducer during both submersion and withdrawal from the liquid, a buoyancy graph can be plotted, from which the surface tension forces active on the sample surface can be calculated. These forces can be used to determine the spread, or contact angle, of water on the surface. The contact angle is indicative of the degree of surface wetability and therefore the relative hydrophobicity of a surface. If a surface is highly hydrophilic, water will spread widely on the surface, resulting in low contact angle of less than 90°. Conversely, a contact angle of between 90° and 180° indicates a hydrophobic surface, as the spread of water is much reduced.

To measure the contact angle of each titanium surface, a Dynamic Contact Angle Analyzer 312 (Cahn Instruments Inc., Thermo Electron Corporation) was used. Each disc was suspended at the same distance above double distilled water, at room temperature, before being submerged and withdrawn at a rate of 30μm/s. A buoyancy graph based on the force applied to the disc at each position during submersion and withdrawal was generated by Cahn Application Software (Thermo Electron Corporation). The advancing contact angle was calculated using the least squares analysis provided in the software package. Six discs of each surface were examined, with the contact angles averaged and standard error of the mean calculated using Minitab statistical software (Minitab Inc).

2.2.2.5 Stability of TCP Coated Surfaces

In order to investigate if immersion during culture of cells causes the dissolution of the TCP coating, discs were placed into mineralising media and left at 37°C, 5% CO_2 for a period of 1, 2 and 5 days. Profilometry was used to measure the R_a values of surfaces from all three time points as described in section 2.2.2.2, while XPS broad spectrum analysis was carried out as described in section 2.2.2.3 on surfaces from the 5 day time point. Triplicate specimens were used in all experiments. Significance between R_a values from soaked TCP coated surfaces and un-soaked TCP coated surfaces was determined using Student's T test. P values below .05 at a 95% confidence interval were held to be statistically significant.

2.2.3 Morphological Characterisation of Adherent Bone Marrow Stromal Cells on Titanium Surfaces

As a proof of principal that bone marrow stromal cells could be successfully cultured and differentiated on all three experimental titanium surfaces, BMSCs were isolated and cultured on each surface. Growth media was supplemented such that BMSCs would differentiate down the osteoblast lineage.

2.2.3.1 BMSC Isolation and Culture

BMSCs were isolated from the femurs of 28 day old male Wistar rats. Rats were sacrificed via CO_2 asphyxiation and dipped in 70% ethanol to sterilize the outer skin. Femurs were then dissected from the rats and placed into 10x antibiotic media, consisting of α-MEM (Gibco, Invitrogen, Paisley, UK) supplemented with 10% v/v penicillin/streptomycin (Sigma-Aldrich, Dorset, UK). In a sterile environment, the both ends of the femur were removed and the bone marrow flushed out into a 50ml falcon tube using 15ml of culture

media for each femur. Culture media consisted of α-MEM (Gibco) supplemented with 10% foetal calf serum (FCS) (Sigma-Aldrich), 1% penicillin/streptomycin (Sigma-Aldrich), 1% 10^{-8}M Dexamethasone (Sigma-Aldrich), 1% 10mM β-Glycerophosphate (Sigma-Aldrich), and 1% 50ug/ml Ascorbic acid (Sigma-Aldrich). After centrifugation at 1000 RPM for 5 mins, the pellet was dispersed into 500μls of collagenase/dispase (Sigma-Aldrich) and incubated for 20 mins at 37°C. Following incubation, 5ml of culture media was added to the tube and it was centrifuged at 1000g for 5 mins, and the supernatant decanted. The pellet was then resuspended in 10ml of alpha MEM and passed through a 40μm filter (Falcon) to generate a single cell suspension. Cells were counted using a hematocytometer. Cell concentration was adjusted to $36x10^5$ cells/ml by the addition of culture media, and 50μl droplets were seeded onto titanium discs in 24 well plates, resulting in a seeding density of $1x10^5$ cells/cm^2. The plate was then incubated at 37°C and 5% CO_2 for 2 hrs before the wells were filled with 2ml of culture media. BMSCs were cultured for 7 days prior to fixation and visualisation, with media changes every two days.

2.2.3.2 SEM Imaging of BMSCs

In order to view cell morphology on the three titanium surfaces, cells were visualised using scanning electron microscopy. Following 7 days of culture, discs containing BMSCs were placed in a fresh 24 well plate, washed once with tris-buffered solution (TBS) and fixed for 1 hr with a 2% paraformaldehyde (Sigma-Aldrich) solution. The discs were air dried for 24 hrs before being prepared for SEM and visualised in the same manner as for the titanium surfaces, described previously in section 2.2.2.1.

2.2.3.3 Fluorescent Imaging of BMSC

In order to visualize the actin cytoskeleton and vinculin focal adhesion sites of the BMSCs cultured on the titanium surfaces, phalloidin-FITC and anti-vinculin antibodies, visualised with a Texas Red conjugated secondary antibody were used. Following 7 days of culture, titanium discs were placed in a fresh 24 well plate, washed once for 5 mins with TBS and fixed as described above in section 2.2.3.2. Cells were permeabilized with a 0.3% Triton-X 100 (Sigma-Aldrich) solution for 15 mins, washed in TBS and blocked with 1% bovine serum albumin (BSA) (Sigma-Aldrich) for 30 mins at room temperature. Cells were then stained with a 1μg/ml Phalloidin-FITC (Sigma-Aldrich) solution diluted 1:16 with TBS for 1 hr at 4°C, washed three times in TBS for 5 mins each time prior to addition of a goat anti-rat IgG vinculin antibody (Sigma-Aldrich), diluted 1:50 in TBS and 1% BSA, for 1 hr. For two separate negative controls, one disc was incubated for an hr 1% BSA with the primary antibody excluded, while another was incubated with a non immunogenic isotype IgG (Sigma-Aldrich) substituted for the primary antibody. After a 3x 5 mins washes in TBS, a solution containing both bisbenzaminde (Sigma-Aldrich) diluted 1:100 in TBS as a nuclear counter stain and an anti-goat IgG-Texas Red conjugated secondary antibody (Sigma-Aldrich) diluted 1:100 in TBS and 1% BSA was added for 1 hr. Finally after a series of 3x 5 mins washes, the discs were removed from their wells, mounted with cover-slips on glass slides using Fluorosave mounting media (Calbiochem, San Diego, USA) and visualized using a Zeiss Axiovert 200M microscope with a mercury lamp.

2.3 Results

2.3.1 SEM of Titanium Surfaces

Figure 2.1a showed the relatively smooth topography of the machined surface, albeit with machining lines visible. In Figure 2.1b, the grit blasted/acid etched surface was shown to have a much rougher topography, with visible 'impact craters' and debris from the alumina grit. The visible peaks resulting from the grit blasting had relatively smooth faces from the acid etching, yet still rose to form fairly jagged points. In contrast, the TCP coated surface, shown in Figure 2.1c, showed a series of raised rounded protrusions, due to the TCP coating, which appeared to totally cover the titanium surface.

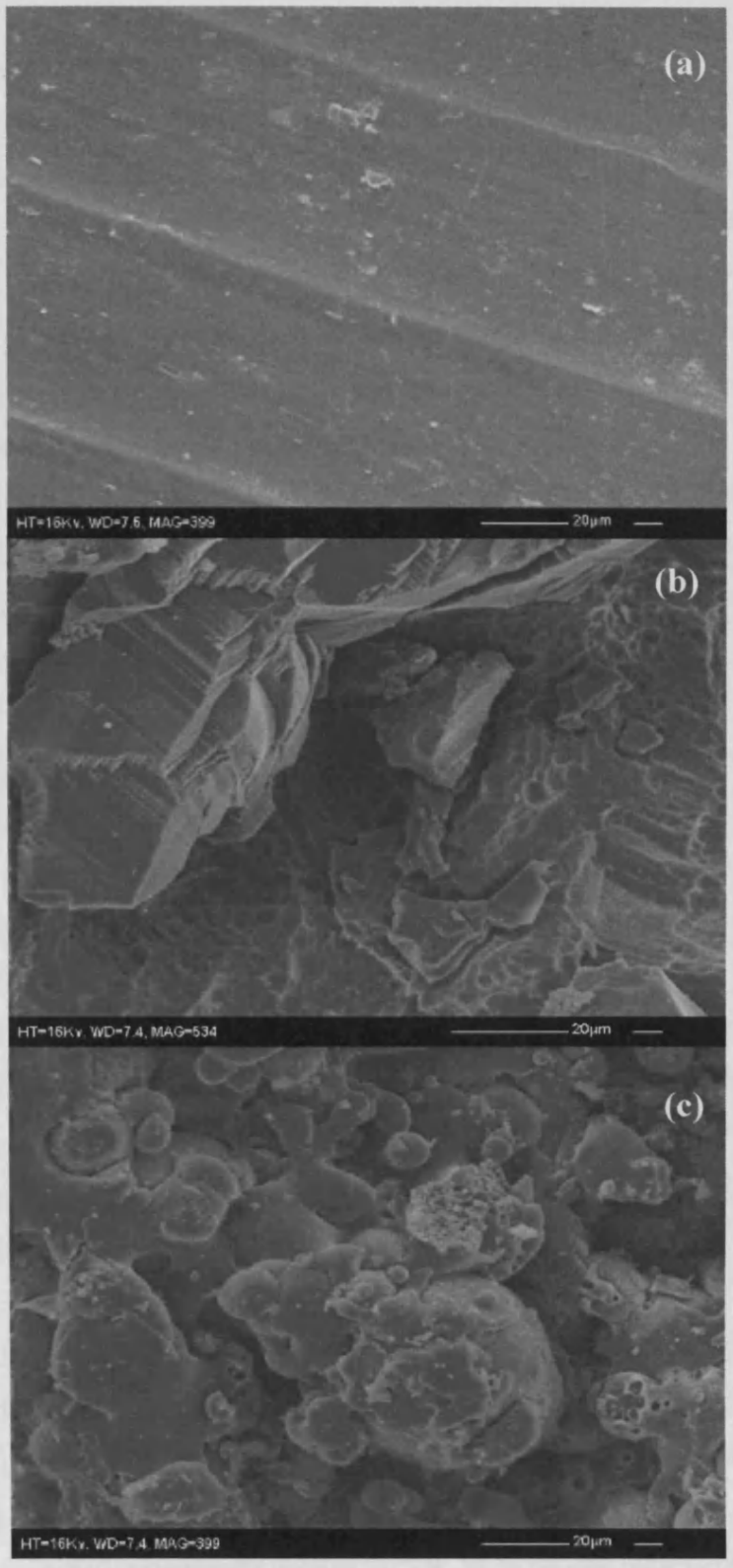

Figure 2.1: Typical images obtained by SEM of a titanium surfaces **(a)** machined, **(b)** grit blasted and acid etched, and **(c)** TCP coated.

2.3.2 Characterisation of Surface Roughness by Profilometry

The three dimensional image of the machined surface produced following profilometry, shown in Figure 2.2a, showed a largely smooth topography, although machining lines formed depressed regions, causing some variation in the topography. In the centre of each machined disc, there was one raised peak, located in the centre of each disc as a consequence of the machining process. With a replicated average R_a value of only .09μm (Table 2.1), the machined surface possessed a relatively smooth surface. The second batch of titanium discs had a replicated average R_a of .26μm (Table 2.1), which although higher than the first batch average, is still relatively smooth. In terms of topographical appearance, both batches were similar.

In contrast, the three dimensional image showed that the grit blasted/acid etched surface, shown in Figure 2.2b, was significantly rougher, with a series of 'peaks' and 'valleys' distributed over the sample area. These appeared to be random in their distribution, as they were created by the impact of alumna grit particles and the action of hydrofluoric acid across the titanium surface. A replicated average R_a of 1.51μm (Table 2.1) denotes this surface as being much rougher than the machined surface. In the second batch of grit blasted/acid etched discs, a replicated average R_a of 2.71μm (Table 2.1) was observed. This is substantially rougher than the first batch of discs, despite having a similar topographical appearance to the surfaces in the first batch.

Finally, the three dimensional image of the TCP coated surface in Figure 2.2c showed a roughened surface with higher and more densely packed 'peaks' than the grit blasted/acid etched surface. Deeper 'valleys', compared to the grit blasted/acid etched surface were also evident from the compiled and single traces. The rounded protrusions visible in the SEM of the TCP coated surface were not as evident from the three dimensional image from profilometry, possibly due to the probe recording them as sharper peaks. TCP coating resulted

in the roughest of the three surfaces with a replicated average R_a of 2.09μm (Table 2.1) for the first batch. The second batch of TCP coated surfaces was found to be substantially rougher with a replicated average R_a of 6.08μm (Table 2.1), although their overall topographical appearance was similar to that of the first batch, albeit with relatively deeper 'valleys' and higher 'peaks.'

There were some differences observed in the second batch of discs in terms of the surface roughness values. While the machined surfaces from both batches had similar R_a values, the roughness values for the grit blast/acid etched surface were much lower than in the first batch, while the TCP coated surfaces were seen to be much rougher than those in the first batch. In a similar sequence to the first batch of titanium discs, the machined was the smoothest surface, followed by the grit blasted/acid etched surface and finally the TCP coated surface was by far the roughest.

Soaking TCP coated surfaces from the second batch of discs in mineralizing culture media did not reveal any significant changes in the R_a values observed over time (Table 2.2). P Values resulting from Students T test comparison between soaked and un-soaked R_a values were as follows: 1 day: $p=0.40$, 2 day: $p= 0.26$, and 5 day: $p= 0.14$.

Figure 2.2(a)

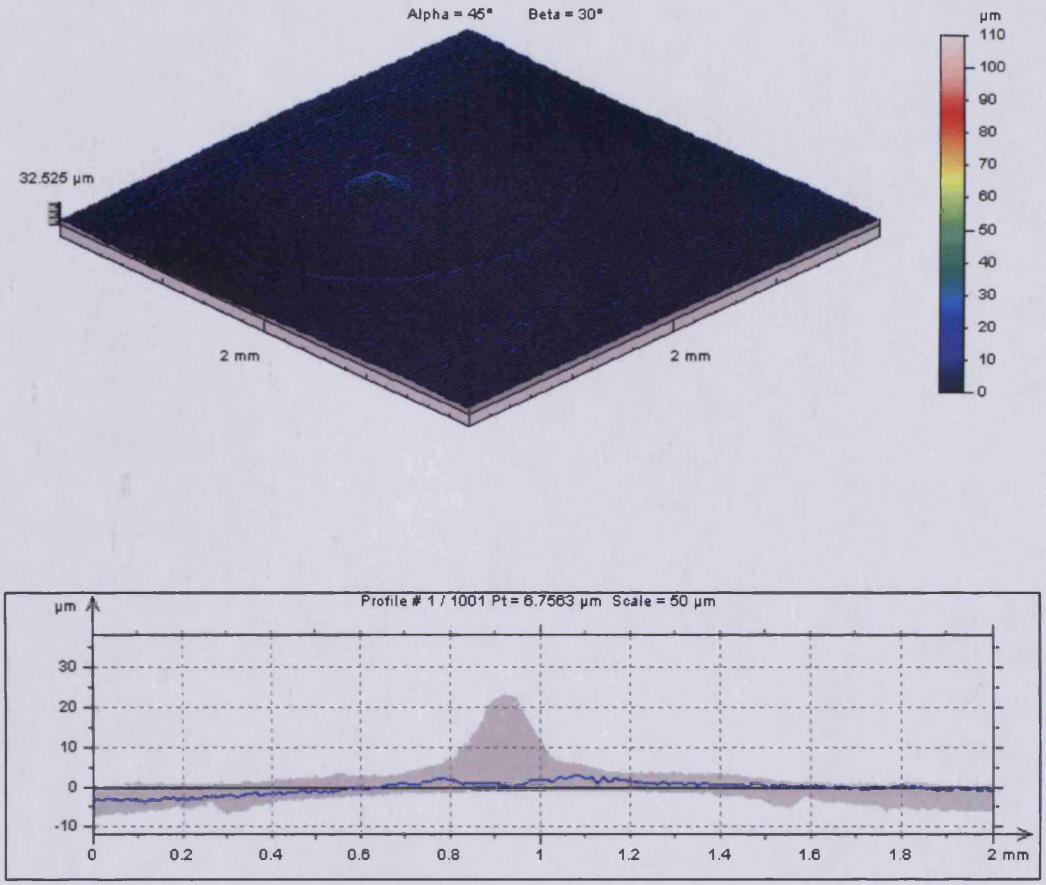

Figure 2.2: Typical examples of the 3 dimensional images (upper box) and traces (lower box) of the machined **(a)**, grit blast/acid etched **(b)** and TCP coated **(c)** surfaces generated by the Talysurf. In the traces, the grey area is composed of 1001 individual traces made over the sample area of 2mm by 2mm. Each trace has a space of 2µm in between them, due to the diameter of the stylus head. After all 1001 traces are compiled, a mean line is drawn (shown at 0 on the y axis) and the arithmetic mean of the deviations from this line are calculated, indicated by the blue line, giving a value for average roughness, or Ra.

Figure 2.2(b)

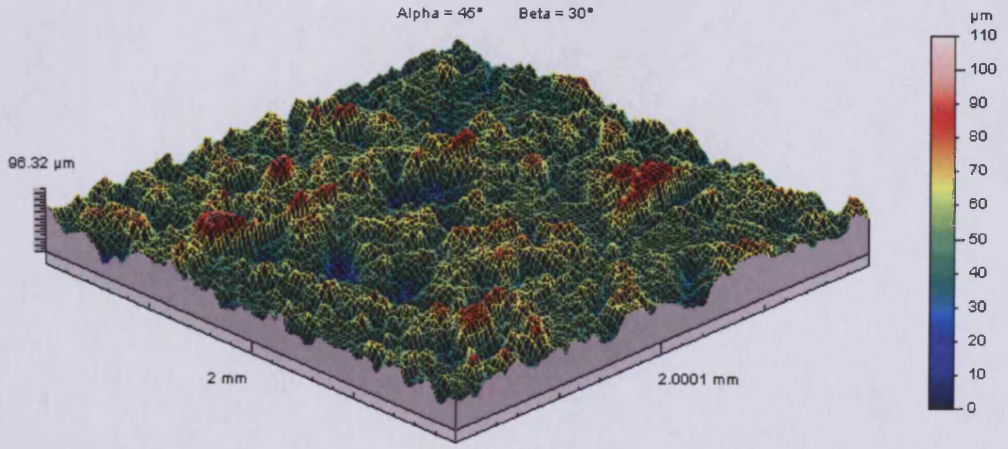
Alpha = 45°
Beta = 30°
98.32 µm
2 mm
2.0001 mm
µm
110
100
90
80
70
60
50
40
30
20
10
0

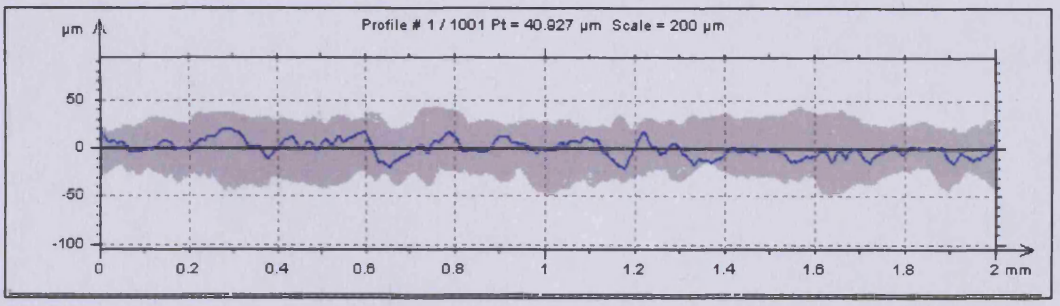
Profile # 1 / 1001 Pt = 40.927 µm Scale = 200 µm
µm
50
0
-50
-100
0
0.2
0.4
0.6
0.8
1
1.2
1.4
1.6
1.8
2 mm

Figure 2.2(c)

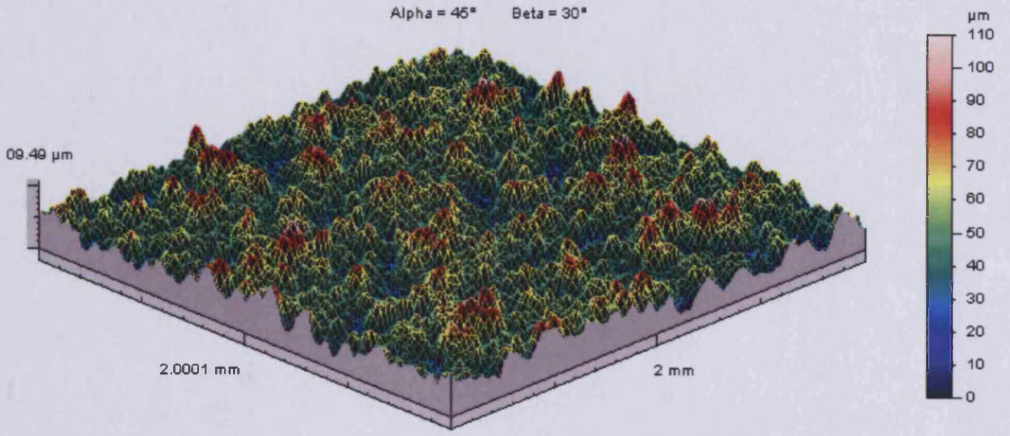
Alpha = 45°
Beta = 30°
09.49 µm
2.0001 mm
2 mm
µm
110
100
90
80
70
60
50
40
30
20
10
0

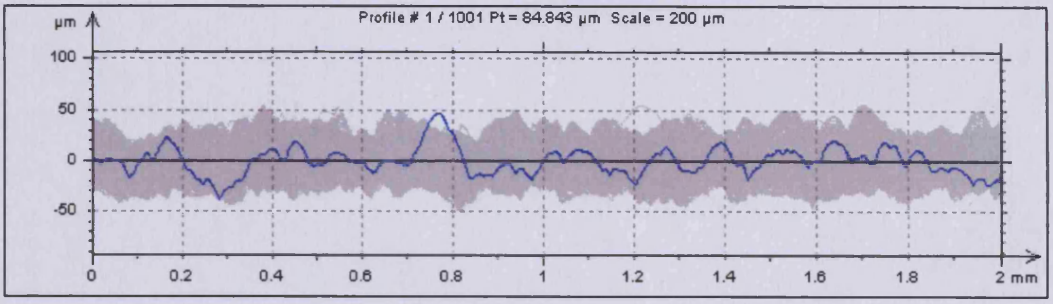
Profile # 1 / 1001 Pt = 84.843 µm Scale = 200 µm
µm
100
50
0
-50
0
0.2
0.4
0.6
0.8
1
1.2
1.4
1.6
1.8
2 mm

Surface	Average Roughness (R_a) Batch 1	Average Roughness (R_a) Batch 2
Machined (n=3)	0.09μm SD+/-0.02	0.26μm SD+/- 0.05
Alumina Grit Blasted, HF Acid Etched (n=3)	1.51μm SD+/-0.17	2.71μm SD+/- 0.24
Alumina Grit Blasted, Acid Etched, Tri-Calcium Phosphate (TCP) Coated (n=3)	2.09μm SD+/-0.14	6.08μm SD+/- .64

Table 2.1: Average roughness values from all three surfaces in both batches of discs supplied.

Surface	Average Roughness (R_a) 1 Day	Average Roughness (R_a) 2 Day	Average Roughness (R_a) 5 Day
Alumina Grit Blasted, Acid Etched, Tri-Calcium Phosphate (TCP) Coated and Soaked (n=3)	6.22μm SD+/-.1	6.05μm SD+/-.06	6.32μm SD+/-.2

Table 2.2: Profilometry data showing Ra values for 2nd batch TCP coated surfaces soaked in mineralizing culture media for 1, 2 and 5 days.

2.3.3 Surface Chemical Analysis of Titanium Surfaces

2.3.3.1 Broad Spectrum X-Ray Photoelectron Spectroscopy (XPS)

Broad spectrum XPS scans for the machined surface shown in Figure 2.3(a) had substantial peaks for both oxygen and titanium, which indicated the presence of a titanium oxide layer. A nitrogen peak was also present, which was probably the result of residual nitrogen from the passivation process. Carbon was also shown to be present in relatively high levels, probably due to carbon contamination of the surface. There were also a number of other elements present in trace amounts: Al, Pb, P, Ca, Zn, Na, and Mg, as shown in Table 2.3.

XPS data for the grit blasted/acid etched surface, shown in Figure 2.3(b) again showed substantial peaks for titanium and oxygen, which suggested the presence of a titanium oxide layer on the surface. Residual amounts of fluoride and aluminium were shown to be present as the result of the alumna grit blasting and hydrofluoric acid etching process. Carbon contamination was again seen at the surface, resulting in a substantial carbon peak. There were also several other trace elements present on the surface, but comprised a less diverse list that of the machined surface, specifically Na, Zn, and P, as shown in Table 2.3.

The broad spectrum scans of the TCP coated surface, shown in Figure 2.3(c) showed no titanium peak, indicating that the titanium surface had been totally covered by the TCP coating. A large oxygen peak was present however, which may indicate an oxide layer on the TCP. As would be expected, calcium and phosphorous from the TCP coating were present on the surface. Carbon contamination was also seen, although it was less prevalent compared to the other two surfaces. Although there were some contaminants on the surface, namely Si and N, these are much fewer in number than on the other two surface types (Table 2.3).

The XPS analysis of the second batch of discs showed that they had relatively similar surface chemistry to those of the first batch, with similar proportions of the main elements seen between both batches. There were, however, some differences in the trace elements present on the surfaces between the two batches.

Soaking TCP coated discs from the second batch in mineralizing culture media for 5 days did not reveal any substantial changes in the surface chemistry of the discs (Figure 2.5), with the only difference being the absence of trace amounts of N and Na from the soaked surfaces (Table 2.4). It does not therefore appear that the TCP coating was dissolved by soaking in culture media.

2.3.3.2 Narrow Spectrum XPS

In order to more closely examine the presence of fluoride, nitrogen and phosphorous, elements known to contribute to the bioactivity of a surface, narrow spectrum analyses were produced. The narrow spectrum scans shown for all surfaces in Figure 2.4, fluoride appeared to be present in the greatest amount on the girt blasted and acid etched surfaces, while nitrogen was only present in large amounts on the machined surfaces. Phosphorous was highly variable between replicates, with a large amount appearing on the TCP coated surfaces, but definite peaks were seen on the machined surfaces as well.

Narrow spectrum XPS revealed similar proportions of nitrogen, fluoride and phosphorous between the first and second batches of discs.

Figure 2.3(a)

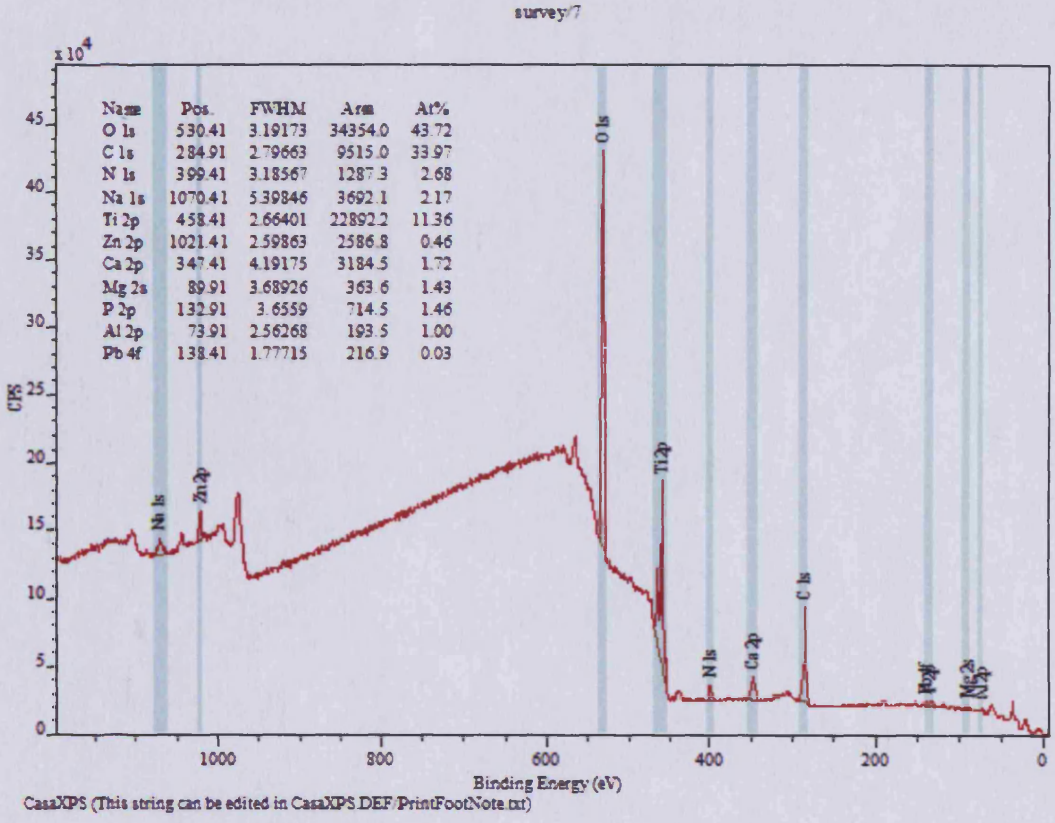

Figure 2.3: Typical examples of the broad survey XPS traces obtained from Machined **(a)**, Grit blasted/Acid Etched **(b)**, and TCP coated surfaces **(c)**. Peaks showing the electron counts on the y axis determine the relative proportion of electrons released, while their location on the X axis shows the binding energy of the electrons, which determines the element the peak represents. In the corner of each trace, a table gives the species, X-axis position, the full width at half maximum (FWHM) of each peak, the area of each peak and the percentage of the total electrons detected for each element. All experiments were performed in triplicate.

Figure 2.3(b)

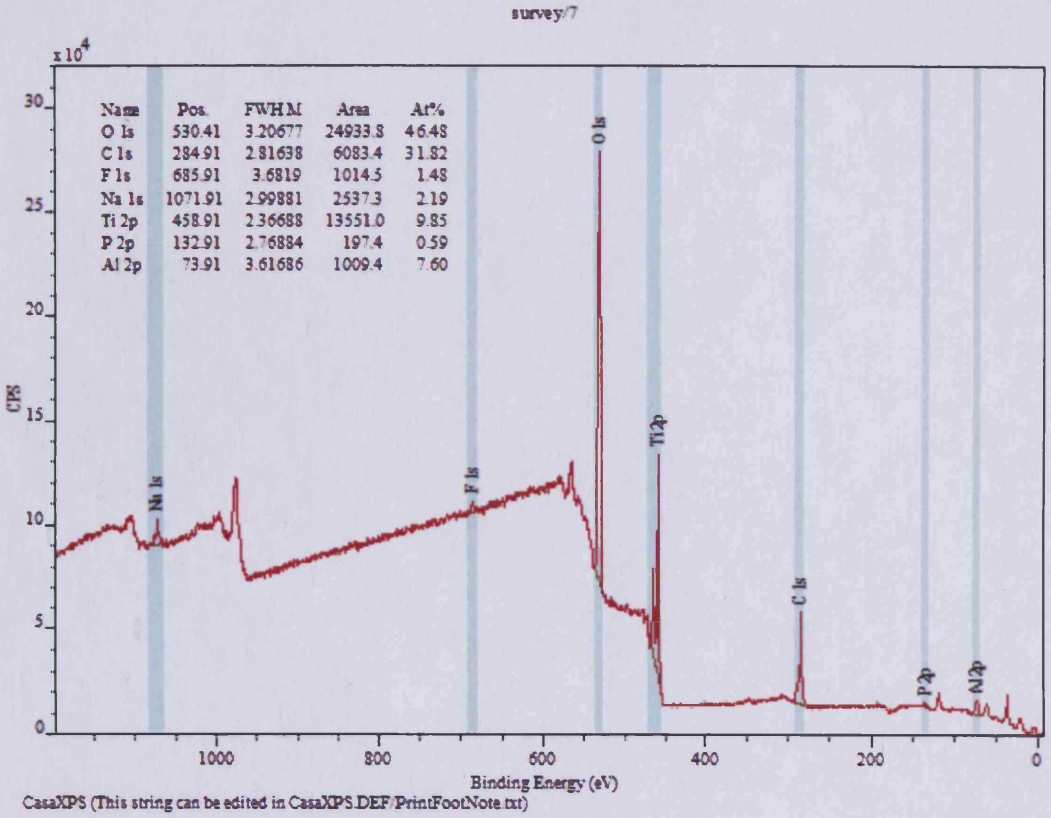
survey/7
x 10^4
Name Pos. FWHM Area At%
O 1s 530.41 3.20677 24933.8 46.48
C 1s 284.91 2.81638 6083.4 31.82
F 1s 685.91 3.6819 1014.5 1.48
Na 1s 1071.91 2.99881 2537.3 2.19
Ti 2p 458.91 2.36688 13551.0 9.85
P 2p 132.91 2.76884 197.4 0.59
Al 2p 73.91 3.61686 1009.4 7.60
CPS
Na 1s
F 1s
O 1s
Ti2p
C 1s
P2p
Al2p
Binding Energy (eV)
CasaXPS (This string can be edited in CasaXPS.DEF/PrintFootNote.txt)

Figure 2.3(c)

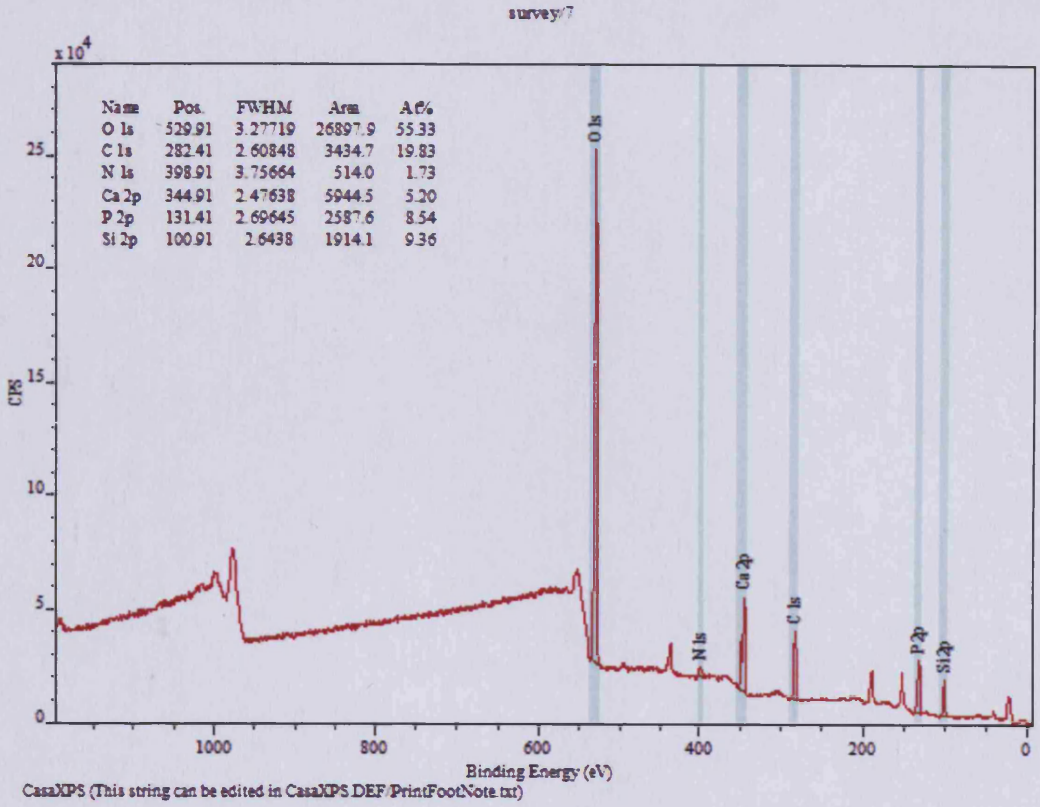
survey/7
x 10^4
Name Pos. FWHM Area At%
O 1s 529.91 3.27719 26897.9 55.33
C 1s 282.41 2.60848 3434.7 19.83
N 1s 398.91 3.75664 514.0 1.73
Ca 2p 344.91 2.47638 5944.5 5.20
P 2p 131.41 2.69645 2587.6 8.54
Si 2p 100.91 2.6438 1914.1 9.36
O 1s
N 1s
Ca 2p
C 1s
P 2p
Si 2p
CPS
Binding Energy (eV)
CasaXPS (This string can be edited in CasaXPS.DEF/PrintFootNote.txt)

Figure 2.4: Typical examples of the narrow spectrum scans for each surface for Fluoride (top), Nitrogen (middle) and Phosphorous (bottom). In all traces, A_1 and A_2 designate duplicate machined surfaces, B_1 and B_2 grit blasted and acid etched surfaces and C_1 and C_2 TCP coated surfaces.

Figure 2.4

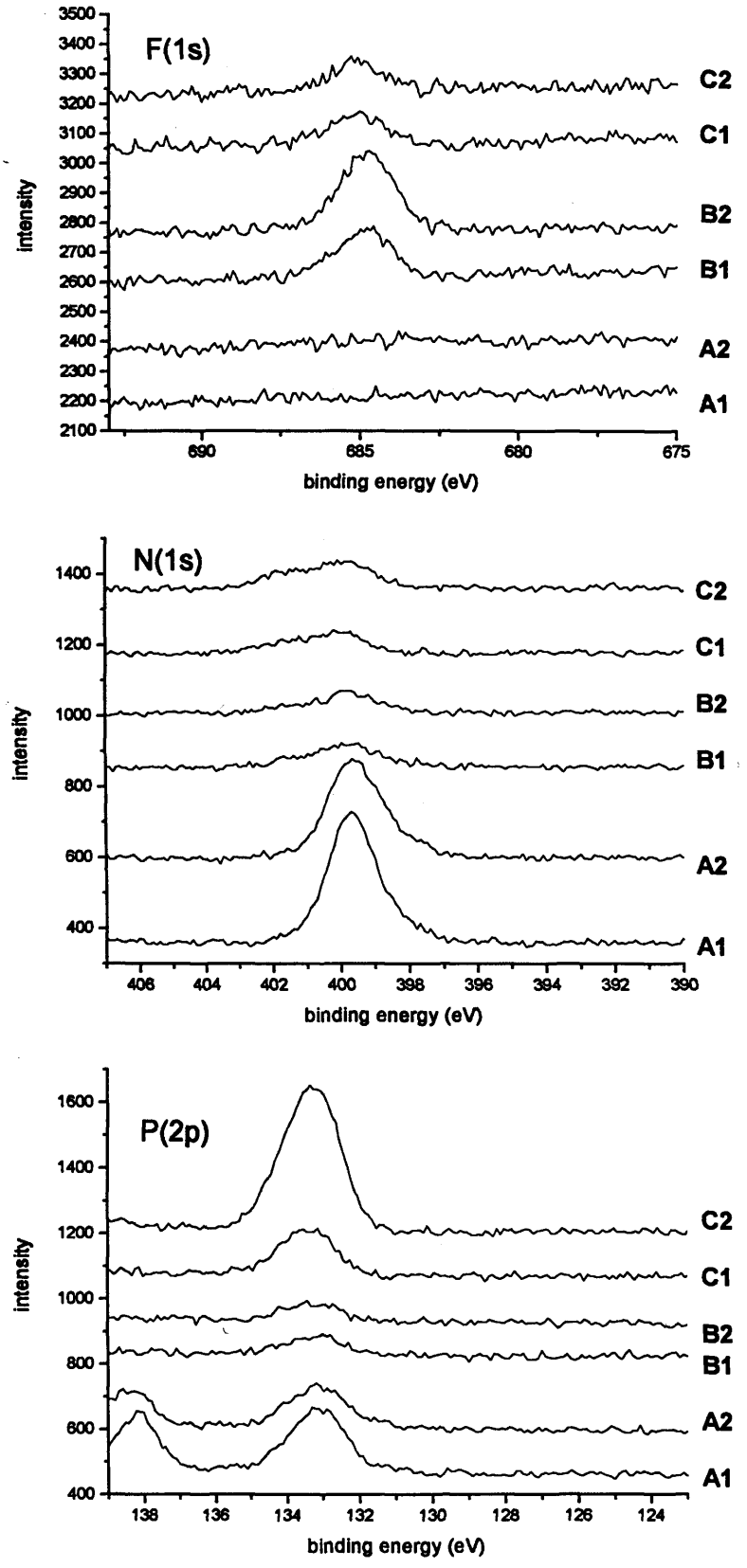
F(1s)
intensity
binding energy (eV)
C2
C1
B2
B1
A2
A1
N(1s)
intensity
binding energy (eV)
C2
C1
B2
B1
A2
A1
P(2p)
intensity
binding energy (eV)
C2
C1
B2
B1
A2
A1

Surface	Elements Present at Surface, Batch 1	Elements Present at Surface, Batch 2
Machined (n=3)	**Main:** Ti, O, C **Trace:** Al, Pb, P, Ca, Zn, Na, Mg, N	Main: Ti, O, C Trace: P, S, Ca, N
Alumina Grit Blasted, HF Acid Etched (n=3)	**Main:** Ti, O, C **Trace:** F, Na, Zn, Al, P	Main: Ti, O, C Trace: F, Al, P, N, Ca
Alumina Grit Blasted, Acid Etched, Tri-Calcium Phosphate (TCP) Coated (n=3)	**Main:** O, C, Ca, P **Trace:** Si, N	Main: O, C, Ca, P Trace: Si, Na, N

Table 2.3: Elements found by XPS on all three surfaces for the two batches supplied. The distinction between trace or main elements is a subjective one, with the categorisation arrived at on the examination of the relative proportions present on each surface.

Figure 2.5

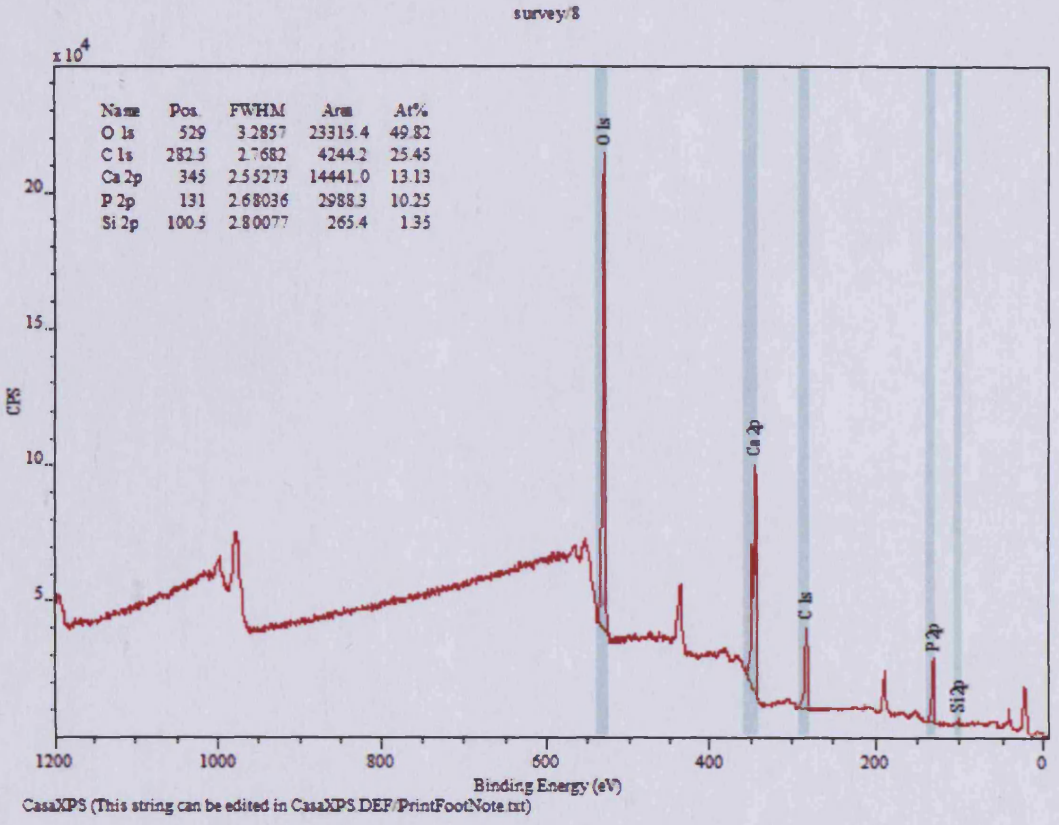

Figure 2.5: A broad spectrum XPS trace from 2nd batch TCP surfaces soaked in mineralizing culture media for 5 days. Surface chemistry was only different in the absence of N and Na on the soaked surfaces. Ti is still not present on the surface and relatively high levels of Ca and P are seen. This suggests that immersion in media does not cause dissolution of the TCP coating.

Surface	Elements Present at Surface
Alumina Grit Blasted, Acid Etched, Tri-Calcium Phosphate (TCP) Coated, Soaked for 5 Days (n=3)	**Main:** O, C, Ca, P **Trace:** Si

Table 2.4: Elements found on the surface of TCP coated discs after soaking for 5 days in culture media.

2.3.4 Hydrophobicity of Titanium Surfaces

The average values obtained following contact angle analysis are presented in Table 2.5. There were only relatively small differences between the advancing contact angles of the three surfaces, and all were under 90°, indicating that all three surfaces were hydrophilic, with the grit blasted/acid etched surface being the least hydrophilic and the TCP coated the most hydrophilic.

Hydrophobicity analysis showed similar contact angles between the first and second batches of discs (Table 2.5).

Surface	Average Advancing Contact Angle Batch 1	Average Advancing Contact Angle Batch 2
Machined (n=6)	82.87°+/-1.62	80.32°+/-2.10
Alumina Grit Blasted, HF Acid Etched (n=6)	87.17°+/-.308	86.3 °+/-.276
Alumina Grit Blasted, Acid Etched, Tri-Calcium Phosphate (TCP) Coated (n=6)	77.17°+/-.975	74.64 °+/-1.36

Table 2.5: Replicated average value s for the advancing contact angles of the three surfaces for the two batches supplied. Values are plus or minus the standard deviation.

2.3.5 Culture of Bone Marrow Stromal Cells (BMSCs) on Surfaces

To establish the potential for the cell adherence and differentiation of the three experimental surfaces, BMSCs were isolated and grown on the surfaces. Their morphology and distribution were analyzed using both SEM and fluorescent imaging.

2.3.5.1 SEM Imaging of BMSCs

When examined using SEM, cells were found to be attached to all three surfaces. On the machined surface, shown in Figure 2.6a, cells showed a rounded morphology. Images from the grit blasted/acid etched surface in Figure 2.6b show cells with a more elongated morphology. Cells attached to the TCP coated surface, shown in Figure 2.6c, were widely spread across the surface and were fewer in number than on the other two surfaces. The morphology of cells on the TCP and grit blasted/acid etched surfaces resembled each other more than those seen on the machined surface.

Figure 2.6a

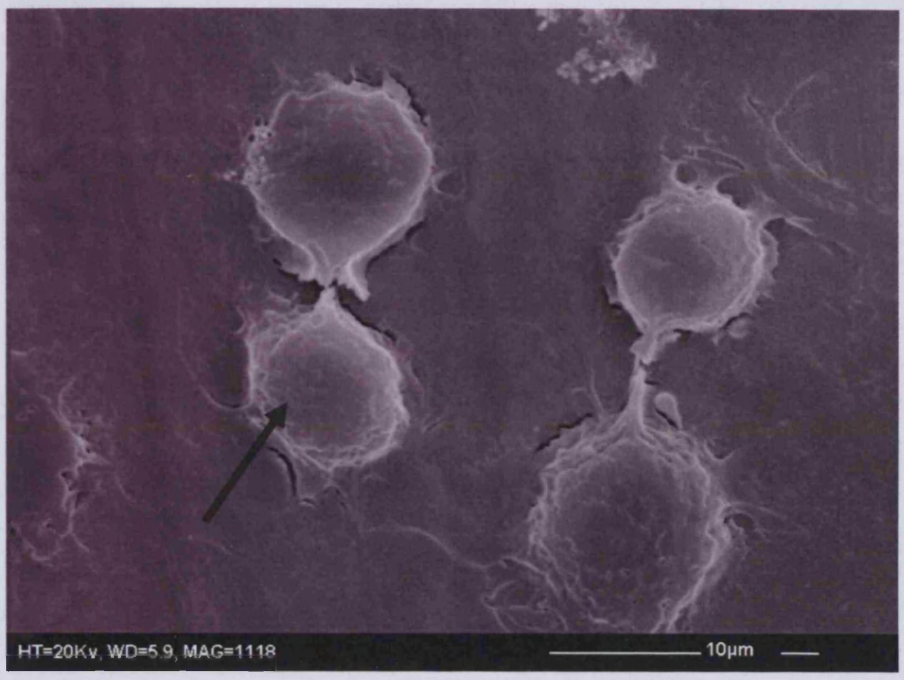

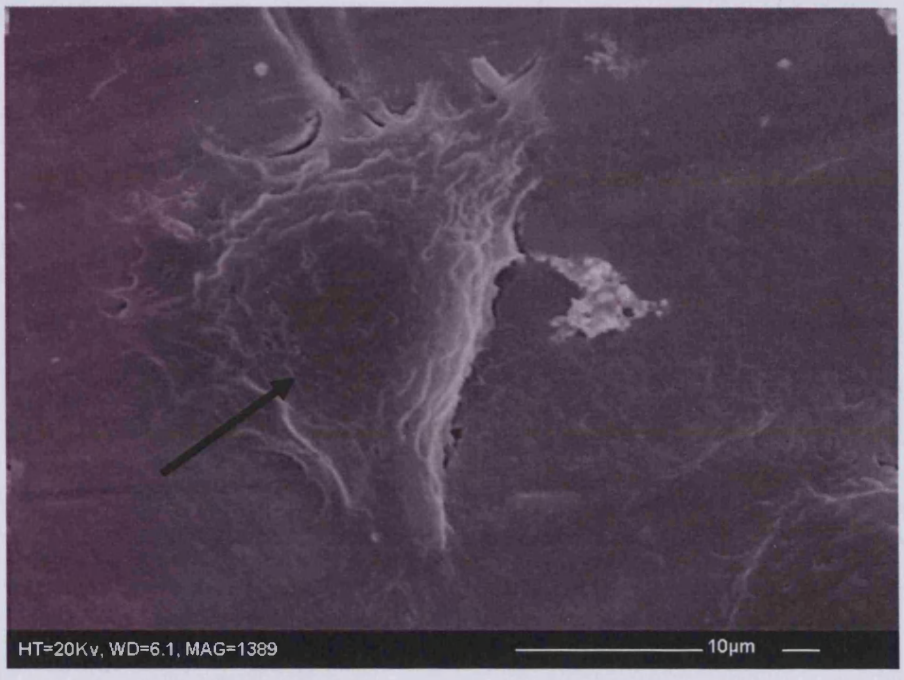

Figure 2.6: SEMs of BMSCs grown on the machined **(a)**, grit blasted and acid etched **(b)**, and TCP coated **(c)** surfaces. Cells are indicated by arrows.

Figure 2.6b

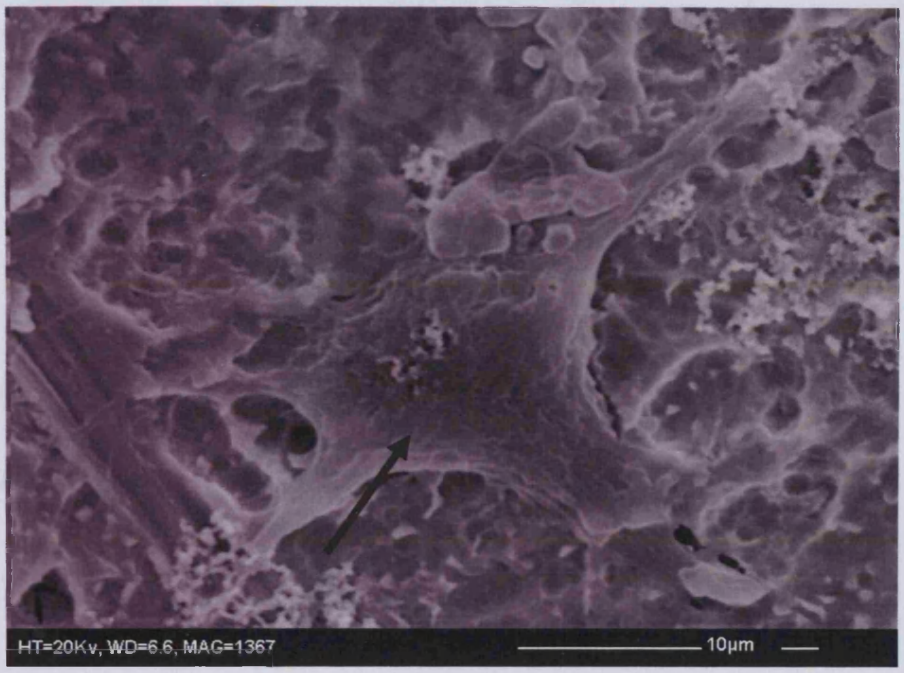

Figure 2.6c

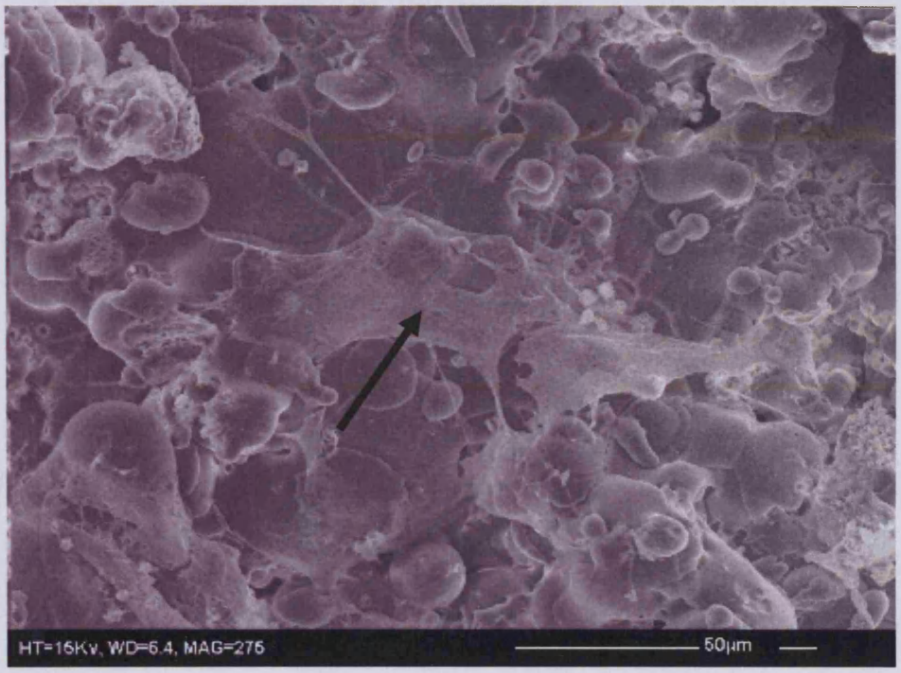

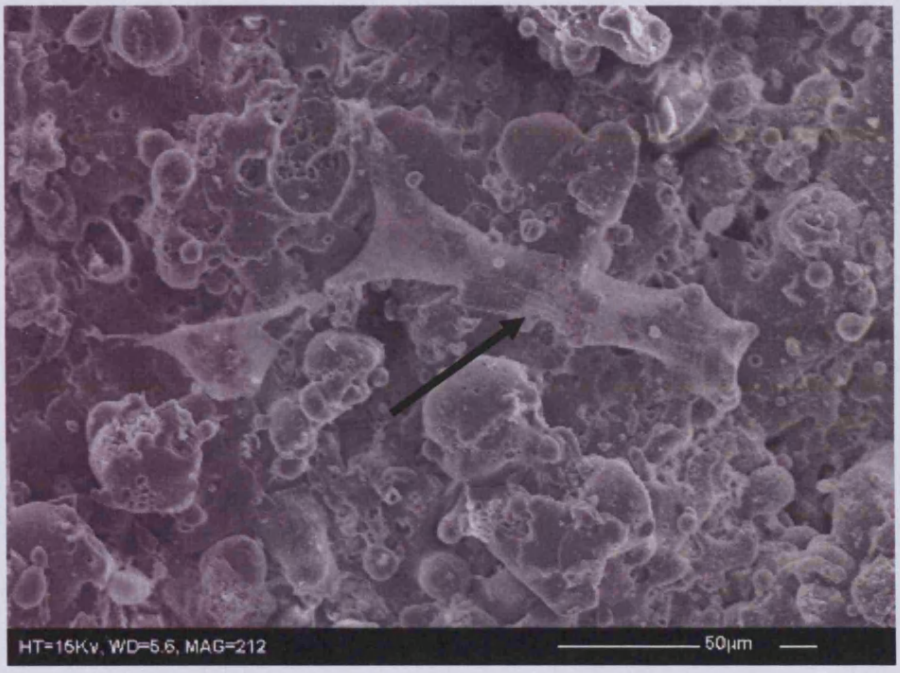

2.3.5.2 Visualisation of the BMSC Cytoskeleton and Focal Adhesion Points

Adherent cells were found on both the machined and grit blasted/acid etched surfaces. Some differences in terms of the cytoskeletal arrangement and the distribution of focal adhesion sites were observed between cells grown on each surface. On the machined surface, shown in Figure 2.7a, cells were relatively large with a rounded morphology and had a well developed cytoskeleton, with a number of focal adhesion sites located at the end of cytoskeletal projections. These cells also tended to be spread out widely across the surface. In contrast, cells grown on the grit blasted/acid etched surface, seen in Figure 2.7b, showed a more compact, elongated morphology and had a number of densely packed focal adhesion sites closely associated with the cell bodies, demonstrated by the intense red staining seen in this area. They were observed to be generally more densely packed than cells grown on the machined surface. All isotype and vinculin primary antibody excluded negative controls showed minimal immuno-staining, indicating that the staining observed was specific for vinculin focal adhesion points. Unfortunately, auto-fluorescence from the TCP coating prevented the fluorescent imaging of cells adherent on the TCP coated surface.

Figure 2.7a

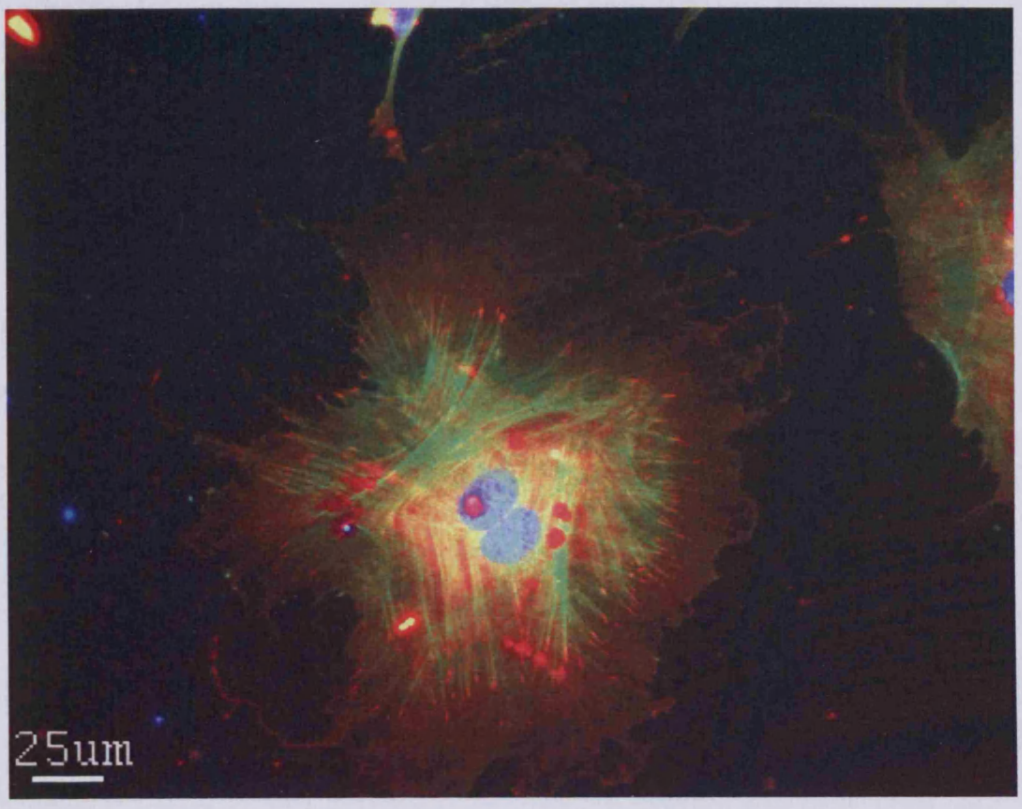

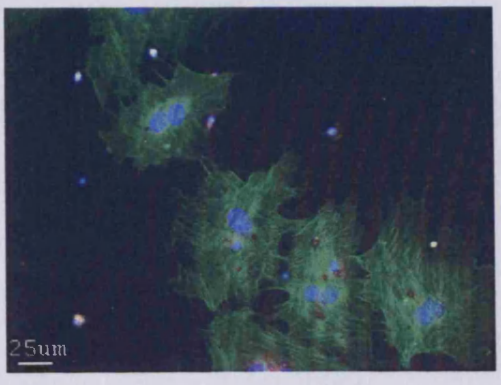

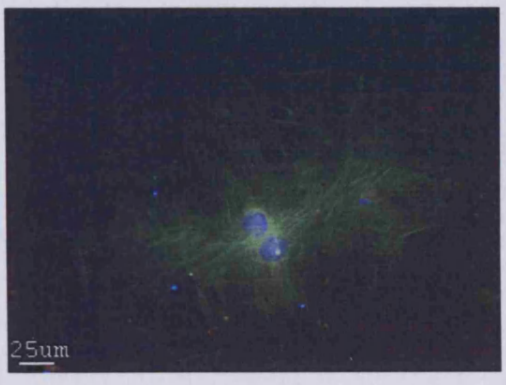

Figure 2.7: Images of rat BMSCs grown on the three different titanium surfaces. In the fluorescent images from the machined **(a)** and grit blasted and acid etched surface **(b)**, the actin cytoskeleton is stained green, with the nuclei stained blue and the focal adhesion sites stained red. Below each image are the negative controls with the isotype control on the left and the primary antibody excluded on the right.

Figure 2.7b

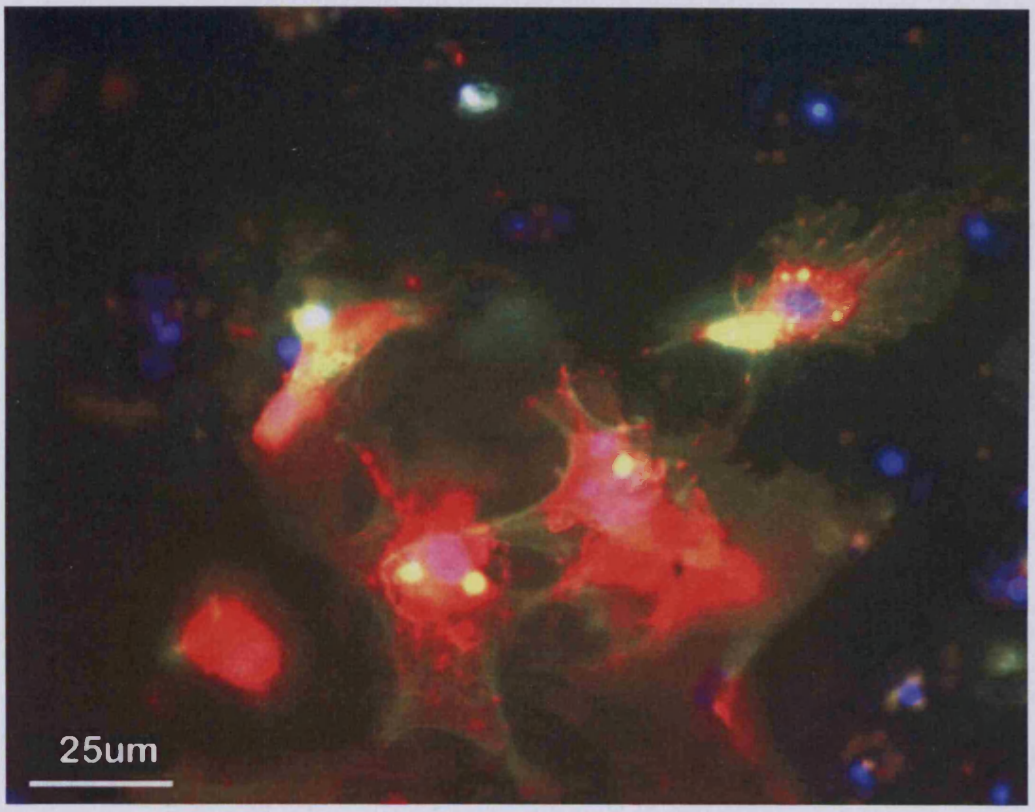

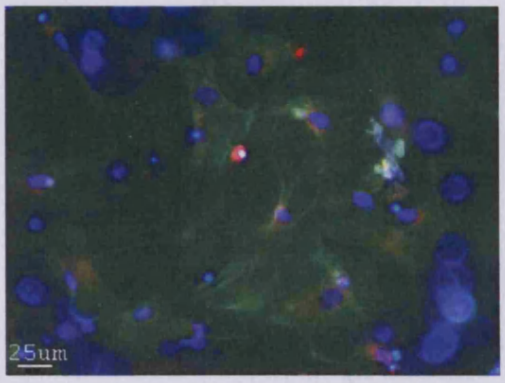

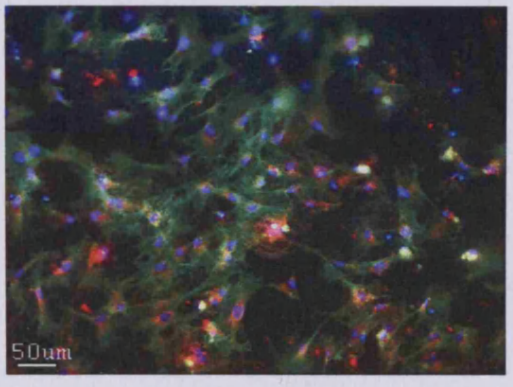

2.4 Discussion

This chapter has been successful in providing a full characterisation of the three experimental surfaces, in terms of their topography and physiochemical properties. Furthermore, the studies presented have established that all of the surfaces are capable of supporting BSMC adhesion. The differences seen in the properties of all three surfaces have been shown to have some influence on the pattern of adhesion and morphology of attached BMSCs.

All of the experimental surfaces were shown to be hydrophilic. Hydrophilicity has been widely reported to be important for implant surfaces in terms of their ability to absorb plasma proteins during the initial formation of the fibrin clot and therefore for the initial adhesion and differentiation of osteoblast progenitor cells (Buser et al. 2004; Schwarz et al. 2009; Tsukimura et al. 2008; Zhao et al. 2005) Alterations to a titanium surface, for example roughening by grit blasting/acid etching, is known to increase surface hydrophobicity by enhancing the potential for carbon contamination (Rupp et al. 2006; Zhao et al. 2005). This is because roughening a titanium surface generally leads to a thicker hydrophilic titanium oxide layer, which has a high surface energy, thus forming a favourable environment for the attachment of atmospheric carbon compounds (Rupp et al. 2006; Schwarz et al. 2009; Zhao et al. 2005). As these compounds accumulate, they decrease the overall surface energy and hydrophilicity of the surface (Rupp et al. 2006; Zhao et al. 2005). Within the present study, it was found that both the machined surface and the Grit blasted/acid etched surface have similar average contact angle values and also similar levels of carbon contamination. This may be the reason why these surfaces were found to be less hydrophilic, with an average advancing contact angle closer to 90°. The TCP coated surface had the lowest levels of carbon contamination, which may explain its relative hydrophilicity.

The full impact of hydrophilicity on the osseointegrative potential of each of these surfaces in an *in vivo* situation cannot be assessed here on the basis of

the work contained in this chapter. Upon referring to the literature, however, it is widely held that hydrophilic surfaces are more desirable than hydrophobic ones (Buser et al. 2004; Schwarz et al. 2009; Zhao et al. 2005). There are however, implications for the surface hydrophobicity in terms of the cell seeding technique used in the *in vitro* model of BMSC attachment described. Cells were seeded in droplets, and the more hydrophobic the surface, the less these droplets tended to spread over the surface. This means that with increasing hydrophobicity, the initial distribution of BMSCs across the surface increased in density, which may affect the initial adhesion and distribution of cells, as BMSC activity and growth kinetics have been shown to be influenced by the initial seeding density (Kamalia et al. 1992). When droplets were placed on the TCP coated surface, it was apparent that the droplets spread significantly more than on the other two surfaces, resulting in a lower initial clustering of cells on the surface, which may be a factor in the relatively low density of cells observed on the surface after one week in culture. The hydrophilicity of each surface may therefore have an impact on the performance of the *in vitro* model used here.

The elemental composition of titanium surfaces is widely thought to influence both the behaviour of osteoblast progenitor cells and the osseointegration of titanium implants (Buser et al. 2004; Le Guéhennec et al. 2007; Tsukimura et al. 2008; Zhao et al. 2005). Specifically, one of the most important aspects of the surface chemistry is the titanium oxide layer, which occurs spontaneously in atmospheric conditions and has been shown to have significant biological activity both *in vitro* and *in vivo* (Buser et al. 2004; Tsukimura et al. 2008; Zhao et al. 2005). The thickness of this layer can be increased or decreased by various surface treatments and, as noted previously, is a major reason for the carbon contamination seen in the chemical analysis of the surfaces (Buser et al. 2004; Le Guéhennec et al. 2007; Tsukimura et al. 2008; Zhao et al. 2005). From the broad spectrum XPS scans, it is clear that specific components of the oxide layer observed on the three experimental surfaces varied depending on the surface modification. On both the machined and grit blasted/acid etched surfaces, the presence of a titanium oxide layer was detected. There are, however, possible differences in the specific composition of these

oxide layers, for example the oxide layer on the machined surface was shown to contain nitrogen from the passivation process. Fluoride, present on the grit blasted/acid etched surface, has been shown to affect osteoblast function (Waddington and Langley 1998, 2003), and it has been reported that alumina, also found on this surface as a by-product of grit blasting, may do the same (Bellows et al. 1999; Le Guéhennec et al. 2007; Malluche 2002). These elements along with the other surface contaminants observed, could alter the specific properties of the oxide layers. In contrast, there is no titanium oxide layer on the TCP surface as the titanium is completely covered by TCP. Therefore, the oxide layer seen on this surface was probably largely comprised of calcium or phosphorous. This difference in the composition of the reactive oxide layer may explain the reduced carbon contamination and thereby influences the relative hydrophilicity of this surface. Alterations in the composition and properties of the reactive oxide layer is likely to have implications for BMSCs grown on each surface and may be responsible for some of the differences in cell morphology and distribution observed between cells grown on the three experimental surfaces (Arys et al. 1998; Sittig et al. 1999; Zhao et al. 2005). It is also of note that profilometry and XPS results indicate that the TCP layer was stable under the culture conditions used, and did not dissolve off during the culture of adherent BMSCs.

In addition to altering the composition of the reactive oxide layer, grit blasting and acid etching and TCP coating were shown to decrease the overall number of surface contaminants compared to the machined surface. Contaminants found on surfaces in the current study, for example Zn, Pb, Na, and Si are relatively common contaminants in titanium implants, due to the reactive nature of titanium, and may have a negative influence on cell-surface interaction and the process of osseointegration (Arys et al. 1998; Sittig et al. 1999; Zhao et al. 2005). The decrease in the number of surface contaminants observed may be due to the ablation of the titanium surface, which may serve to remove some of these elements and is therefore a possible beneficial effect of roughening or coating implant surfaces.

Each of the treatments produced a titanium surface which had a distinct topography, both in terms of the average roughness and general appearance. All surfaces had an average roughness value of less than 10μm and are therefore classified as micro rough surfaces (Bagno and Di Bello 2004; Le Guéhennec et al. 2007). The machined surface had a surface roughness which is comparable to other surfaces in the literature which are considered to be 'smooth' (Bagno and Di Bello 2004; Le Guéhennec et al. 2007) while the grit blasted/acid etched surface and TCP coated surfaces had roughness profiles which are similar to many other blasted and etched surfaces, although are notably much lower than those of typical plasma sprayed surfaces (Bagno and Di Bello 2004; Le Guéhennec et al. 2007). It has been suggested that surfaces with an average roughness of greater than 2μm are outside the range of optimal roughness (Le Guéhennec et al. 2007) and only the TCP coated surface approaches this value in the first batch. The second batch surfaces, aside from the machined surface, tended to be rougher, particularly the TCP coated surface. It is a possibility that such high R_a values may have a deleterious effect on BMSC attachment and differentiation.

Generally, the 3D traces produced by profilometry reproduced with great fidelity the images obtained by SEM. A notable exception was the TCP coated surface. In the SEM, the TCP surface was shown to have much more rounded projections, while the image produced by profilometry shows much sharper peaks. This may be due to the fact that the profilometer probe is displaced sharply as it moves over a rounded surface and records it as a peak instead. The R_a values generated should not have been unduly affected however, as the probe would still have accurately recorded the height of the projections and the depths of the 'valleys' in between them. It is possible that the general profile of the roughened topography, i.e. sharp peaks as seen in the grit blasted/acid etched surface as opposed to rounded projections as seen in the TCP coated surface affect cell behaviour in addition to the average roughness of the surface.

An important proof of concept for this work was to actually grow BMSCs on each surface in order to investigate any obvious cellular differences which

might be brought on by alterations in surface conditions. Cells were shown to be capable of adhering to and differentiating on all of the surfaces. On the relatively flat machined surface, there was space available for cells to spread out, resulting in a flattened morphology and more widely distributed focal adhesion points. In contrast, on the rougher grit blasted/acid etched surface, the cells adhered onto irregular 'peaks', resulting in focal adhesion points which clustered around the cell body and adopted a more elongated appearance. There was also a tendency for cells to populate 'valleys' formed by the process of grit blasting/acid etching, resulting in a more tightly packed appearance across the surface. The low number and sparse distribution of cells seen in each field of view on the TCP coated surface may be due to its high roughness reducing cell adherence, or its higher hydrophilicity leading to a greater spreading of the cells during seeding. Some cells did adhere to the surface however, and the similarity of morphology compared to the cells observed on the grit blasted/acid etched surfaces indicates that this particular elongated shape may be the result of rougher topography.

In summary, all of the surface treatments produced surfaces with unique physiochemical properties. It has also been demonstrated that all surfaces support the attachment and viability of BMSCs, and each surface appears to influence cell morphology and distribution. The relative contribution of surface hydrophobicity, chemistry and topography to any cellular differences is unclear from the data presented within this chapter, although it is well supported by the literature that all three factors act in concert, forming a complex and dynamic environment for cell-surface interaction. Each facet of the surface environments characterised in this chapter no doubt has a bearing on the attachment, metabolic activity and behaviour of BMSCs grown on them, and also influences implant performance in an *in vivo* situation.

Chapter 3: The Effects of Modified Titanium Surfaces on Bone Marrow Stromal Cell Behaviour

3.1 Introduction

One of the most important aims of the modification of titanium dental implant surfaces is to increase the attachment, proliferation and osteoid matrix production of osteoblast progenitor cells around the implant site, promoting rapid healing and enhancing the process of osseointegration (Bagno and Di Bello 2004; Ellingsen et al. 2006; Le Guéhennec et al. 2007). Dental implants which accomplish more rapid and complete bone healing and osseointegration, allowing 'one step' implants for example, would be advantageous clinically by decreasing 'chair time', thus decreasing the cost of placement. Rapid bone healing around the implant would also reduce the chances of infection and thus peri-implantitis, further improving patient outcomes (Davies 2003; Le Guéhennec et al. 2007; Zhao et al. 2005). There are a number of factors however, like the sheer number of effects modifying a surface has on its characteristics, which complicates the process of defining the optimal surface characteristics for osseointegration.

The process of osseointegration begins with the initial placement of the implant, which results in an immediate trauma around the site of implantation, leading to the formation of a fibrin clot. Crucially, the elements found in the fibrin clot, for example TGF-β, PDGF, fibronectin and indeed fibrin itself, facilitate the attachment and differentiation of a variety of cell types, including osteoblast progenitor cells, forming a cell rich granulation tissue around the implant site (Davies 2003; Haga et al. 2008; Hughes et al. 2006; Joos et al. 2006). This granulation tissue, under the influence of a wide variety of local and systemic signals, provides an environment conducive to the formation and multiplication of osteoblast-like cells, which in turn produce an osteoid matrix consisting of mainly type I collagen and diverse of non-collagenous proteins such as osteopontin, osteonectin, osteocalcin, and bone sialoprotein among others, which then undergoes mineralisation. As this newly formed bone is remodelled by the combined activity of

osteoblast and osteoclast cells, the implant is ultimately surrounded by dense cortical bone attached to the implant surface and thereby being fully osseointegrated (Davies 2003; Haga et al. 2008; Hughes et al. 2006; Joos et al. 2006). Both the topography and the surface chemistry of the titanium surface influence this process, in terms of initial surface interaction with the fibrin clot, attachment and differentiation of osteoblast progenitor cells, and the pattern of osteoid matrix deposition and mineralisation (Abrahamsson et al. 2004; Chung et al. 2008; Le Guéhennec et al. 2007; Shibli et al. 2007; Sul et al. 2006; Trisi et al. 2003; Zhao et al. 2005).

It has been widely reported that roughened surfaces with a thick oxide layer induce osteoblast differentiation and the subsequent production of osteoid matrix *in vitro* (Deligianni et al. 2001; Qu et al. 2007; Salido et al. 2007; Schneider et al. 2003; Tsukimura et al. 2008; Zhao et al. 2005) and enhance osseointegration *in vivo* (Buser et al. 2004; Cho and Park 2003; Cochran et al. 1998; Franchi et al. 2007; Schwarz et al. 2007; Sul et al. 2005; Sul et al. 2001; Wennerberg et al. 1998). In the initial phase of osseointegration, such surfaces are proposed to increase the absorption of plasma proteins during the initial formation of the fibrin clot (Deligianni et al. 2001; Park and Davies 2000). As the initial fibrin clot gives way to a cell-rich granulation tissue, surfaces with these particular characteristics may also enhance the differentiation of osteoblast progenitor cells into mature osteoblasts, leading to a greater number of osteoid producing cells and thereby enhancing the potential for osseointegration (Qu et al. 2007; Salido et al. 2007; Schneider et al. 2003). Roughened surfaces with a thick oxide layer have been reported to enhance the production of osteoid matrix proteins, influence the pattern of matrix deposition and enhance mineralised tissue apposition, resulting in a stronger anchorage for dental implants (Bernd et al. 2008; Buser et al. 2004; Cho and Park 2003; Le Guéhennec et al. 2007; Qu et al. 2007). Calcium phosphate coatings, introduced onto implant surfaces as osteogenic agents, have also been reported to influence the process of osteoblast differentiation to varying degrees and have and also directly influence the topography and surface chemistry (Bigi et al. 2005; Daculsi et al. 2003; Lacefield 1999; Le Guehennec et al. 2008; Montanaro et al. 2002).

Despite the widely reported influences of roughened surfaces on the process of osseointegration, the exact mechanisms by which surface topography influences the behaviour of osteoblast cells remain to be elucidated, as does the optimal topography and surface chemistry for the osseointegrating dental implants. Although much of the literature clearly suggests that various characteristics of different titanium surfaces directly influence osteoblast progenitor cell behaviour, it is difficult to determine the relative importance of each surface characteristic's influence over the process of osseointegration (Le Guéhennec et al. 2007; Tsukimura et al. 2008; Zhao et al. 2005). It is unclear if a roughened implant surface with a thick oxide layer owes its greater osseointegrative potential, compared to a smoother surface, to the enhanced attachment of mesenchymal progenitor cells, increased differentiation of these cells into osteoblasts, altered osteoblast secretory activity, provision a better scaffold for the deposition of osteoid matrix and mineralisation or some combination of the above factors. The plethora of methods currently used to modify the chemistry and topography of titanium surfaces (Bagno and Di Bello 2004; Le Guéhennec et al. 2007), and the wide range of both *in vitro* and *in vivo* models which have been used to examine the effects of surface modification on the process of osseointegration (Bachle and Kohal 2004; Davies 1996; Joos et al. 2006) further complicate defining optimal conditions. A surface may be roughened by two different methods which could result in the surface having the same R_a value; the nature of the roughness achieved however may be different in terms the distribution of the resulting topography. For example, the features can be regularly or irregularly distributed across a surface, which would also have an impact on the surface chemistry (Bagno and Di Bello 2004; Zhao et al. 2005). Thus, beyond the roughness of a surface, the pattern of surface roughness may influence the process of osseointegration, rendering direct comparisons even more difficult as each surface will have unique, individual characteristics.

In order to investigate the osseointegrative potential of modified titanium surfaces, it is critical to characterise them in terms of their topography and surface chemistry characteristics before examining their effect on osteoblast cells, as has been done in the previous chapter. In this chapter, an *in vitro* rat model which utilises bone marrow stromal cells was used to investigate the effects of modified titanium

surfaces on the adhesion of BMSCs and their expression of osteoid matrix markers at both the mRNA and protein level. Examination of these factors determined which aspects of osteoblast cell activity are influenced by titanium surface characteristics and how these affect the overall process of bone formation. Ultimately, this will provide information about the suitability of each surface for supporting osteoblast progenitor cells and thereby allow inferences to be made about the osseointegrative potential of each surface in an *in vivo* situation.

3.2 Materials and Methods

3.2.1 Bone Marrow Stromal Cell (BMSC) Isolation and Culture on Titanium Surfaces

In order to assess the influence of titanium surfaces on osteoblast like cells, BMSCs were extracted from rat femurs and cultured on the experimental surfaces as described in Chapter 2. Studies were then performed to determine the initial survival of BMSCs on each of the surfaces in addition to their mRNA and protein expression profiles. It was the aim of these experiments to establish the ability of each experimental surface to support the initial adhesion, survival and bone matrix synthesis of osteoblast progenitor cells.

3.2.1.1 BMSC Isolation and Culture

Rat femurs were obtained as described in section 2.2.3.1 and washed in media prepared as described in section 2.2.3.1. Due to the low cell numbers obtained through the method described in this section, alterations in the method of cell isolation and culture were made to select for a higher proportion of BMSCs to seed onto each of the titanium surfaces. Cells were also seeded directly onto the bottom of plastic wells to serve as controls. Ends of 4 femurs were removed in a sterile environment and the bone marrow flushed out into a single T-75 tissue culture flask using 15mL of the mineralising culture media, prepared as described in section 2.2.3.1. Cells were incubated at 37°C and 5% CO_2, allowing the BMSCs to adhere to the bottom of the flask, while the non-adherent cells remained in suspension and were removed when the culture media was changed after 24 hrs. This served to create a BMSC rich cell population which could be used for further experiments. Culture media was changed every 2 days during the culture period. After 5 days in culture, adherent BMSCs were incubated with 5mL of Accutase (Sigma Aldrich) for 5 mins at 37°C in order to detach them from the flask, centrifuged, counted and

seeded onto surfaces, as described in section 2.4.3. Seeded cells cultured for 5, 7, 9 and 12 days prior to experimental use.

3.2.2 Scanning Electron Microscopy (SEM)

Visualization of cells on the titanium discs was carried out at the 7 day post seeding time point. Cells were fixed in 2% paraformaldehyde and examined using SEM as described in section 2.2.3.2.

3.2.3 Analysis of BMSC Survival over Time by Direct Counting

In order to investigate the number of BMSCs remaining on the four different surfaces over time, cells were recovered from the discs and counted in order to determine the proportion of initially seeded cells remaining attached to the surfaces at 1 hr, 1, 3 and 5 days after seeding. To recover cells, the discs were removed from their culture wells at the appropriate time point and placed into a fresh 24 well plate and washed twice with PBS. Each disc was incubated in 500µl of Accutase (Sigma Aldrich) for 5 mins at 37°C. After incubation, 500µl of PBS was added to each well and the entire 1mL was recovered by pipetting up and down several times. Recovered cells were then counted using a hematocytometer and expressed as a proportion of the total number of cells originally seeded ($1.8x10^5$ cells per disc). Cell counts were performed in triplicate generated from three replicates of each experimental surface and the experiment was repeated once in its entirety.

3.2.4 BMSC mRNA Expression Profiles on Experimental Surfaces

In order to investigate the capability of each experimental surface to support the production of osteoid matrix by BMSCs, RT-PCR was carried out on RNA extracted from cells grown on each surface at 5, 7, and 12 days post seeding. Specifically the presence of mRNA from a range of bone and osteoblast cell markers was examined. The presence of chondrocyte and adipocyte specific mRNA was also

investigated in order to investigate BMSC differentiation on each surface under mineralising conditions. This work was repeated in its entirety, meaning that there was an experimental replicate, using a single biological sample each time.

3.2.4.1 RNA Extraction

At 5, 7 and 12 days post-seeding, discs were recovered, placed in a fresh 24 well plate and washed twice with PBS. Cells grown on plastic as controls were simply washed twice in PBS. RNA extraction was carried out using the RNeasy™ mini kit (Qiagen, Crawley, UK). This kit consists of RLT lysis buffer, RW1 and RPE wash buffers and spin columns containing membranes which bind RNA. A volume of 350µl RLT buffer containing 0.1% 2-β-mercaptoethanol (Sigma Aldrich) was placed directly onto cells adherent to each experimental surface. Lysate from 5 discs of each surface type (and 5 wells containing cells grown directly on plastic) were pooled in order to ensure sufficient RNA was extracted for RT-PCR. The lysate was first placed into QIAshredder™ columns (Qiagen) and centrifuged at 13,600g for 2 mins in order to homogenise them. An equal volume of ethanol (Sigma Aldrich) was added to each lysate prior to placing it into an RNeasy™ spin column, which served to increase the attachment of RNA to the column membranes. Columns were centrifuged at 12,000g, binding the RNA to their membranes. 350µl of RW1 wash buffer was added to each column prior to centrifugation at 12,000g for 30 sec. In order to reduce the chances of genomic DNA contamination, 10µl of DNase enzyme (Qiagen) was added to each column, which were then incubated at room temperature for 15 mins, prior to another RW1 buffer wash. Two washes with 500µl of RPE buffer were carried out by centrifugation at 12,000g for 30 sec each. Finally, the column was centrifuged at 12,000g for 1 min in order to dry the membrane and the RNA was then eluted by adding 40µl of sterile water and centrifuging at 12,000g for 1 min.

3.2.4.2 RNA Quantification

Total RNA quantification was carried out using the Nanovue™ spectrophotometer (GE Healthcare). The absorbance at 260:280nm ratio of all samples was between 1.7 and 2.1, indicating RNA purity.

3.2.4.3 Reverse Transcription

Reverse transcription (RT) reactions were set up by the addition of 500ng total RNA (final volume dependent on the concentration of RNA) to 10µl of 5x 1st Strand Buffer (Invitrogen), 1µl of 200U/µl Superscript II reverse transcriptase (Invitrogen), 1µl of 40U/mL RNase Inhibitor (Promega), 10µl 10mM PCR Nucleotide Mix (Promega), and 2.5µl Random Primers (Promega). All reaction volumes were made up to a total of 50µl with sterile water. For each RT reaction performed, a water negative control was established by substituting sterile water for RNA. RT-negative controls were set up excluding the reverse transcriptase RNA. For this control, 500ng RNA was used from each of the surfaces at the 7 day post seeding time point, all of which had sufficient RNA. All reactions were run on a G-storm™ GS1 thermal cycler (Genetic Research Instrumentation Ltd, Braintree, UK) with an initial denaturing step of 95°C for 5 mins, followed by an annealing step at 25°C for 10mins, elongation at 42°C for 60 mins and 95°C for 5 mins as a final denaturing step. All resulting cDNA was stored at -20°C for use in PCR reactions.

3.2.4.4 Polymerase Chain Reaction (PCR)

All PCR reactions were set up by the addition of 1µl of cDNA/control generated by reverse transcription to 10µl 5x Green GoTaq™ Flexi Buffer (Promega), 4µl 25mM MgCl, 1µl 10mM PCR Nucleotide Mix, .5µl 5U/µl GoTaq™ DNA Polymerase, 2.5µl 0.04µg/µl Forward Primer (Table 3.1), and 2.5µl 0.04µg/µl Reverse Primer (Table 3.1). All reaction volumes were made up to 50µl with sterile water. Reactions were run on a G-storm™ GS1 thermal cycler (Genetic Research Instrumentation Ltd)

with an initial denaturing step of 95°C for 5mins, followed by 30 cycles of a 1 min 95°C denaturing step, a 1 min 56°C annealing step and a 1 min 72°C extension step. A final extension step at 72°C for 5 mins was run, ending the reaction. All PCR products were stored at 4°C until visualisation.

Primer	Sequences 5'-3'	Product Size	Reference
Osteocalcin	F:ATGAGGACCCTCTCTCTGCTC R:GTGGTGCCATAGATGCGCTTG	293bp	(Alvarez et al. 1997)
Alkaline Phosphatase	F: TGATCACTCCCACGTTTTCA R: CTGGGCCTGGTAGTTGTTGT	202bp	(Kono et al. 2007)
Collagen Type I	F:GGTCTTCCTGGCTTAAAGGG R:GCTGGTCAGCCCTGTAGAAG	313bp	(Murphy et al. 1999)
Runx2	F:CCAGATGGGACTGTGGTTACC R:ACTTGGTGCAGAGTTCAGGG	381bp	(Gilbert et al. 2002)
Osteonectin	F:CTGCAGAAGAGATGGTGGCGG R:CAGGCAGGGGGCAATGTATTTG	395bp	(Hack-Young Maeng 2002)
Osteopontin	F:GGAGTCCGATGAGGCTATCAA R:TCCGACTGCTCAGTGCTCTC	189bp	(Fu et al. 2008)
BSP	F:CTGCTTTAATCTTGCTCTG R:CCATCTCCATTTTCTTCC	211bp	(Emi and Yorimasa 2002)
Collagen Type II	F:ACTTTCCTCCGTCTACTGTC R:CCTATGTCCACACCAAATTCC	320bp	(Tholpady et al. 2003)
Collagen Type III	F:AGATGCTGGTGCTGAGAAG R:TGGAAAGAAGTCTGAGGAAGG	134bp	(Tholpady et al. 2003)
MSX-2	F:CCGCCTCGGTCAAGTCGGAAA R:AGGGCTCATATGTCTTGGCGG	92bp	(Tsuruoka et al. 2007)
Sox-9	F:CCCTTCAACCTCCCACACTACAGC R:TGTGTAGACGGGTTGTTCCCAGTG	249bp	(Schumacher et al. 2008)
PPARγ	F:GGAAAGACAACAGACAAATCAC R:GAACTTCACAGCAAACTCAAAC	408bp	(Tholpady et al. 2003)
β-Actin	F:TGAAGATCAAGATCATTGCTCCTCC R:CTAGAAGCATTTGCGGTGGACGATG	155bp	(Gatto et al. 2008)

Table 3.1: A list of all primer sequences used in PCR reactions. A primer Blast search was run on each primer sequence in order to ensure specificity for the intended amplification targets. β-Actin was used as a housekeeping gene.

3.2.5 Visualisation of PCR Products

PCR products were visualised on ethidium bromide impregnated TBE agarose gels. 5x TBE buffer, used for both to make agarose gels and as a running buffer, contained 0.5M tris-base (Sigma Aldrich), 0.5M boric acid (Sigma Aldrich), 0.03M EDTA (Sigma Aldrich) and had a pH of 8.1. TBE buffer was diluted 10 times to a concentration of 0.5x prior to use.

3.2.5.1 Agarose Gel Preparation

100mL 1% agarose gels were prepared (Sigma Aldrich) using 0.5x TBE buffer. Agarose was dissolved into solution by heating in a microwave prior to the addition of 7µl of ethidium bromide (Promega). The agarose solution was immediately poured into a casting tray and left to cool.

3.2.5.2 Running Agarose Gels and Product Visualisation

10µl of each PCR product were loaded into wells on the agarose gel. In addition each get also contained 7µl of a 100bp DNA ladder (Promega). The loaded gel was run in 0.5x TBE buffer at 125mA for 45 mins. Gels were removed from the casting tray and placed on a Gel Doc™ scanner (Bio-Rad, Hemel Hempstead, UK). Products were visualised using UV light and images captured using Quantity One image analysis software (BioRad).

3.2.6 Protein Expression Profile of BMSCs Grown on Experimental Surfaces

In order to determine if mRNA expression led to the expression of bone matrix proteins by BMSCs, protein was extracted from cells grown on the experimental surfaces and plastic controls. Protein extracts were run on 4-12% Bis-tris gels and Western blots were used to investigate the expression of several non-collagenous proteins found in bone matrix.

3.2.6.1 Protein Extraction

Protein was extracted from BMSCs grown on the experimental surfaces and plastic controls at 5 day and 12 days post seeding, using a protein extraction buffer containing 4M GuCl, 0.03M EDTA and 0.05M Tris HCl. Immediately prior to use, one Complete™ protease inhibitor cocktail tablet (Roche, Hertfordshire, UK) was dissolved in the extraction buffer, per 50mL of extraction buffer as per manufacturers' instructions. Discs were removed from their culture wells and placed into fresh 24 well plates and washed twice for 5 mins PBS. BMSCs grown on plastic as controls were simply washed twice for 5 mins with PBS. After the addition of 1mL of extraction buffer to each well, samples were left at 4°C for 48 hrs with constant agitation. Extracts were collected and centrifuged at 1,000g for 5 mins. The resulting supernatants were collected and desalted using Centriprep spin columns (Millipore, Billerica, USA) prior to freeze-drying overnight and resuspension in 2mLs of distilled water. All samples were homogenized by sonification and stored at -20°C.

3.2.6.2 Protein Quantification

Protein concentration in the samples was determined using a BCA protein assay kit (Pierce, Northumberland, UK). The addition of a BCA reagent containing bicinchoninic acid and cupric sulfate to a solution containing protein leads to the peptide bonds in the protein reducing copper ions in a manner proportional to the amount of protein in the sample, which are in turn chelated by the bicinchoninic acid. This leads to the formation of a purple product which can be measured by absorbance, indicating the relative protein concentration in a given sample.

For each assay, a standard curve was generated by adding 25µl of known BSA standards in a range of concentrations from 20µg/ml to 2,000µg/ml to triplicate wells of a 96 well plate. 25µl of each protein extract was placed into triplicate wells of the same plate. The BCA reagent was prepared combining 'Reagent A', a sodium bicinchoninate solution with 'Reagent B', a cupric sulphate solution in a 50:1 ratio. 200µl of the combined sodium bicinchoninate/cupric sulphate solution was added to each well containing either sample or standard and incubated at 37°C for 30 mins. Absorbance at 570nm was read using on a Microplate™ reader (BioTek Instruments Limited). A best fit line through the standard curve generated by the absorbance values of the BSA standards allowed the concentration of the protein samples to be determined. The linearity of the best fit line through the standard curve was assessed using regression analysis and it was found to have $R^2>0.9$, indicating linearity (Instant Package, Graph Pad Software, San Diego, USA). Protein samples were diluted to an equal concentration of 30µg/mL.

3.2.6.3 Protein Separation Using Bis-Tris Gels

30μg/mL protein samples were diluted 1:1 with a protein sample buffer containing 26% (v/v) 0.5M Tris HCl, 21% (v/v) glycerol, 42% (v/v) of 10% (w/v) SDS in distilled water, 10 %(v/v) of 2-β-mercaptoethanol and 1% (v/v) of 0.5% (w/v) bromophenol blue in distilled water (final protein concentration 15μg/mL). Samples were boiled for 10 mins prior to loading into pre-cast NuPAGE® 4-12% Bis-Tris gels (Invitrogen). Gels were run in NuPAGE® running buffer (Invitrogen) diluted 1:20, as per manufacturers' instructions. 500μl of Nupage® antioxidant reagent (Invitrogen) was also added to the gel tank. Gels were run for 35 mins at 120mA.

3.2.6.4 Protein Electroblot

Proteins were transferred to a Hydrobond P 0.45μm blotting membrane (Amersham), prepared by soaking in methanol for 5 mins and subsequently for 5 mins in protein transfer buffer, containing 0.03M Tris base, 0.2M glycine, 10% (v/v) of methanol and 1% (v/v) of 20% (w/v) SDS in distilled water. The NuPAGE® blotting module (Invitrogen) was used for the electroblot. Three sponges were soaked in the protein transfer buffer and placed into the blotting module. Two pieces of Whatman number 1 filter paper (GE Healthcare) soaked in transfer buffer were placed atop the sponges followed by the bis-tris gel containing the separated protein samples, the prepared Hydrobond P blotting membrane, and two further pieces of soaked filter paper. Finally two more sponges soaked in protein transfer buffer were placed atop the filter paper, completing the transfer 'sandwich'. Proteins were transferred for 1 hr at 160mA in protein transfer buffer prior to the recovery of the blotting membrane.

3.2.6.5 Protein Detection

The blotting membrane was placed in a 50mL falcon tube and blocked in a 5% w/v milk (Sainsbury's) in TBS solution for 1 hr. Primary antibodies (Table 3.2) were diluted ratio with 5% w/v milk in TBS and incubated with the membrane overnight at 4°C with agitation and subsequently washed in TBS 3 times for 5 mins. Appropriate secondary antibodies (Table 3.2) conjugated with horse radish peroxidise (HRP) were diluted in a 5% w/v milk solution and incubated with the membrane for 1 hr at room temperature with agitation and washed in TBS 3 times for 5 mins. Finally, an ECL Plus substrate reagent (GE Healthcare) was added to the membrane for 3 mins. Chemoluminescence was detected by exposing the membrane to Hyperfilm (Amersham) and developed using a Curix 60 auto-developer (AGFA, Mortsel, Belgium) which passed exposed film through a developer (AGFA), a fixative (AGFA) and a wash in distilled water. Blocking peptides for the antibodies used to detect osteonectin and osteopontin were used to produce negative controls, and are also listed in Table 3.2. Primary antibodies were incubated at 37°C for 30mins with a 10x excess of blocking peptide prior to use in the detection protocol. Blocking peptides for the antibody used to detect BSP were not available. All Western blots were replicated once.

Primary antibody	Antibody source	1° isotype and dilution used	HRP 2° and dilution used
Anti-rat Bone Sialoprotein	Larry Fisher	IgG; Rabbit polyclonal; 1:50	Goat anti-rabbit IgG; 1:5,000 (Santa Cruz)
Anti-rat Osteopontin (P-18)	Santa Cruz Biotechnology, Inc., CA, USA	IgG; Goat polyclonal; 1:30	Rabbit anti-goat IgG 1:5,000 (Santa Cruz)
Anti-rat Osteonectin (H-14)	Santa Cruz Biotechnology, Inc., CA, USA	IgG; Goat polyclonal; 1:30	Rabbit anti-goat IgG 1:5,000 (Santa Cruz)
Osteopontin Blocking Peptide (P-18)	Santa Cruz Biotechnology, Inc., CA, USA	n/a	n/a
Osteonectin Blocking Peptide (H-14)	Santa Cruz Biotechnology, Inc., CA, USA	n/a	n/a

Table 3.2: Antibodies used in Western Blot and Their Dilutions. Also listed are the blocking peptides used as negative controls.

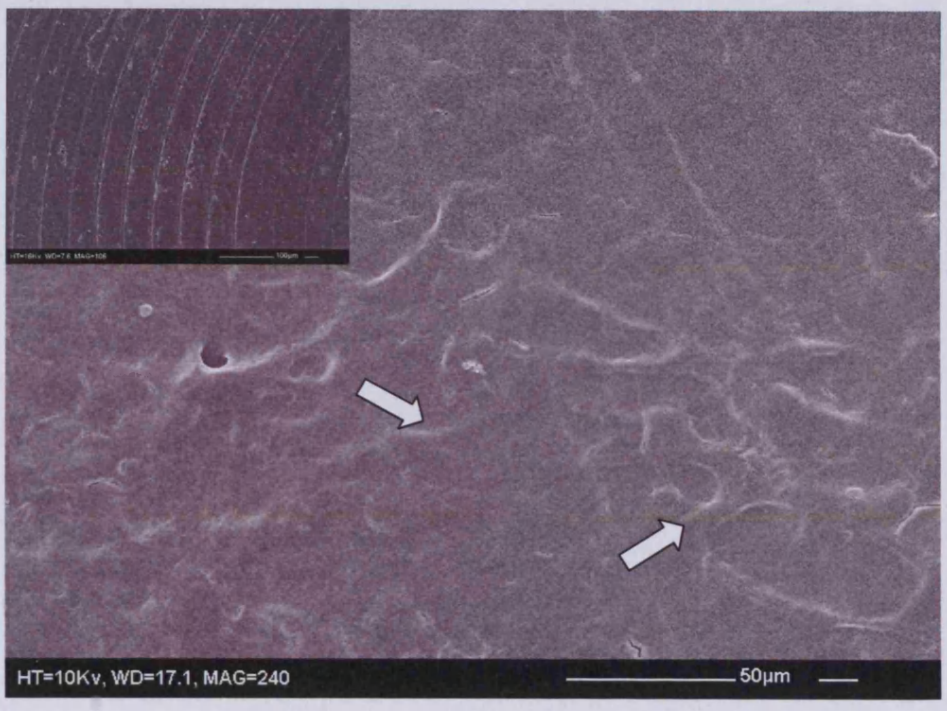

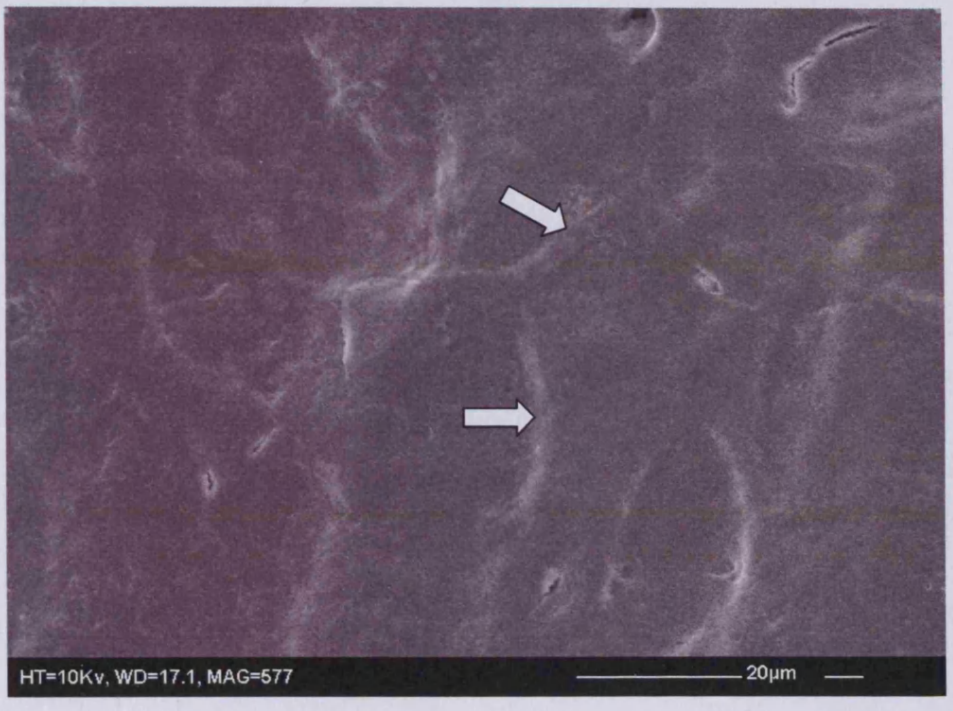

Figure 3.1: Typical SEM images of machined discs after BMSC seeding and culture for 7 days. Cells appear to be covered by a thin layer of matrix material. Examples of cells are indicated by arrows. Inset on the upper image is an SEM image of a surface with no cells seeded.

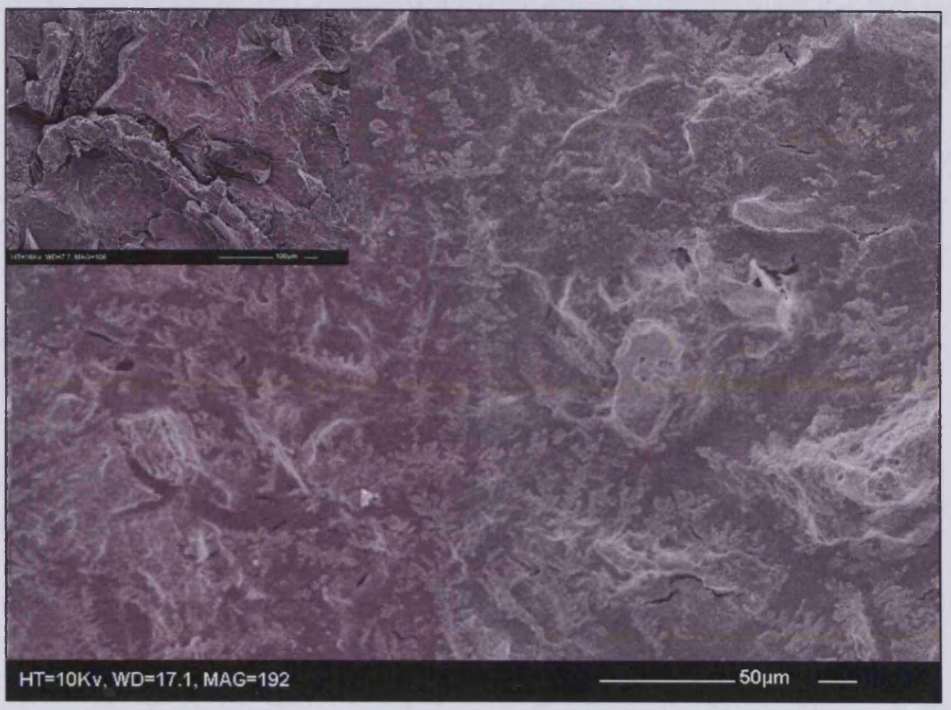

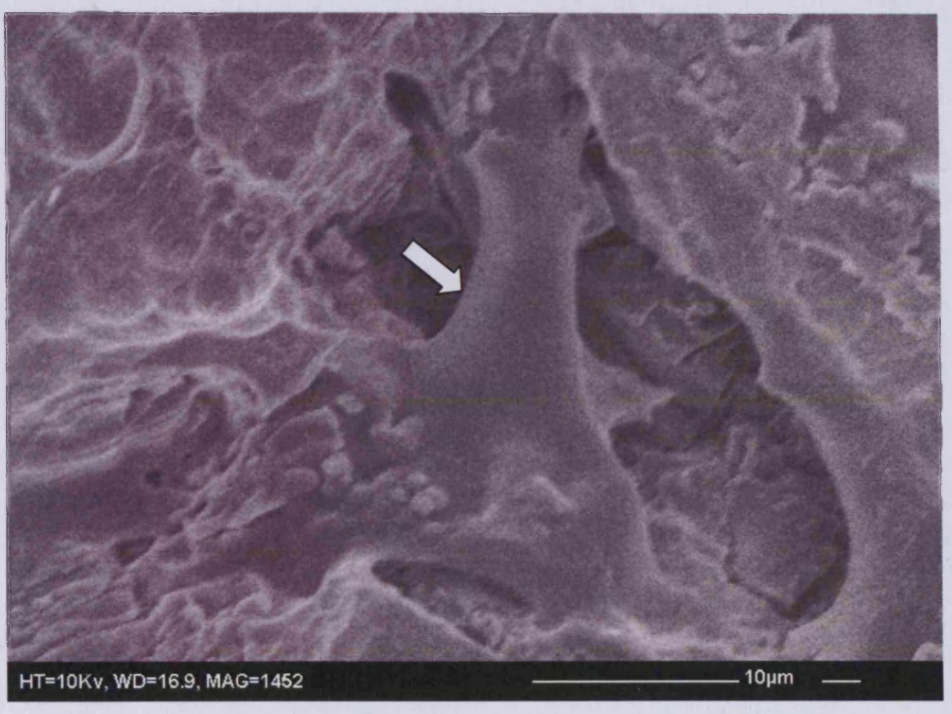

Figure 3.2: Typical SEM images of grit-blast/acid etched discs after BMSC seeding and culture for 7 days. Above, the topographical low points (or 'valleys') appear to be partially filled in with matrix material. Inset is an SEM image of a surface with no cells seeded. Below, a cell partially encased in this material, which is indicated by an arrow.

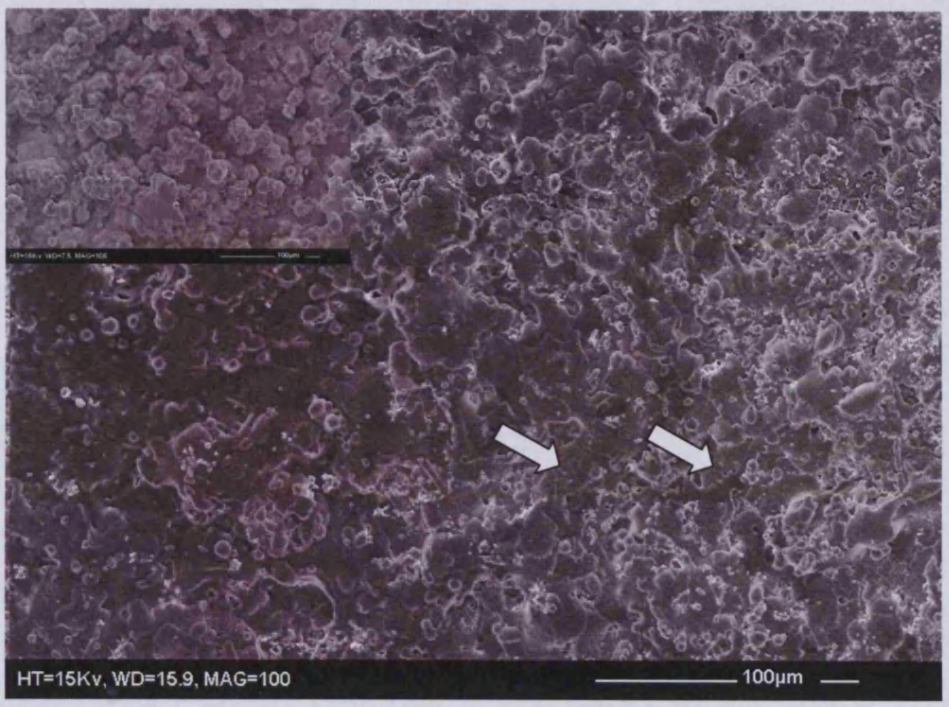

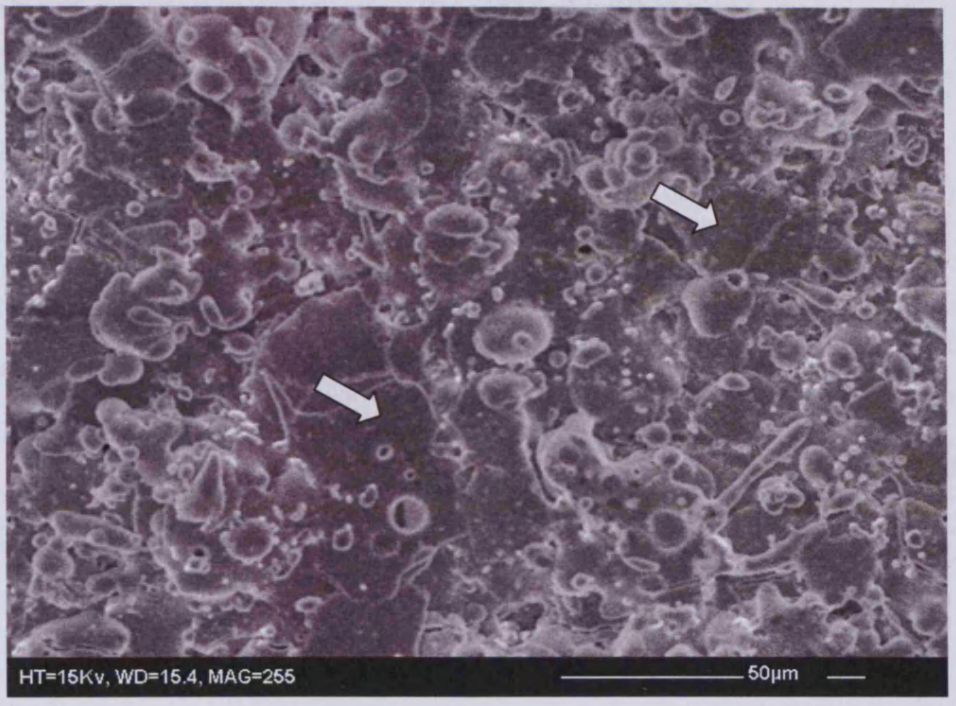

Figure 3.3: Typical SEM images of BMSCs seeded onto TCP coated discs and cultured for 7 days. Although no cells are clearly visible at the surface, matrix material is visible around the topographical features. Examples of this matrix are indicated by arrows. Inset on the upper image is an SEM image of a surface with no cells seeded.

3.3.2 Recovery of Cells from Experimental Surfaces

Figure 3.4 shows a graph of the percentage of cells recovered from the different surfaces across five post-seeding time points. Generally the initial number of cells recovered after 1 hr was very low compared to the number seeded, although this proportion increased over time on all surfaces. At all time points, the highest proportion of cells was recovered from the machined surface. There were generally not large differences between the other three experimental surfaces in terms of the proportion of cells recovered, although the initial recovery of cells 1 hr seeding was lower from the TCP coated surface relative to the other surfaces.

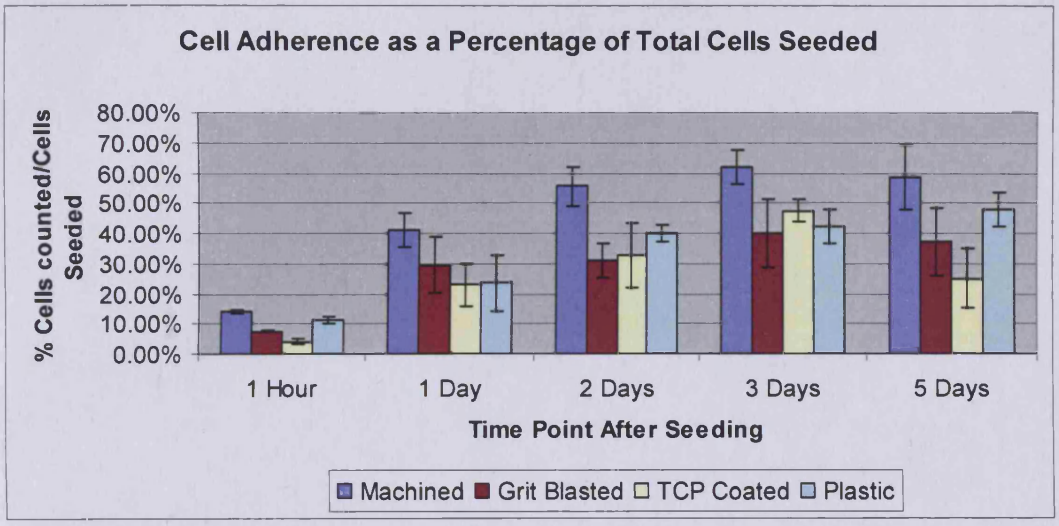

Figure 3.4: A graph showing the percentage of cells recovered at different post-seeding time points from each experimental surface. The percentage of cells recovered was based on the total number of cells seeded. The graph represents the averaged results of triplicate cultures in 2 experimental replicates. Error bars represent standard error of the mean.

3.3.3 BMSC mRNA Expression

The mRNA expression profiles at 5, 7 and 12 days post-seeding for osteoblast markers of BMSCs cultured on the experimental surfaces are shown in Figures 3.5 and 3.6. All osteoblast markers investigated were found to be strongly expressed by BMSCs on all surfaces and at all three post-seeding time points. BMSC expression of the chondrocyte markers Sox9 and Col II and the adipocyte marker pparγ across the experimental surfaces is shown in Figures 3.7 and 3.8. Bands for pparγ appeared across all surfaces at all time points, although generally they were faint. An exception to this was the band from the TCP coated surface at 5 days post-seeding which was noticeably stronger. Bands for pparγ were visibly stronger on plastic at all time points, with a particularly strong band at 12 days post-seeding. There is also a second faint band for pparγ present at all three time points on the plastic surface which does not correspond to an expected product size. This may be an artefact due to PCR machine failure, as the heating blocks were not maintaining consistent temperatures around the time the reactions from the plastic surfaces were carried out. No bands for Col II were seen from any surface at any time point. Faint bands for Sox9 were also visible across all titanium surfaces at all time points. Tables 3.3a-c and Tables 3.4a-c summarise the RT-PCR results, with '++' indicating clear strong bands, '+' indicating clear bands, 'faint' indicating barely visible bands and '–' denoting negative. Neither water controls nor RT negative controls showed any product formation, except for small bands of less than 50bp, which are likely primer-dimer.

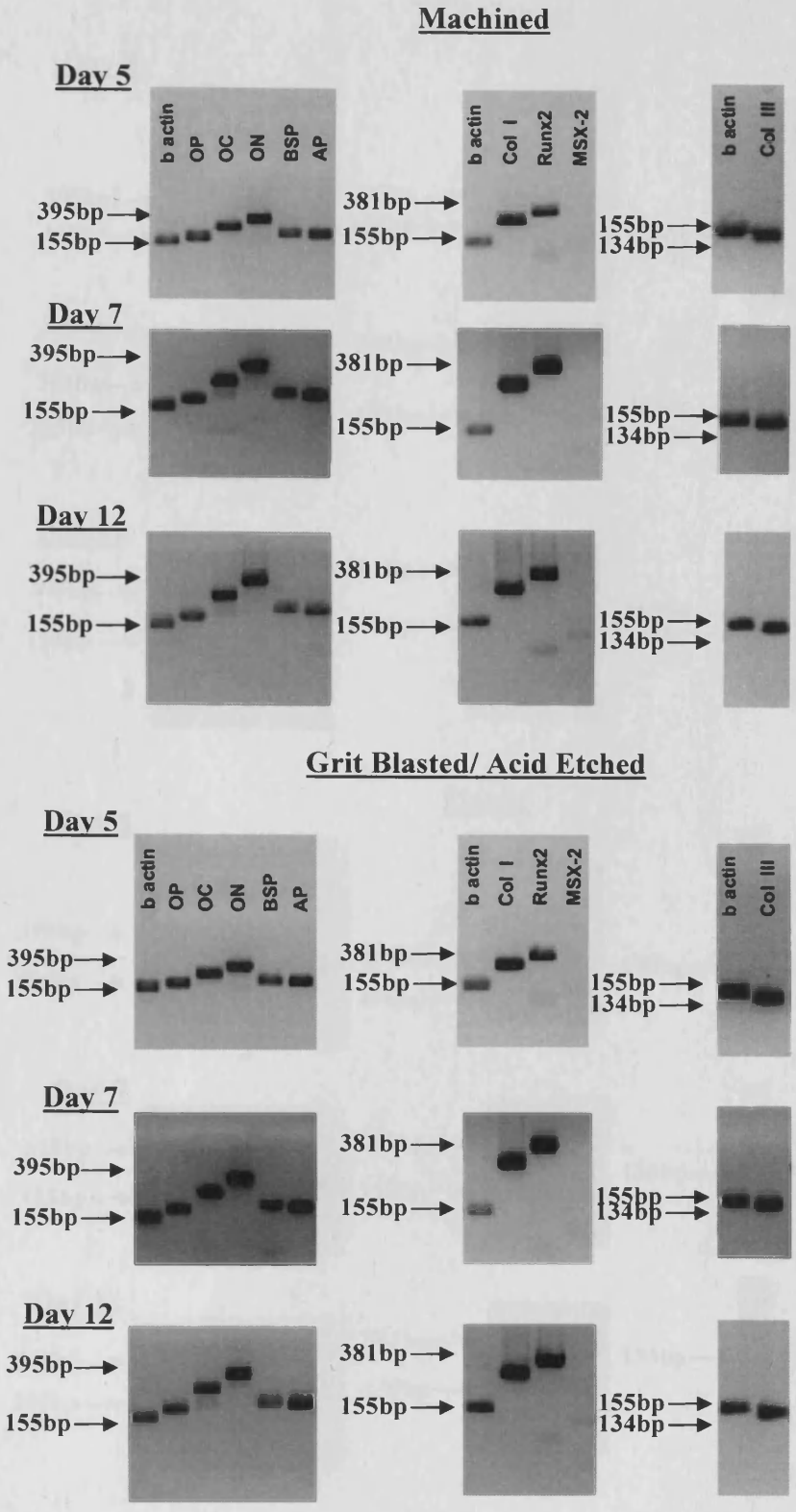

Figure 3.5: RT-PCR results showing the mRNA expression profile of BMSCs cultured on the machined and grit blasted/acid etched surfaces at different post-seeding time points. β actin was used as a house keeping gene. OP-osteopontin, OC-osteocalcin, ON-osteonectin, BSP-bone sialoprotein, AP-alkaline phosphatase, Col I-type I collagen, Col III-type III collagen. Product band sizes are estimated based on their relative position to a 100kb DNA ladder.

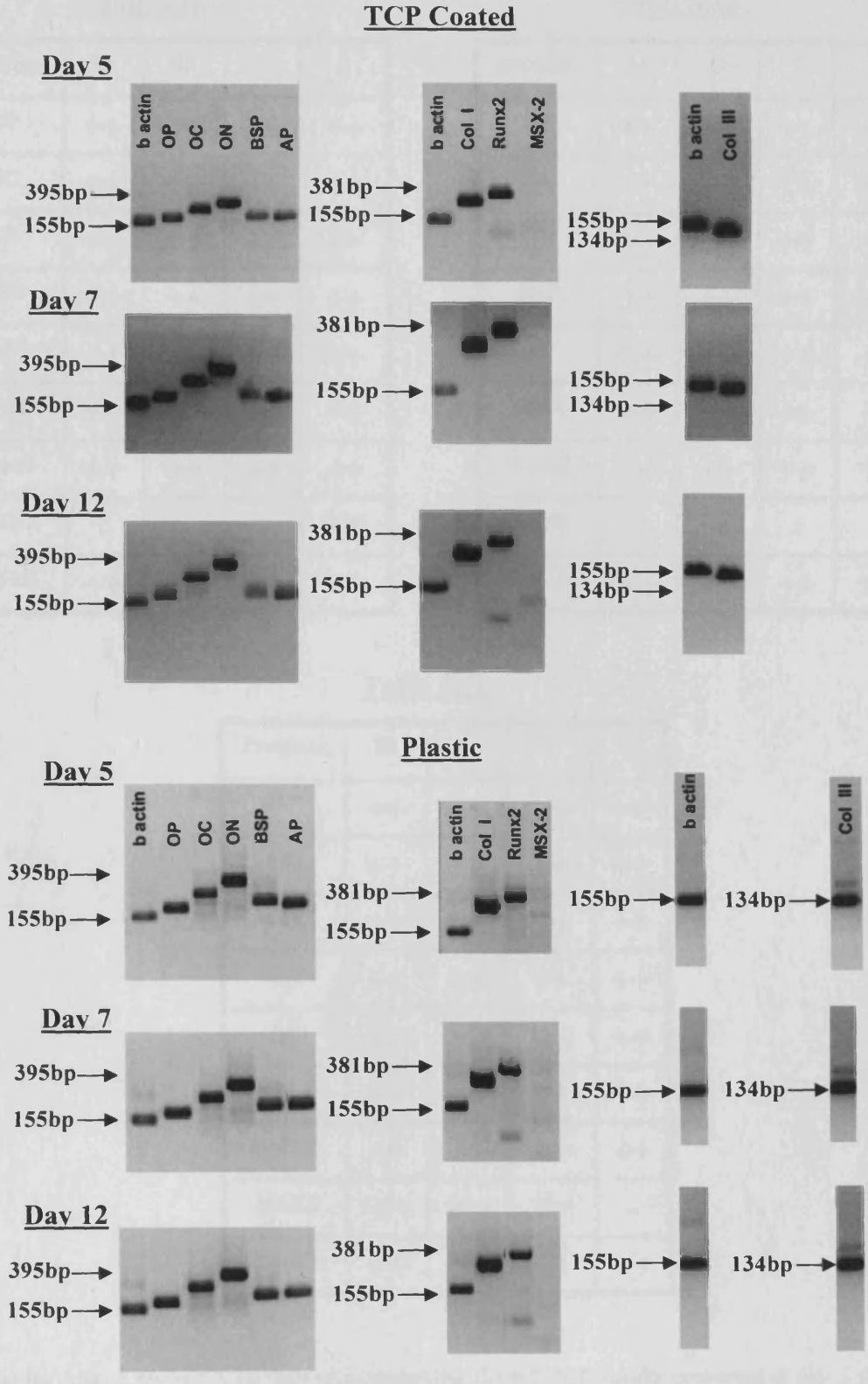

Figure 3.6: RT-PCR results showing the mRNA expression profile of BMSCs cultured on TCP coated and plastic surfaces at different post-seeding time points. β actin was used as a house keeping gene. OP-osteopontin, OC-osteocalcin, ON-osteonectin, BSP-bone sialoprotein, AP-alkaline phosphatase, Col I-type I collagen, Col III-type III collagen. Product band sizes are estimated based on their relative position to a 100kb DNA ladder.

Table 3.3a

Product	M	G	T	P
OP	++	++	++	++
OC	++	++	++	++
ON	++	++	++	++
BSP	++	++	++	++
AP	++	++	++	++
Col I	++	++	++	++
Runx2	++	++	++	++
MSX2	-	-	-	faint
Col III	++	++	++	++

Table 3.3b

Product	M	G	T	P
OP	++	++	++	++
OC	++	++	++	++
ON	++	++	++	++
BSP	++	++	++	++
AP	++	++	++	++
Col I	++	++	++	++
Runx2	++	++	++	++
MSX2	-	-	-	-
Col III	++	++	++	++

Table 3.3c

Product	M	G	T	P
OP	++	++	++	++
OC	++	++	++	++
ON	++	++	++	++
BSP	++	++	++	++
AP	++	++	++	++
Col I	++	++	++	++
Runx2	++	++	++	++
MSX2	faint	faint	faint	-
Col III	++	++	++	++

Tables 3.3a, 3.3b and 3.3c: Tables summarising the RT-PCR results presented at day 5 (**3.3a**) day 7 (**3.3b**) and day 12 (**3.3c**) post-seeding time points. M-machined, G-grit blasted/acid etched, T-TCP coated, P-Plastic, OP-osteopontin, OC-osteocalcin, ON-osteonectin, BSP-bone sialoprotein, AP-alkaline phosphatase, Col I-type I collagen, Col III-type III collagen. '++' indicates clear strong bands, '+' indicates clear bands, 'faint' indicates barely visible bands and '–' denotes no band.

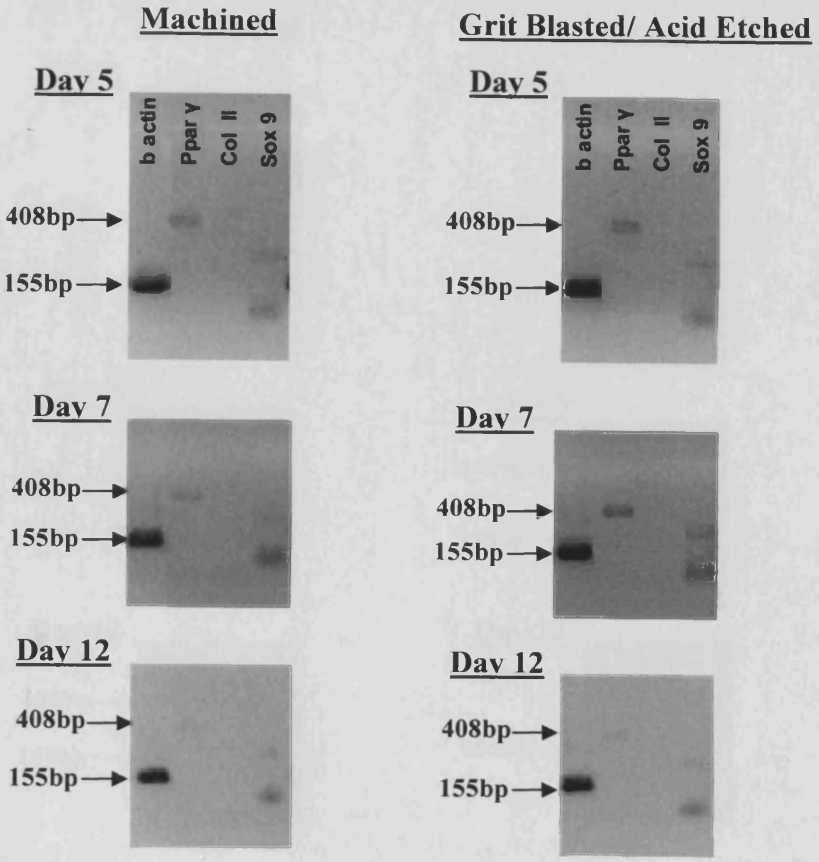

Figure 3.7: RT-PCR results showing an mRNA expression profile of BMSCs cultured on the machined and grit blasted/acid etched surfaces at different post-seeding time points. β actin was used as a house keeping gene. Col II-type II collagen. Product band sizes are estimated based on their relative position to a 100kb DNA ladder.

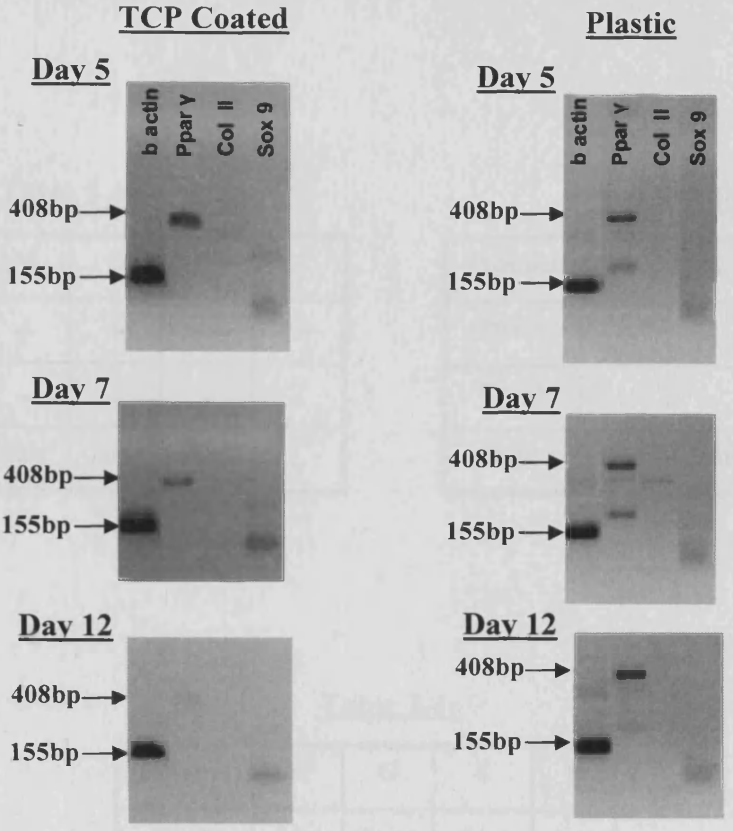

Figure 3.8: RT-PCR results showing an mRNA expression profile of BMSCs cultured on the TCP coated and plastic surfaces at different post-seeding time points. β actin was used as a house keeping gene. Col II-type II collagen. Product band sizes are estimated based on their relative position to a 100kb DNA ladder.

Table 3.4a

Product	M	G	T	P
Pparγ	+	+	++	++
Col II	-	-	-	-
Sox9	faint	faint	faint	-

Table 3.4b

Product	M	G	T	P
Pparγ	+	+	+	++
Col II	-	-	-	-
Sox9	faint	faint	faint	-

Table 3.4c

Product	M	G	T	P
Pparγ	faint	faint	faint	++
Col II	-	-	-	-
Sox9	faint	faint	faint	+

Tables 3.4a, 3.4b and 3.4c: Tables summarising the RT-PCR results presented at day 5 (**3.4a**) day 7 (**3.4b**) and day 12 (**3.4c**) post-seeding time points. M-machined, G-grit blasted/acid etched, T-TCP coated, P-Plastic, Col II-type II collagen. '++' indicates clear strong bands, '+' indicates clear bands, 'faint' indicates barely visible bands and '–' denotes no band.

3.3.4 Protein Expression Profiles of BMSCs

Western blots showing the protein expression profile of BMSCs cultured on the experimental surfaces for 5 and 12 days post-seeding are shown in Figures 3.9 and 3.10. In Figure 3.9, bands indicating the expression of BSP were seen across all surfaces at both time points with the exception of the plastic surface at 5 days post seeding. Figure 3.9 also shows that OP was expressed on the machined and plastic surfaces at 12 days post-seeding and to a lesser extent on grit-blasted/acid etched surface at the same time point. There are a large number of OP degradation products visible. ON, shown in Figure 3.10 had a similar expression pattern, with the machined and plastic surfaces having a relatively high level of expression at 12 days post-seeding, with a much lower level of expression seen on the grit blasted/acid etched surface at the same time point. Figure 3.11 shows the negative control blots, where the primary antibody was pre-incubated with a blocking peptide. No immuno-reactivity was detected in either negative control.

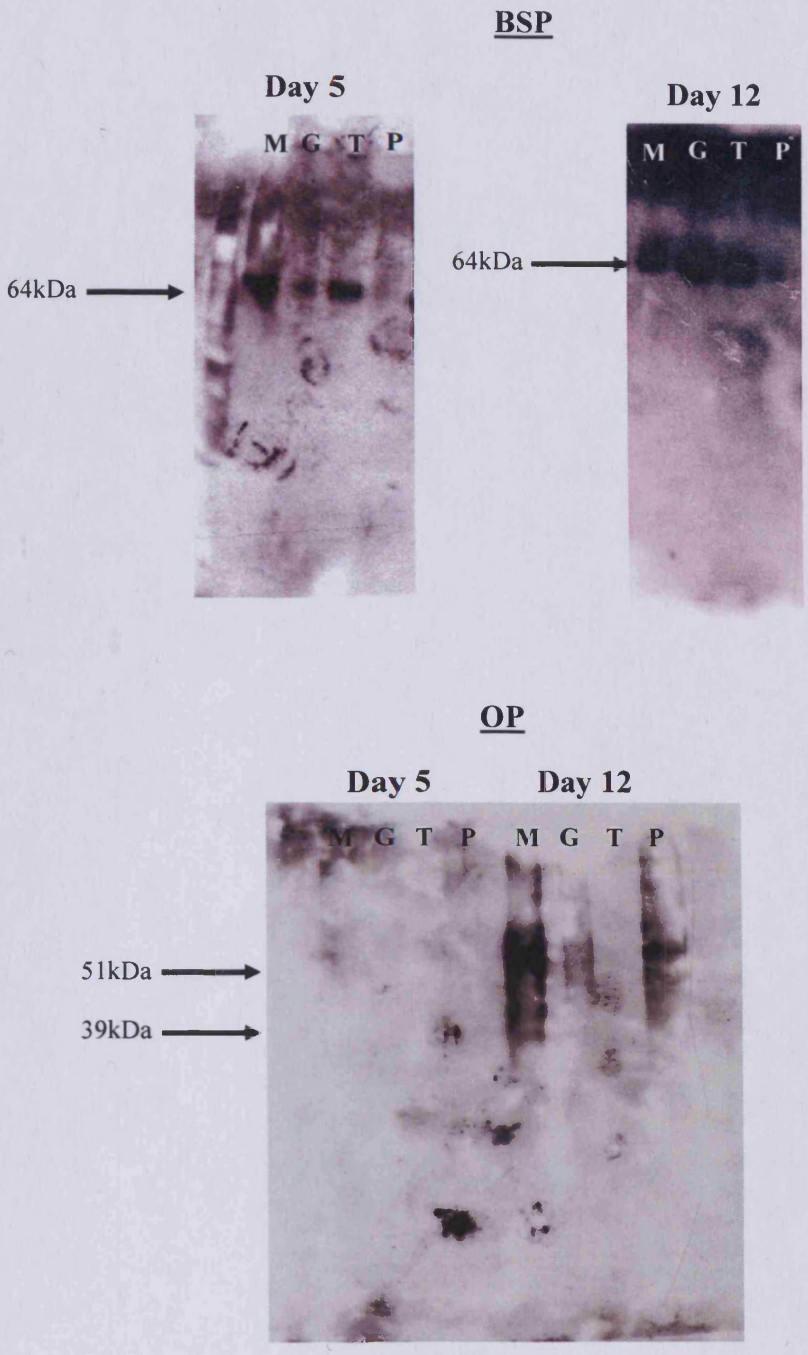

Figure 3.9: Western blot results showing the expression of bone sialoprotein and osteopontin by BMSCs grown on different surfaces at 5 and 12 day post-seeding time points.

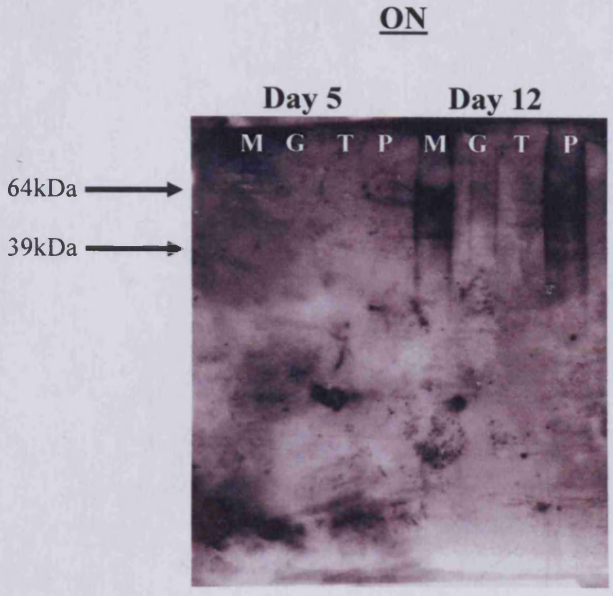

Figure 3.10: Western blot results showing the expression of osteonectin by BMSCs grown on different surfaces at 5 and 12 day post-seeding time points.

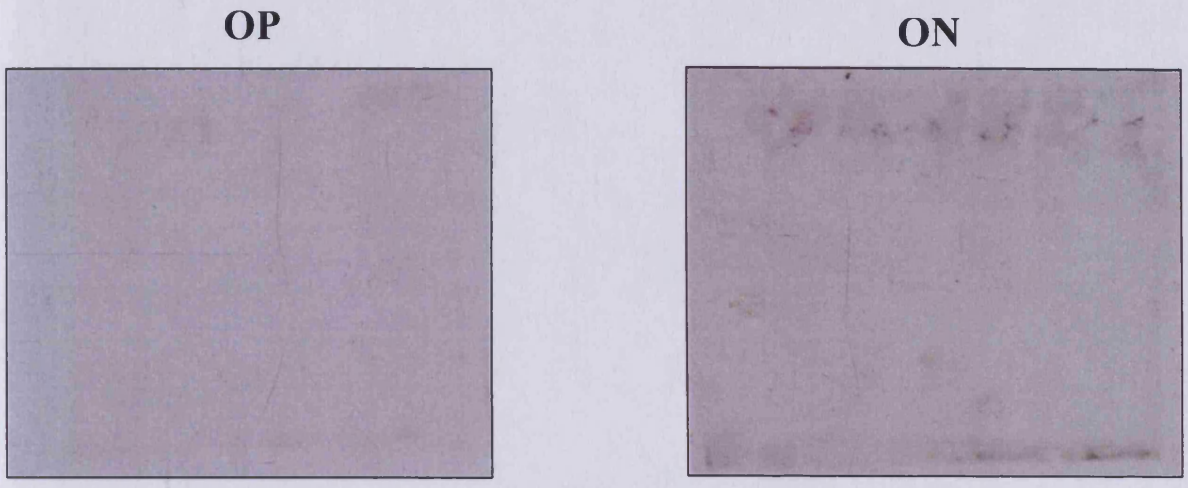

Figure 3.11: Negative controls for Western blots, in which the primary antibody was incubated with a blocking peptide prior to use in the blot. OP-osteopontin, ON-osteonectin.

3.4 Discussion

The results of this chapter have shown that cultured BMSCs attach to all experimental surfaces. It is also interesting to note that the mRNA expression profiles of cells across all surfaces were highly similar, suggesting that the cellular activity at the transcriptional level remained largely unchanged regardless of the surface the cells were cultured on. Titanium, regardless of the surface treatment, also appeared to promote osteoblast over adipocyte differentiation by suppressing the expression of pparγ mRNA compared to a plastic control. At the level of protein secretion, surface treatment did appear to have an influence on cellular activity, as BMSCs cultured on the TCP coating showed variations in the matrix, which may influence the osseointegrative potential of this surface treatment. The patterns of matrix deposition may have been influenced by the surface topography, with the rougher grit blast/acid etched and TCP coated surfaces producing a thicker layer in apposition to the matrix than the machined surface. This could result in better mechanical interlocking and is therefore of critical important when considering the osseointegrative potential of a surface.

From the cell recovery at 1 hr post-seeding, it is a possibility that the machined surface had the highest rate of initial cell attachment. In contrast, the TCP coated surface, which was also the roughest of the experimental surfaces, had the lowest rate of initial attachment, which may have significant consequences for the osseointegrative potential of this surface treatment. The proportion of cells recovered from all experimental surfaces generally increased over time, demonstrating that all of the experimental surfaces were capable of supporting adherent BMSC populations. Interestingly however, the highest proportion of cells was recovered from the machined surface at all post-seeding time points, indicating that it may be this surface which most favours cell expansion over time. BMSCs cultured on the rougher grit blasted/acid etched and TCP coated surfaces, along with the plastic control, had a lower proportional recovery over time. This trend may indicate that smoother titanium surfaces are more favourable to the attachment of osteoblast progenitor cells, which has been widely reported in the literature (Bachle and Kohal

2004; Kieswetter et al. 1996b; Kim et al. 2006; Mustafa et al. 2001). Alternately, cells could simply be more difficult to recover from the rougher surfaces, as cells adherent within the topographical features would be less accessible to the Accutase. Further, cells on these surfaces, having encased themselves in matrix, may have undergone apoptosis. It is therefore difficult to interpret these results in terms of the functional osseointegrative potential of each surface, as they are simply a measure of how many cells were available for recovery from each surface over time as opposed to an assessment of their ability to induce and sustain matrix production.

The desire to assess the functional ability of each experimental surface to support the production of osteoid matrix, and therefore the process of osseointegration, was the primary motivation for carrying out mRNA expression profiles for BMSCs grown on them. Interestingly, the expression profiles of BMSCs from all experimental surfaces had a very high degree of similarity. It is clear from the results that all surfaces are capable of supporting a population of cells which express mRNA for a wide range of osteoblast markers. This is well supported in the literature, with a range of modified titanium surfaces having been shown to support osteoblast differentiation (Balloni et al. 2009; Marinucci et al. 2006; Masaki et al. 2005; Ponader et al. 2008; Qu et al. 2007; Schneider et al. 2003; Tsukimura et al. 2008). As RT-PCR is at best a semi-quantitative method, it is impossible to comment directly on the absolute levels of mRNA expression between the different titanium surfaces, however the results do show that osteoblast markers are clearly expressed by BMSCs cultured on all of the surfaces, while chondrocyte and adipocyte markers generally had low levels of expression. Using quantitative PCR to directly measure the differences in the levels of mRNA expression between cells cultured on the different experimental surfaces would have allowed more subtle differences in cell activity that could not be detected using the methods employed here to be clarified. The drawback to such methodology is the cost and time involved; rarely is it possible to examine a broad range of markers using quantitative PCR. Rather it would be useful to examine several key indicators of osseointegrative activity and examine them in more detail using this technique

BMSCs cultured on all surfaces were also found to weakly express pparγ and Sox 9, which may be the result of residual mRNA copies for these markers initially present in cells, despite the BMSCs apparently being primarily switched to an osteoblast cell type. The noticeably stronger expression of pparγ by BMSCs cultured on the plastic surface is noteworthy, as it may indicate that titanium surfaces, no matter their surface treatment, promote differentiation down the osteoblast lineage, as opposed to the adipocyte lineage. In fact, at 12 days post-seeding, there are only strong, clear pparγ product bands from the plastic surface, which may indicate that osteoblast differentiation is better supported by the titanium surfaces compared to the plastic control over time. These results would have no doubt been strengthened by the addition of a positive control, such RNA from an chondrocyte cell line, which could have confirmed any negative findings, for example in the case of Sox 9.

There are conflicting accounts in the literature regarding the influence of surface characteristics on osteoblast gene expression. Using quantitative PCR, Ponader et al (2008) found no differences in the expression of OC, BSP, AP or Col I by human osteoblasts grown on a smooth machined surface and a number of surfaces highly roughened by electron beam. This is in contrast to other groups using quantitative PCR, which have found alterations in the expression of osteoblast markers in cells grown on variously modified titanium surfaces (Masaki et al. 2005; Schneider et al. 2003). Similarly, there have been many reports of osteoblast marker expression being influenced by the modification of titanium surfaces using semi-quantitative comparison of RT-PCR product band intensities (Balloni et al. 2009; Marinucci et al. 2006; Qu et al. 2007; Tsukimura et al. 2008). On the whole, the results presented in this chapter would tend to support the position that alterations in the titanium surface do not substantially influence the mRNA expression of BMSCs.

Based on the Western blot results presented, it is apparent that there are some differences in the composition of the matrix produced by cells cultured on the experimental surfaces, despite BMSCs cultured on these surfaces having a broadly similar mRNA expression profiles. The cells on the TCP coated surface appeared to express only BSP, demonstrating that cells cultured on this surface produce the least 'complete' matrix after 12 days. It appears that cells grown on the experimental

titanium surfaces are influenced in terms of the secretion of non-collagenous matrix proteins. This finding may indicate that the TCP coated surface is the least favourable for osseointegration. Equally, the weaker expression of ON and OP on the grit blast/acid etched surface compared to the machined and plastic surfaces may indicate a reduced osseointegrative potential. It has, however, been reported in the literature that there are different possible compositions of bone, each containing a unique mix of non collagenous proteins. Trabecular bone for example, has been found to contain substantially higher levels of osteonectin than cortical bone, while cortical bone contains a higher proportion of osteocalcin (Ninomiya et al. 1990). The precise functions of these non-collagenous matrix proteins are poorly understood, especially in terms of their relative contribution to the mechanical function of bone (Gorski 1998; Ninomiya et al. 1990). Therefore, while it could be assumed that an ideal bone matrix would contain all of the non-collagenous matrix proteins, it is somewhat difficult to speculate as to what an optimal ratio for their occurrence would be or to categorically state that the matrix produced by BMSCs grown on the TCP coated surface is inferior.

Differences in the structure of the matrix depositions by BMSCs cultured on the different experimental surfaces are obvious from the SEM images. On the machined surface, the BMSCs appear to have distributed themselves evenly over the surface prior to synthesizing a thin sheet of matrix material. In contrast, BMSCs cultured on the grit blasted/acid etched and TCP surfaces appear to have migrated into the 'valleys' created by the alterations to surface topography and filled them with matrix material, resulting in a thicker layer of matrix material in apposition to the titanium surface. It has been widely reported in the literature that implants with rougher surfaces have higher rates of osseointegration *in vivo* (Al-Nawas et al. 2008; Buser et al. 2004; Buser et al. 1991; Franchi et al. 2007; Gotfredsen et al. 1995). This may be attributed to surface roughening creating a greater surface area in opposition to bone, which in turn causes higher bone matrix apposition to the surface (Cooper 2000; Le Guéhennec et al. 2007). Based on the observed patterns of matrix deposition, it is a possibility that the thin later of matrix in direct apposition to the machined titanium surface would show a lesser degree of mechanical interlocking with surrounding bone compared that allowed by the in-filling of topographical

features on the grit blasted/acid etched surface and the TCP coated surface. This higher potential for mechanical interlocking may result in better osseointegrative potential *in vivo* for the roughened surfaces, despite the observed similarity in influence the experimental surface treatments had on BMSC activity *in vitro*.

An intriguing possibility raised by this work is that surface treatments may exert an influence over osseointegration by their mechanical interaction with bone as a tissue, rather than influencing osteoblast differentiation directly on a cellular level. Due to the complexities inherent in the process of bone formation and the diverse factors which can influence this process however, it is likely that *in vivo* investigations, described in Chapters 5 and 6, will be of use in further understanding the ways in which titanium surface treatments affect the process of osseointegration.

Chapter 4: The Effects of Modified Titanium Surfaces on the Expression of Inflammatory Cytokines and Control of Bone Resorption

4.1 Introduction

The process of inflammation, and the cytokines which mediate it, play an important role in the osseointegration of titanium dental implants. Placement of a titanium implant results in an initial trauma and local tissue damage, leading directly to the release of a cascade of pro-inflammatory cytokines (Davies 2003; Hughes et al. 2006; Le Guéhennec et al. 2007). In particular, the inflammatory cytokines interleukin 1-β (IL-1β), tumour necrosis factor α (TNFα) and interleukin 6 (IL-6) are well known to influence the process of bone formation (Bellido et al. 1997; Boyce et al. 1989; Erices et al. 2002; Gowen et al. 1988; Hanazawa et al. 1986; Hughes et al. 2006; Nanes 2003). These inflammatory mediators function synergistically to influence the process of osseointegration at different levels, from mediating osteoblast differentiation and bone matrix production, to controlling bone remodelling through the modulation of osteoclast function. Similarly, a variety of growth factors are also heavily involved in the regulation of osteoblast differentiation and function, an important example being TGFβ1 (Centrella et al. 1994; Hughes et al. 2006; Robey et al. 1987). It is therefore relevant to examine the potential influence of variously modified titanium surfaces on the production and activity of these factors, as surfaces which minimize the expression of inflammatory mediators while maximizing the expression of pro-osteogenic factors would be favourable for osseointegration.

The inflammatory response in the context of treatment with dental implants is complex and at times apparently contradictory. On one hand, acute phase inflammation in response to the initial placement of an implant is not only unavoidable, but is also necessary for the stimulation of the bone repair process (Davies 2003; Hughes et al. 2006; Le Guéhennec et al. 2007). Conversely, if

expression of inflammatory cytokines persists around the implant site it causes a number of deleterious effects, leading to a general delay in the healing process, increasing the risk of fibrous encapsulation and, ultimately, stimulation of bone resorption by osteoclasts (Boyle et al. 2003; Davies 2003; Hughes et al. 2006; Le Guéhennec et al. 2007). While the initial inflammatory response is a crucial step in the process of bone repair, a prolonged one is highly deleterious to it. Inflammation is a complex and many aspects of it, particularly the processes by which it is regulated, are poorly understood. It is clear however, that a delicate and tightly controlled balance is required for rapid and complete bone healing and therefore optimal osseointegration of titanium implants.

The cytokines involved in the inflammatory response are multifunctional and have a variety of roles depending on the context of their expression. Specifically, their roles in and effects on the healing process are dependant on when in this processes they are expressed, and also on the concurrent expression of other cytokines. For example, IL-1 has been variously shown to inhibit osteoblast production of bone matrix (Stashenko et al. 1987), increase osteoblast progenitor proliferation and differentiation (Lange et al. 2009) and to increase bone mineralization (Ding et al. 2009). TNFα, in contrast, has a broadly suppressive effect on osteoblast proliferation, differentiation and production of matrix components (Abbas et al. 2003; Gowen et al. 1988; Rosenquist et al. 1996). Relatively little is known about the functions of IL-6, although it is thought to inhibit osteoblast proliferation, whilst stimulating differentiation in the presence of its soluble receptor (Bellido et al. 1997; Erices et al. 2002; Iwasaki et al. 2008). The regulation of these cytokines is equally complex. IL-1β, for example, is a key regulator of the inflammatory process and is known to modulate osteoblast production of TNFα and IL-6 (Hughes et al. 2006; Ishimi et al. 1990; Wei et al. 2005). Inflammatory cytokines present around an implant site may not only exert direct effects on the surrounding tissues, but also influence the process of bone repair indirectly through the modulation of other cytokines, adding to the overall complexity of the situation.

Another crucial way in which inflammatory cytokines exert control over the process of osseointegration is through the control of osteoclast activity, and therefore

bone resorption. IL-1β, TNFα and IL-6 can all upregulate osteoblast expression of RANKL, leading to a potent stimulation of bone resorption through RANKL/RANK mediated osteoclast activation (Boyle et al. 2003; Hsu et al. 1999; Lerner 2004; O'Brien et al. 2000; Teitelbaum 2000). IL-1β and TNFα also influence the negative feedback control of osteoclast activation by stimulating osteoblast production of OPG, which competitively binds to RANKL, preventing it from activating RANK (Brandstrom et al. 1998; Vidal et al. 1998). These inflammatory cytokines are intimately involved in the maintenance of a RANKL/OPG ratio which directly regulates bone resorption. As the control of bone resorption has obvious implications to the osseointegration of dental implants, it is critical that any investigation into the influence of surface modification on osteoblast activity considers its impact on the expression of both the inflammatory mediators and signalling molecules involved.

As bone healing progresses, the initial inflammation around the implant site is resolved and the process of bone repair commences under the direction of a variety of growth factors. One such growth factor, TGFβ1, is a crucial component of a complex regulatory cascade which is involved in the initial recruitment of osteoblast progenitor cells (Centrella et al. 1994; Hughes et al. 2006; Janssens et al. 2005). The specific activity of TGFβ1 is contextual and may vary based on its ratio of expression with other growth factors, but it has been found to specifically drive the early phases of the osteoblast differentiation pathway, particularly in terms of driving the proliferation of osteoblast progenitor cells (Centrella et al. 1994). Additionally, TGFβ1 enhances OPG expression, making it an inhibitor of osteoclast activation and therefore bone resorption (Boyle et al. 2003). TGFβ1 has also been reported to suppress the TNFα potentiated production of IFNγ by dendritic precursor cells (Koutoulaki et al. 2010), suggesting that it may have anti-inflammatory properties, although IFNγ may also suppress the formation of osteoclasts, complicating the issue (Xu et al. 2010). The effects of surface modifications on the production of TGFβ1 by osteoblasts is therefore of interest in investigating favourable conditions for the osseointegration of dental implants.

It is clearly important to consider the influence of surface modification on the inflammatory process, due to the wide ranging impact it has on osteoblast

differentiation and activity and its direct mediation of bone resorption. In this chapter therefore, the same *in vitro* model used in the previous chapter, to investigate BMSC expression of osteoblast markers on the different experimental surfaces, will be employed to investigate the expression of several inflammatory cytokines at both the mRNA and protein level. Additionally, due to the involvement of osteoblasts in the regulation of osteoclast activity and the obvious relevance of this to the process of osseointegration, the expression of RANKL and OPG mRNA will be considered. TGFβ1 mRNA expression will also be investigated, due to its central role in the regulation of the osteoblast differentiation pathway, its role in the inhibition of osteoclast activation and its possible anti-inflammatory properties. Investigating the expression of these elements by osteoblasts cultured on the experimental surfaces aims to give a clearer understanding of how these surface modifications may affect the process of osseointegration.

4.2 Materials and Methods

4.2.1 Bone Marrow Stromal Cell (BMSC) Isolation and Culture on Titanium Surfaces

BMSCs were extracted from rat femurs and cultured on the experimental surfaces as described in section 3.2.1.1.

4.2.2 BMSC mRNA Expression Profiles on Experimental Surfaces

The mRNA expression of the inflammatory cytokines IL-1β, TNFα, and IL-6, the osteoclast regulatory elements OPG and RankL and the growth factor TGFβ1 by BMSCs grown on the experimental titanium surfaces and plastic controls were investigated using RT-PCR. mRNA was extracted at 5, 7 and 12 days post-seeding as described in section 3.2.4.1. Quantification of mRNA and RT-PCR reactions were carried out as described in sections 3.2.4.2, 3.2.4.3 and 3.2.4.4 respectively. Information about the primers used in the PCR reactions is given in Table 4.1.

Primer	Sequences 5'-3'	Product Size	Reference
IL-1β	F:GACAGAACATAAGCCAACAAG R:GTCAACTATGTCCCGACCATT	335bp	(Wheeler et al. 2000)
TNFα	F:TACTGAACTTCGGGGTGATTGGTCC R:CAGCCTTGTCCCTTGAAGAGAACC	295bp	(Nadeau et al. 1995)
IL-6	F:CAAGAGACTTCCAGCCAGTTGC R:TTGCCGAGTAGACCTCATAGTGACC	614bp	(Nadeau et al. 1995)
OPG	F:TGGCACACGAGTGATGAATGCG R:GCTGGAAAGTTTGCTCTTGCG	538bp	(Myers et al. 1999)
RankL	F:ACGCAGATTTGCAGGACTCGAC R:TTCGTGCTCCCTCCTTTCATC	493bp	(Myers et al. 1999)
TGFβ1	F:AAGAAGTCACCCGCGTGCTA R:GGCACTGCTTCCCGAATG	118bp	(Gurantz et al. 2005)
β-Actin	F:TGAAGATCAAGATCATTGCTCCTCC R:CTAGAAGCATTTGCGGTGGACGATG	155bp	(Gatto et al. 2008)

Table 4.1: A list of all primer sequences used in PCR reactions. A primer Blast search was run on each primer sequence in order to ensure specificity for the intended amplification targets B-Actin was used as a housekeeping gene.

4.2.3 Visualisation of PCR Products

PCR products were visualised by running on ethidium bromide impregnated agarose gels as described in section 3.2.5.1. Gel images were captured as described in section 3.2.5.2.

4.2.4 Detection of BMSC Expression of IL-1β and TNFα by ELISA

The level of IL-1β and TNFα synthesis was measured by enzyme-linked immunosorbent assay (ELISA). Media supernatants were collected from cultures of BMSCs grown on the experimental surfaces for 5, 7, and 12 days after seeding. Commercial ELISA Development Kits (Peprotech, NJ, USA) were used. These kits contain capture antibodies specific to the protein being investigated, biotinylated detection antibodies, avidin-HRP, and standards which are comprised of a fixed amount of the protein of interest.

4.2.4.1 Collection of Culture Supernatants

Culture supernatants were collected by pipette from the BMSC cultures on the experimental titanium surfaces and plastic controls at 5, 7 and 12 days post-seeding. Collected supernatants were frozen at -20°C until required.

4.2.4.2 ELISA Plate Preparation

96-well plates (Fisher Scientific) were coated with the appropriate capture antibody diluted to 2μg/mL with a diluent buffer containing 0.05% v/v Tween-20 and 0.01% w/v BSA in TBS and incubated overnight at room temperature. Wells were then washed 4x with wash buffer (0.05% v/v Tween-20 in TBS). In order to

minimize non specific binding, plates were blocked for 1 hr with blocking buffer (1% w/v BSA in TBS). Plates were once again washed 4x in wash buffer.

4.2.4.3 ELISA Standard Preparation

Standards for ELISAs were prepared by diluting the appropriate supplied protein standards in a range from 3ng/mL to 0.05ng/mL using 2 fold dilutions with diluent buffer. 100µl of each standard concentration were added in triplicate to each coated ELISA plate. Triplicate wells containing only diluent buffer were used as a zero.

4.2.4.4 ELISA

100µl of each collected supernatant sample were added in triplicate to coated plates and incubated for 2 hrs at room temperature. Plates were then washed 4x with wash buffer, before 100µl of biotinylated detection antibody diluted to 0.5µg/mL in diluent buffer were added to each well. Plates were incubated for 2 hrs at room temperature before 4 further washes in wash buffer. 100µl of avidin-HRP diluted 1:2,000 with diluent buffer was added to each well and incubated for 30 mins at room temperature, prior to a final 4 washes in wash buffer. SureBlue™ TMB (Insight Biotechnology, Wembley, UK) was used as a peroxidase substrate and 50µl was added to each well prior to a 30 min incubation at room temperature. The peroxidase reaction was stopped using 50µl TMB stop solution (Insight Biotechnology). Experiments were performed in duplicate.

4.2.4.5 ELISA Signal Detection and Quantification

ELISA plate absorbance was read at 405nm on a Microplate™ reader (BioTek Instruments Limited). A best fit line through the standard curve generated by the absorbance values of the standards allowed the concentration of IL-1β or TNFα in the collected supernatant samples to be determined.

4.3 Results

4.3.1 BMSC mRNA Expression

The mRNA expression profile at 5, 7 and 12 days post-seeding of BMSCs cultured on the experimental surfaces is shown in Figure 4.1. RANKL was only found to be faintly expressed by cells cultured on the grit blasted/ acid etched surface at the 12 day post-seeding time point. Faint OPG bands were seen from all titanium surfaces at 5 days-post seeding, while the band from the plastic surface at this time point was much stronger. Strong bands for OPG were visible from all surfaces at 7 and 12 days post-seeding. IL-1β appeared to be expressed only by BMSCs cultured on the plastic surface. Bands indicating TNFα expression were seen from cells cultured on all surfaces, although were faint from the titanium surfaces at 5 days-post seeding, in contrast to the strong band seen from the plastic surface, which remains at days 7 and 12 post-seeding. BMSCs cultured on the machined and grit blasted/acid etched surface showed increasing expression of TNFα over days 7 and 12 post-seeding, while BMSCS on the TCP coated surface showed a uniformly weak expression over these time points. Very faint bands for IL-6 were visible from BMSCs cultured on all surfaces at all time points, except for the TCP coated surface from which no bands are seen.TGFβ1 expression was seen from BMSCs cultured on every surface at every time point. Tables 4.2a-c summarise the RT-PCR results, with '++' indicating clear strong bands, '+' indicating clear bands, 'faint' indicating barely visible bands and '-' denoting negative. Neither water controls nor RT negative controls showed any product formation, except for small bands of less than 50bp, which are likely primer-dimer.

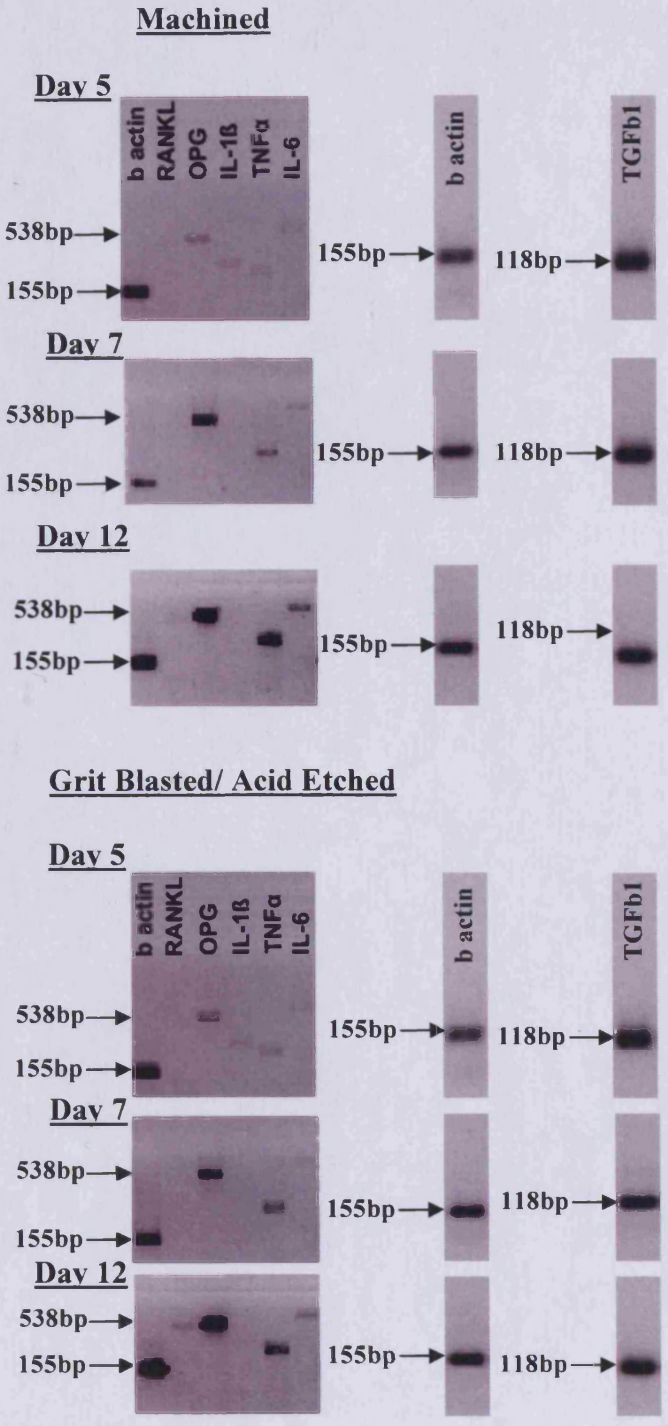

Figure 4.1: RT-PCR results showing an mRNA expression profile of BMSCs cultured on the machined and grit blasted/acid etched surfaces at the different post-seeding time points. β actin was used as a house keeping gene. RANKL - Rank ligand, OPG - Osteoprotegerin, IL-1β - Interleukin 1β, TNFα – Tumour Necrosis Factor α, IL-6 - Interleukin 6, TGFb1- Transforming Growth Factor β1. Product band sizes are estimated based on their relative position to a 100kb DNA ladder.

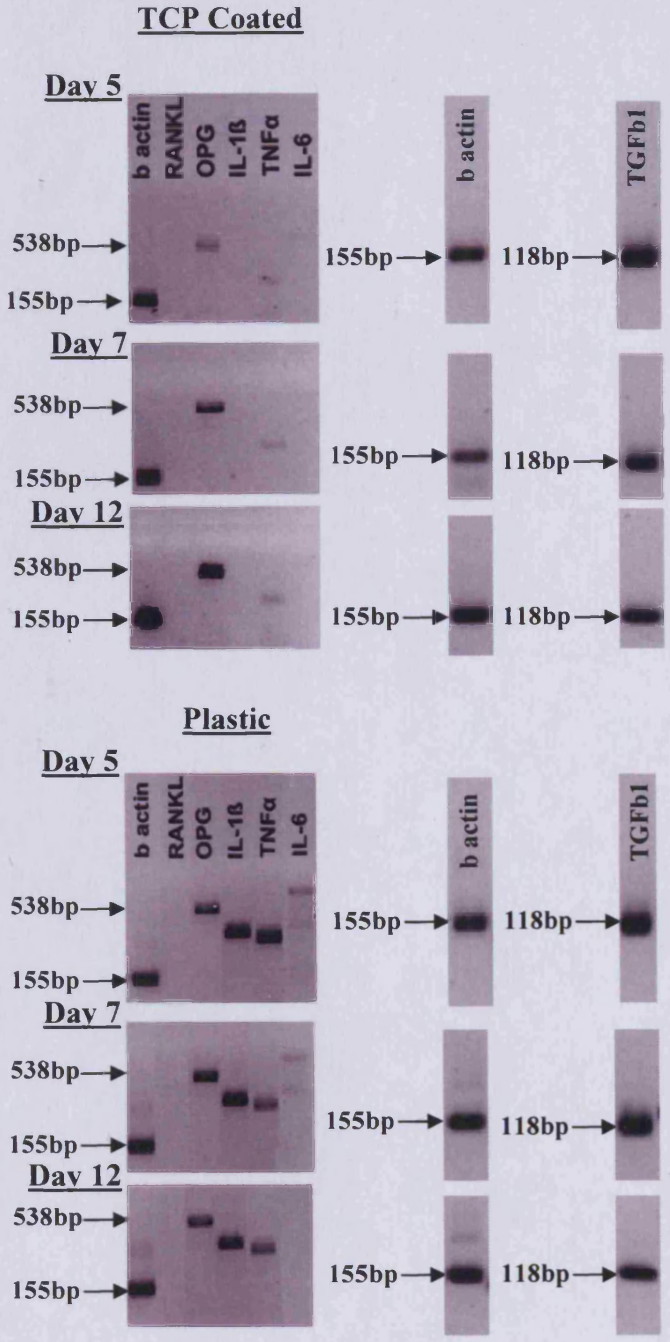

Figure 4.2: RT-PCR results showing an mRNA expression profile of BMSCs cultured on the TCP coated and plastic surfaces at the different post-seeding time points. β actin was used as a house keeping gene. RANKL - Rank ligand, OPG - Osteoprotegerin, IL-1β - Interleukin 1β, TNFα – Tumour Necrosis Factor α, IL-6 - Interleukin 6, TGFb1- Transforming Growth Factor β1. Product band sizes are estimated based on their relative position to a 100kb DNA ladder.

Table 4.2a

Product	M	G	T	P
RANKL	-	-	-	-
OPG	+	+	+	++
IL-1β	faint	faint	-	++
TNFα	faint	faint	faint	++
IL-6	faint	faint	-	+
TGFβ1	++	++	++	++

Table 4.2b

Product	M	G	T	P
RANKL	-	-	-	-
OPG	++	++	++	++
IL-1β	-	-	-	++
TNFα	+	+	faint	+
IL-6	faint	faint	-	faint
TGFβ1	++	++	++	++

Table 4.2c

Product	M	G	T	P
RANKL	-	faint	-	-
OPG	++	++	++	++
IL-1β	-	-	-	++
TNFα	++	++	faint	+
IL-6	+	+	-	-
TGFβ1	++	++	++	++

Tables 4.2a, 4.2b and 4.2c: Tables summarising the RT-PCR results presented at day 5 **(4.2a)** day 7 **(4.2b)** and day 12 **(4.2c)** post-seeding time points. M-machined, G-grit blasted/acid etched, T-TCP coated, P-Plastic, RANKL - Rank ligand, OPG - Osteoprotegerin, IL-1β - Interleukin 1β, TNFα – Tumour Necrosis Factor α, IL-6 - Interleukin 6, TGFβ1- Transforming Growth Factor β1. '++' indicates clear strong bands, '+' indicates clear bands, 'faint' indicates barely visible bands and '–' denotes no band.

4.3.2 TNFα and IL-1β ELISAs

Graphs showing the standard curves generated from both the TNFα and IL-1β ELISAs are shown in Figure 4.4. No detectable levels of either protein were found in the culture supernatants of BMSCs cultured on any of the experimental surfaces at any time point. The standard curves, however, show that there was immunoreactivity in the ELISAs, as the absorbance increased with increasing concentrations of the standards.

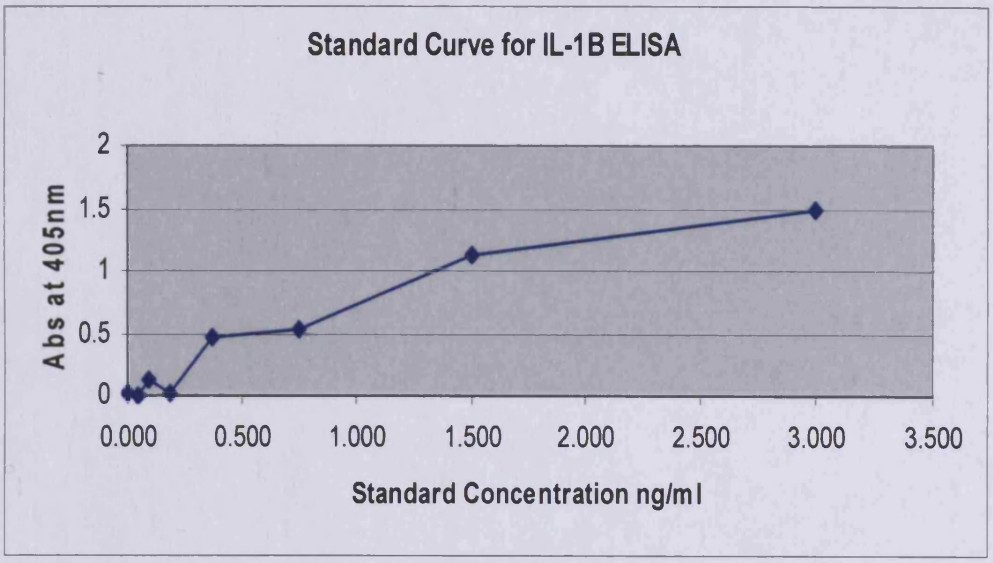

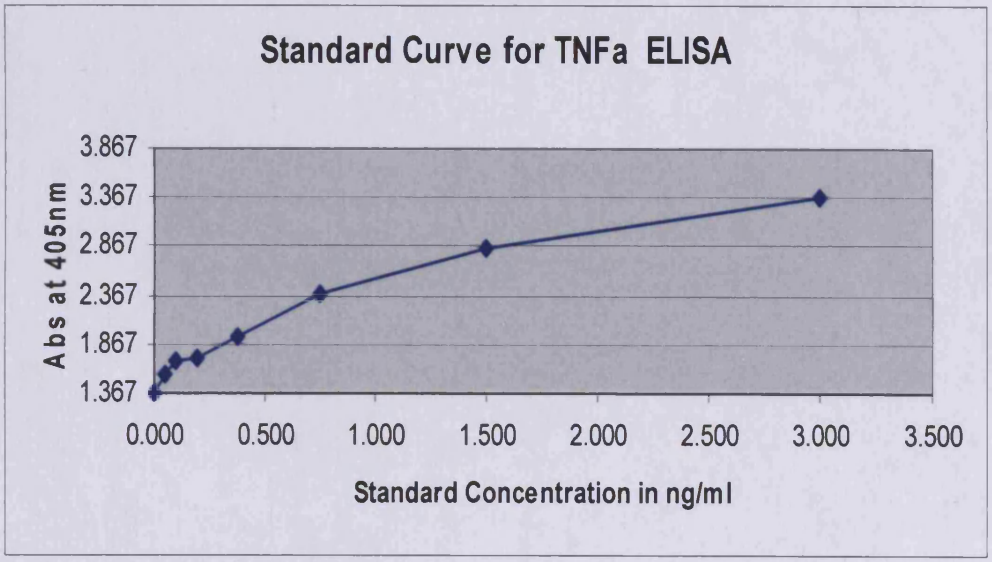

Figure 4.4: Standard curves generated by the IL-1β and TNFα ELISAs. Neither protein was detected in the culture supernatant, but the standard curves show immunoreactivity with the standards.

4.4 Discussion

In this chapter, the data presented have shown that there are differences in the IL-1β mRNA expression profiles of BMSCs grown on titanium surfaces versus plastic controls, which may indicate potential differences in the inflammatory response of BMSCs to different surfaces. A reduction was also observed in the expression of TNFα mRNA by BMSCs cultured on the TCP coated surface, which would likely be favourable to bone formation. Interestingly however, neither IL-1β nor TNFα appeared to be released by BMSCs cultured on any surface. BMSCs from all surfaces appeared to generate osteogenic signals through the expression of OPG and TGFβ1 mRNA.

One of the key findings presented in this chapter is that all of the titanium surfaces appeared to suppress the expression IL-1β mRNA compared to the plastic control surface at all time points investigated and that this phenomena was independent of surface treatment. This is significant due to the complex role that this cytokine plays in the process of osteoblast differentiation and function; there have been contradictory reports over the effect of IL-1β on osteoblast differentiation and function. It was initially reported that IL-1β inhibits the production and secretion of bone matrix proteins by osteoblasts *in vitro*, particularly after sustained exposure (Canalis 1986; Stashenko et al. 1987). Conversely, it has been also been shown that IL-1β increases the differentiation and proliferation of pre-osteoblasts *in vitro* (Lange et al. 2009), and promotes mineralisation while decreasing Runx2 expression *in vitro* (Ding et al. 2009). *In vivo*, an initial inflammatory response involving IL-1β may be necessary to initiate the healing process by stimulating osteoblast progenitor cell proliferation, but this response would need to be quickly suppressed to allow the formation of new bone. Although the overall influence of IL-1β on the process of osseointegration is not fully understood, it is clearly a key regulatory element in the early osteoblast differentiation pathway. Therefore, the observed suppression of IL-1β mRNA expression by titanium surfaces, particularly at the later post-seeding time points, may enhance the osseointegrative potential of surfaces and thereby serve to enhance bone formation *in vivo*. Alternatively, the increase in IL-1β expression by

BMSCs cultured on plastic surfaces may have been caused by an increase in macrophage adherence to these surfaces, as these cells are a primary source of IL-1β *in vivo*.

Overall, TNFα has a deleterious effect on bone formation and has been shown to broadly inhibit the production of bone matrix components by osteoblasts and also to inhibit osteoblast proliferation (Gowen et al. 1988; Rosenquist et al. 1996) and differentiation via the suppression of Runx2 (Abbas et al. 2003; Gilbert et al. 2002). The expression profile of TNFα mRNA by BMSCs varied somewhat across the different surfaces, with stronger bands for the machined and grit blasted/acid etched surfaces at each subsequent time point, while the band strength decreased for the plastic surface over time. In contrast, the TCP coated surfaces had minimal TNFα expression at all time points. An increased expression of TNFα mRNA over time by BMSCs cultured on the machined and grit blasted/acid etched surfaces is therefore somewhat surprising, given the apparent suppression of IL-1β by these surfaces. This however, did not appear to affect their ability to produce bone matrix material, as was shown in Chapter 3. Likewise, the lower expression of TNFα by BMSCs cultured on the TCP coated surface did not appear to confer any particular advantages to the formation of bone matrix. It is therefore difficult to gauge the important of this finding. All bands for IL-6 mRNA were consistently faint, which is somewhat surprising as TNFα has been shown to increase osteoblast production of IL-6 (Dai et al. 2006). Therefore, it might be expected that those surfaces which caused an increased expression of TNFα may have caused a corresponding increase in IL-6 expression by BMSCs cultured on them.

The direct regulation of osteoclast activity by osteoblasts through the RANKL/OPG pathway has been previously characterized (Boyle et al. 2003). OPG mean product band intensity from the titanium surfaces increased over time, while the mean band intensity from the plastic surface remained relatively constant at all post-seeding time points. RANKL mRNA, in contrast, was only faintly expressed by BMSCs cultured one surface at a single post-seeding time point. *In* vivo, the ratio of RANKL expression versus OPG expression directly regulates the level of osteoclast activation and therefore the process of bone resorption (Boyle et al. 2003). In

BMSCs cultured on the experimental surfaces, this ratio was found to be highly in favour of OPG expression, suggesting that the adherent BMSCs are suppressing osteoclast activity and therefore bone resorption. It is peculiar that RANKL is not widely expressed in conjunction with OPG, and there is no doubt that appropriate positive controls, for example RT-PCR reactions using RNA from an osteoblast cell line, would have served to clarify this issue.

TGFβ1 mRNA was found to be expressed by BMSCs cultured on all of the experimental surfaces at all time points. This is indicative of both the osteoblast phenotype and of bone matrix production, as TGFβ1 is produced along with the bone matrix proteins and is sequestered in the bone matrix (Hughes et al. 2006). Therefore, this result confirms the fact that all of the experimental surfaces were capable of supporting populations of osteoblast progenitor cells and the production of matrix.

A surprising finding presented in the chapter was the lack of either IL-1β or TNFα in the culture supernatants despite the presence of both cytokines at the transcriptional level. Although BMSCs cultured on the plastic surface had IL-1β mRNA copies present at all time points, they apparently did not secrete it at detectible levels. This would indicate that cells either did not move from transcription to translation of IL-1β or that the protein remained in intracellular storage as a pro-peptide, perhaps due to a lack of a stimulus for release (Ferrari et al. 2006). Similarly, TNFα mRNA was detected yet the cytokine itself was not found in any culture supernatants, possibly due to a lack of translation or because the cytokine was stored in an inactive form by BMSCs. Unfortunately, further speculation is beyond the scope of the investigations carried out here.

The most notable difference observed between the mRNA expression profiles of BMSCs cultured on the experimental surfaces was the apparent suppression of IL-1β by titanium as opposed to plastic. With the exception of the reduced expression of TNFα mRNA in BMSCs cultured on the TCP coated surface, none of the experimental titanium surfaces showed any outstanding effects on cells which would indicate a higher osseointegrative potential. On the contrary, cells from all surfaces

showed mRNA expression of OPG and TGFβ1, suggesting a suppression of bone resorption and the presence of a population of active osteoblast-like cells, both of which would be favourable to osseointegration.

Chapter 5: The Osseointegration of Titanium Dental Implants in an In Vivo Rat Model of Type II Diabetes Mellitus

5.1 Introduction

Titanium dental implants have a high clinical success rate in healthy individuals where there is ample good quality bone around the implant site. There are many individuals however, with conditions which prevent them from being able to benefit from treatment with dental implants. A prime example of such a condition is diabetes mellitus (DM). DM is a metabolic disorder, which is characterised by chronic hyperglycaemia, and has two types, type I and type II. Type I DM, or insulin dependent diabetes, is caused by the destruction of insulin producing beta cells in the pancreas by an auto-immune response, thus eliminating the ability to produce insulin. Approximately 5 to 10 percent of individuals with DM have type I, making it the minority variant (Graves et al. 2006). Type II DM, or non-insulin decedent diabetes, is caused by a desensitisation of the tissues to insulin, which is brought on by sustained hyperglycaemia. This type of DM is by far the most prevalent, with the remaining 90 to 95 percent of cases consisting of type II diabetes (Graves et al. 2006). It is estimated that more than 150 million individuals worldwide have type II DM (Zimmet et al. 2003).

The placement of dental implants in diabetic individuals has proven to be controversial. Although there are reports of implants being well tolerated in diabetic patients (Klokkevold and Han 2007; Morris et al. 2000), diabetes is often held to be a contraindication for treatment, with higher failure rates reported in diabetic individuals (Fiorellini et al. 2000; Morris et al. 2000; Valero et al. 2007). This may be explained by the fact that diabetes has been repeatedly shown to impair the process of bone formation and thereby significantly delay the process of osseointegration (Hasegawa et al. 2008; He et al. 2004; Kwon et al. 2005; Liu et al. 2007b; Shyng et al. 2006; Siqueira et al. 2003). Although the specific cause for this delay in healing remains to be fully elucidated, it is thought that a slower attachment

of tissue to the implant surface allows opportunities for bacterial invasion, leading to infection and sustained inflammation, resulting in an impairment of bone formation in diabetic individuals (Graves et al. 2006; Valero et al. 2007). For example, it has been demonstrated that monocytes harvested from individuals with type I DM have increased levels of TNF-α and IL-1β in response to bacterial LPS (Salvi et al. 1997a; Salvi et al. 1997b), which would lead to increased inflammatory tissue damage and therefore impaired healing in diabetic individuals. It is possible that certain aberrations exist in the activity of osteoblast cells in DM, leading to altered function and therefore have an impact on the process of bone repair around an implant site.

In order to investigate possible mechanisms behind the delay in healing around implants in diabetic individuals and how different titanium surfaces could affect it, an *in vivo* rat model has been developed in conjunction with Osaka Dental University in Japan (Sakai et al. 2008). This model involves the removal of an incisor and subsequent placement of titanium dental implants with a machined surface into the resulting socket. The progression of mandibular bone healing following the placement of a titanium implant allows bone healing to be observed at a series of post-operative time points, and osteogenic activity around an actual implant site can be assessed by the presence of various cellular markers. A model of type II DM, the Goto-Kakizaki (GK) rat (Goto et al. 1975), which exhibits spontaneous hyperglycaemia leading to impaired insulin sensitivity, allows the process of osseointegration to be studied in the context of this disease state. This model has previously been used to investigate the removal torques of implant placed in GK rats compared to normal controls. Interestingly, these were found to be significantly higher in diabetic animals, despite the fact that a small decrease in bone formation around the diabetic implant site was observed histologically (Sakai et al. 2008).

There have been a number of *in vivo* models which suggest that both type I and type II DM decrease the level of osseointegration of titanium implants in both rats and mice (Fiorellini et al. 1999; Hasegawa et al. 2008; Kwon et al. 2005; McCracken et al. 2000; McCracken et al. 2006; Nevins et al. 1998; Shyng et al. 2006; Siqueira et al. 2003). Many of these studies have been carried out in models

where implants were inserted into the tibia or femurs of animals, presumably due to the ease of access, with the aim of modelling the progression of osseointegration of a dental implant. Although this clearly provides useful information about the effects of bone repair around titanium implants, it is entirely possible that there are regional differences in the way the bone repair process is affected by DM. Furthermore, in the tibia, the environment in which bone healing takes place is entirely different from the oral cavity. For example, exposure to the oral flora no doubt has a substantial impact on the inflammatory process, as does the constant exposure of the oral cavity to the external environment. As an altered response to various infectious agents is thought to be a major factor in the delayed healing seen around dental implants in DM (He et al. 2004; Valero et al. 2007), taking these factors into account when considering the clinical situation in humans is of critical importance. In addition, the cell populations involved in the bone repair process would almost certainly be different between the tibia and the oral cavity. Using an *in vivo* model which involves the direct insertion of implants into the mandible can therefore only give a clearer representation of the clinical situation than insertion of implants into a more peripheral site.

Within the present study, basic haematoxylin and eosin (H&E) staining was used to gauge the level of bone healing around the implant site in both normal and diabetic animals at 1, 3, 9 and 12 week post-operative time points. Staining with alizarin red served to detect tissue mineralisation. Several biomarkers specific to different stages in the osteoblast differentiation process were also selected for immunolocalisation in order to track the progression of osteoblast progenitor cells through this process around the implant sites in both the normal and disease states. Stro-1 is a cell surface marker associated with mesenchymal stem cells and osteoblast progenitor cells early in their differentiation, indicating the presence of progenitor cells recently migrated from the bone marrow and the remnants of the PDL (Stewart et al. 1999; van den Dolder and Jansen 2007; Walsh et al. 2000). The cell proliferation marker proliferating cell nuclear antigen (PCNA) was used to identify the presence of mitotic cells. Cellular proliferation around the implant site indicates a healing response involving the proliferation of a variety of cell types, including osteoblast progenitor cells. Osteopontin (OP), an early osteoblast marker which serves a role in cellular adhesion and osteocalcin (OC), a later osteoblast

marker known to be an inducer of mineralization (Hughes et al. 2006), were chosen to label mature osteoblasts. Finally, the presence of transforming growth factor β1 (TGF β1), a powerful stimulator of early osteoblast proliferation and a critical factor in matrix synthesis (Centrella et al. 1992; Janssens et al. 2005) was also examined.

Due to the trauma involved in the initial placement of the implant, cytokines such as IL-1β and TNFα would normally be secreted around the implant site by activated macrophages. The presence of these potent inflammatory mediators, which are known to inhibit bone formation and are involved in bone resorption (Bertolini et al. 1986; Boyce et al. 1989; Ellies and Aubin 1990; Hughes et al. 2006; Nanes 2003), normally wanes as the healing process advances. These cytokines were therefore immunolocalised along with the pan specific macrophage marker F4/80 around the implant sites in both normal and diabetic animals in order to examine their expression during the healing process in both the normal and disease state. Sustained expression of these cytokines and the presence of the cells which are critical modulators of them may be a key mechanism behind the delayed bone healing observed in DM. The development of a model of implant osseointegration in DM permits the study of the effects of DM on the process of bone healing at the cellular level, serving to elucidate differences in cell behaviour which contribute to delays in bone healing, and thereby worsen clinical outcomes in implant treatment

5.2 Materials and Methods

5.2.1 Preparation of Mandibles

Implant procedures were performed by Diago Sakai and Joji Okazaki at the Dental University of Osaka Japan on both 10 week old male Wistar and Goto and Kakizaki (GK) rats, as described in Sakai et al (2008). All experimental protocols involving these animals were reviewed and approved by the Animal Committee of Osaka Dental University (approval number 08-03009), and conformed with the procedures described in the 'Guiding Principles for the Use of Laboratory Animals' handbook at the Laboratory Animal Facilities in the Institute of Osaka Dental Research, Osaka Dental University. The continuously erupting incisors of the rats were trimmed at 14, 11, 7 and 4 days prior to extraction in order to stimulate eruption (Figure 5.1a). This served to loosen the incisors, facilitating an extraction which minimally disrupted surrounding tissues. Pre-treatment trimming procedures were carried out under infiltration anaesthesia with isoflurane (Isoflurane Rhodia™, Nissan Chemical Industries Ltd., Tokyo, Japan). Tooth extraction was carried out under the general anaesthetic sodium pentobarbital (Nembutal®, Dainippon Pharmaceutical Co., Ltd. Osaka, Japan) delivered by intra peritoneal injection (Figure 5.1b). Blood samples were collected immediately after tooth extraction and blood glucose levels measured using the Acensia Contour™ glucose monitoring system (Bayer Medical Co. Ltd., Tokyo, Japan). Blood glucose levels in the GK rats were found to be significantly higher than in control animals. The implant sockets were then curetted to remove debris and the majority of the periodontal ligament. Machined titanium alloy (Ti-6Al-4V) implants with a length of 17.0mm and a 1.2mm diameter (SNK Screwpost Ti-tan®, Dentsply-Sankin K.K. Tokyo, Japan). Implants were immediately placed in the socket (Figure 5.1c). Rats were then sacrificed by intra peritoneal injection of sodium pentobarbital (Nembutal®, Dainippon Pharmaceutical Co) at post-operative time points of 1, 3, 9 and 12 weeks. Animals were finally fixed by perfusion with 10% neutral-buffered formalin, extracted and sent to the Cardiff in formalin for processing.

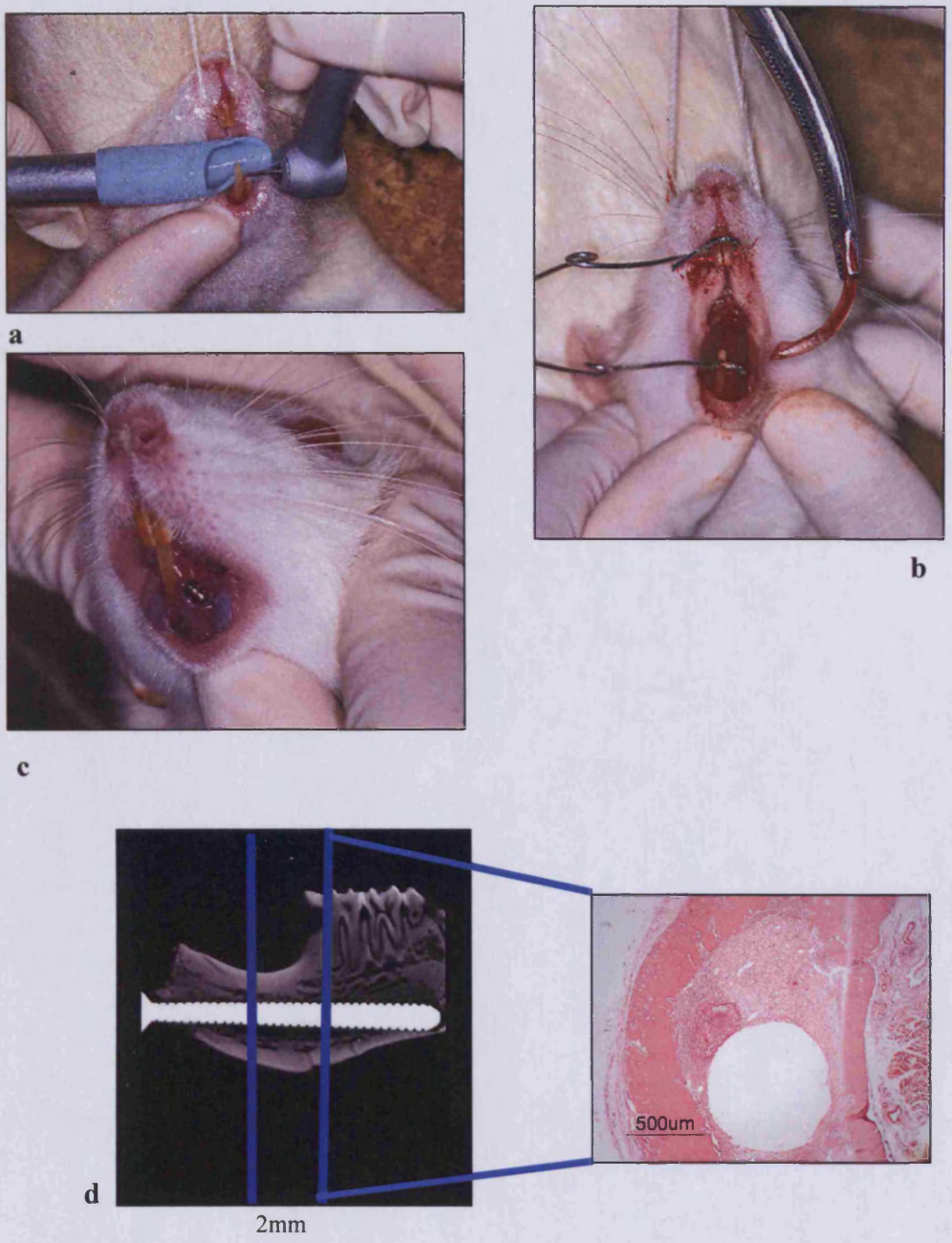

Figure 5.1: Schematic of implant placement and histological processing. Pre-treatment trimming of mandibles in shown in (**a**), followed by incisor extraction (**b**) and placement of implants (**c**). In (**d**) a radiograph of an implant in a mandible is shown, along with an example an of a tissue section, which were taken such that they were perpendicular to the implant socket. All sections shown come from a 2mm section near the middle of the mandible, between the two lines shown in (d).

5.2.2 Processing of Mandibles

Implants were removed from the mandibles by carefully unscrewing them out of the socket. After removal of the ramus and condyle, the mandibles were then cut into approximately 2mm thick sections running perpendicular to the implant socket using a bone saw (Figure 5.1d) and placed in 10% formic acid with agitation for 72 hs to demineralise the tissue sections. The tissue sections were then placed in biopsy cassettes and processed using a processing machine (Shandon Pathcentre), which passed them through a series of 70, 90, and 100% graded alcohol soaks which served to dehydrate them, cleared them with a xylene rinse and finally impregnated them with molten paraffin wax (Raymond Lamb, UK). Tissue sections were then removed from the processing machine and embedded in paraffin wax (Raymond Lamb). 5μm sections were cut on a rotary microtome (Leica) and mounted on poly-L-lysine coated glass slides (Sigma Aldrich) before being placed in an oven at 65°C overnight in order to improve tissue adhesion and sections were stored at room temperature in closed boxes until required.

5.2.3 Haematoxylin and Eosin Staining

Sections were stained with haematoxylin and eosin (H&E) using an automated staining machine, in order to visualize the area around the implant site. Firstly, the automated staining system passed the slide mounted sections through a heater to dry them. Tissue sections were then passed through a series of xylene, graded alcohol and water rinses in order to remove all paraffin and rehydrate them. The sections were then immersed in haematoxylin which stains the nucleus of cells blue, washed and blued in Scott's tap water, and differentiated in 1% acid alcohol. After a further rinse in tap water, sections were stained with eosin which stains cytoplasmic components red. Finally, the sections were rinsed in tap water, dehydrated in alcohol and immersed in xylene. Cover slips were mounted onto the sections using DPX mounting medium (Raymond Lamb). Images were captured using an Olympus AX70 microscope incorporating a Nikon DXM 1200 digital camera and ACT-1 software.

5.2.4 Alizarin Red Staining

In order to assess the level of mineralization in the tissues around the implant sites, sections were stained with alizarin red, which stains areas rich in calcium ions bright red, indicating a degree of mineralization. Although sections had undergone demineralization, there was still enough residual calcium remaining in the tissue sections to stain with alizarin red. Sections were deparaffinized with xylene for 10 mins, rinsed with industrial methylated spirit (IMS) for 5 mins and washed in tap water for 5 mins. Sections were circled using a paraffin pen (Sigma Aldrich). 0.1% w/v alizarin red, adjusted to pH 5.5 with ammonium hydroxide, was applied to each slide for approximately 5 mins. Slides were then rinsed with tap water, washed with IMS for 5 mins and cleared with xylene for 5 mins. Cover slips were applied to slides using DPX glue, and images taken using an Olympus AX70 microscope incorporating a Nikon DXM 1200 digital camera and ACT-1 software.

5.2.5 Immunohistochemistry

5.2.5.1 Preparation of Sections

Sections were deparaffinized with xylene for 10 mins, rinsed with industrial methylated spirit (IMS) for 5 mins and washed in tap water for 5 mins. Sections were circled with a paraffin pen. For the immunolocalisation of TGFβ1, IL-1β, TNFα and F4/80, antigen retrieval was performed by treating the tissue sections with 24μg/mL protinase K (Sigma Aldrich) for 10 mins at 37°C. After this step the sections were washes three times in TBS for 5 min. Finally in order to quench endogenous peroxidase activity, sections were incubated at room temperature in 3% hydrogen peroxide for 10 mins. This was followed by three further 5 min washes with TBS.

5.2.5.2 Immunolocalisation

Immunodetection of PCNA, osteopontin, osteocalcin, TGFβ1, IL-1β, TNFα and F4/80 was carried out using a Vectastain Universal IgG Kit (Vector Laboratories) and a DAB perioxidase kit (Vector Laboratories). Non specific binding of antibodies was blocked by incubating with 1% w/v normal horse serum, diluted in tris buffered solution (TBS), for 1 hr at room temperature. After blocking, sections were incubated with the appropriate IgG primary antibody (Table 1) at the appropriate dilution in 1% w/v horse serum in TBS at 4°C overnight. As a negative control for each experiment, a non-immunogenic IgG_1 control antibody (Sigma Aldrich) was substituted for the primary within the protocol or the primary was excluded altogether and was with blocking serum. Sections were washed three times for 5 min with TBS, and the universal secondary antibody (Vector Laboratories) diluted with 100µl of normal blocking serum (Vector Laboratories) in TBS was applied for 30 mins. Appropriate dilutions for both primary and secondary antibodies were determined experimentally and are given in Table 1. Following incubation with the secondary antibody, sections were again washed three x5 min with TBS and incubated with the 'ABC' reagent (Vector Laboratories) for 30 mins. The 'ABC' reagent, which is an avidin-biotin complex which acts as a signal amplifier, was prepared by adding two drops of 'reagent A', containing avidin, and two drops of 'reagent B', containing biotin, into 5mL of TBS. Sections were washed three x5 min for a final time and incubated with a 3, 3'diaminobenzidine (DAB) peroxidase made up using a DAB substrate kit (Vector Laboratories) for approximately 2 mins. The substrate solution was made up by adding the following kit contents to 5ml of distilled water as per the manufacturer's instructions: 100µl Buffer Stock Solution, 200µl DAB stock Solution, 100µl Hydrogen Peroxide Solution and 100µl Nickel Solution. Finally, slides were rinsed in tap water, counterstained with 0.1% w/v methyl green for approximately 1 min, rinsed in industrial methylated spirit for 5 mins and cleared with xylene for 5 mins. Cover slips were applied to sections using DPX glue, and images taken using an Olympus AX70 microscope incorporating a Nikon DXM 1200 digital camera and ACT-1 software. All immunolocalisations were performed in duplicate.

5.2.5.3 Stro-1 Localization

The primary antibody to Stro-1 is an IgM class antibody and therefore the Vectastain Kit was not appropriate for use. Instead, sections were blocked with 5% goat serum (Sigma Aldrich) for 20 mins and incubated with the IgM primary antibody or negative controls overnight (Table 1 for dilution details). After washing two x5 min with TBS sections were incubated with the secondary antibody, a biotinylated goat anti-mouse IgM antibody (Vector Laboratories) for 30 mins. Sections were then treated with the ABC reagent from the Vecastain universal kit and immuno-reactivity detected using the DAB peroxidase substrate as described in the previous section.

Primary antibody	Antibody source	1° isotype and dilution used	Biotinylated 2° and dilution used
Anti-human Stro-1	National Hybridoma Bank	IgM; Mouse polyclonal; 1:25	Goat anti-mouse IgM; 1:600
Anti-rat PCNA (PC10)	Santa Cruz Biotechnology, Inc., CA, USA	IgG; Mouse monoclonal; 1:25	Vectastain Universal IgG; 1:100
Osteopontin (recombinant OPN human origin; FMb-14)	Santa Cruz Biotechnology, Inc., CA, USA	IgG; Mouse monoclonal; 1:50	Vectastain Universal IgG; 1:100
Osteocalcin (amino acid 1-95 mouse OCN; FL-95)	Santa Cruz Biotechnology, Inc., CA, USA	IgG; Rabbit polyclonal; 1:50	Vectastain Universal IgG; 1:100
IL-1ß (Anti rat B122)	eBioscience, CA, USA	IgG; Armenia Hamster polyclonal; 1:50	Vectastain Universal IgG; 1:100
TNFα (N-terminus mouse origin; L-19)	Santa Cruz Biotechnology, Inc., CA, USA	IgG; Goat polyclonal; 1:50	Vectastain Universal IgG; 1:100
TGFß 1 (c-terminus human origin; v)	Santa Cruz Biotechnology, Inc., CA, USA	IgG; Rabbit polyclonal; 1:50	Vectastain Universal IgG; 1:100
F4/80 (Anti-Rat Pan macrophage marker ab15637)	Abcam, MA, USA	IgG; Mouse monoclonal; 1:40	Vectastain Universal IgG; 1:100

Table 5.1: A list of primary antibodies, along with dilutions of primary and secondary antibodies used.

5.2.5.4 Semi-Quantification of Immunohistochemical Results

Positively stained cells were counted using the Image Pro-Plus version 6.0.0.260 image analysis software (Media Cybernetics Inc. Bethesda, MD). This software allows colors to be manually selected from an image and continuous objects, which are these colors, are designated as 'positive'. From each section, images were taken from five random fields of view around the implant socket. On each of these 5 images, positive cells in 5 $100\mu m^2$ areas around the implant site were counted and averaged, giving a semi-quantitative value for the number of average positive cells per $100\mu m^2$ in 5 random fields of view. Overall average cell counts from the 5 random fields of view were calculated alongside the standard error of the mean.

5.3 Results

5.3.1 Haematoxylin & Eosin Histology

Figures 5.2-5.5 show that bone healing appeared to be delayed in the diabetic animal, especially at the earlier time points. In Figure 5.2, a cell rich granulation tissue (GT) is visible around the implant socket in both normal and diabetic animals at one week post-operation. No bone formation appeared to have occurred at this stage in either animal. By three weeks post-operation (Figure 5.3) however, although a substantial amount of the granulation tissue was still visible in the sections from both animals, there was evidence of new bone growth around the implant socket in the normal animal. This is in stark contrast to the diabetic animal, which had granulation tissue around the implant site at this time point. At nine weeks post-operation (Figure 5.4), bone healing had advanced considerably around the normal implant socket, with only a small amount of granulation tissue evident. In the area around the diabetic implant socket, some newly formed bone was visible, although less than that in the normal animal. In both the normal and diabetic animals at twelve weeks post-operation (Figure 5.5), a substantial amount of bone formation had taken place, with little difference visible between the two animals.

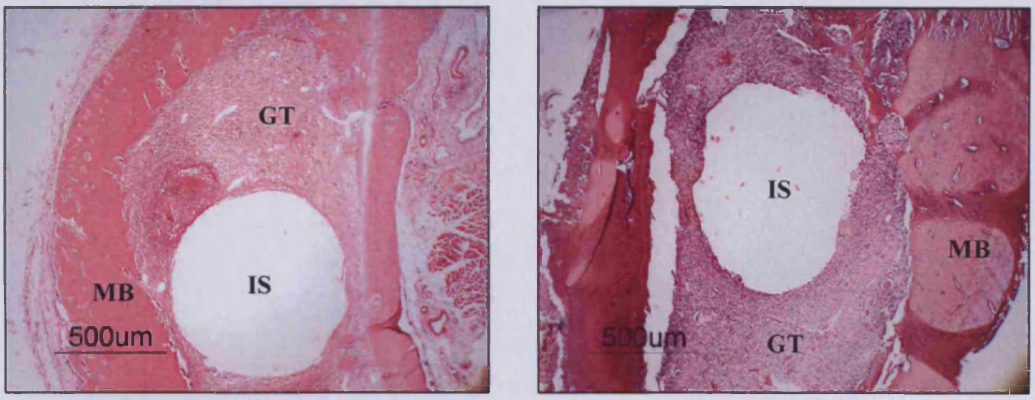

a b

Figure 5.2: H&E stained sections obtained from a normal (a) and diabetic (b) rat at one week post-operation. MB indicates mandibular bone, IS indicates the implant socket and GT the granulation tissue.

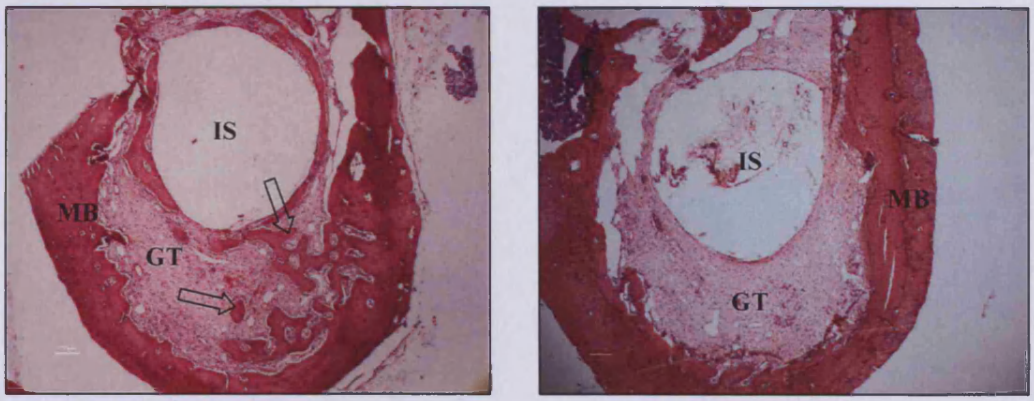

c d

Figure 5.3: H&E stained sections obtained from a normal (**c**) and diabetic (**d**) rat at three weeks post-operation. MB indicates mandibular bone, IS indicates the implant socket and GT the granulation tissue. Newly formed bone is indicated by arrows.

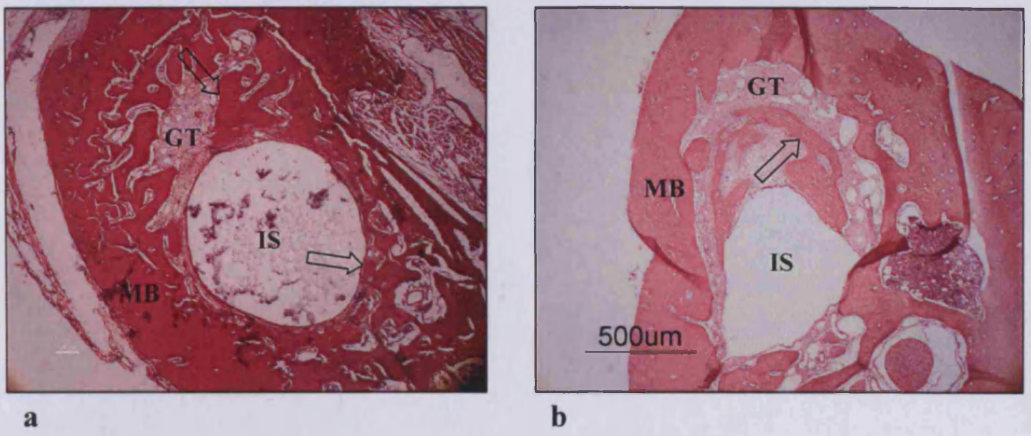

Figure 5.4: H&E stained sections obtained from a normal (**a**) and diabetic (**b**) rat at nine week post-operation. MB indicates mandibular bone, IS indicates the implant socket and GT the granulation tissue. Newly formed bone is indicated by arrows.

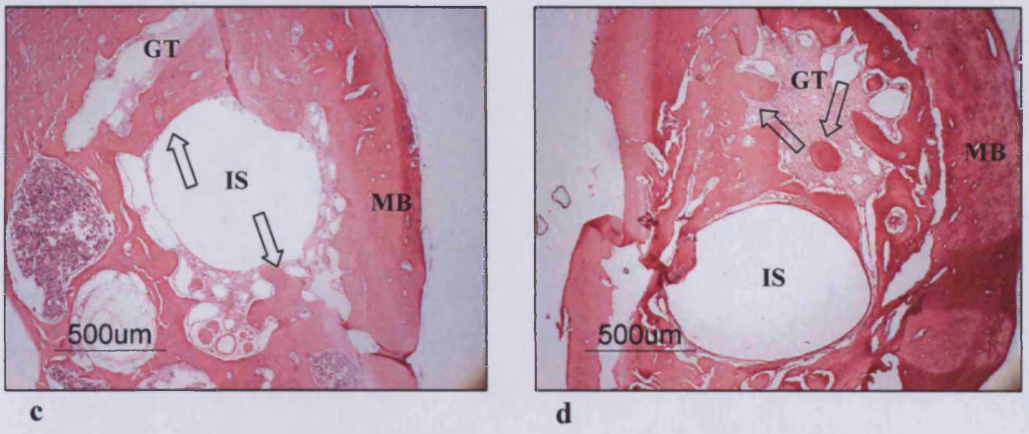

Figure 5.5: H&E stained sections obtained from a normal (**c**) and diabetic (**d**) rat at twelve weeks post-operation. MB indicates mandibular bone, IS indicates the implant socket and GT the granulation tissue. Newly formed bone is indicated by arrows.

5.3.2 Alizarin Red Staining

Images obtained following the staining of mineral residue with alizarin red are shown in Figures 5.6-5.9. The results concur with those from H&E staining. At one week post operation (Figure 5.6), no bright red staining was visible on sections from either the normal or diabetic animal, which indicated that no mineralisation has taken place around either implant site at this time point. By three week post-operation however (Figure 5.7), areas of bright red staining were visible around the normal implant site, indicating the deposition of mineral at these locations. This is in contrast to the diabetic implant site, around which there was no evidence of mineralisation at this time point. In the sections from nine weeks post-operation however (Figure 5.8), areas of bright red staining were visible around the edges of newly formed bone in both normal and diabetic animals, although there were noticeably fewer of these in the diabetic animal. There was a similar situation at twelve weeks post-operation (Figure 5.9), with bright red staining appearing at the edges of newly formed bone around implant sites in both animals.

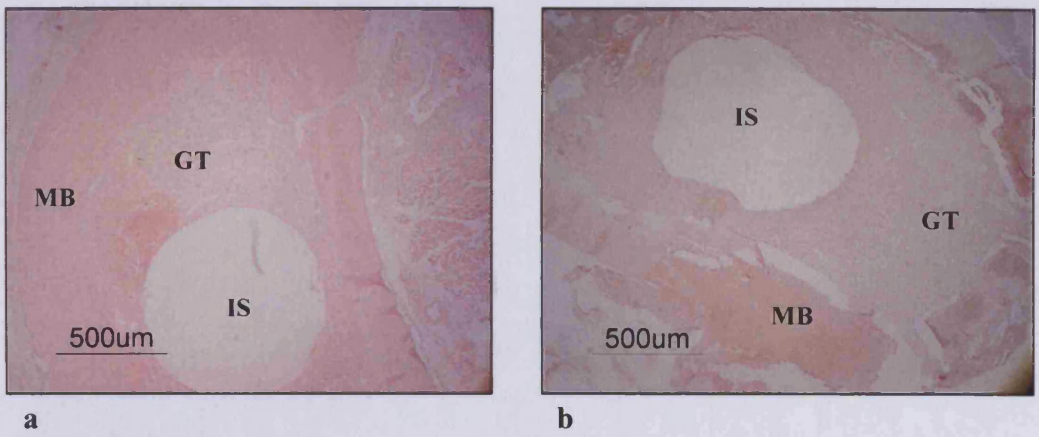

Figure 5.6: Alizarin red stained sections from a normal (**a**) and diabetic (**b**) rat at one week post-operation. The implant site is indicated by IS, granulation tissue by GT and mandibular bone by MB.

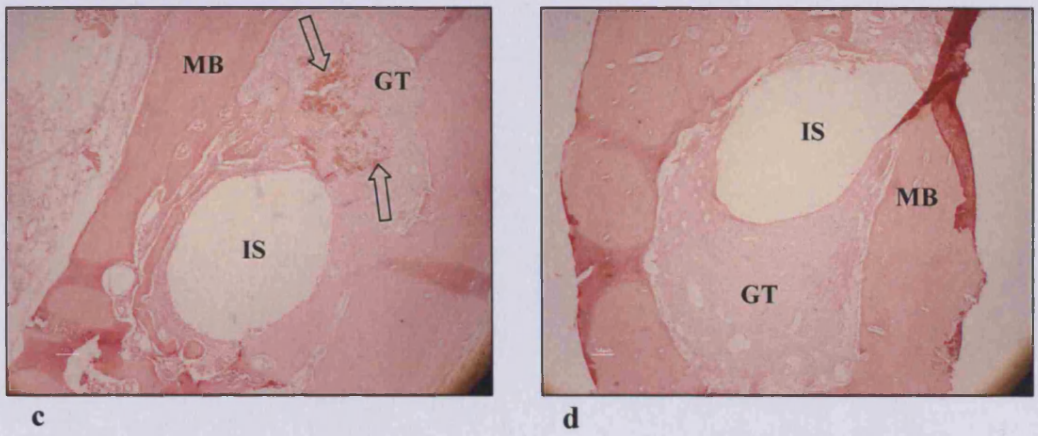

Figure 5.7: Alizarin red stained sections a normal (**c**) and diabetic (**d**) rat at three weeks post-operation. Around the normal implant socket (IS) bright red staining is visible (indicated by arrows) and is evidence of mineralisation. Granulation tissue is indicated by GT and mandibular bone by MB.

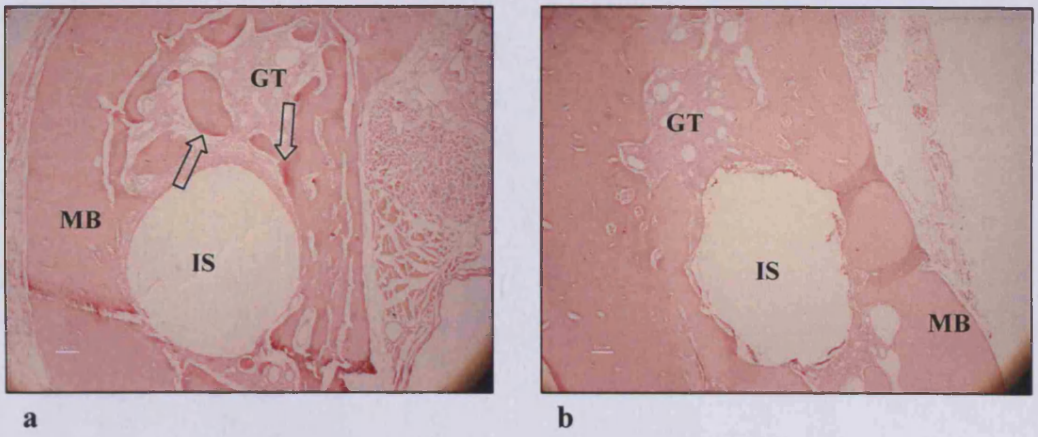

Figure 5.8: Alizarin red stained section from a normal (**a**) and diabetic (**b**) rat at nine weeks post-operation. The implant site is indicated by IS, granulation tissue by GT and mandibular bone by MB. Areas of bright red staining are indicated by arrows.

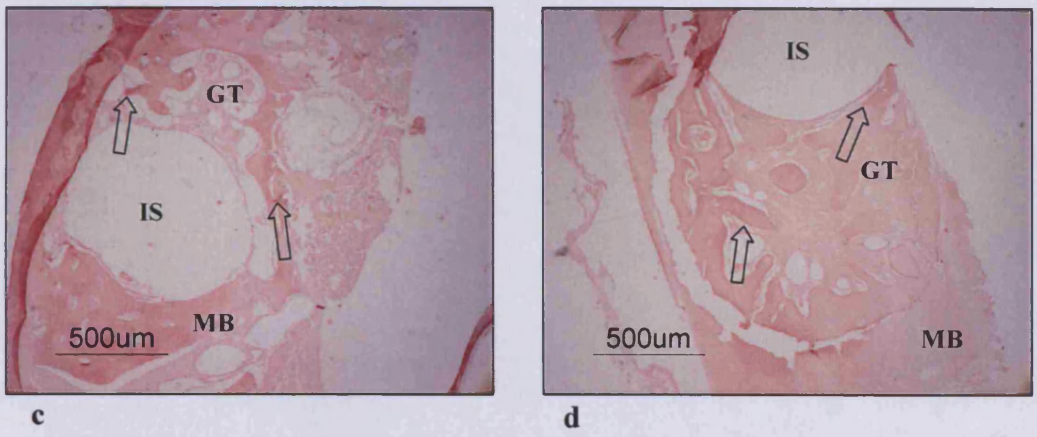

Figure 5.9: Alizarin red stained sections from a normal (**c**) and diabetic (**d**) rat at twelve weeks post-operation. Around the normal implant socket (IS) bright red staining is visible (indicated by arrows) and is evidence of mineralisation. Granulation tissue is indicated by GT and mandibular bone by MB.

5.3.3 Immunolocalisation of Stro-1

Images obtained from the immunolocalisation of mesenchymal progenitor cells are shown in Figures 5.10-5.12. Stro-1 expression is indicated by brown cellular staining. There were not any substantial differences between normal and diabetic animals in the number of these cells present around the implant sites at any time point. At one week post-operation, Stro-1 was found to be present around the implant sites of both diabetic and normal rats (Figure 5.10). Expression of Stro-1 at three weeks post-operation (Figure 5.11) was much reduced in both animals, with only a very few positive cells seen around the implant sites. At nine weeks post-operation (Figure 5.12), there was no population of Stro-1 positive cells which could be identified around the implant site in either normal or diabetic animals. Figure 5.13 shows a graph of the average number of Stro-1 positive cells per $100\mu m^2$ in tissue sections from both animals over one, three and nine weeks post-operation. Images of immunolocalisation of Stro-1 at twelve weeks post-operation are not shown due to the lack of Stro-1 expression in either animal at twelve weeks post-operation.

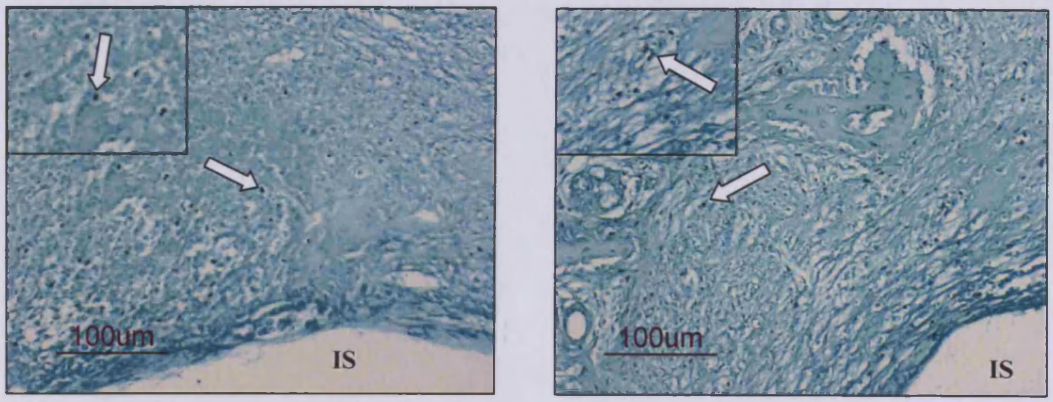

a b

Figure 5.10: Immunolocalisation of Stro-1 in tissue sections from a normal (**a**) and diabetic (**b**) rat at one week post-operation. Positive cells are indicated by arrows. Where visible, the implant socket is indicated by IS. Inset into both images are a magnified areas of the images.

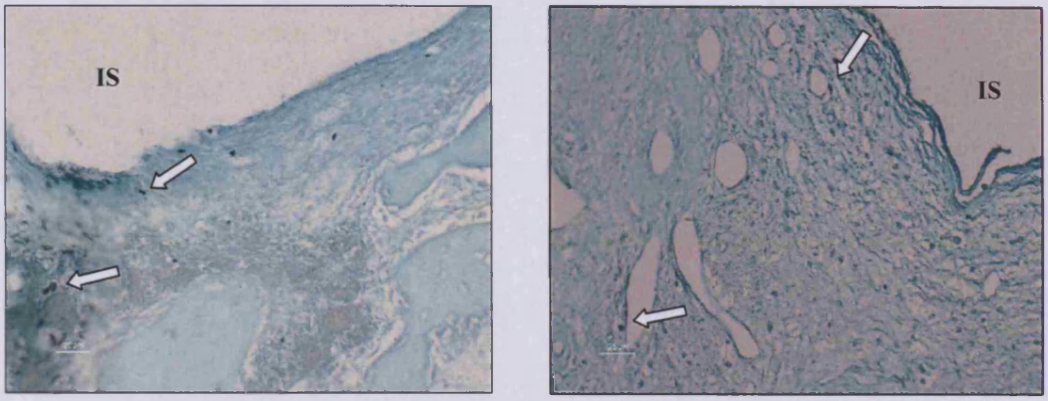

c d

Figure 5.11: Immunolocalisation of Stro-1 in tissue sections from a normal (**c**) and a diabetic (**d**) rat at three weeks post-operation. Positive cells are indicated by arrows. The implant socket, where visible is indicated by IS.

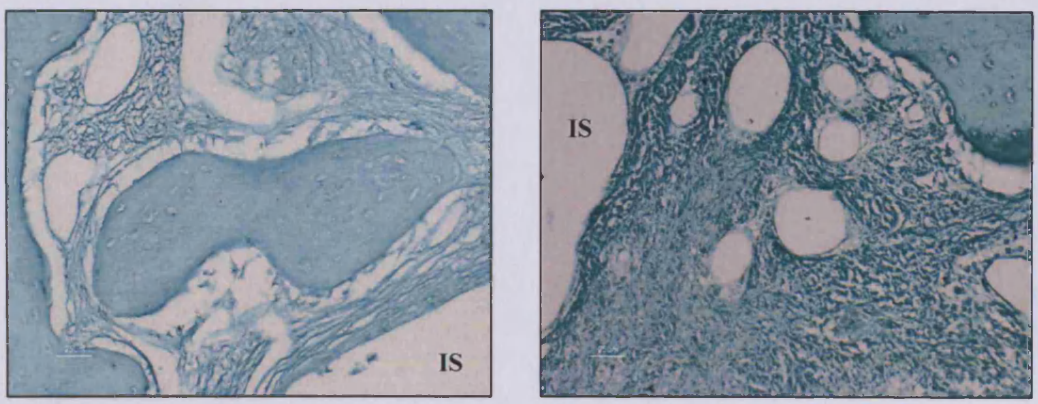

a b

Figure 5.12: Immunolocalisation of Stro-1 in tissue sections from a normal (**a**) and a diabetic (**b**) rat at nine weeks post-operation. The implant socket, where visible is indicated by IS.

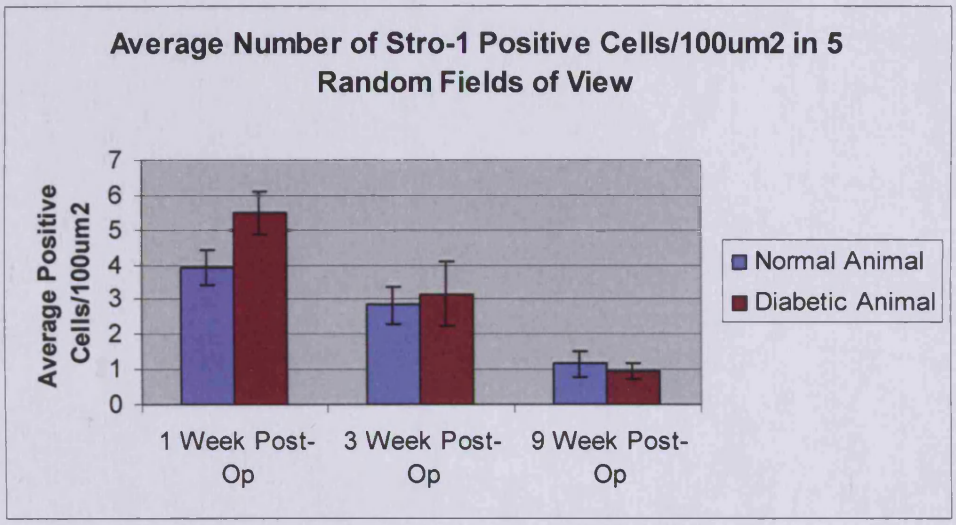

Figure 5.13: Graph of the average number of Stro-1 positive cells per $100\mu m^2$ in five random fields of view over one, three and nine weeks post operation.

5.3.4 Immunolocalisation of PCNA

Images resulting from the immunolocalisation of proliferating cell nuclear antigen (PCNA) are shown in Figures 5.14-5.17. PCNA positivity is indicated by brown cellular staining. In the diabetic condition, there was a prolonged expression of PCNA compared to normal controls. PCNA was not highly expressed in sections from either normal or diabetic animals at one week post-operation, although higher levels were observed in the normal animal (Figure 5.14). This is in contrast to three weeks post-operation (Figure 5.15), when a high degree of PCNA positivity was seen around both normal and diabetic implant sites. At nine weeks post-operation (Figure 5.16) however, PCNA was not widely expressed around the normal implant site, but was expressed at a higher level around the diabetic implant site. At twelve weeks post-operation (Figure 5.17), PCNA did not appear to be expressed around the implant site in sections from either normal or diabetic animals. Figure 5.18 shows a graph of the average number of PCNA positive cells per $100\mu m^2$ in tissue sections from both animals over all four time points.

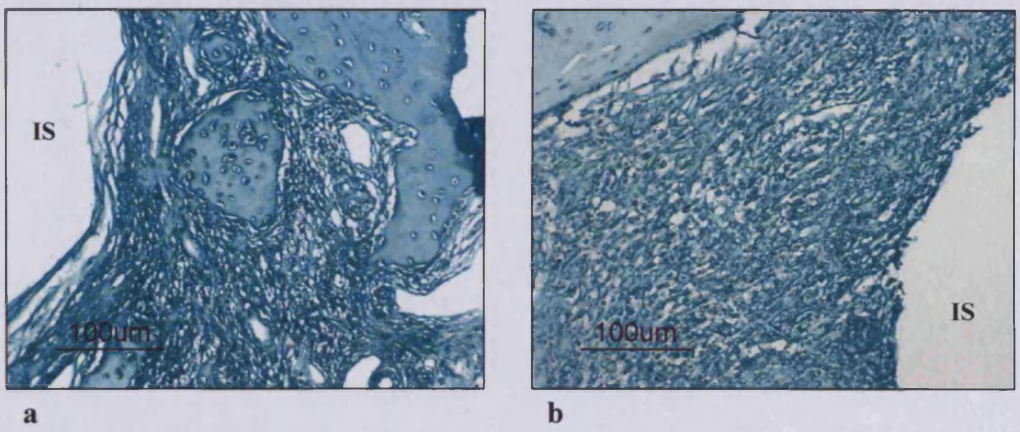

Figure 5.14: Immunolocalisation of PCNA in tissue sections from a normal (**a**) and a diabetic (**b**) rat at one week post-operation. The implant socket is indicated by IS.

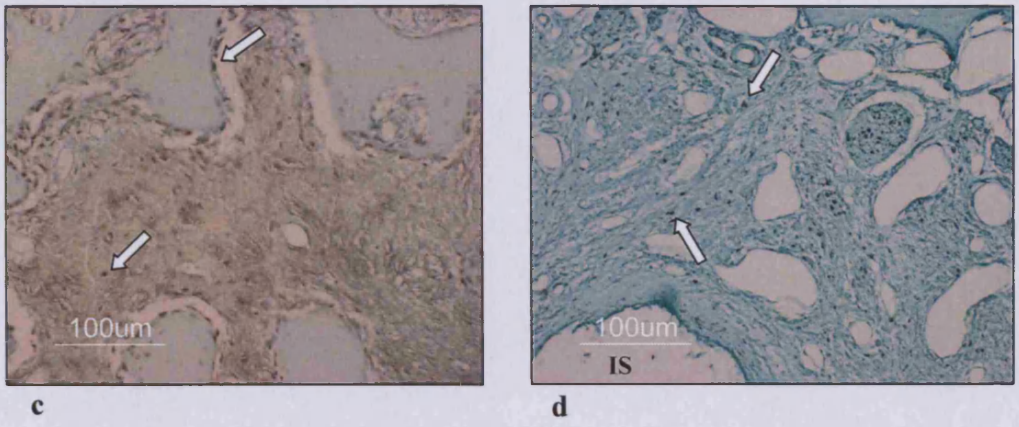

Figure 5.15: Immunolocalisation of PCNA in tissue sections from a normal (**c**) and a diabetic (**d**) rat at three weeks post-operation. Positive cells are indicated by arrows. The implant socket, where visible, is indicated by IS.

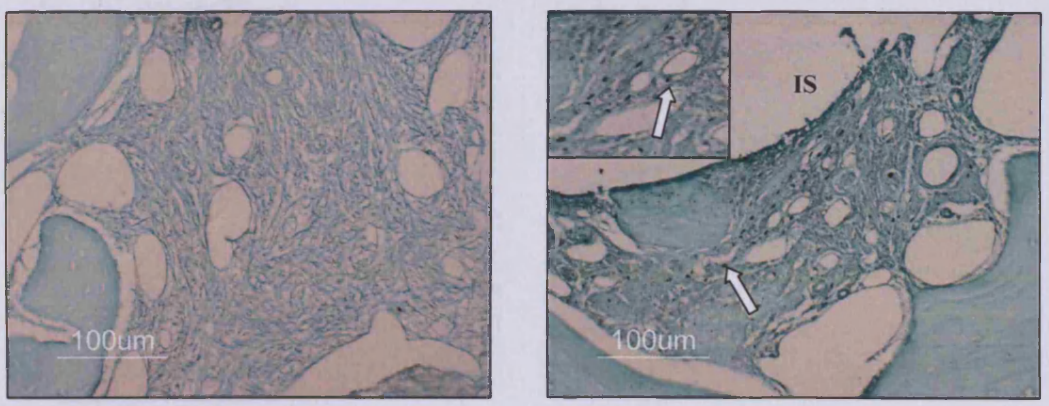

a b

Figure 5.16: Immunolocalisation of PCNA in tissue sections from both a normal (**a**) and a diabetic (**b**) rat at nine weeks post-operation. Examples of positive cells are indicated by arrows. Where visible, the implant socket is indicated by IS. Inset into image **b** is a magnified area of the image.

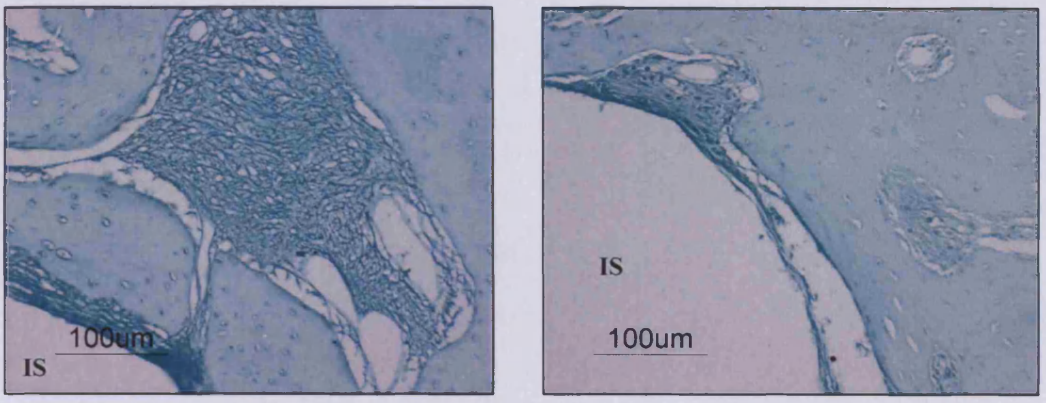

c d

Figure 5.17: Immunolocalisation of PCNA in tissue sections from both a normal (above) and a diabetic (below) rat at twelve weeks post-operation. The implant socket, where visible, is indicated by IS.

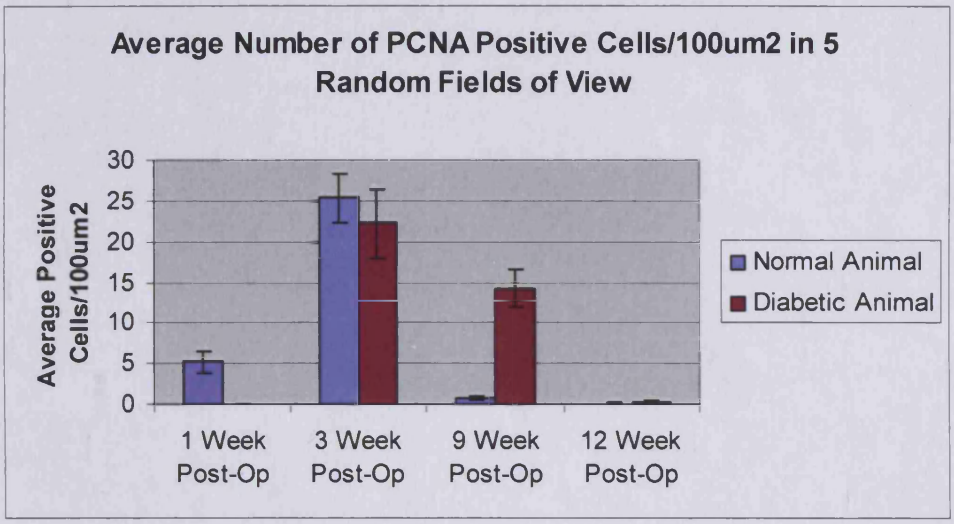

Figure 5.18: Graph of the average number of PCNA positive cells per $100\mu m^2$ in five random fields of view over one, three, nine and twelve weeks post operation.

5.3.5 Immunolocalisation of Osteopontin

Images obtained from the immunolocalisation of osteopontin are shown in Figures 5.19-5.22. Osteopontin expression is indicated by brown cellular staining and followed approximately the same pattern as PCNA expression, with a prolonged expression in the diabetic condition. At one week post-operation osteopontin was present in a relatively low level around the implant sites of both normal and diabetic animals (Figure 5.19). By three weeks post-operation (Figure 5.20), osteopontin was expressed at high levels around the implant site in both normal and diabetic animals, with much lower levels of expression in the normal animal by nine weeks post-operation. In contrast, the expression of osteopontin in the diabetic animal at this time point was higher, being comparable to the three week post-operative level (Figure 5.21). Finally, at twelve weeks post-operation (Figure 5.22), there was very little osteopontin expression around the implant site in either animal. Figure 5.23 shows a graph of the average number of osteopontin positive cells per $100\mu m^2$ in tissue sections from both animals over all four time points.

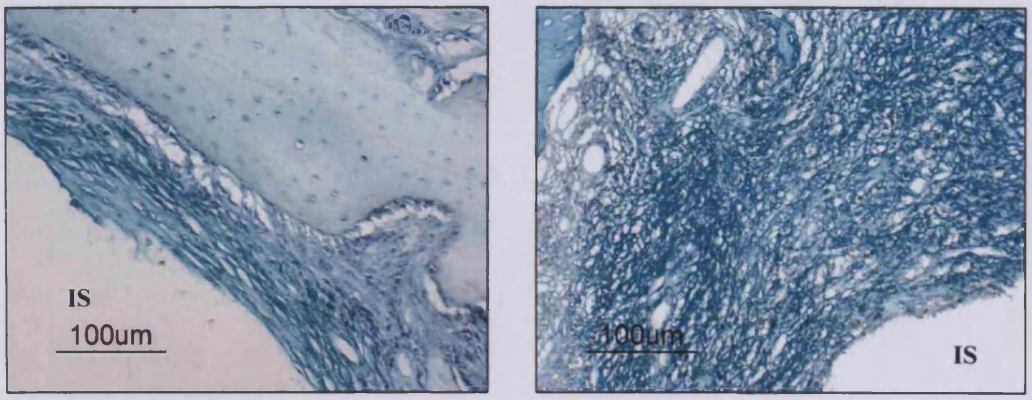

a b

Figure 5.19: Immunolocalisation of osteopontin in tissue sections from both a normal (**a**) and a diabetic (**b**) rat at one week post-operation. The implant socket, where visible, is indicated by IS.

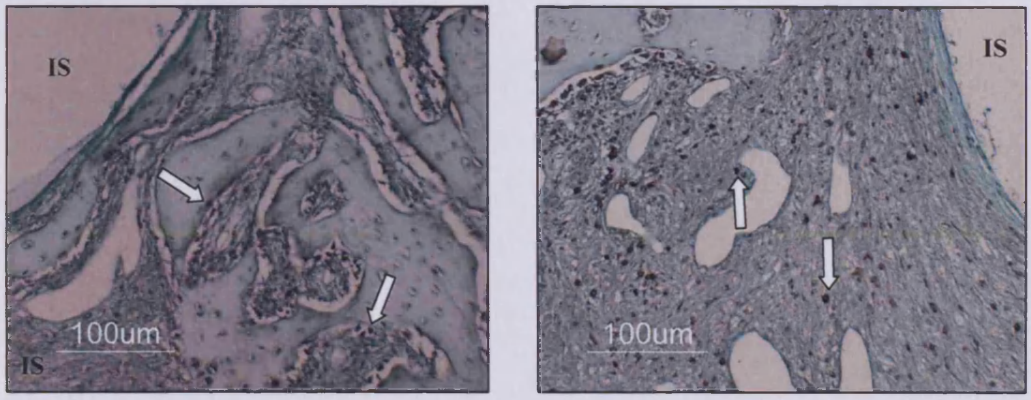

c d

Figure 5.20: Immunolocalisation of osteopontin in tissue sections from both a normal (**c**) and a diabetic (**d**) rat at three weeks post-operation. Positive cells are indicated by arrows. The implant socket, where visible, is indicated by IS.

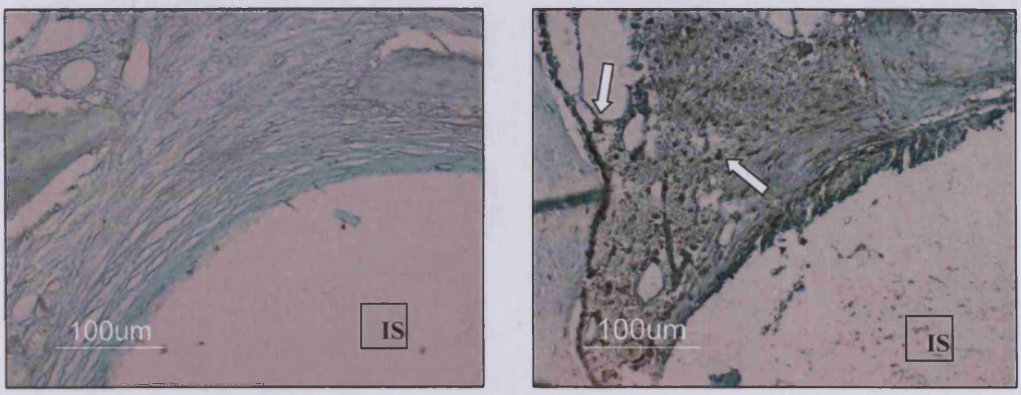

a b

Figure 5.21: Immunolocalisation of osteopontin in tissue sections from both a normal (**a**) and a diabetic (**b**) rat at nine weeks post-operation. Examples of positive cells are indicated by arrows. The implant socket, where visible, is indicated by IS.

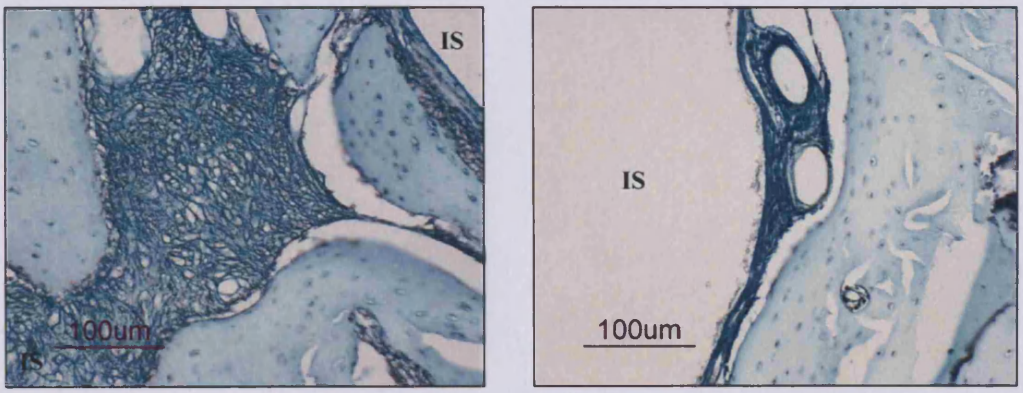

c d

Figure 5.22: Immunolocalisation of osteopontin in tissue sections from both a normal (**c**) and a diabetic (**d**) rat at twelve weeks post-operation. The implant socket, where visible, is indicated by IS.

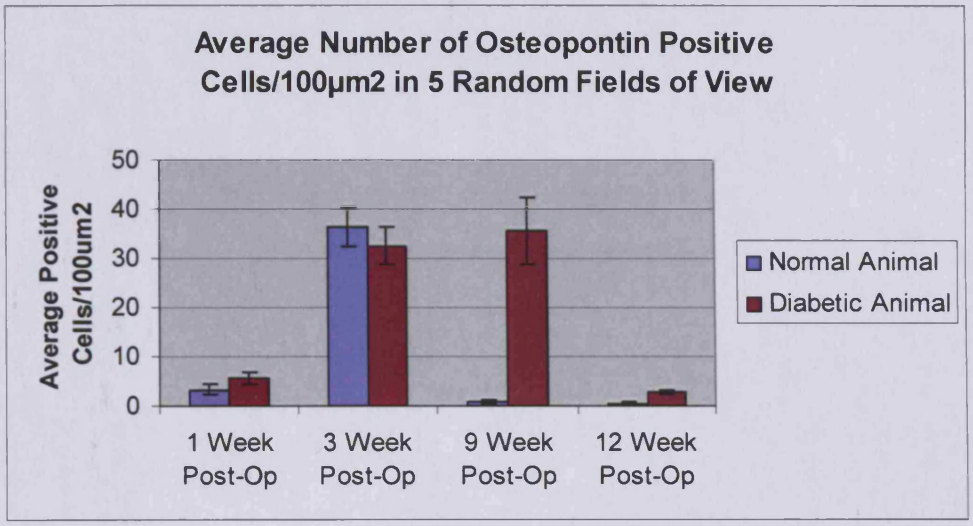

Figure 5.23: Graph of the average number of osteopontin positive cells per $100\mu m^2$ in five random fields of view over one, three, nine and twelve weeks post operation.

5.3.6 Immunolocalisation of Osteocalcin

Images obtained from the immunolocalisation of osteocalcin are shown in Figures 5.24-5.27. Osteocalcin expression is indicated by brown cellular staining. Overall, expression of osteocalcin appeared to take place earlier in the normal animals compared to their diabetic counterparts. No expression of osteocalcin was observed at one week post-operation in either animal (Figure 5.24). At three weeks post-operation (Figure 5.25), there was a significantly higher level of expression around the implant site in the normal animal compared to the diabetic animal. The opposite situation exists at nine weeks post-operation (Figure 5.26), where there was minimal expression around the implant site in the normal animal, while there was a higher degree of expression around the diabetic implant site. By twelve weeks post operation (Figure 5.27), there was not a substantial expression of osteocalcin around the implant sites in either animal, although the level of expression in the normal animal was slightly higher. Figure 5.28 shows a graph of the average number of osteocalcin positive cells per $100\mu m^2$ in tissue sections from both animals over all four time points.

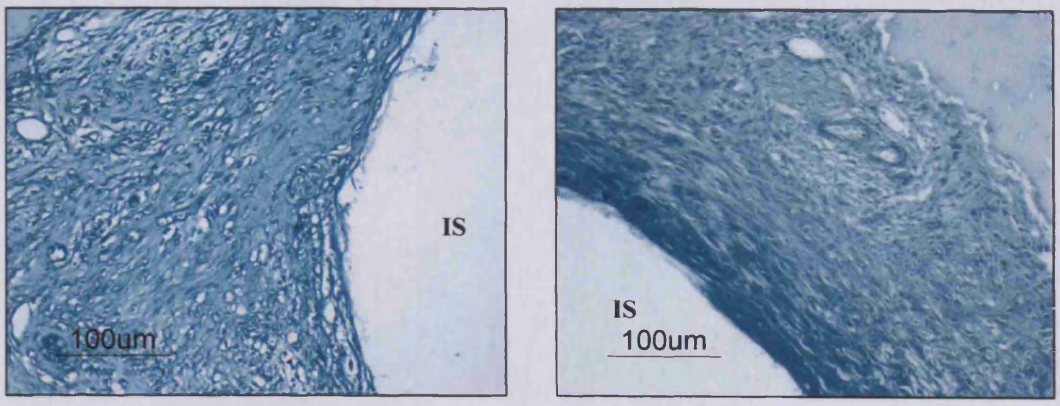

Figure 5.24: Immunolocalisation of osteocalcin in tissue sections from both a normal (**a**) and a diabetic (**b**) rat at one week post-operation. The implant socket is indicated by IS.

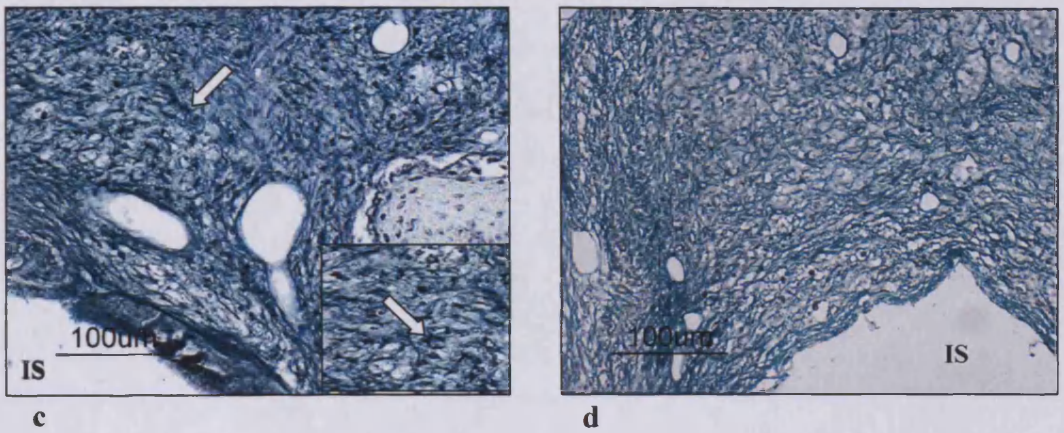

Figure 5.25: Immunolocalisation of osteocalcin in tissue sections from a normal (**c**) and a diabetic (**d**) rat at three weeks post-operation. Examples of positive cells are given by arrows. The implant socket, where visible, is indicated by IS. Inset into image **c** is a magnified area of the image.

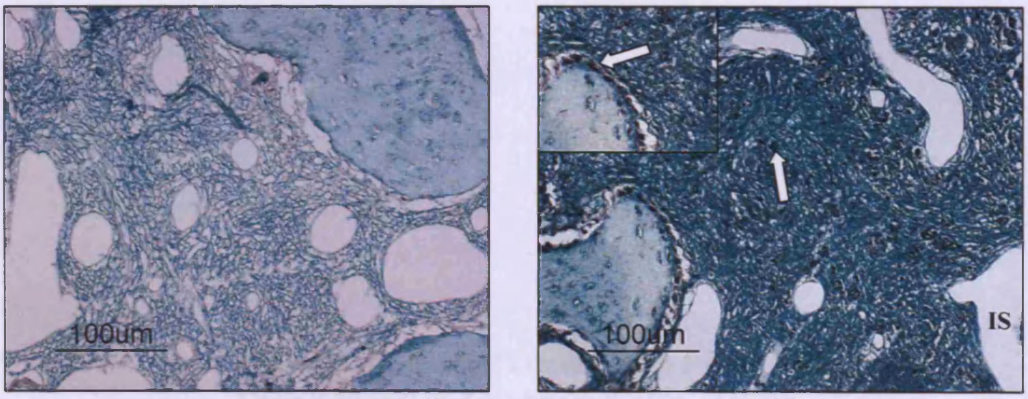

a b

Figure 5.26: Immunolocalisation of osteocalcin in tissue sections from both a normal (**a**) and a diabetic (**b**) rat at nine weeks post-operation. The implant socket is indicated by IS. Inset into image **b** is a magnified area of the image.

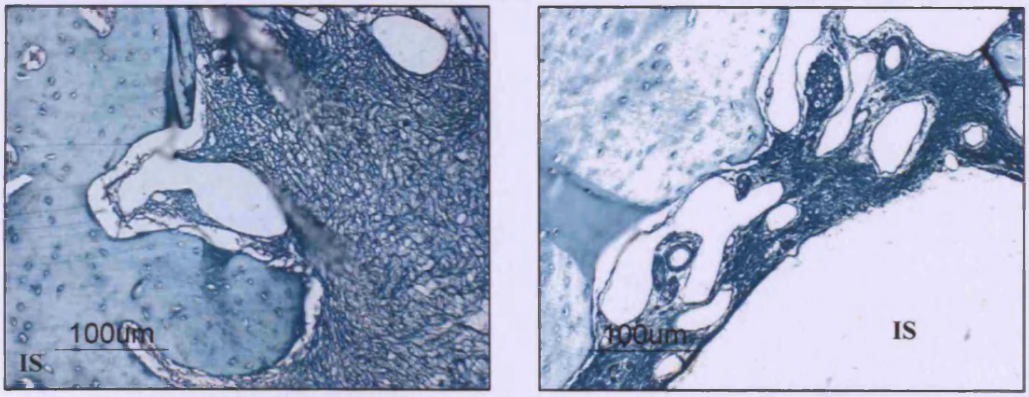

c d

Figure 5.27: Immunolocalisation of osteocalcin in tissue sections from both a normal (**c**) and a diabetic (**d**) rat at twelve weeks post-operation. The implant socket, where visible, is indicated by IS.

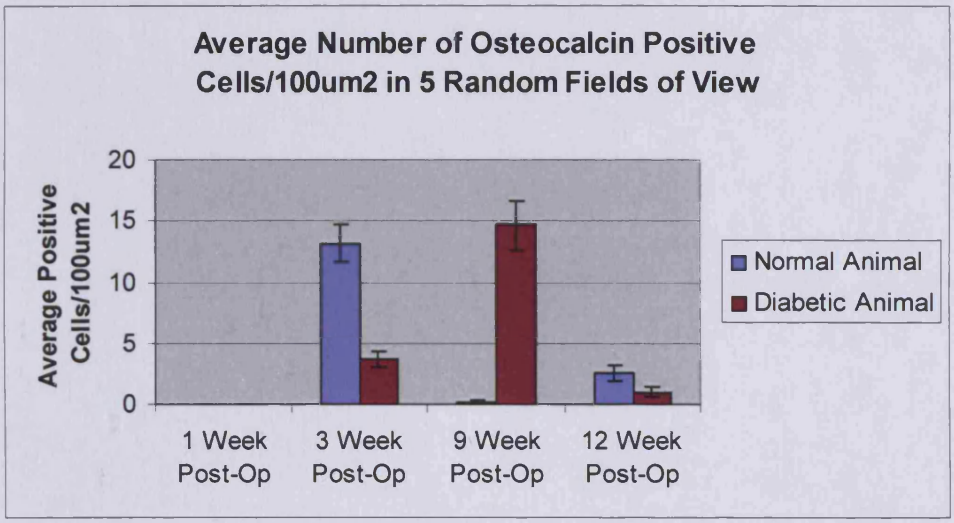

Figure 5.28: Graph of the average number of osteocalcin positive cells per $100\mu m^2$ in five random fields of view over one, three, nine and twelve weeks post operation.

5.3.7 Immunolocalisation of TGFβ1

Images obtained from the immunolocalisation of TGFβ1 are shown in Figures 5.29-5.32. TGFβ1 expression is indicated by brown cellular staining. Expression of TGFβ1 appeared to be delayed in the diabetic condition, as opposed to an early peak of expression in the normal animals. TGFβ1 expression was higher at week 1 post-operation in the normal animal compared to its diabetic counter-part at (Figure 5.29). At 3 weeks post operation however, similar levels of TGFβ1 expression were observed around both the normal and the diabetic implant site (Figure 5.30). TGFβ1 was seen around both implant sites at 9 weeks post operation, although at a lower level in the normal animal (Figure 5.31). Finally, at the 12 week time point, expression was higher in the normal animal (Figure 5.32). Figure 5.33 shows a graph of the average number of TGFβ1 positive cells per $100\mu m^2$ in tissue sections from both animals over all four time points.

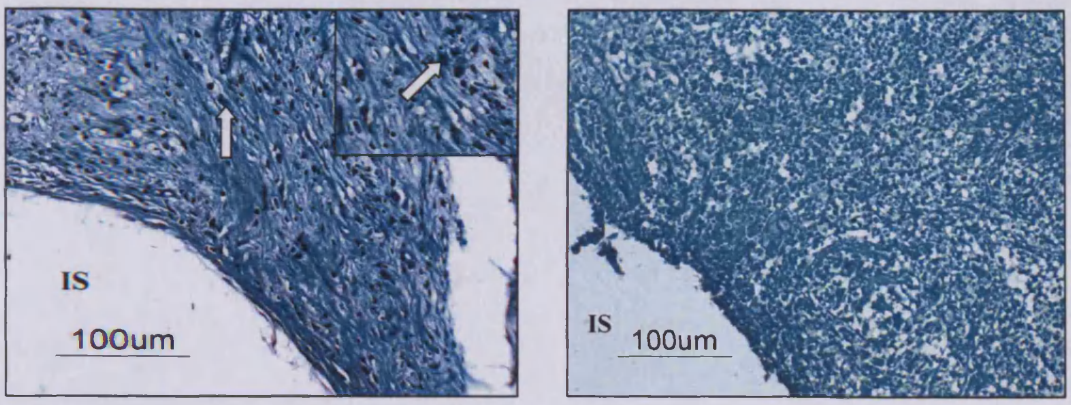

Figure 5.29: Immunolocalisation of TGFβ1 in tissue sections from both a normal (**a**) and a diabetic (**b**) rat at one week post-operation. Examples of positive cells are indicated by arrows. The implant socket is indicated by IS. Inset into image **a** is a magnified area of the image.

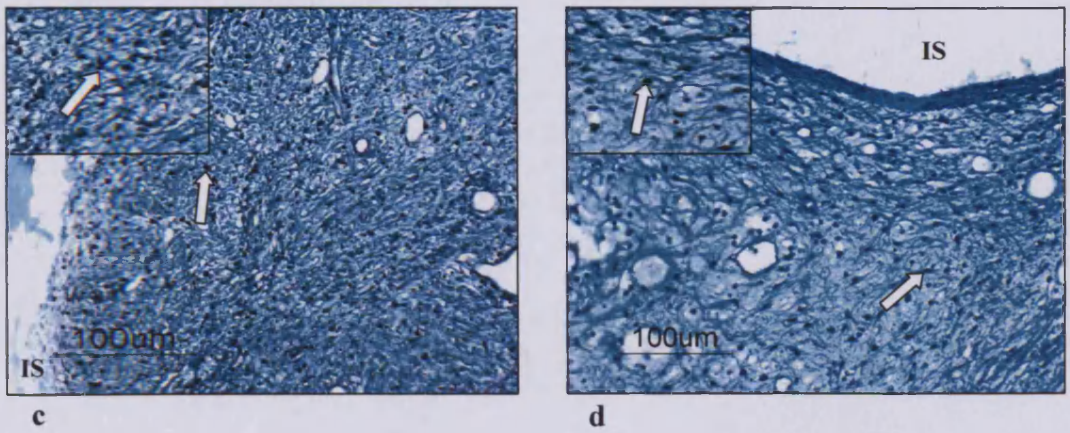

Figure 5.30: Immunolocalisation of TGFβ1 in tissue sections from both a normal (**c**) and a diabetic (**d**) rat at three weeks post-operation. Example of positive cells are indicated by arrows. The implant socket, where visible, is indicated by IS. Inset into both images are a magnified areas of the images.

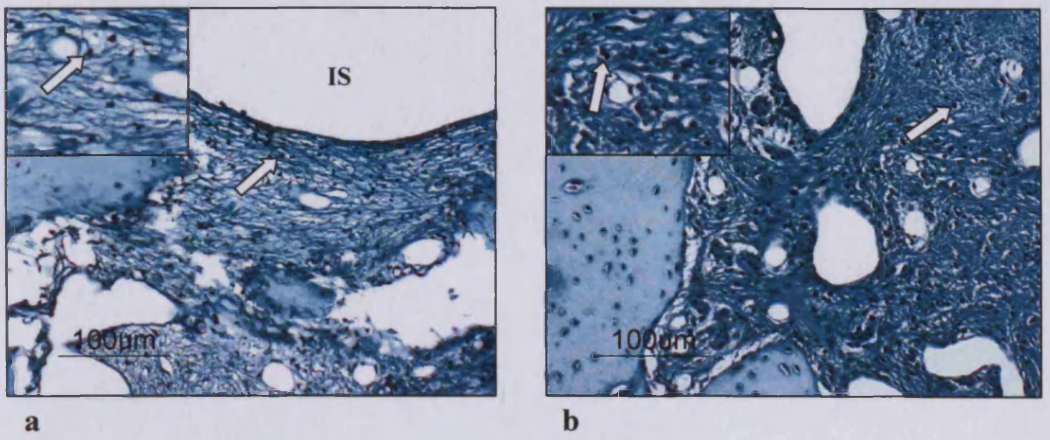

Figure 5.31: Immunolocalisation of TGFβ1 in tissue sections from both a normal (**a**) and a diabetic (**b**) rat at nine weeks post-operation. Examples of positive cells are indicated by arrows. The implant socket, where visible is indicated by IS. Inset into both images are a magnified areas of the images.

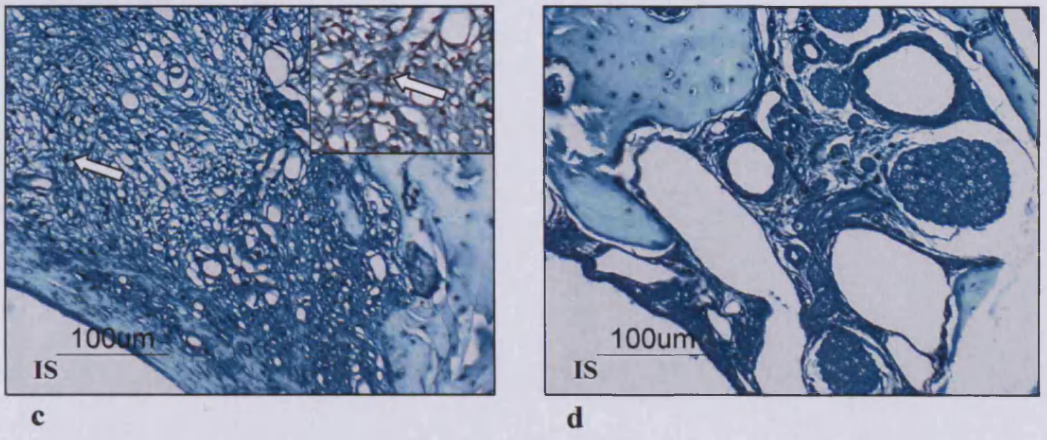

Figure 5.32: Immunolocalisation of TGFβ1 in tissue sections from both a normal (**c**) and a diabetic (**d**) rat at twelve weeks post-operation. Example of positive cells are indicated by arrows. The implant socket, where visible, is indicated by IS. Inset into image **c** is a magnified area of the image.

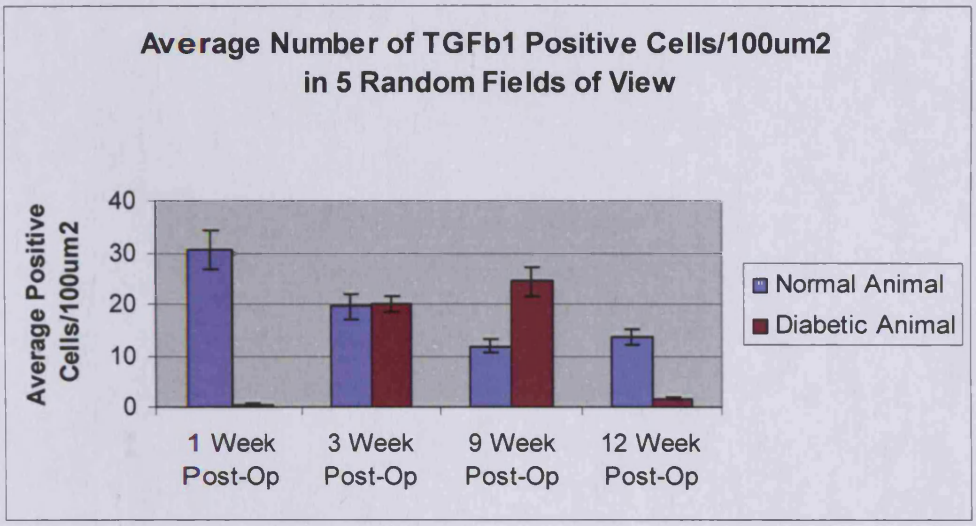

Figure 5.33: Graph of the average number of TGFβ1 positive cells per $100\mu m^2$ in five random fields of view over one, three, nine and twelve weeks post operation.

5.3.8 Immunolocalisation of IL-1β

Images obtained from the immunolocalisation of IL-1β are shown in Figures 5.34-5.37. IL-1β positivity is indicated by brown cellular staining. IL-1β expression appeared to be delayed in the diabetic healing process, with an early expression around the normal implant site which was not seen around the diabetic. At one-week post operation, expression of IL-1β was evident around the normal implant site but was absent from the diabetic (Figure 5.34). At three weeks post-operation, IL-1β was expressed around the implant site in both normal and diabetic animals, although expression was higher in the normal animal (Figure 5.35). At both the 9 (Figure 5.36) and 12 (Figure 5.37) week time points, no expression was seen in either animal. Figure 5.38 shows a graph of the average number of IL-1β positive cells per $100\mu m^2$ in tissue sections from both animals over all four time points.

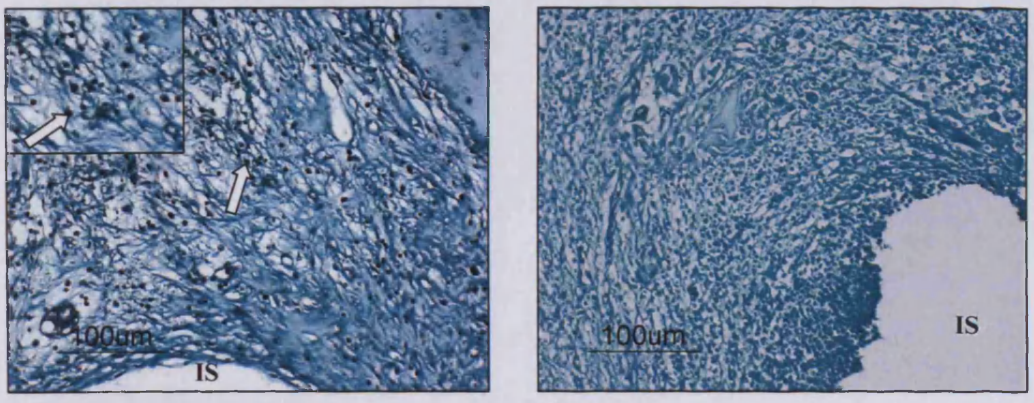

a b

Figure 5.34: Immunolocalisation of IL-1β in tissue sections from both a normal (**a**) and a diabetic (**b**) rat at one week post-operation. Examples of positive cells are indicated by arrows. The implant socket, where visible, is indicated by IS. Inset into image **a** is a magnified area of the image.

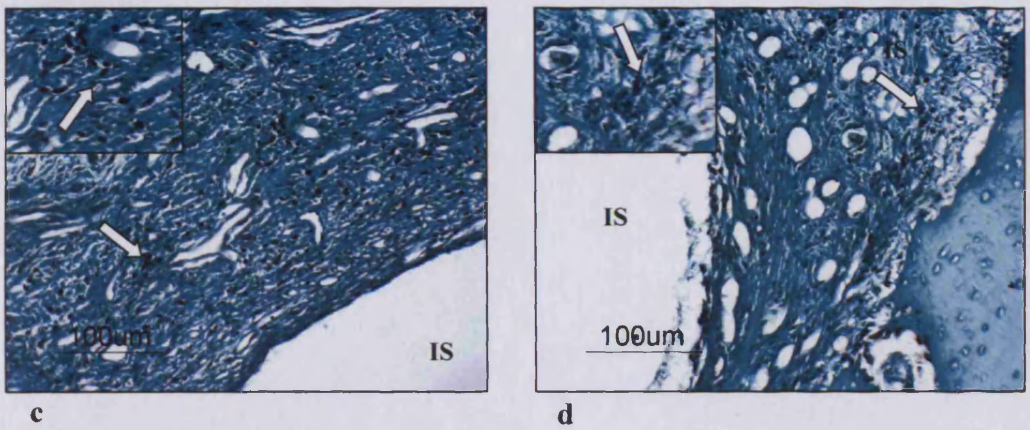

c d

Figure 5.35: Immunolocalisation of IL-1β in tissue sections from both a normal (**c**) and a diabetic (**d**) rat at three week post-operation. Examples of positive cells are indicated by arrows. The implant socket, where visible, is indicated by IS. Inset into both images are a magnified areas of the images.

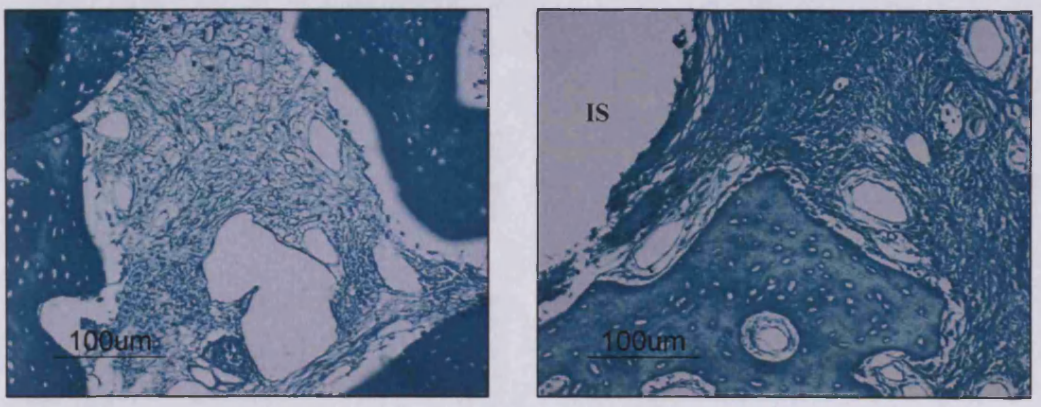

a b

Figure 5.36: Immunolocalisation of IL-1β in tissue sections from both a normal (**a**) and a diabetic (**b**) rat at nine week post-operation. The implant socket, where visible, is indicated by IS.

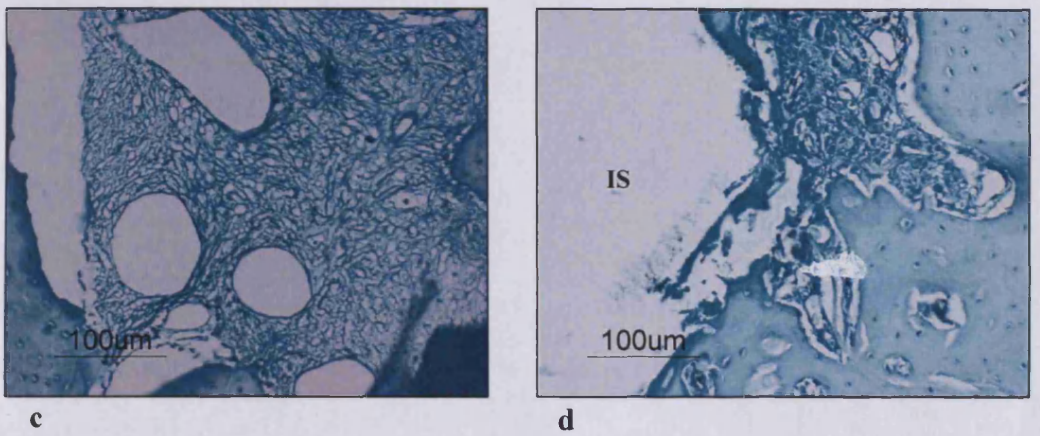

c d

Figure 5.37: Immunolocalisation of IL-1β in tissue sections from both a normal (**c**) and a diabetic (**d**) rat at twelve week post-operation. The implant socket, where visible, is indicated by IS.

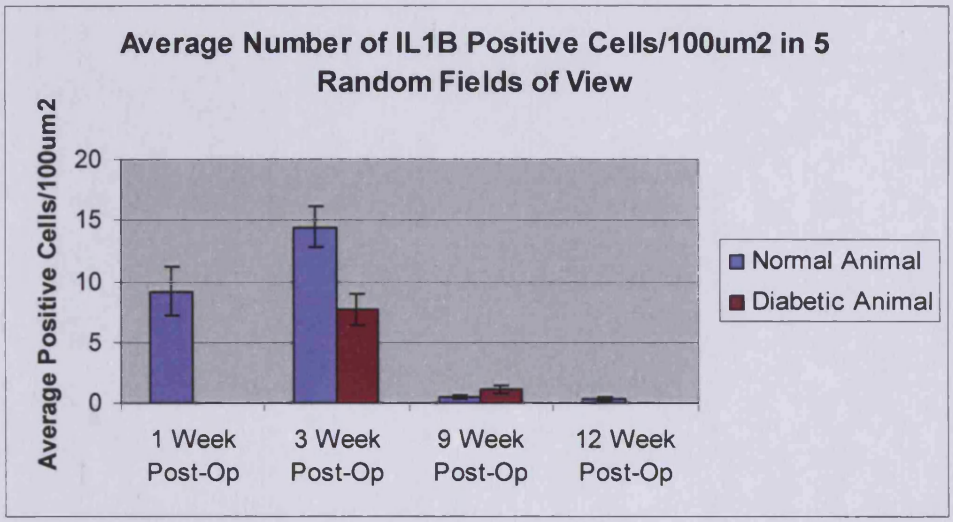

Figure 5.38: Graph of the average number of IL1-β positive cells per 100μm^2 in five random fields of view over one, three, nine and twelve weeks post operation.

5.3.9 Immunolocalisation of TNFα

Images obtained from the immunolocalisation of TNFα are shown in Figures 5.39-5.42. TNFα positivity is indicated by brown cellular staining. TNFα was only seen to be expressed in the diabetic animal at the 3 week post operative time point and expression levels were relatively low (Figure 5.40). Figure 5.43 shows a graph of the average number of TNFα positive cells per $100\mu m^2$ in tissue sections from both animals over all four time points.

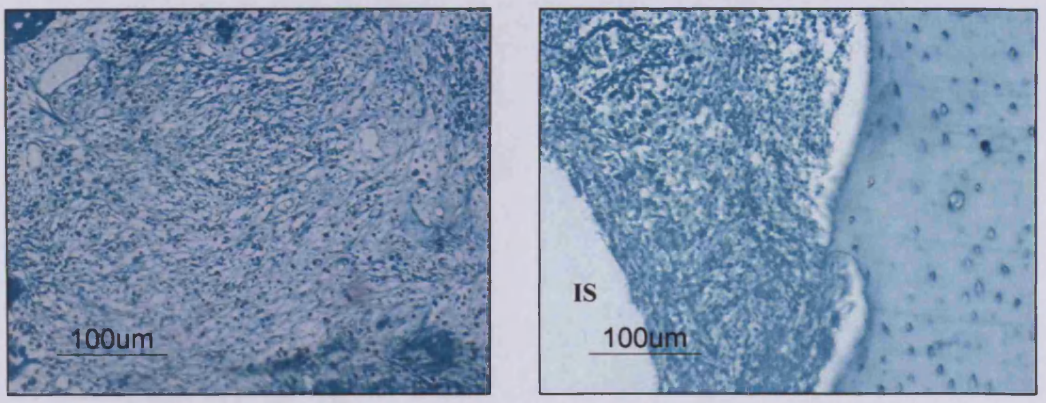

a b

Figure 5.39: Immunolocalisation of TNFα in tissue sections from both a normal (**a**) and a diabetic (**b**) rat at one week post-operation. The implant socket, where visible, is indicated by IS.

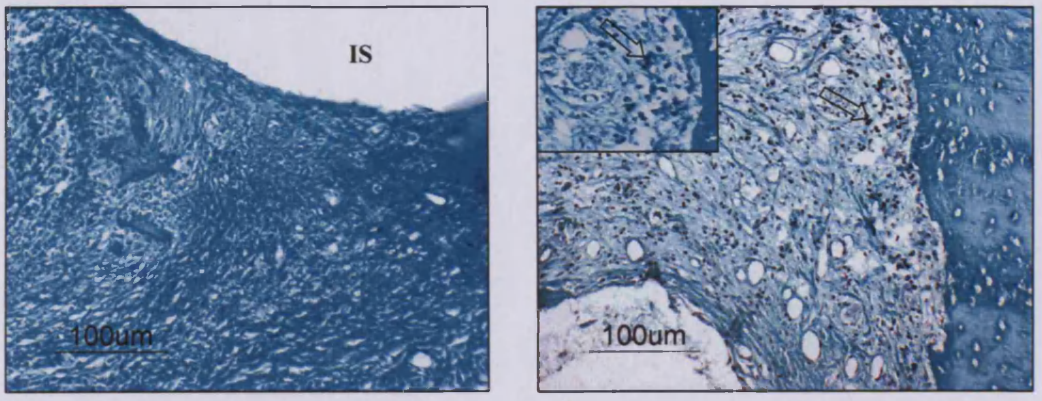

c d

IS

Figure 5.40: Immunolocalisation of TNFα in tissue sections from both a normal (**c**) and a diabetic (**d**) rat at three weeks post-operation. Examples of positive cells are indicated by arrows. The implant socket, where visible, is indicated by IS. Inset into image **d** is a magnified area of the image.

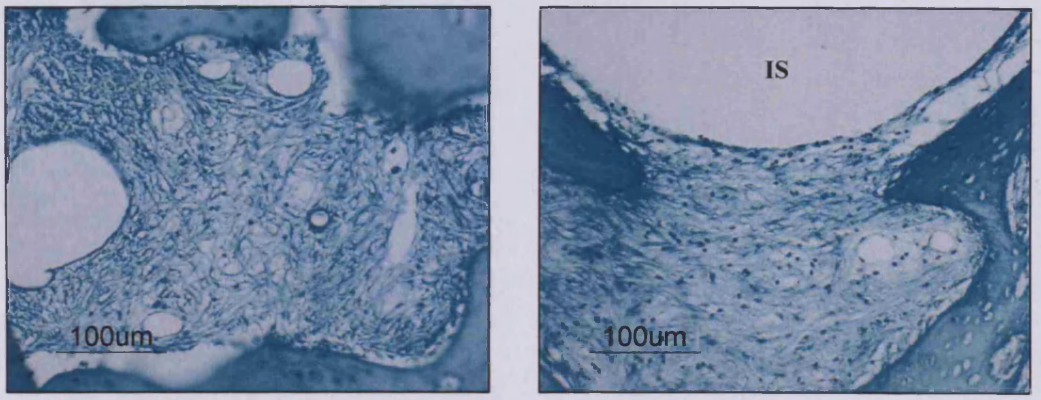

a b

Figure 5.41: Immunolocalisation of TNFα in tissue sections from both a normal (**a**) and a diabetic (**b**) rat at nine weeks post-operation. The implant socket, where visible, is indicated by IS.

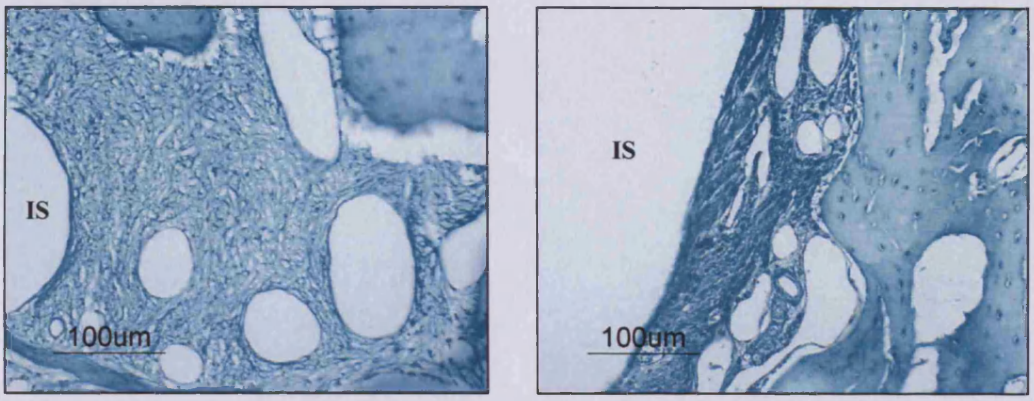

c d

Figure 5.42: Immunolocalisation of TNFα in tissue sections from both a normal (**c**) and a diabetic (**d**) rat at twelve weeks post-operation. The implant socket, where visible, is indicated by IS.

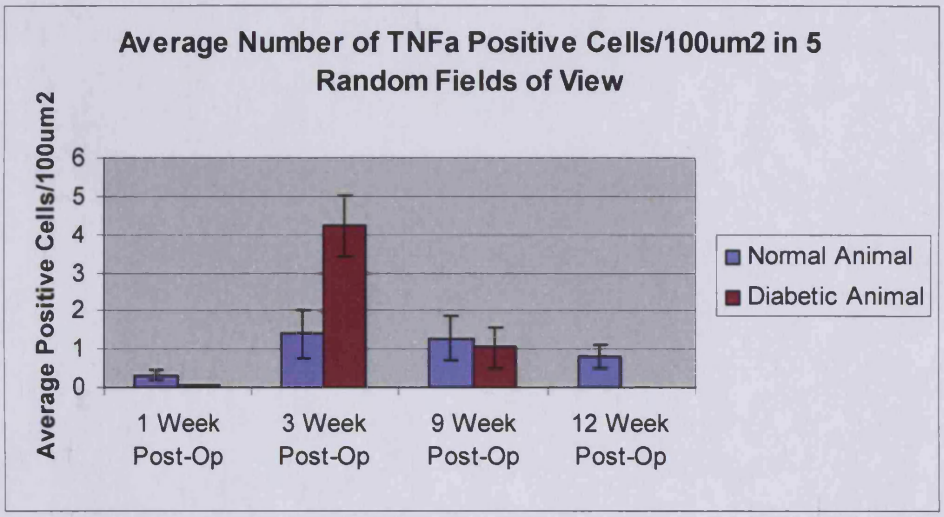

Figure 5.43: Graph of the average number of TNFα positive cells per 100μm^2 in five random fields of view over one, three, nine and twelve weeks post operation.

5.3.10 Immunolocalisation of F4/80

Images obtained from the immunolocalisation of F4/80 are shown in Figures 5.44-5.47. F4/80 positivity is indicated by brown cellular staining. Cells positive for the pan specific macrophage marker F4/80 were apparent in the healing tissue around the normal implant site at one week post-operation, in contrast to the diabetic implant site at this time point, around which no expression was seen (Figure 5.44). Conversely, at 3 weeks post operation, no F4/80 expression appeared around the normal implant site, while there was expression around the diabetic implant site (Figure 5.45). Figure 5.46 shows that there is even higher expression of F4/80 around the diabetic implant site at 9 weeks post-operation, while there is no expression around the normal implant site. At 12 weeks post operation, there does not appear to be any staining around either normal or diabetic implant sites (Figure 5.47). Figure 5.48 shows a graph of the average number of F4/80 positive cells per $100\mu m^2$ in tissue sections from both animals over all four time points.

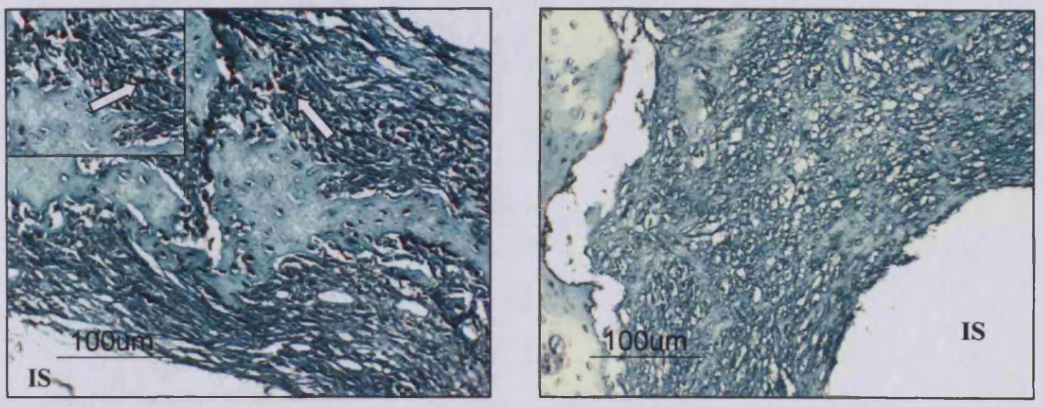

a b

Figure 5.44: Immunolocalisation of F4/80 in tissue sections from both a normal (**a**) and a diabetic (**b**) rat at one week post-operation. Examples of positive cells are indicated by arrows. The implant socket, where visible, is indicated by IS. Inset into image **a** is a magnified area of the image.

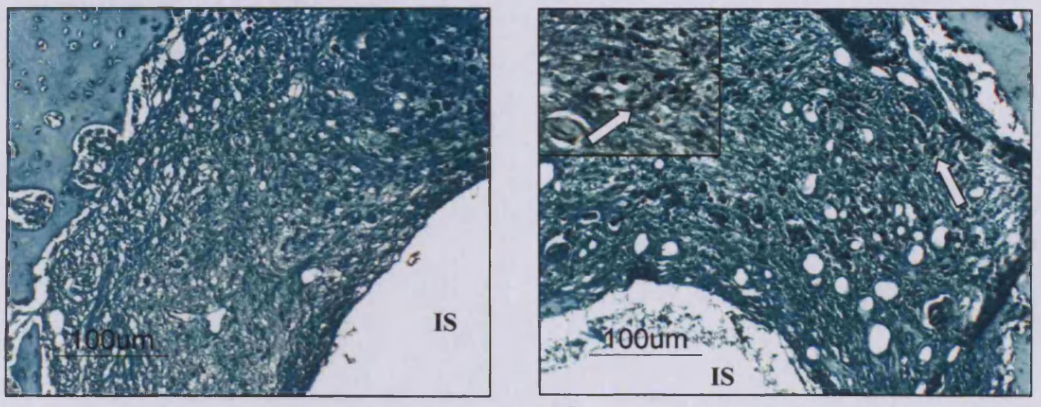

c d

Figure 5.45: Immunolocalisation of F4/80 in tissue sections from both a normal (**c**) and a diabetic (**d**) rat at three weeks post-operation. Examples of positive cells are indicated by arrows. The implant socket, where visible, is indicated by IS. Inset into image **b** is a magnified area of the image.

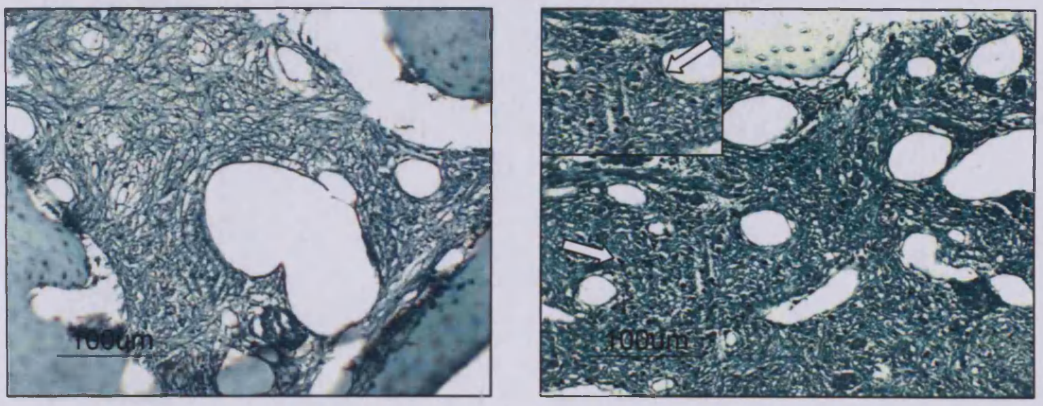

a b

Figure 5.46: Immunolocalisation of F4/80 in tissue sections from both a normal (**a**) and a diabetic (**b**) rat at nine weeks post-operation. Examples of positive cells are indicated by arrows. The implant socket, where visible, is indicated by IS. Inset into image **b** is a magnified area of the image.

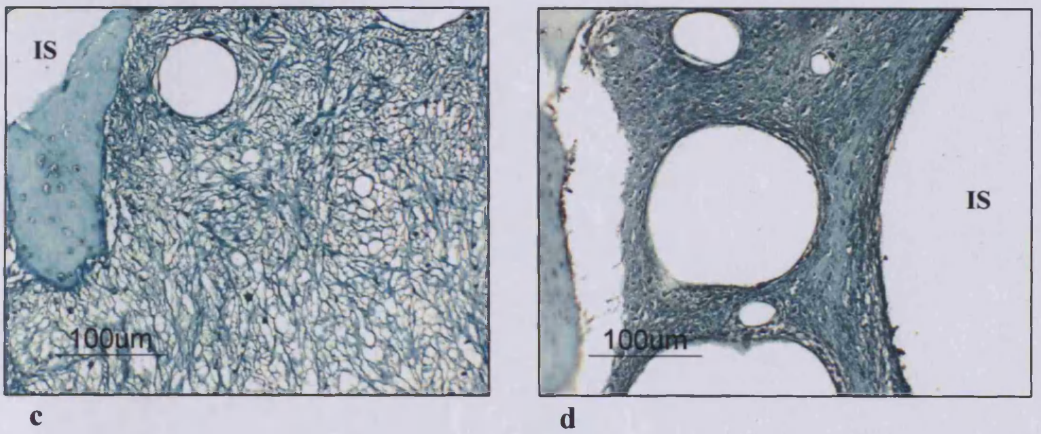

c d

Figure 5.47: Immunolocalisation of F4/80 in tissue sections from both a normal (**c**) and a diabetic (**d**) rat at twelve weeks post-operation. The implant socket, where visible, is indicated by IS.

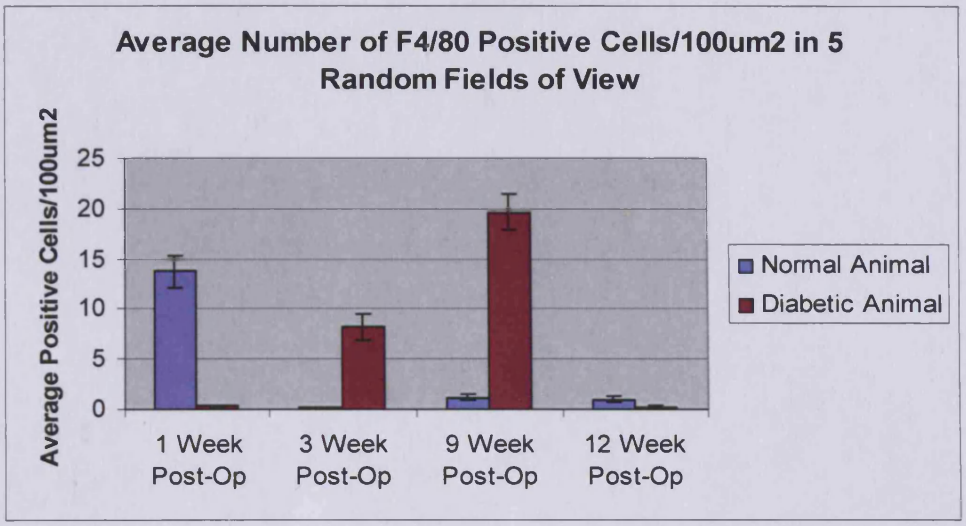

Figure 5.48: Graph of the average number of F4/80 positive cells per $100\mu m^2$ in five random fields of view over one, three, nine and twelve weeks post operation.

5.3.11 Negative Controls

Typical examples of both non-immunogenic IgG (IgM for Stro-1) and primary excluded negative controls for all immunolocalisations performed are shown in Figure 5.49. Both of these negative controls were performed for all tissue sections at all time points and none showed any positive staining.

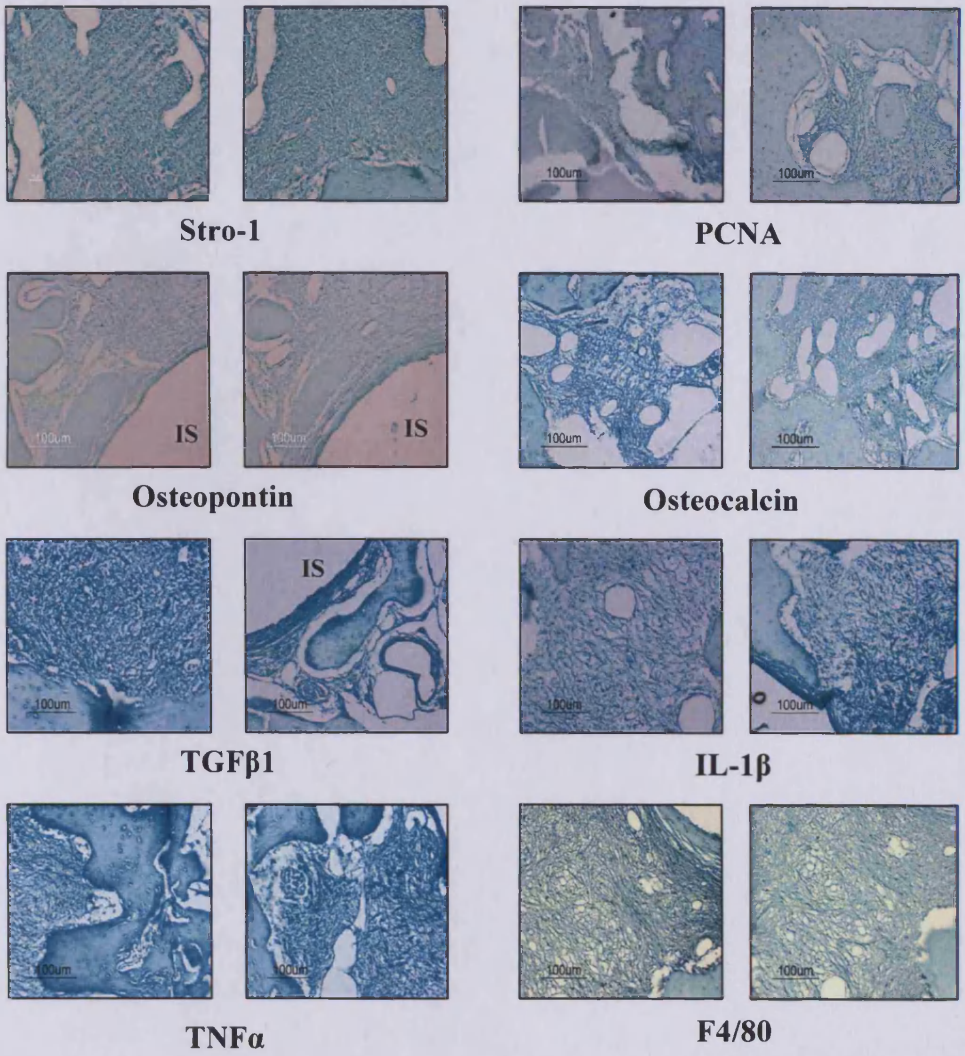

Figure 5.49: Typical examples of negative controls which had the primary antibody excluded (**left**) and a negative control in which a non-immunogenic IgG antibody (non-immunogenic IgM in the case of Stro-1) was used in place of the primary IgG (or IgM for Stro-1) antibody (**right**). These controls were performed for every time point and condition and did not demonstrate any positive staining.

5.3.12 Summary of Immunohistochemistry Results

A flow chart summarising the temporal appearance of the markers examined by immunohistochemistry in both normal and diabetic mandibles is shown in Figure 5.50.

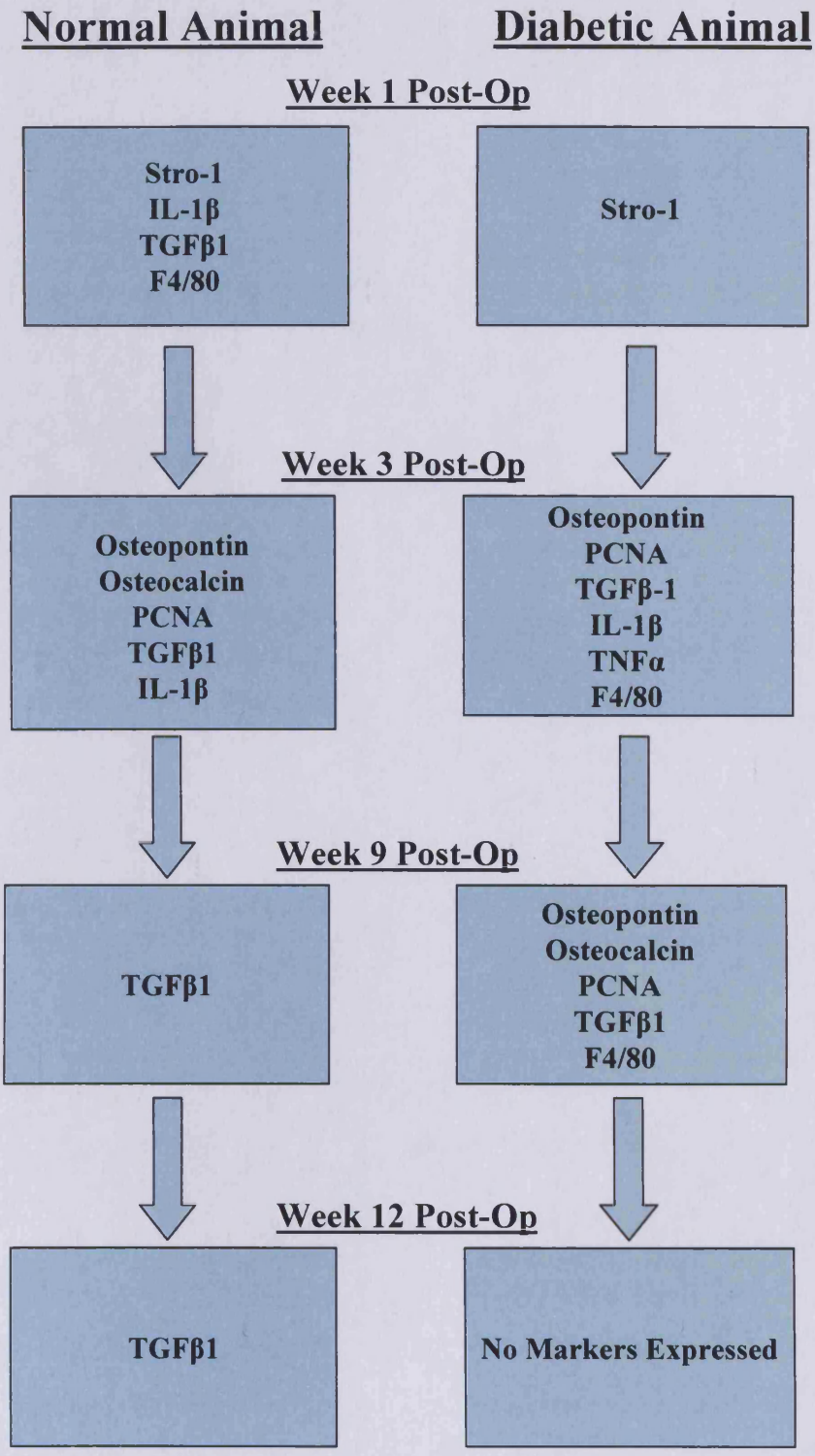

Figure 5.50: A flow chart summarising the immunohistochemistry results at the different time points around the normal and the diabetic implant sites.

5.4 Discussion

The results presented in this chapter show the effectiveness of the *in vivo* model of osseointegration as a means to contrast progression of healing around titanium dental implants in both a normal and a clinically relevant disease state, type II DM. Although bone healing occurred around the implant site in both normal and diabetic animals, diabetic bone healing was shown to be delayed compared to the normal animal, and there were substantial differences in the temporal expression of bone markers, inflammatory cytokines, the growth factor TGFβ1 and the presence of macrophages around the implant site. These results, which indicate behavioural differences between cells around normal and diabetic implant sites, may serve to partially elucidate the cellular basis of the delay in healing observed in diabetic bone.

It is widely reported that there is a delay in bone healing associated with DM (Hasegawa et al. 2008; Kwon et al. 2005; Liu et al. 2007b; McCracken et al. 2000; Shyng et al. 2006; Siqueira et al. 2003), which is in agreement with the histology results presented in this chapter. Although both animals appear to have developed granulation tissue around the implant site by one week post-operation, delayed formation of new bone and deposition of calcium were apparent in the GK rats compared to normal controls. This was particularly evident at 3 weeks post-operation, at which time new bone and tissue mineralisation were seen adjacent to the implant site in the normal animal, while there was no indication of these bone healing responses in the diabetic animal. Healing was again seen to be delayed in the diabetic animal at 9 weeks post-operation, while by 12 weeks post-operation, the diabetic animal had an almost identical amount of bone around the implant socket compared to its normal counterpart, suggesting that osseointegration was occurring in the diabetic animal, but at a substantially slower rate than in the normal animal. The time frame observed for delayed healing in diabetic bone corresponds with much of the literature, although few have investigated diabetic bone healing at a time point as late as 12 weeks (Hasegawa et al. 2008; Kwon et al. 2005; McCracken et al. 2000; Shyng et al. 2006; Siqueira et al. 2003).

One finding presented herein, that is of particular interest, is that the observed delay in bone healing in the diabetic animals did not appear to be the result of the failure of mesenchymal stem cells (MSCs) to arrive at the site of the injury. The expression pattern of Stro-1, a marker for these cells, was the same for both normal and diabetic animals at all time points investigated. This would suggest that MSCs, present in their niche in bone marrow adjacent to the implant site, responded to the extraction of the incisor and placement of the implant, migrated to the site of the injury and infiltrated the granulation tissue and thus were present in both the normal and diabetic animal at 1 week post-operation. Thus it does not appear that either a lack of response from these cells, or an impairment of their ability to migrate to the site of injury were responsible for the observed delayed healing response in diabetes. It is possible, therefore, that this delay arises from alterations in the behaviour of the cells present.

The cell proliferation marker PCNA appeared around the normal implant site at one week post-operation at low levels yet was not expressed around the diabetic implant site until 3 weeks post-operation. It has been previously reported that PCNA expression is delayed in an obese rat model of type II DM bone healing compared to normal controls 2 weeks after an injury to tibia bone (Liu et al. 2007b). Similarly, it has been reported that PCNA is reduced in rat models of type I diabetic bone healing 7 days after controlled femoral fractures (Gebauer et al. 2002; Tyndall et al. 2003). Not only do the results presented in this chapter correspond with the reported delay in the expression of PCNA during the early phase of the diabetic bone healing process, but additionally demonstrate the persistence of PCNA expression around the diabetic implant site at 9 weeks post-operation, in contrast to the corresponding normal implant site. This could suggest that the proliferative response of cells to injury was delayed in the diabetic condition, perhaps contributing to the observed delay in diabetic bone healing. Furthermore, the sustained proliferative response observed around the diabetic implant site could indicate a sustained inflammatory response, with the proliferation of immune cells such as macrophages, or a delay in the differentiation of proliferating MSCs into post-mitotic osteoblast progenitor cells around the implant site, both of which would likely lead to a delay in bone formation. Certainly, positive staining for F4/80, indicating the presence or macrophages,

corresponds with the persistence of cell proliferation around the diabetic implant site at 9 weeks post-operation.

Also of interest are the differences in the expression of the osteoblast markers osteopontin (OP) and osteocalcin (OC) between normal and diabetic animals. OP, which is expressed early in the process of osteoblast differentiation, has a wide array of functions including playing a role in the attachment of cells, including differentiating osteoblasts, to matrices (Sodek et al. 2000). The differences in the expression of OP around the diabetic and normal implant sites followed a similar pattern to the differences in PCNA expression, in that OP was present around both implant sites at 3 weeks post-operation, yet persisted around the diabetic implant site at 9 weeks post-operation, by which point it had ceased around the normal. Continued expression of OP around the diabetic implant site could indicate a delay in the progression of osteoblast differentiation, as it is typically expressed in the early stages of this process (Hughes et al. 2006; Sodek et al. 2000). OP also has a number of other complex functions in wound healing however, including a chemo-attractant and anti-apoptotic signal for macrophages, neutrophils, T-cells, fibroblasts and endothelial cells as well as osteoblast progenitor cells via CD 44 interaction (Ashkar et al. 2000; Denhardt et al. 2001; O'Regan et al. 1999; Wang and Denhardt; Weber et al. 1996). Interestingly, macrophage numbers, as indicated by F4/80 positivity, were much higher around the diabetic implant site at 9 weeks post-operation, which corresponded to the observed persistence of OP and may indicate that OP is playing a role in the continued recruitment of macrophages and possibly other immune cells. This would lead to an extended inflammatory response, which would certainly contribute to a delay in the bone healing process.

OC expression, in contrast to that of OP, is seen to be delayed around the diabetic implant site. While there were high levels of expression around the normal implant site at 3 weeks post-operation, similar levels were not seen in the diabetic animal until 9 weeks post-operation. OC is an osteoblast specific protein which is considered to be an indicator of a mature osteoblast phenotype, and has been proposed to halt the process of bone formation and begin the process of bone remodelling, thus participating the final stage of bone maturation (Boskey et al.

1998; Ducy et al. 1996). Therefore, a temporal delay in the expression of OC, such as was observed in the diabetic animal, would indicate that the osteoblast differentiation pathway is somehow disrupted in type II DM, leading to a delay in process of bone healing.

TGFβ1 is known to be involved in the early phases of the osteoblast differentiation pathway, where it is suggested to be responsible for driving the expansion of osteoblast progenitor cells (Centrella et al. 1994; Hughes et al. 2006). Conversely TGFβ1 has been shown to suppress terminal osteoblast differentiation and the process of mineralisation (Maeda et al. 2004). The expression of TGFβ1 around the normal implant site was at its highest level at 1 week post-operation, with a subsequent decrease to much lower levels at each subsequent time point. These novel findings would indicate that TGFβ1 may be functioning to create a pool of osteoblast progenitor cells at the outset of the healing response, which would then undergo differentiation into more mature osteoblasts as expression decreased. In contrast, around the diabetic implant site, expression of TGFβ1 was not seen until 3 weeks post-operation and was maintained until 9 weeks post-operation. This fits with the delay and prolongation of cell proliferation, continued expression of OP and the delay in OC expression observed in the diabetic animals. If TGFβ1 expression was delayed around the implant site in the diabetic animal, it could cause a delay and subsequent elongation of the initial proliferative phase of osteoblast progenitor cells, which would impair the process of osteoblast differentiation causing the observed alterations in OP and OC expression, in this way contributing to the observed delay in the process of bone formation.

The study presented in this chapter also demonstrated some differences in the expression of inflammatory cytokines between normal and diabetic animals. Differences in the temporal expression of IL-1β and TNFα between normal and diabetic animals may play a role in the observed delay in diabetic bone healing. IL-1β is an inflammatory cytokine with a vast number of complex functions attributed to it. In the context of bone, it has been reported to both inhibit osteoblast proliferation and increase bone formation (Hanazawa et al. 1986; Ohmori et al. 1988) and conversely it may increase osteoblast proliferation while inhibiting

differentiation and thus bone formation, particularly at lower concentrations (Canalis 1986; Ellies and Aubin 1990; Rickard et al. 1993). In the context of the results presented here, IL-1β expression was seen around the normal implant site at 1 and 3 weeks post-operation, as opposed to only at 3 weeks post-operation around the diabetic implant site. It may be that the early expression of IL-1β is the result of a normal early inflammatory response, concomitant with the presence of macrophages around the normal implant site at 1 week post-operation, which served to stimulate the process of osteoblast progenitor cells proliferation, before resolving and enabling the process of osteoblast differentiation and thus bone formation to continue. The delay in IL-1β expression seen around the diabetic implant site may indicate a disruption in the normal process of inflammation and stimulation of bone healing.

TNFα expression, by contrast, was only seen at 3 weeks post-operation in the diabetic animal, and then at a relatively low level. Generally, TNFα is known as inflammatory cytokine which has deleterious effects on the process of bone healing, inhibiting both osteoblast proliferation and differentiation (Bertolini et al. 1986; Gowen et al. 1988) and stimulating bone resorption (Nanes 2003). It is difficult to interpret what the impact of TNFα expression on the process of diabetic bone healing may be, as it is only expressed at a relatively low level at a single post-operative time point. TNFα expression would however, indicate an inflammatory response around the implant site, which would almost certainly impair bone healing, leading to the delay observed in the diabetic animals.

It is an unfortunate fact that only a single animal from each experimental group was available for study at each time point, meaning that there was an N of 1. This work would have been considerably strengthened by the addition of replicate animals; limitations were enforced however, by the sheer distance involved in the collaboration that produced this work. Initially, replicate animals were sought and some replicate mandibles were delivered. Upon inspection of these mandibles however, it was apparent that a large number of implants had not undergone osseointegration, and histological examination revealed evidence of fibrous encapsulation, possibly resulting from infections and incomplete healing. These

replicates were therefore judged to be unusable. Unfortunately time and budgetary constraints did not allow further animals to be obtained from Japan.

In summary, the data presented in this chapter have shown that there is a delay in bone healing around a dental implant site in a rat model of type II DM. Possible causes for the observed delay appear to include a prolongation of cell proliferation and OP expression around the implant site, leading to a delay in progression of the osteoblast differentiation pathway as evidenced by the delay in the expression of OC. Differences in the expression of TGFβ1 around the implant site may contribute to this delay, particularly as the onset of expression is delayed in the diabetic animal. It is also possible that an altered inflammatory response, seen in the variations of the presence of macrophages and expression of IL-1β and TNFα around the implant site, is either partially responsible or a result of the other differences observed between the normal and diabetic implant sites and almost certainly is involved in the observed delay in diabetic bone healing. It is difficult to speculate further from the data presented here however as to possible mechanisms for the observed findings, however these results will hopefully contribute to a greater understanding of the delayed healing which has been widely observed in DM, particularly in relation to titanium dental implants. If the mechanisms by which osseointegration of dental implants is delayed in DM were to be better understood, it is possible that this information could be translated into therapies which would improve outcomes for diabetic individuals, thus broadening their access to treatment.

Chapter 6: The Osseointegration of Modified Titanium Surfaces in Rat Mandibles

6.1 Introduction

As discussed in detail within the introduction of this thesis, the bone repair process which takes place around the site of a titanium dental implant has several key phases. Fibrin clot formation, the activation and resolution of the inflammatory response, the initiation of bone formation and the bone remodelling process all interact in order to bring about the final osseointegration of the implant (Davies 2003; Hughes et al. 2006). The regulation of the progression of these phases is highly complex, and it is nearly impossible to consider all aspects of it when attempting to accurately model this process *in vitro*. An *in vitro* model involving osteoblast-like cells being cultured on titanium surfaces under mineralising conditions has been described this thesis, and examples of many similar model systems can be found in the literature (Deligianni et al. 2001; Qu et al. 2007; Salido et al. 2007; Schneider et al. 2003; Tsukimura et al. 2008; Zhao et al. 2005). These models are useful as they serve to simplify a highly complex process, thereby allowing the direct impact of surface modification on osteoblast activity to be investigated and interpreted. As a result of this simplification however, these models disregard important aspects of osseointegration, making it difficult to define the influence that alterations in surface parameters such as topography and chemistry have on this process in a clinical situation, when these implants are placed in patients. The use of an *in vivo* model of osseointegration, which can model all aspects of the process of osseointegration, is therefore a key component in determining potential clinical benefits of surface modification.

An *in vivo* rat model of dental implant osseointegration, developed in conjunction with Osaka Dental University in Japan (Sakai et al. 2008), has been described in this thesis and was used to investigate the effects of DM on the osseointegration of implants with machined surfaces. In this chapter however, the same model system was used to investigate the osseointegration of titanium dental

implants with modified titanium surfaces. These surfaces were modified in the same way as the titanium discs used in the *in vitro* investigations described in this thesis. This provides a direct link between observations made regarding the behaviour of osteoblast progenitor cells attached to each of the experimental surfaces and the impact of these surfaces on the process of bone healing upon their insertion into a rat mandible. It has been previously reported in the literature that a variety of modified surfaces have enhanced osseointegration *in vivo* (Buser et al. 2004; Cho and Park 2003; Cochran et al. 1998; Franchi et al. 2007; Schwarz et al. 2007; Sul et al. 2005; Sul et al. 2001; Wennerberg et al. 1998). It may be the case that, due to the complexities of the bone repair process, osteoblast progenitor cells behave similarly on two differently modified surfaces *in vitro*, while these surface modifications have implications for the osseointegrative potential of an implant *in vivo*. This possibility therefore renders the use of this model critical to the investigation of the impact of titanium surface modification on osseointegrative potential.

The work described in Chapter 3 questioned whether the modification of titanium surfaces caused accelerated bone formation or improved mechanical interlocking with bone matrix, resulting in better bone attachment. The use of *in vivo* model of the osseointegration of modified titanium surfaces will serve to further clarify this issue. In this model, improved osseointegration response to a given surface would be indicated by an accelerated formation of bone in apposition to that surface. H&E and alizarin red staining were therefore used to histologically assess the progression of bone healing at 1, 3, 9 and 12 week post-operative time points around sites where implants with machined, grit blasted/acid etched and TCP coated surfaces were placed. This served to detect any influences these surface modifications might have had on implant osseointegration over time. It is also a possibility that, in addition to altering bone formation, surface modifications may lead to changes in osteoblast progenitor cell recruitment, proliferation and differentiation around implant sites. Therefore, immunolocalisations were carried out for Stro-1, PCNA, OP and OC in order to detect changes in cell activity brought about by implant surface modification.

The use of an *in vivo* model of osseointegration of titanium implants in a rat mandible in this chapter represents a close approximation of the clinical situation and is perhaps one of the closest available. Ultimately, it is the bone healing response to a surface in an *in vivo* situation which determines its suitability for use clinically, irrespective of its effects on attached osteoblast progenitor cells *in vitro*. Therefore using this model to investigate the osseointegrative potential of each experimental surface is the logical extension of the other investigations described in this thesis and will generate useful data which is directly relevant to determining the effects of modified titanium surfaces on the process of osseointegration.

6.2 Materials and Methods

6.2.1 Preparation of Mandibles

All implant procedures were carried out at the Dental University of Osaka Japan on 24 10-week old male Wistar rats, as described in Sakai et al (2008). All experimental protocols involving these animals were reviewed and approved by the Animal Committee of Osaka Dental University (approval number 08-03009), and conformed with the procedures described in the 'Guiding Principles for the Use of Laboratory Animals' handbook at the Laboratory Animal Facilities in the Institute of Osaka Dental Research, Osaka Dental University. Incisors were trimmed prior to extraction as described in section 5.2.1, in order to stimulate eruption. Anaesthetic was applied and tooth extraction followed by curette was carried out as described in section 5.2.1. Implants were produced and prepared by Osteo-Ti (Guernsey) and included a machined, grit blasted/acid etched surface and a TCP coated surface. These surface treatments were carried out as for the titanium discs, described in section 2.2.1. Animals were sacrificed at post-operative time points of 1, 3, 6, 9 and 12 weeks, fixed and mandibles extracted as described in section 5.2.1.

6.2.2 Processing of Mandibles

Implants were removed from mandibles, cut into approximately 2mm thick sections running perpendicular to the implant socket using a bone saw and demineralised as described in section 5.2.2. Demineralised tissue sections were placed in biopsy cassettes and processed by machined as described in section 5.2.2. Processing of mandibles was carried out as described in section. 5.2.2. The processed tissue sections were embedded in paraffin wax and 5μm sections were cut as described in section 5.2.2. Sections were then mounted on poly-L-lysine coated glass slides (Sigma Aldrich) before being placed in an oven at 65°C overnight.

6.2.3 Haematoxylin and Eosin Staining

Sections were stained with haematoxylin and eosin (H&E) using an automated staining machine, in order to assess the level of bone healing around the implant site (described in section 5.2.3). Images were captured using an Olympus AX70 microscope incorporating a Nikon DXM 1200 digital camera and ACT-1 software.

6.2.4 Alizarin Red Staining

In order to assess the level of mineralization in the tissues around the implant sites, sections were stained with alizarin red as described in section 5.2.4.

6.2.5 Immunohistochemistry

6.2.5.1 Preparation of Sections

Mounted sections were deparaffinized and endogenous peroxidase activity quenched with 3% hydrogen peroxide as described in section 5.2.5.1. For the immunolocalisation of TGFβ1, IL-1β, TNFα and F4/80, antigen retrieval was performed using 24μg/mL protinase K (Sigma Aldrich) as described in section 5.2.5.1.

6.2.5.2 Immunolocalisation

Immunodetection of PCNA, osteopontin, osteocalcin, TGFβ1, IL-1β, TNFα and F4/80 was carried out using a Vectastain Universal IgG Kit (Vector Laboratories) and a DAB peroxidase kit (Vector Laboratories) as described in section 5.2.5.2. As a negative control for each experiment, a non-immunogenic IgG_1 control

antibody (Sigma Aldrich) was substituted for the primary within the protocol or the primary was excluded altogether and was with blocking serum. Cover slips were applied to sections using DPX glue, and images taken using an Olympus AX70 microscope incorporating a Nikon DXM 1200 digital camera and ACT-1 software. All immunolocalisations were performed in duplicate. Details of all antibodies used are given in Table 5.1

6.2.5.3 Stro-1 Localization

Immunodetection of Stro-1 was carried out as described in section 5.2.5.3, without the Vectastain Kit, as the primary antibody to Stro-1 is an IgM class antibody. Details of the Stro-1 antibody are given in Table 5.1.

6.2.5.4 Semi-Quantification of Immunohistochemical Results

The results of the immunolocalisation experiments were semi-quantified as described in section 5.2.5.4. In order to statistically compare the number of positive cells per $100\mu m^2$ present around the sites of the different implants, a Kruskal-Wallis test was used, as there were three treatment groups to be compared at each time point (Instant Package, Graph Pad Software). A Dunn post test was used to compare the three groups to each other. Non-parametric statistical tests were performed as the n numbers were too small to assume normality or equal variance. P values below .05 at a 95% confidence interval were held to be statistically significant.

6.3 Results

6.3.1 Haematoxylin & Eosin Histology

Figures 6.1-6.4 show that bone healing appeared to progress at approximately the same rate around the implant sites for all three treated implant implants. Further, there was no difference between the three surfaces or the amount of contact versus distance osteogenesis at any time point. In Figure 6.1, a cell rich granulation tissue (GT) is visible around the implant sockets of all three surface treatments at one week post-operation. By three weeks post-operation (Figure 6.2) however, there was evidence of new bone growth around all three implant sockets. At nine weeks post-operation (Figure 6.3), bone healing had advanced considerably around all of the implant sockets. Figure 6.4 shows that bone healing was nearly complete around the machined and grit blasted/acid etched implant sites at twelve weeks post-operation, while a large amount of granulation tissue was seen around the TCP coated implant site, with very little evidence of bone healing. This was replicated in both experimental animals.

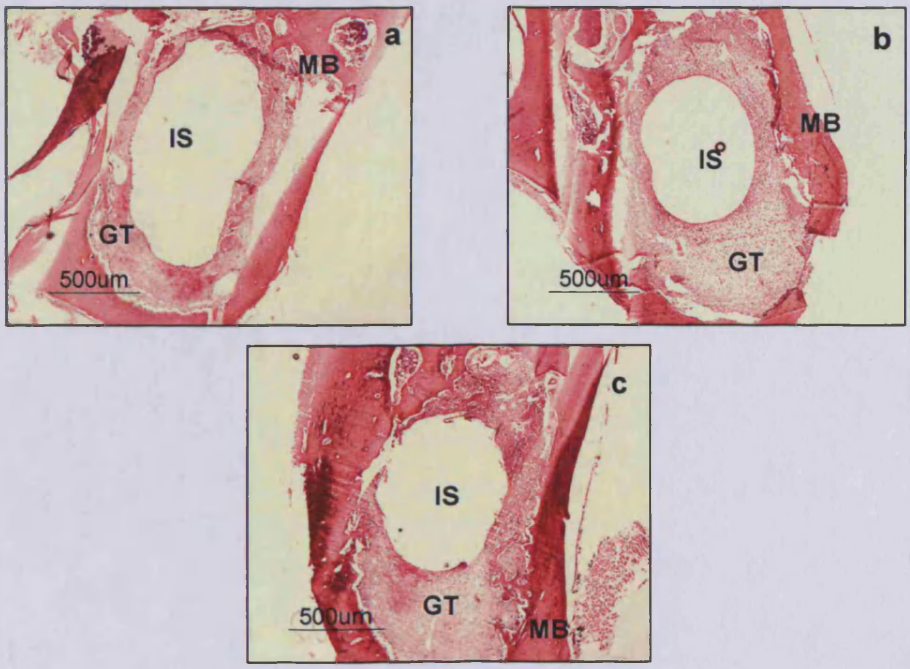

Figure 6.1: H&E stained sections obtained from rat mandibles with machined (a) grit blasted/acid etched (b) and TCP (c) coated implants one week post-operation. MB indicates mandibular bone, IS indicates the implant socket and GT the granulation tissue.

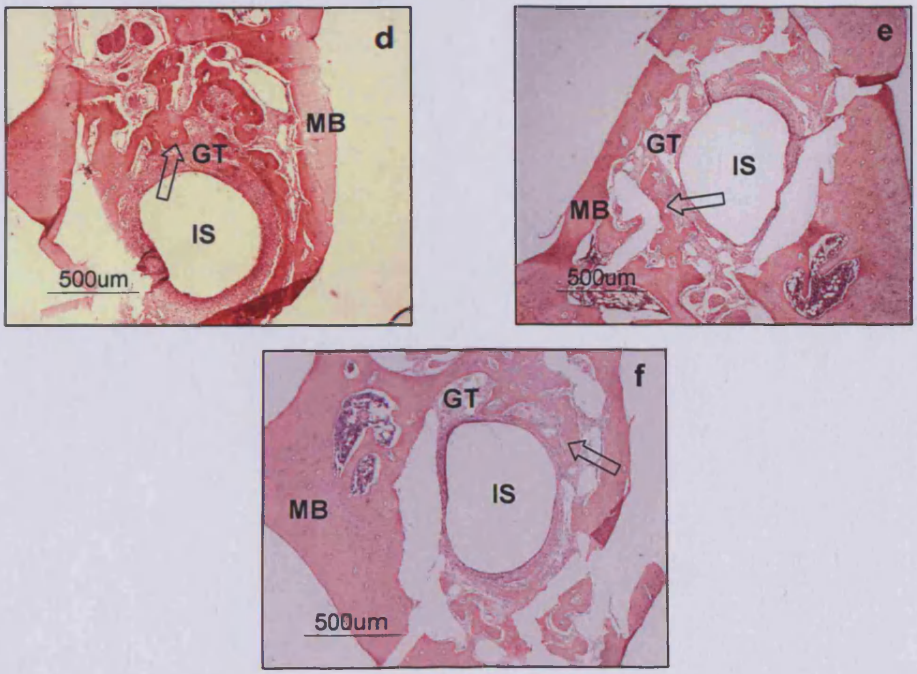

Figure 6.2: H&E stained sections obtained from rat mandibles with machined (d) grit blasted/acid etched (e) and TCP coated (f) implants three weeks post-operation. MB indicates mandibular bone, IS indicates the implant socket and GT the granulation tissue. New bone is indicated by arrows.

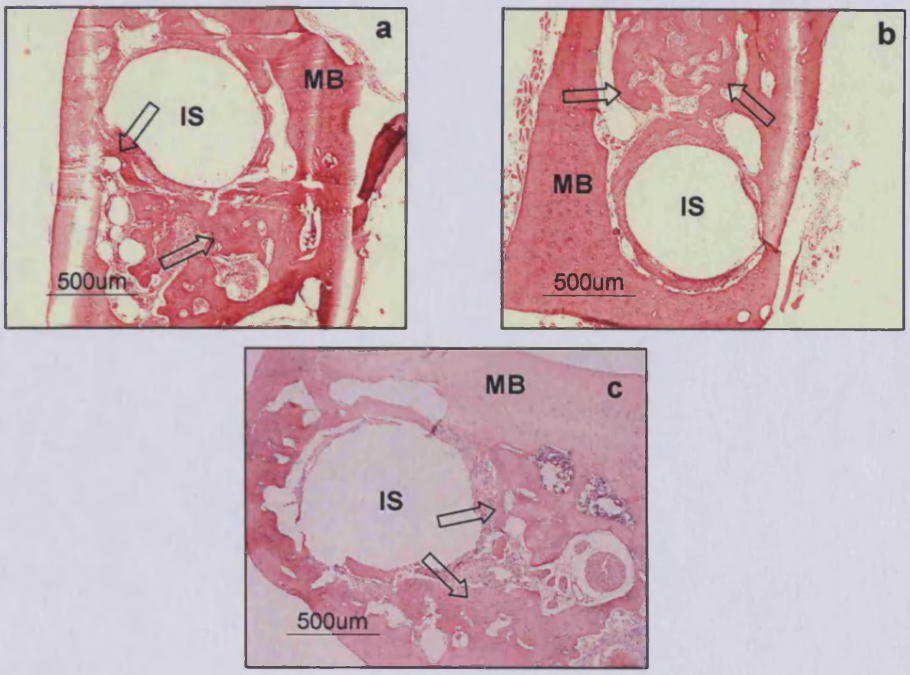

Figure 6.3: H&E stained sections obtained from rats with machined (a) grit blasted/acid etched (b) and TCP (c) coated implants nine weeks post-operation. MB indicates mandibular bone and IS indicates the implant socket. New bone is indicated by arrows.

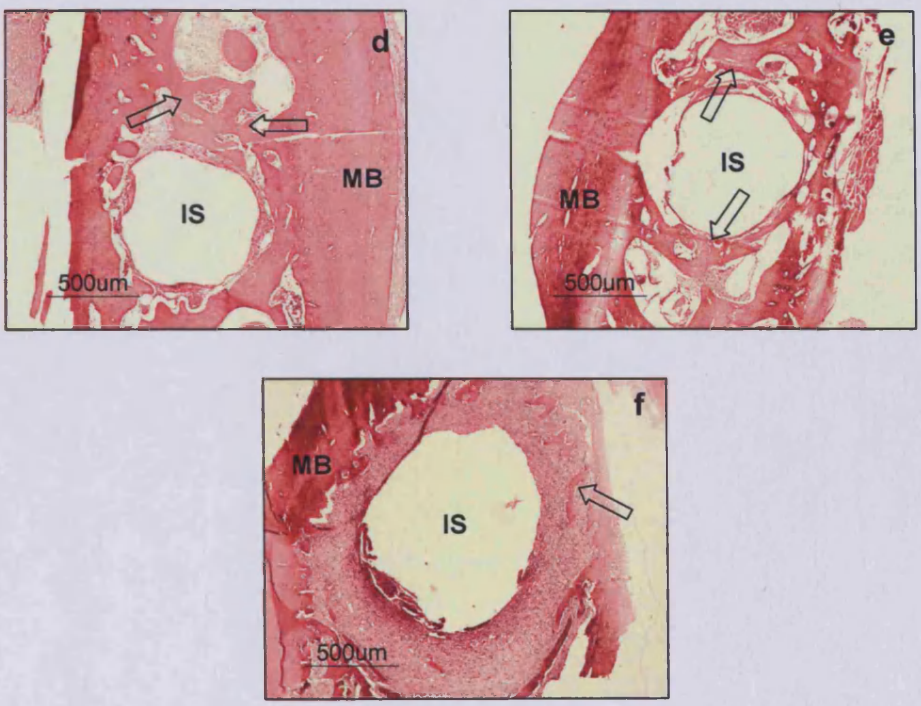

Figure 6.4: H&E stained sections obtained from rat mandibles with machined (d) grit blasted/acid etched (e) and TCP coated (f) implants twelve weeks post-operation. MB indicates mandibular bone and IS indicates the implant socket. New bone is indicated by arrows.

6.3.2 Alizarin Red Staining

Images obtained following the staining of mineral residue with alizarin red are shown in Figures 6.5-6.8. The results concur with those from H&E staining. At one week post operation (Figure 6.5), no newly formed mineralised bone was visible around any of implant sites. At three and nine weeks post-operation (Figure 6.6-6.7), areas of bright red staining were visible, particularly at the edges of newly formed bone tissue, indicating tissue mineralisation. In the sections from twelve weeks post-operation (Figure 6.8), areas of bright red staining were visible at the edges of newly formed bone around the machined and grit blasted/acid etched implant sites due to the small amount of bone formation around the TCP coated implant site at this time point, little staining was seen.

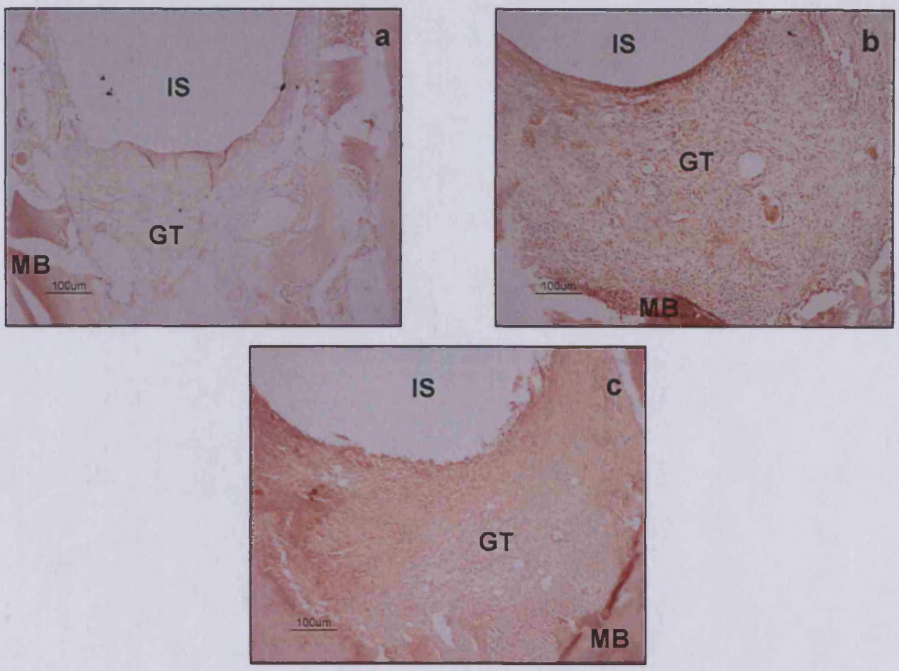

Figure 6.5: Alizarin red stained sections obtained from rat mandibles with machined (a) grit blasted/acid etched (b) and TCP (c) coated implants one week post-operation. MB indicates mandibular bone, IS indicates the implant socket and GT the granulation tissue.

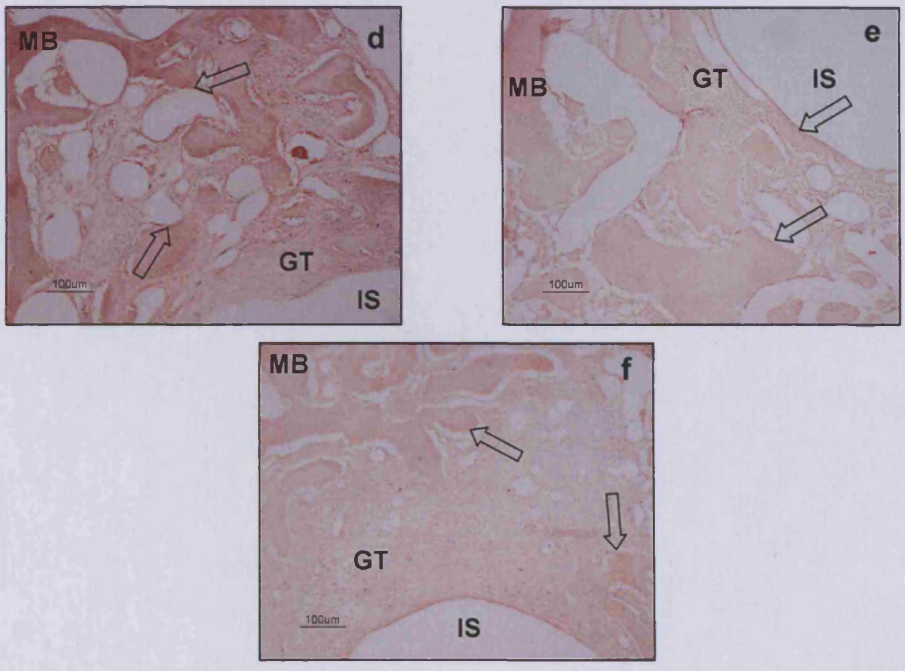

Figure 6.6: Alizarin red stained sections obtained from rat mandibles with machined (d) grit blasted/acid etched (e) and TCP coated (f) implants three weeks post-operation. MB indicates mandibular bone, IS indicates the implant socket and GT the granulation tissue. Areas of positive staining are indicated by arrows.

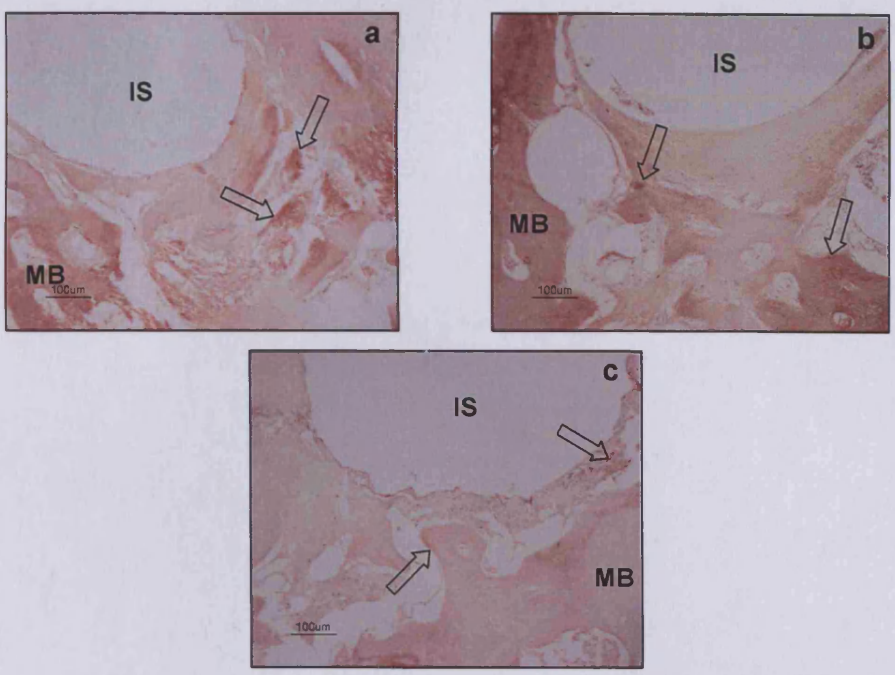

Figure 6.7: Alizarin red stained sections obtained from rat mandibles with machined (a) grit blasted/acid etched (b) and TCP (c) coated implants nine weeks post-operation. MB indicates mandibular bone and IS indicates the implant socket. Areas of positive staining are indicated by arrows.

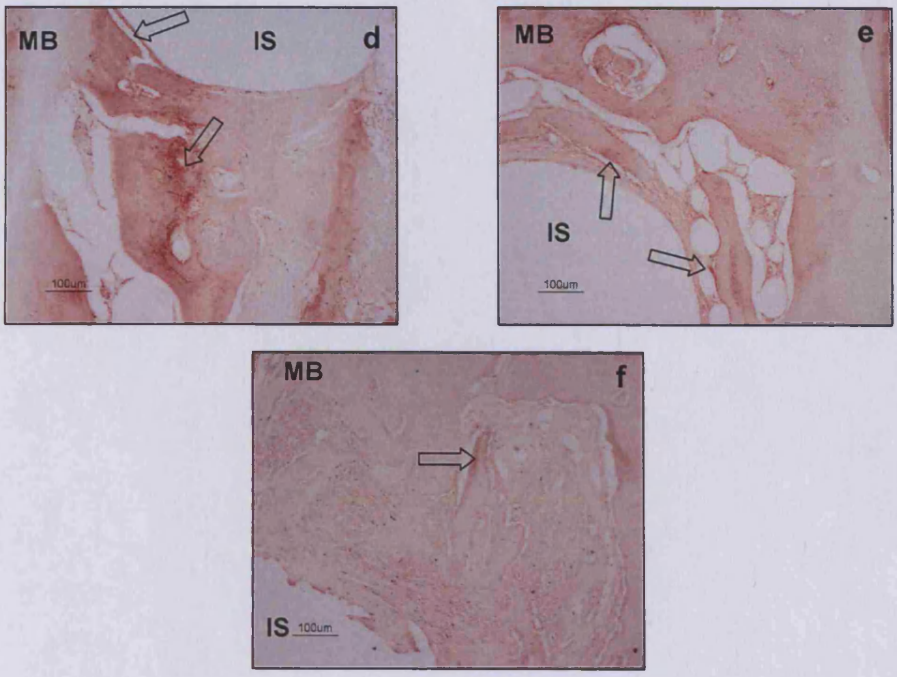

Figure 6.8: Alizarin red stained sections obtained from rat mandibles with machined (d) grit blasted/acid etched (e) and TCP coated (f) implants twelve weeks post-operation. MB indicates mandibular bone and IS indicates the implant socket. Areas of positive staining are indicated by arrows.

6.3.3 Immunolocalisation of Stro-1

Stro-1 positive cells were not found around any implant sites at any time point. Images resulting from the immunolocalisation of Stro-1 around the implant site of all three experimental implants at one week post operation are shown in Figure 6.9. Images from three, nine, and twelve weeks are not shown.

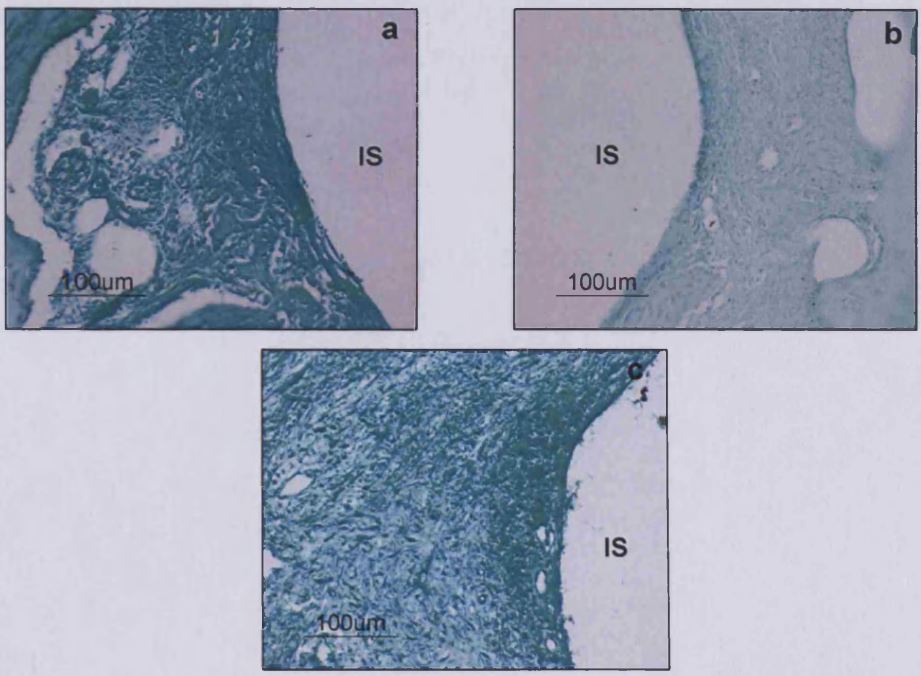

Figure 6.9: Immunolocalisation of Stro-1 in sections obtained from rat mandibles with machined (a) grit blasted/acid etched (b) and TCP (c) coated implants one week post-operation. IS indicates the implant socket.

6.3.4 Immunolocalisation of PCNA

Images resulting from the immunolocalisation of proliferating cell nuclear antigen (PCNA) are shown in Figures 6.10-6.11. Positive staining for PCNA is indicated by brown cellular staining. The temporal expression pattern of PCNA was the same around the three surface treated implant sites, with positive cells only seen at one week post-operation (Figure 6.10). The levels of PCNA expression were not found to be significantly different around the three implant sites at this time point. Figure 6.11 shows no positive staining around any of the three implant sites at three weeks post-operation. There was no staining around any implant sites at either nine or twelve weeks post-operation and the images are not shown. Figure 6.12 shows a graph of the average number of PCNA positive cells per $100\mu m^2$ in tissue sections around all implant sites over the four time points. The graph represents the average number of positive cells per $100\mu m^2$ around the implant sites of two animals per surface treatment per time point. P values shown in a table indicate that there is no significant difference in the level of expression around any of the experimental implant sites at one week post operation. As there was no positive staining at three, nine or twelve weeks post-operation no statistical tests were performed for these time points.

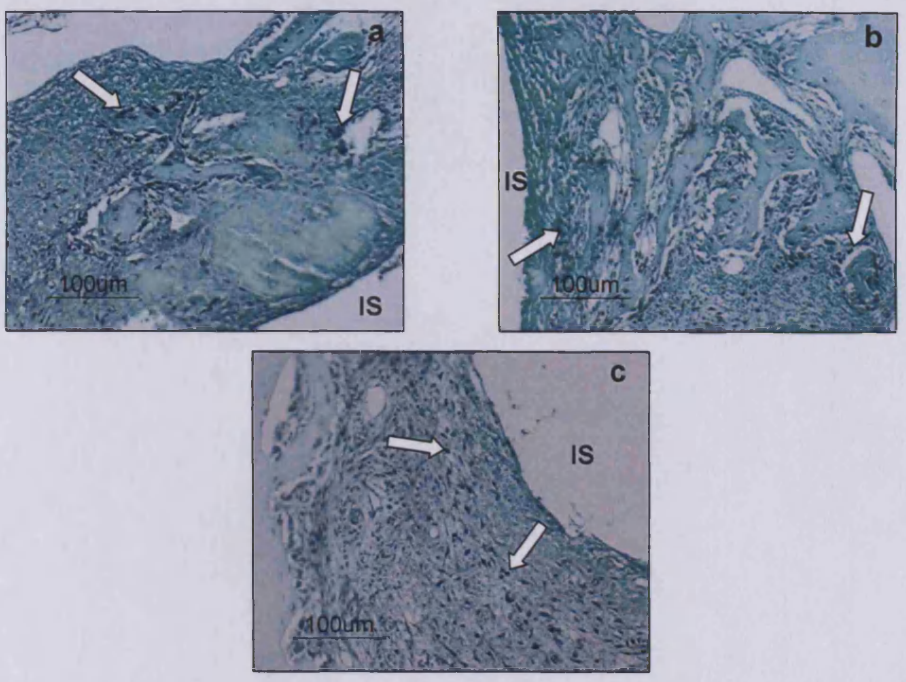

Figure 6.10: Immunolocalisation of PCNA in sections obtained from rat mandibles with machined (a) grit blasted/acid etched (b) and TCP (c) coated implants one week post-operation. IS indicates the implant socket. Examples of positive cells are indicated by arrows.

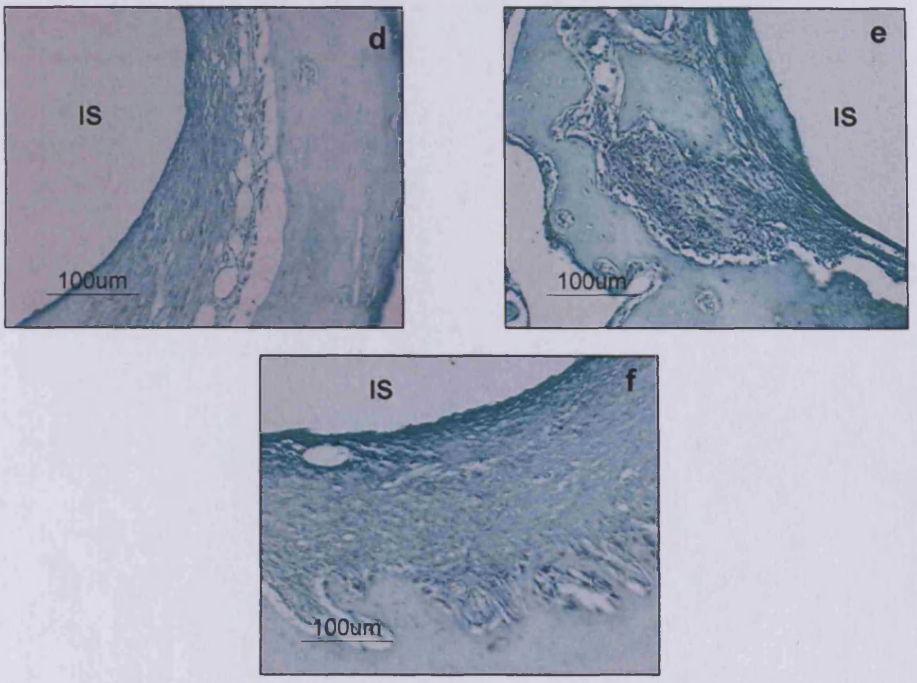

Figure 6.11: Immunolocalisation of PCNA in sections obtained from rat mandibles with machined (d) grit blasted/acid etched (e) and TCP coated (f) implants three weeks post-operation. IS indicates the implant socket.

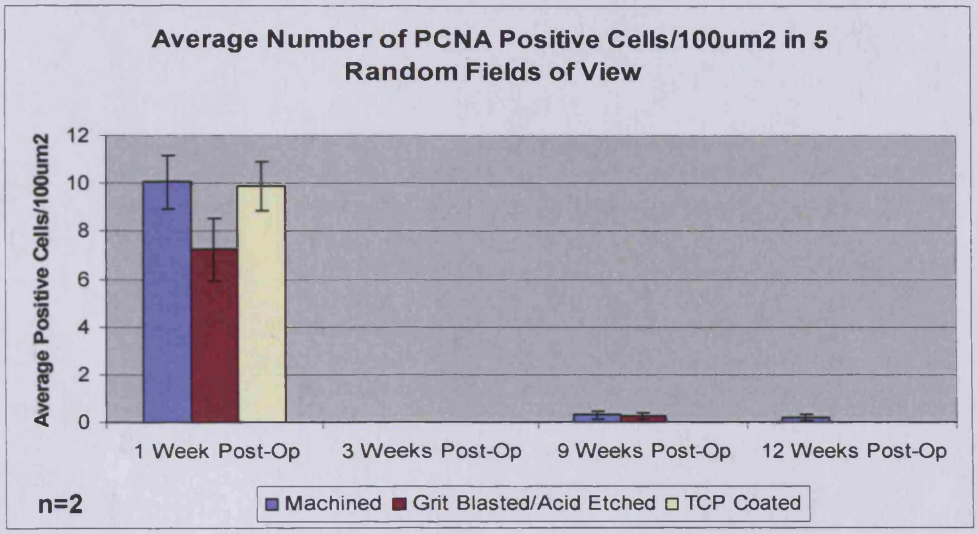

Week 1 Post-Operation	P = 0.0719
Machined v Grit Blasted/Acid Etched	P > 0.05
Machined v TCP Coated	P > 0.05
Grit Blasted/Acid Etched v TCP Coated	P > 0.05

Figure 6.12: Graph of the average number of PCNA positive cells per 100μm^2 in five random fields of view over one, three, nine and 12 weeks post-operation. P values resulting from a Kruskal-Wallis test are given in a table.

6.3.5 Immunolocalisation of Osteopontin

Images obtained from the immunolocalisation of osteopontin are shown in Figures 6.13-6.14. Osteopontin expression is indicated by brown cellular staining. The temporal expression pattern of OP was the same around the three surface treated implant sites, with positive cells only seen at three weeks post-operation (Figure 6.13). The levels of OP expression were not found to be significantly different around the three implant sites at this time point. At nine weeks post-operation, no staining is seen around any of the experimental implants (Figure 6.14). No staining was seen around any implant site at one or twelve weeks post-operation and images are not shown. Figure 6.15 shows a graph of the average number of osteopontin positive cells per $100\mu m^2$ in tissue sections from all implant sites over the four time points. The graph represents the average number of positive cells per $100\mu m^2$ around the implant sites of two animals per surface treatment per time point. P values shown in a table indicate that there is no significant difference in the level of expression around any of the experimental implant sites at three weeks post operation. As there was no positive staining at one, nine or twelve weeks post-operation no statistical tests were performed for these time points.

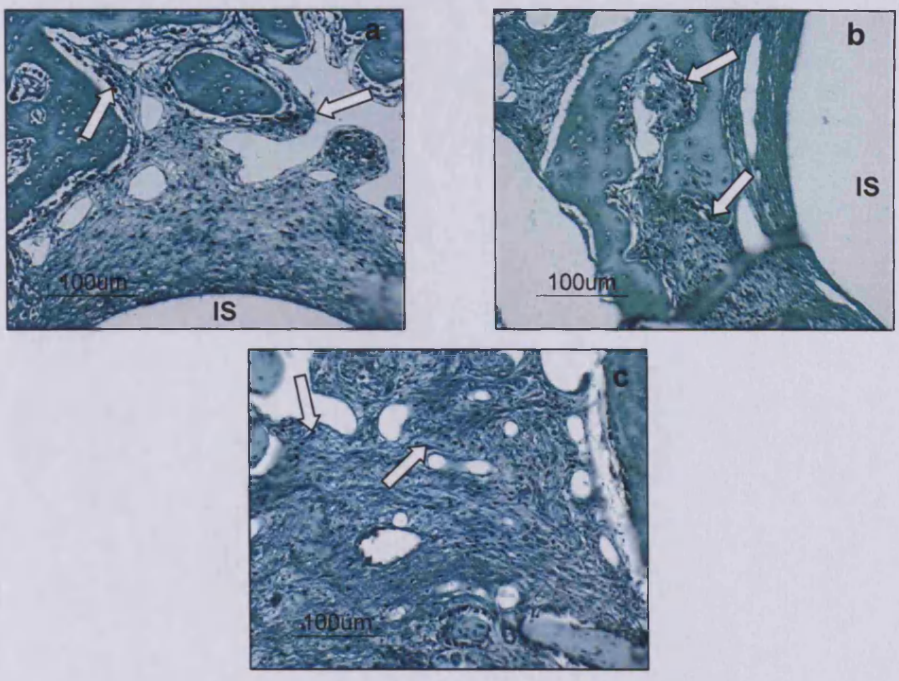

Figure 6.13: Immunolocalisation of OP in sections obtained from rat mandibles with machined (a) grit blasted/acid etched (b) and TCP (c) coated implants three weeks post-operation. IS indicates the implant socket. Examples of positive cells are indicated by arrows.

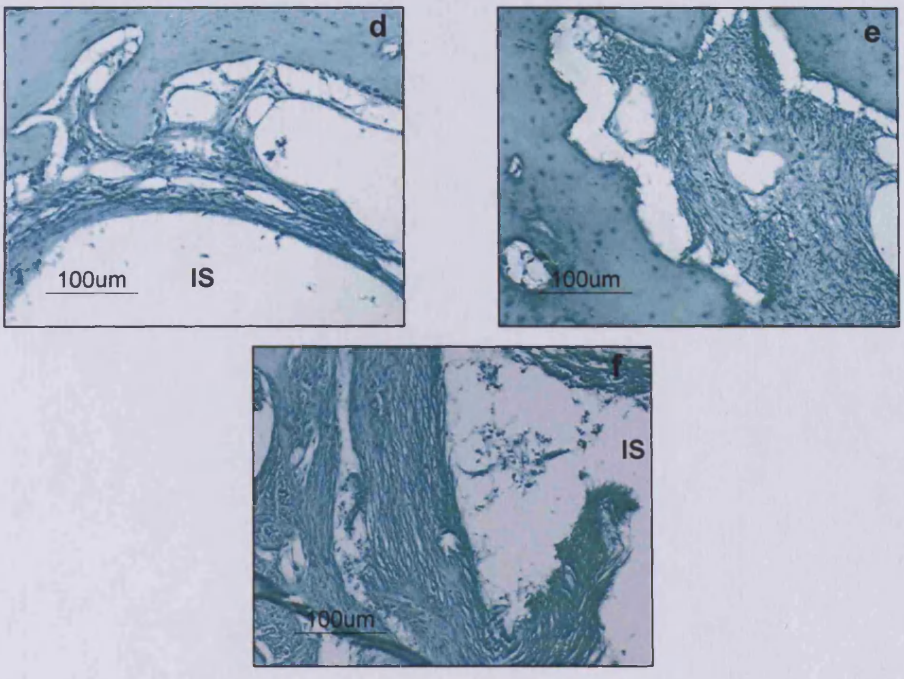

Figure 6.14: Immunolocalisation of OP in sections obtained from rat mandibles with machined (d) grit blasted/acid etched (e) and TCP coated (f) implants nine weeks post-operation. MB indicates mandibular bone and IS indicates the implant socket.

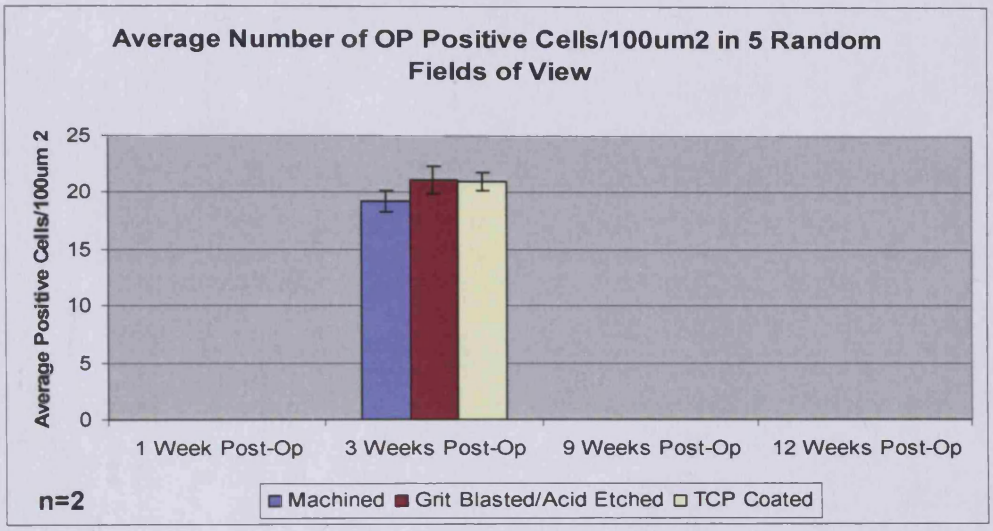

Week 3 Post-Operation	P= 0.3324
Machined v Grit Blasted/Acid Etched	P > 0.05
Machined v TCP Coated	P > 0.05
Grit Blasted/Acid Etched v TCP Coated	P > 0.05

Figure 6.15: Graph of the average number of OP positive cells per 100μm^2 in five random fields of view over one, three, nine and twelve weeks post operation. P values resulting from a Kruskal-Wallis test are given in a table.

6.3.6 Immunolocalisation of Osteocalcin

Images obtained from the immunolocalisation of osteocalcin are shown in Figures 6.16-6.18. Cells positive for osteocalcin are stained brown. The temporal expression pattern of OC was similar around the three surface treated implant sites with positive cells seen primarily at nine and twelve weeks post-operation (Figures 6.17-6.18), while staining was minimal at three weeks post-operation (Figure 6.16). The levels of OC expression were not found to be significantly different around the three implant sites at any time point. No staining was seen at one week post-operation around any of the implant sites and the images are not shown. Figure 6.19 shows a graph of the average number of osteocalcin positive cells per $100\mu m^2$ in tissue sections from all implant sites over the four time points. The graph represents the average number of positive cells per $100\mu m^2$ around the implant sites of two animals per surface treatment per time point. P values shown in tables indicate that there is no significant difference in the level of expression around any of the experimental implant sites at three, nine or twelve weeks post operation. As there was no positive staining at one week post-operation no statistical tests were performed for this time point.

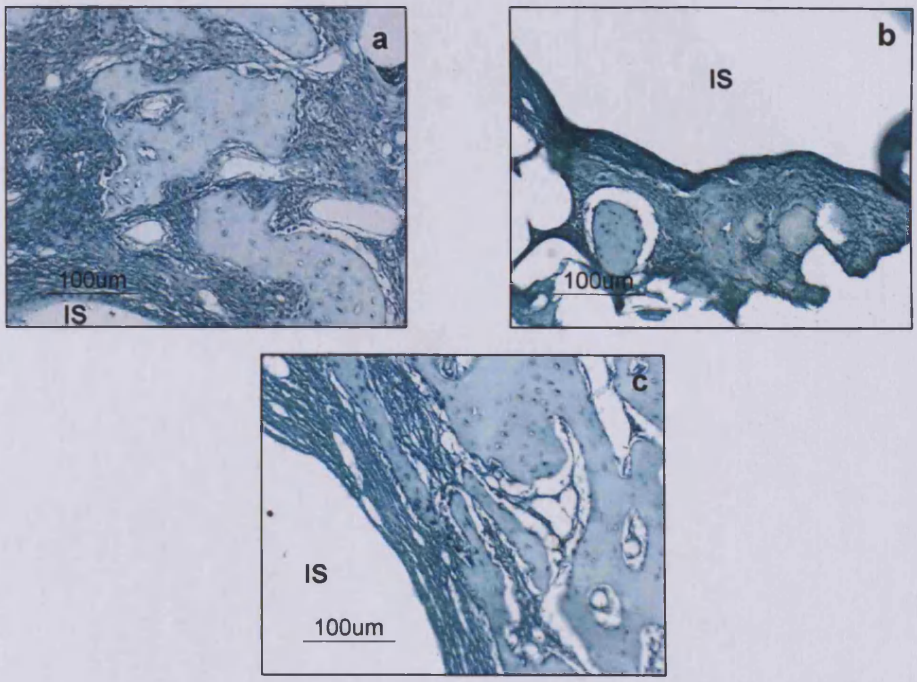

Figure 6.16: Immunolocalisation of OC in sections obtained from rat mandibles with machined (a) grit blasted/acid etched (b) and TCP (c) coated implants three weeks post-operation. IS indicates the implant socket.

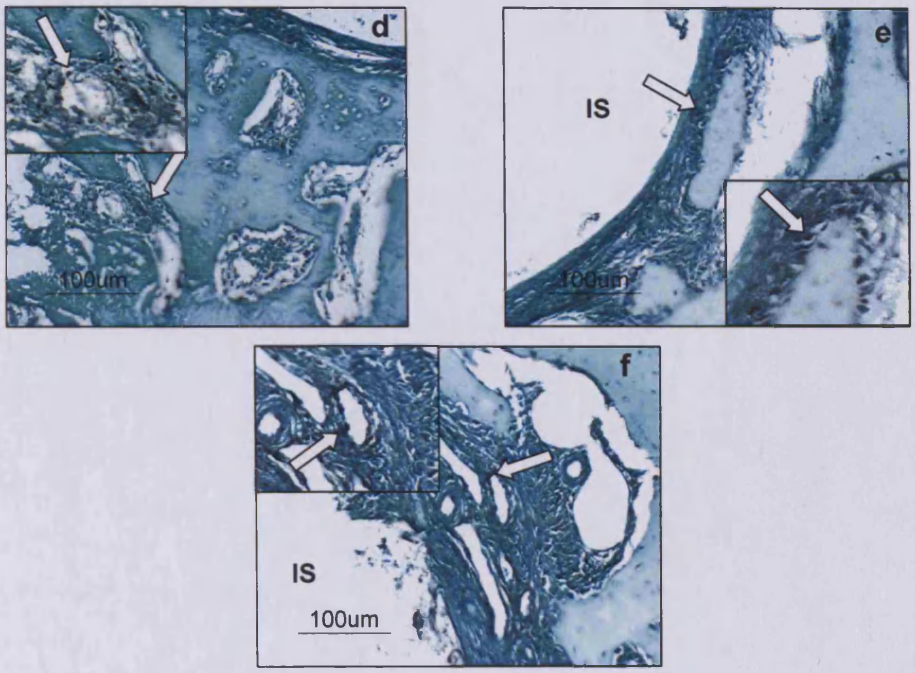

Figure 6.17: Immunolocalisation of OC in sections obtained from rat mandibles with machined (d) grit blasted/acid etched (e) and TCP coated (f) implants nine weeks post-operation. IS indicates the implant socket. Examples of positive cells are indicated by arrows. Inset into all images are magnified areas of the images.

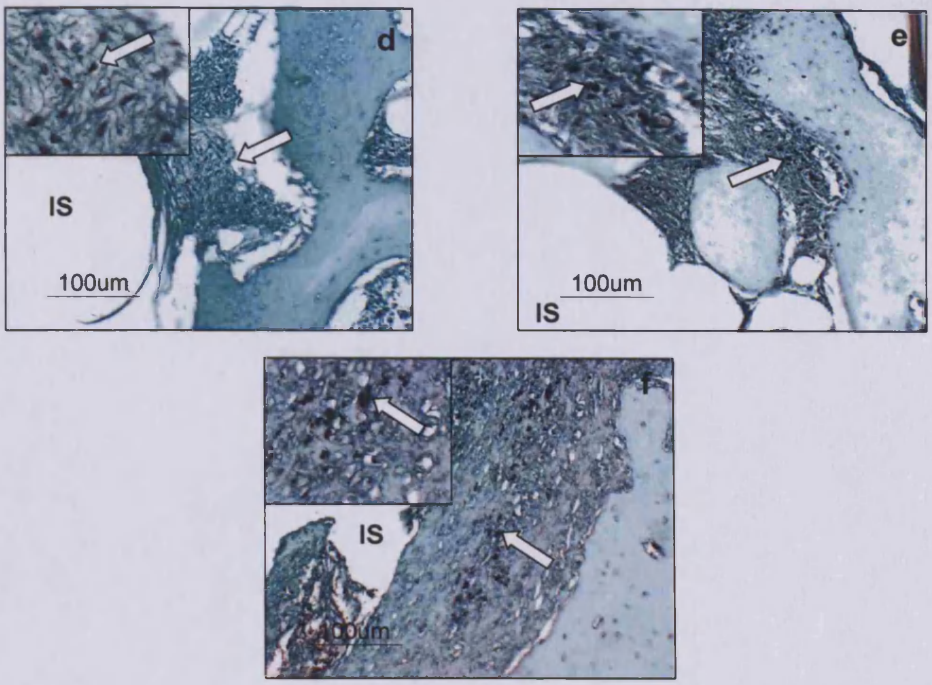

Figure 6.18: Immunolocalisation of OC in sections obtained from rat mandibles with machined (a) grit blasted/acid etched (b) and TCP (c) coated implants twelve weeks post-operation. IS indicates the implant socket. Examples of positive cells are indicated by arrows. Inset into all images are magnified areas of the images.

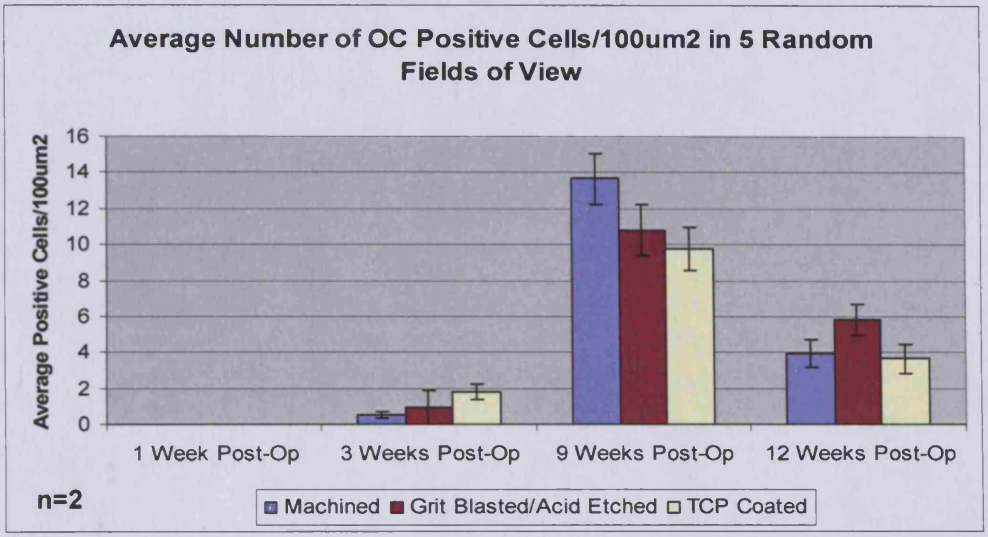

Week 3 Post-Operation	P= 0.0717
Machined v Grit Blasted/Acid Etched	P > 0.05
Machined v TCP Coated	P > 0.05
Grit Blasted/Acid Etched v TCP Coated	P > 0.05

Week 9 Post-Operation	P= 0.1423
Machined v Grit Blasted/Acid Etched	P > 0.05
Machined v TCP Coated	P > 0.05
Grit Blasted/Acid Etched v TCP Coated	P > 0.05

Week 9 Post-Operation	P= 0.0918
Machined v Grit Blasted/Acid Etched	P > 0.05
Machined v TCP Coated	P > 0.05
Grit Blasted/Acid Etched v TCP Coated	P > 0.05

Figure 6.19: Graph of the average number of OC positive cells per $100\mu m^2$ in five random fields of view over one, three, nine and twelve weeks post operation. P values resulting from a Kruskal-Wallis test are given in a table.

6.3.7 Negative Controls

Typical examples of both non-immunogenic IgG and primary excluded negative controls for all immunolocalisations performed are shown in Figure 6.20. Both of these negative controls were performed for all tissue sections at all time points and none showed any positive staining.

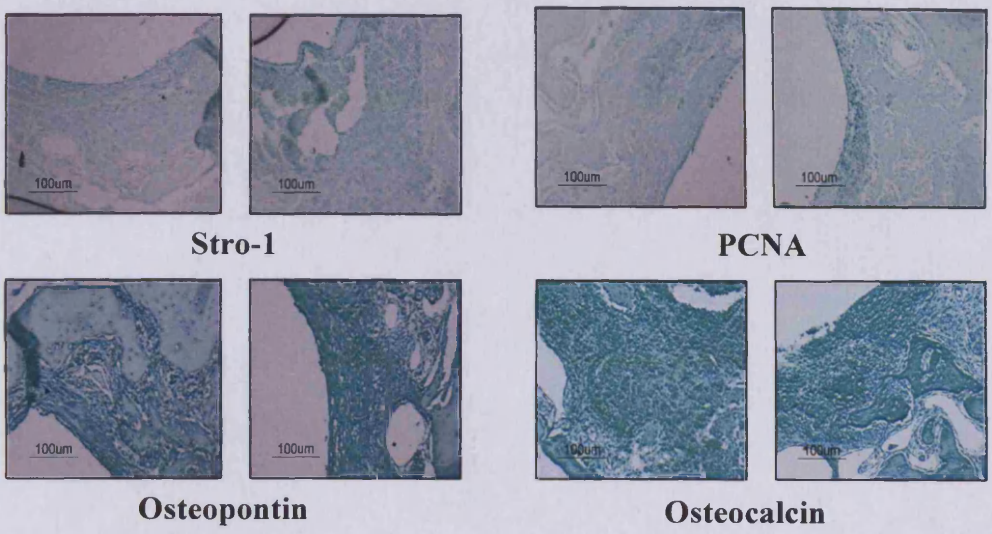

Figure 6.20: Typical examples of negative controls which had the primary antibody excluded (**left**) and a negative control in which a non-immunogenic IgG antibody (non-immunogenic IgM in the case of Stro-1) was used in place of the primary IgG antibody (or IgM for Stro-1) (**right**). These controls were performed for every time point and implant group and did not demonstrate any positive staining.

6.4 Discussion

The use of the *in vivo* model of the osseointegration of modified titanium dental implants described in this chapter has allowed the experimental surface treatments to be tested in conditions which consider all aspects of the complex process of bone formation. Interestingly, it appears from the results presented that there were no temporal differences in the amount of bone healing which took place around the sites of implants with different experimental surface treatments. Furthermore, both cell proliferation and osteoblast markers showed the same temporal pattern of expression around implant sites across all three of the experimental groups. Therefore, it appears that none of the experimental surface treatments had an advantage in promoting the formation of bone in apposition to implants *in vivo*.

From the H&E results presented in this chapter, it is apparent that bone healing occurred at approximately the same rate over time around the implant sites of the machined, grit blasted/acid etched and TCP coated implants. Further, the rate of bone formation was similar to that of the normal animals in Chapter 5. Bone formation also appeared to follow the same pattern over time around all of the experimental implant sites; no differences in the amount of distance or contact osteogenesis were observed. Alizarin red staining showed that mineralisation of the newly formed bone occurred at approximately the same rate around all of the experimental implant sites over time. The rate of bone formation therefore appeared to be neither substantially enhanced nor impaired around any of the experimental implant surfaces, indicating that surface modification had no effect on the rate of osseointegration in this model.

It must be noted that the histological results from around the TCP coated implants at 12 weeks post-operation are likely to be anomalous, as healing appeared to have progressed normally in all animals with TCP coated implants at three and nine weeks post-operation. It is possible that this is the result of an infection around the implant site in these animals, as a large amount of un-mineralised connective

tissue is evident around the implant sites, indicative of fibrous encapsulation. Both animals with TCP coated implants at this time point were affected.

In the literature, accounts differ as to the impact of modifying titanium surfaces on the osseointegration of titanium implants. It has been reported that implant surfaces roughened by acid etching results in a greater the amount of bone formation in apposition to implant surfaces in canine mandibles (Cochran et al. 1998). Acid etching of implants has also been shown to increase the removal torque values of implants placed into rabbit tibiae (Cho and Park 2003), as has the oxidation of implant surfaces (Sul et al. 2005). Franchi and colleagues have reported that grit blasting with zinc particles results in more rapid peri-implant bone formation in sheep tibiae (2007). Likewise, blasting with alumni grit has been shown to enhance bone implant contact in rabbit tibiae (Wennerberg et al. 1998). Conversely, it has also been reported that modifying titanium implants in terms of their topography and surface chemistry does not dramatically influence the process of osseointegration *in vivo*. Grit blasting surfaces has been reported to have no effect on the rate of bone formation in apposition to implants in either mini-pig (Bernd et al. 2008) or canine (Kawahara et al. 2006) mandibles. Based on the evidence in the literature, it seems clear that surface treatments rarely have an adverse affect on osseointegration as it is frequently noted that all surfaces are successfully osseointegrated. It is the speed at which bone is formed in apposition to implants which directly determines an improved surface. It is a possibility that some surface modifications may result in more rapid bone healing around implant surfaces, given the large range of modifications (Bagno and Di Bello 2004). In terms of the results presented here however, no such increase in the rate of bone healing was seen around any of the experimental implant surfaces.

The quality and strength of bone produced in apposition to the implant surfaces was assessed via implant removal torque in Japan at both three and nine weeks post-operation. These results were used in a student thesis in Japan and are therefore only described in the discussion herein. From this data, it appears that removal torque values were similar between the machined and grit blasted/acid etched implants but much higher for TCP coated implants at both time points. It is a

possibility is that the TCP coating, being more porous than titanium, allowed collagen fibres present in the soft tissue to crosslink with pores present on the surface of the coating, leading to increased removal torque values. It is difficult to interpret these findings due to the histological similarities in the progression of bone formation around the sites of implants with the experimental surfaces. Further studies into the mechanical properties of the bone formed around each of the experimental surfaces over time would possibly help to clarify this issue.

Expression of PCNA, OP and OC followed the same temporal pattern around the sites of all of the experimental implants and the level of their expression did not vary significantly between the experimental groups. This suggests that the surface modifications investigated in this thesis had no influence on the activity or proliferation of cells around implant sites *in vivo*. Stro-1 was not expressed around any of the experimental surfaces at one week post-operation, which suggests that surface modification did not affect the recruitment of osteoblast progenitor cells to the implant site. The one week post-operative time point may have been outside the window of Stro-1 expression, which is known to be brief and to occur very early in osteoblast differentiation (Simmons and Torok-Storb 1991). The similar temporal expression of these markers reflects the fact that the experimental surface modifications did not appear to alter the rate of bone healing, as it is certain that any such alterations would be reflected in the pattern of their expression.

It has been reported previously in this thesis that the experimental surface treatments, despite generating a surface with unique characteristics, did not have a great deal of influence on the behaviour of BMSCs *in vitro,* although the protein expression profile of cells cultured on the TCP coated surface was altered. It was therefore possible that this experimental surface would influence the process of osseointegration *in vivo*. The results presented in this chapter however suggest that the experimental surfaces treatments did not increase the rate of bone formation in apposition to implant surfaces. Neither did they alter the proliferative activity of cells surrounding the implant site or the differentiation of adjacent osteoblasts, both key indicators of osseointegration. Broadly speaking, the aim of any surface modification is to increase the speed at which bone is formed apposition to an implant surface, not

only reducing the chances of infection and peri-implantitis, but also the amount of clinical time required for treatment. Based on the *in vivo* results presented here however, it does not appear that any of the experimental surfaces treatments is more advantageous than any other from this standpoint. This chapter generally confirms the results of the previously described *in vitro* experiments using a more complex model of the process of bone healing around titanium dental implants.

Chapter 7: General Discussion

This thesis set out to identify ways in which the modification of titanium surfaces influences the osseointegration of titanium dental implants. To this end, three commercially available treatments were applied to titanium surfaces. These surfaces were then characterised and their effects on the process of osseointegration investigated using both an *in vitro* and *in vivo* model systems. The use of an *in vitro* model allowed cell morphology, attachment, and the mRNA and protein expression profiles of osteoblasts cultured on the experimental surfaces to be examined in isolation, while the *in vivo* model allowed the process of bone formation and cell activity around titanium implants implanted into mandibular bone containing a variety of tissue type to be assessed. Additionally, the *in vivo* model was used to model the process of implant osseointegration in type II DM, a common clinical condition with direct implications for treatment with dental implants. A better understanding of the effects of type II DM on the osseointegration of dental implants may suggest ways in which surfaces could be modified to negate the effects of the disease and thereby secure a better clinical outcome for diabetic individuals.

The systematic characterisation of the experimental surfaces was central to the goal of investigating the ways in which surface modifications influence the process of osseointegration. Variations in the topography, surface chemistry and hydrophobicity are all generally thought to be highly influential on both osteoblast activity and on the formation of bone in apposition to implant surfaces (Le Guéhennec et al. 2007; Zhao et al. 2005). Machining, grit blasting/acid etching and TCP coating were each shown to produce different topographies, with TCP coating producing the roughest surface of the three modifications, followed by grit blasting/acid etching and finally by machining. The experimental surface modifications each produced a distinct surface with respect to topography and elemental content. In contrast, hydrophobicity values were similar for all surfaces and showed that all surfaces were slightly hydrophilic.

Culturing rat bone marrow stromal cells on the experimental surfaces modelled effects of surface modifications directly on osteoblast activity. Some differences were observed in the morphology of cells adherent to the different experimental surfaces, with the machined surface having cells with a rounded morphology and cells on the grit blasted/acid etched and TCP coated surface having a more elongated one. Additionally, cells seemed to attach preferentially to the smoother machined surface than the other two rougher experimental titanium surfaces or even plastic controls. This was in agreement with the convention that smoother surfaces promote cell attachment and proliferation (Bachle and Kohal 2004; Kieswetter et al. 1996a; Kim et al. 2006; Le Guéhennec et al. 2007; Mustafa et al. 2001). Interestingly, the patterns of matrix deposition were seen to be different across the three experimental surfaces, with cells on the machined surface producing matrix in a thin sheet rather than the thick depositions seen to fill the 'valleys' generated by roughening on the grit blasted/acid etched and TCP coated surfaces. Such variations in the matrix deposition raised the possibility that roughened surface topographies may achieve due higher levels of mechanical interlocking between implant surfaces and surrounding bone and may therefore osseointegrate more securely.

Despite differences in cell morphology and the visual appearance of matrix deposition, there was a high degree of similarity in the mRNA expression profiles of cells cultured on the different experimental surfaces. This indicated that cellular activity was broadly the same across all of the modified surfaces and that surface modification did not greatly influence the expression of osteoblast cell marker mRNA. Adherent cells appeared to behave as osteoblasts independently of the surface they were cultured on. This is in contrast with much of the literature which reports that surface modification can influence the expression of osteoblast marker mRNA using both RT-PCR (Balloni et al. 2009; Marinucci et al. 2006; Qu et al. 2007; Tsukimura et al. 2008) and quantitative PCR (Masaki et al. 2005; Schneider et al. 2003). One novel finding from this model was the apparently suppressive effect of titanium on the expression of pparγ compared to plastic, suggestive of an osteogenic

property of titanium as a material. This suppressive effect did not appear to be influenced by the titanium surface characteristics however.

It is a possibility that the observed similarities in cell behaviour are due to the nature of the model system used. Cells were cultured under mineralising conditions, which would have served to drive them down the osteoblast lineage. Therefore, it may be that the observed similarity in cellular mRNA expression across the different experimental surfaces is unsurprising. Despite this possibility however, cells were influenced by the culture conditions in the same way across all the surfaces, which could equally indicate that surface characteristics had less influence on cellular differentiation than did the osteogenic culture media.

Overall, the mRNA expression of inflammatory cytokines and the growth factor TGFβ1 appeared to be broadly similar, with the exception of a decrease in the expression of TNFα mRNA in cells cultured on the TCP coated surface. Similarly cells cultured on all surfaces consistently expressed OPG mRNA, but did not express RANKL, suggesting a net suppression of osteoclast activity. Additionally, all of the titanium surfaces appeared to have a suppressive effect on the production of IL-1β compared to plastic surfaces. Although this possible anti-inflammatory property of titanium confirms its utility as a material to use in dental implants, it did not appear to be affected by surface modification. Neither IL-1β nor TNFα were shown to be released into the supernatants of cultures from any surfaces, although this may be due to the fact that the proteins were stored internally as pro-peptides awaiting the appropriate stimulus for release. Further studies using this model to investigate differences in release of these cytokines from cells cultured on modified surfaces after stimulation with LPS or other pro-inflammatory agents would perhaps serve to clarify this issue.

The composition of the protein matrix produced by adherent cells was shown to be different on the TCP coated surface. It was found to consist of BSP but not ON or OP, despite cultured BMSCs expressing mRNA for these markers. It is difficult to determine if this is relevant to the structural properties of the matrix produce from the use of an *in vitro* model alone, although it is clear evidence of surface

modification affecting the secretion of matrix proteins. There may have been variations in the expression of other bone matrix proteins, and further investigation of those proteins actually produced and secreted by cells may have been revealing, as opposed to investigating their expression at the level of mRNA.

The *in vitro* model showed that bone marrow stromal cells cultured on modified titanium surfaces under mineralising conditions behave in a similar manner in terms of their expression of mRNA for osteoblast markers, osteogenic factors and inflammatory cytokines despite some differences in initial adhesion, morphology, the pattern of matrix deposition and the composition of the matrix deposited. The results presented in this thesis seem to suggest therefore, that the basis for modifying surfaces, improved rates of osseointegration, may be strongly related to an improved the level of mechanical interlocking by variable topography lending itself to increased implant-matrix contact, as opposed to modified surfaces directly influencing the behaviour of individual osteoblasts and accelerating the rate at which bone is deposited. While the data presented suggests that there may be some value in micro-roughening titanium surfaces, in terms of improving mechanical interlocking, there was no strong indication that any of the modifications provided a surface which was optimal for osseointegration. While the observed improvement in mechanical interlocking was most likely the direct result of a roughened topography, it is difficult to separate the influence of surface topography from that of surface chemistry, which may also have played a role. In terms of implant design and manufacture, it may be the case that many commercially available surface modifications do not substantially enhance osteogenic activity by osteoblasts and therefore do not appreciably improve the process of osseointegration.

In order to model the complex nature of osseointegration of titanium dental implants into bone tissue, an *in vivo* model was used. In this way, the limitations of considering the effects of surface modification on osteoblasts as isolated cells were overcome by inserting surface modified implants into bone tissue containing a variety of cell types, an immune response, a blood supply and a healing response. Interestingly, no differences in either the rate of bone healing or in the expression of cell proliferative or osteoblast specific markers were observed around the sites of any

of the modified implants, indicating that surface modification has no effect on the rate of bone formation in apposition to implants. This seems to confirm the general conclusions from the *in vitro* model. It follows that osteoblasts displaying similar cellular behaviour across the modified surfaces would, by extension, indicate that the *in vivo* progression of bone formation around those surfaces would be similar. The literature is somewhat conflicting in terms of the impact of surface modification on *in vivo* model of osseointegration, with reports that it both improves (Cho and Park 2003; Cochran et al. 1998; Sul et al. 2005) and does not affect it (Bernd et al. 2008; Kawahara et al. 2006). It must be noted that all surfaces did appear to undergo successful osseointegration; the speed at which this was accomplished however seemed to be independent of the differences in both surface chemistry and topography between the experimental surfaces.

The data generated by both model systems, coupled with the astronomically high clinical success rates of routine dental implant treatment, suggest that current attempts to develop implant surfaces with higher osseointegrative potentials for routine clinical use through surface roughening and calcium phosphate coating may be largely irrelevant. Research time and resources invested in this area may be better employed elsewhere, for instance investigating implant modifications for use in difficult clinical situations, where patients are not ideal candidates for treatment. For example, it has recently been reported that using surgical techniques which increase the amount of bone fragments around the implant site may be beneficial, as these fragment may stimulate implant osseointegration (Tabassum et al. 2010). Implants with roughened surfaces may similarly serve to increase the number of bone upon implant placement, possibly increasing the rate of osseointegration, particularly in individuals with a compromised bone healing response (Tabassum et al. 2009). Biomimetic coatings containing growth factors such as BMPs, TGFβ, and VEGF or other osteogenic agents could be tailed to specifically improve aspects of various conditions which impair osseointegration such as DM and osteoporosis (Ellingsen et al. 2006; Le Guéhennec et al. 2007; Liu et al. 2007a; Valero et al. 2007). Such advances would not only serve to improve the current understanding of the mechanisms by which these diseases affect bone tissue, but would also increase the access to treatment with implants to patients for whom it is currently contraindicated.

It is often this group from which the greatest clinical need arises, yet it is often not possible for them to receive treatment which would significantly enhance their quality of life.

To this end, the *in vivo* model allowed implant osseointegration to be studied in the context of a clinically relevant disease state, type II DM. Within this thesis, it was found that there was a substantial delay in the rate of bone healing around implants in diabetic animals, and that this delay was underpinned by a variety of alterations in the activity of cells present around the implant site, and the use of this model allowed these to be identified. Foremost among these possible mechanisms was a general delay in differentiation of osteoblasts around the diabetic implant site, but interestingly, not in the appearance of Stro-1 positive mesenchymal progenitor cells, suggesting that migration of these cells to the implant site was unaffected by type II DM. The delay in TGFβ1 expression around the diabetic implant site indicates a delay in the initiation of osteoblast differentiation, as this growth factor is known to be a key mediator of this process, particularly its early phases (Centrella et al. 1994; Janssens et al. 2005). The delayed expression of IL-1β expression in diabetic animals has implications which are less clear. Although it is an inflammatory mediator and is known to inhibit the formation of bone and increase bone resorption (Nguyen et al. 1991), it has been suggested that IL-1β may also have an initial stimulatory effect on osteoblast progenitor cell proliferation and differentiation (Canalis 1986; Hughes et al. 2006), and the observed delay in diabetics may play a role in delaying the process of osteoblast differentiation. Diabetic animals also showed a possibly sustained inflammatory response around their implant sites, as evidenced by elevated TNFα expression and the prolonged presence of macrophages. Delays in diabetic bone healing are well documented in the literature (Hasegawa et al. 2008; Liu et al. 2007b; McCracken et al. 2006; Shyng et al. 2006; Siqueira et al. 2003), and the results presented in this thesis add to this understanding by describing the underlying cellular events associated with this delayed healing.

This *in vivo* model may prove to be useful in further investigating surface modifications which would be useful in treating individuals with a compromised

bone healing response. Herein, it has been used to elucidate possible cellular mechanisms involved in effects of DM on bone repair and could easily be used to investigate the utility of surface modifications for reversing this delay in bone healing. Due to the range of parameters which can be examined in the model using immunohistochemistry, surface modifications could target specific cellular mechanisms disrupted in the disease state. For example, implants with TGFβ1 impregnated coatings may help to compensate for the delayed expression of this growth factor in DM, reducing the delay in bone formation. The experimental surface modifications presented in this thesis could also be investigated in the model; while they did not appear to have any beneficial effects under normal conditions, it is a possibility that they may improve osseointegration in DM. Furthermore, very little is currently known about the characteristics of diabetic osteoblasts. Diabetic Bone marrow stromal cells could be extracted from the diabetic rats used in this model for study *in vitro*, allowing the basic biology of the diabetic osteoblast to be investigated, specifically regarding their responsiveness to a variety of osteogenic growth factors and inflammatory cytokines, or their behaviour under mineralising conditions. This model is also amenable to the investigation of other conditions which impair bone healing, and has been used to study the osseointegration of implants in ovariectomized osteoporotic rats (Kusunoki et al. 2006). It could therefore be used to investigate a wide range of implant modifications in a variety of adverse clinical conditions, with the aim of negating specific aspects of their pathologies.

Over the course of this thesis the osseointegrative potential of three modified titanium surfaces has been compared using both in vitro and in vivo model systems. Overall, it appears that surface modifications investigated had little impact on the differentiation and activity of osteoblasts or on the rate of bone formation around titanium implants, apart from possibly improved bone-implant mechanical interlocking for the rougher surfaces. It is therefore difficult to identify one of the experimental surfaces as having a higher osseointegrative potential. The nearly infinite range of implant modifications available however, means that it is entirely possible that surfaces with different modifications may have performed differently in the models used here. This diversity is cited as one of the key difficulties in defining surface characteristics which are optimal for osseointegration (Bagno and Di Bello

2004). From a clinical perspective, the central tenet of the surface modification of titanium dental implant surfaces is that they should improve patient outcomes. The current clinical value derived from the modification of titanium dental implant in routine cases is unclear, as dental implant treatment seems to have an impressively high success rate regardless of the surface modification. A systematic review of sixteen clinical trials found little evidence to indicate that surface modification improved patient outcome (Esposito et al. 2007). It may be the case, from the standpoint of implant design, that surface modifications do not necessarily lead to more rapid osseointegration; rather the rate of osseointegration in the clinical may depend on factors directly relating to the patient, for example the individual bone healing response and the management of inflammation. Expensive surface treatments carried out to enhance the rate of osseointegration may therefore be of limited value for patients who are good candidates for treatment. The future of surface modification of dental implants may lie with attempting to improve treatment success rates in non-routine more difficult clinical cases, for example individuals who have systemic diseases which affect the process of osseointegration.

References

ABBAS, S., ZHANG, Y.-H., CLOHISY, J. C. & ABU-AMER, Y. 2003. Tumour necrosis factor-[alpha] inhibits pre-osteoblast differentiation through its type-1 receptor. *Cytokine,* 22, 33-41.

ABRAHAMSSON, I., BERGLUNDH, T., LINDER, E., LANG, N. P. & LINDHE, J. 2004. Early bone formation adjacent to rough and turned endosseous implant surfaces. An experimental study in the dog. *Clinical Oral Implants Research,* 15, 381-392.

ABRON, A., HOPFENSPERGER, M., THOMPSON, J. & COOPER, L. F. 2001. Evaluation of a predictive model for implant surface topography effects on early osseointegration in the rat tibia model. *Journal of Prosthetic Dentistry,* 85, 40-46.

ADCOCK, I. M. 2000. Molecular mechanisms of glucocorticosteroid actions. *Pulm Pharmacol Ther,* 13, 115-26.

ALBREKTSSON, T., BRANEMARK, P. I., HANSSON, H. A. & LINDSTROM, J. 1981. Osseointegrated titanium implants. Requirements for ensuring a long-lasting, direct bone-to-implant anchorage in man. *Acta Orthopaedica Scandinavica,* 52, 155-170.

ALIKHANI, M., ALIKHANI, Z., BOYD, C., MACLELLAN, C. M., RAPTIS, M., LIU, R., PISCHON, N., TRACKMAN, P. C., GERSTENFELD, L. & GRAVES, D. T. 2007. Advanced glycation end products stimulate osteoblast apoptosis via the MAP kinase and cytosolic apoptotic pathways. *Bone,* 40, 345-353.

ALLISTON, T., CHOY, L., DUCY, P., KARSENTY, G. & DERYNCK, R. 2001. TGF-beta-induced repression of CBFA1 by Smad3 decreases cbfa1 and osteocalcin expression and inhibits osteoblast differentiation. *Embo J,* 20, 2254-72.

ALLORI, A. C., SAILON, A. M. & WARREN, S. M. 2008. Biological Basis of Bone Formation, Remodeling, and Repairâ€"Part I: Biochemical Signaling Molecules. *Tissue Engineering Part B: Reviews,* 14, 259-273.

ALMEIDA, M., HAN, L., MARTIN-MILLAN, M., O'BRIEN, C. A. & MANOLAGAS, S. C. 2007. Oxidative stress antagonizes Wnt signaling in osteoblast precursors by diverting beta-catenin from T cell factor- to forkhead box O-mediated transcription. *J Biol Chem,* 282, 27298-305.

AL-NAWAS, B., GROETZ, K. A., GOETZ, H., DUSCHNER, H. & WAGNER, W. 2008. Comparative histomorphometry and resonance frequency analysis of implants with moderately rough surfaces in a loaded animal model. *Clinical Oral Implants Research,* 19, 1-8.

ALVAREZ, M., LONG, H., ONYIA, J., HOCK, J., XU, W. & BIDWELL, J. 1997. Rat Osteoblast and Osteosarcoma Nuclear Matrix Proteins Bind with Sequence Specificity to the Rat Type I Collagen Promoter. *Endocrinology,* 138, 482-489.

ANNUNZIATA, M., GUIDA, L., PERILLO, L., AVERSA, R., PASSARO, I. & OLIVA, A. 2008. Biological response of human bone marrow stromal cells to

sandblasted titanium nitride-coated implant surfaces. *Journal of Materials Science: Materials in Medicine,* 19, 3585-3591.

APARICIO, C., GIL, F. J., FONSECA, C., BARBOSA, M. & PLANELL, J. A. 2003. Corrosion behaviour of commercially pure titanium shot blasted with different materials and sizes of shot particles for dental implant applications. *Biomaterials,* 24, 263-273.

ARYS, A., PHILIPPART, C., DOUROV, N., HE, Y., LE, Q. T. & PIREAUX, J. J. 1998. Analysis of titanium dental implants after failure of osseointegration: Combined histological, electron microscopy, and X-ray photoelectron spectroscopy approach. *Journal of Biomedical Materials Research,* 43, 300-312.

ASHKAR, S., WEBER, G. F., PANOUTSAKOPOULOU, V., SANCHIRICO, M. E., JANSSON, M., ZAWAIDEH, S., RITTLING, S. R., DENHARDT, D. T., GLIMCHER, M. J. & CANTOR, H. 2000. Eta-1 (osteopontin): an early component of type-1 (cell-mediated) immunity. *Science,* 287, 860-4.

BACHLE, M. & KOHAL, R. J. 2004. A systematic review of the influence of different titanium surfaces on proliferation, differentiation and protein synthesis of osteoblast-like MG63 cells. *Clinical Oral Implants Research,* 15, 683-692.

BAEUERLE, P. A. & HENKEL, T. 1994. Function and Activation of NF-kappaB in the Immune System. *Annual Review of Immunology,* 12, 141-179.

BAEUERLE, P. A. & HENKEL, T. 1994. Function and activation of NF-kappa B in the immune system. *Annu Rev Immunol,* 12, 141-79.

BAGNO, A. & DI BELLO, C. 2004. Surface treatments and roughness properties of Ti-based biomaterials. *Journal of Materials Science: Materials in Medicine,* 15, 935-949.

BAHT, G. S., HUNTER, G. K. & GOLDBERG, H. A. 2008. Bone sialoprotein-collagen interaction promotes hydroxyapatite nucleation. *Matrix Biology,* 27, 600-608.

BAI, X.-C., LU, D., BAI, J., ZHENG, H., KE, Z.-Y., LI, X.-M. & LUO, S.-Q. 2004. Oxidative stress inhibits osteoblastic differentiation of bone cells by ERK and NF-[kappa]B. *Biochemical and Biophysical Research Communications,* 314, 197-207.

BAIN, G., MÜLLER, T., WANG, X. & PAPKOFF, J. 2003. Activated [beta]-catenin induces osteoblast differentiation of C3H10T1/2 cells and participates in BMP2 mediated signal transduction. *Biochemical and Biophysical Research Communications,* 301, 84-91.

BALINT, E., SZABO, P., MARSHALL, C. F. & SPRAGUE, S. M. 2001. Glucose-induced inhibition of in vitro bone mineralization. *Bone,* 28, 21-28.

BALLONI, S., CALVI, E. M., DAMIANI, F., BISTONI, G., CALVITTI, M., LOCCI, P., BECCHETTI, E. & MARINUCCI, L. 2009. Effects of titanium surface roughness on mesenchymal stem cell commitment and differentiation signaling. *Int J Oral Maxillofac Implants,* 24, 627-35.

BARON, R., RAWADI, G., ROMANROMAN, S. & GERALD, P. S. 2006. Wnt Signaling: A Key Regulator of Bone Mass. *Current Topics in Developmental Biology.* Academic Press.

BARRÈRE, F., VALK, C. M. V. D., MEIJER, G., DALMEIJER, R. A. J., GROOT, K. D. & LAYROLLE, P. 2003. Osteointegration of biomimetic apatite coating applied onto dense and porous metal implants in femurs of goats.

Journal of Biomedical Materials Research Part B: Applied Biomaterials, 67B, 655-665.

BELLIDO, T., BORBA, V. Z. C., ROBERSON, P. & MANOLAGAS, S. C. 1997. Activation of the Janus kinase/STAT (signal transducer and activator of transcription) signal transduction pathway by interleukin-6-type cytokines promotes osteoblast differentiation. *Endocrinology,* 138, 3666-3676.

BELLOWS, C. G., HEERSCHE, J. N. M. & AUBIN, J. E. 1999. Aluminum Accelerates Osteoblastic Differentiation But is Cytotoxic in Long-Term Rat Calvaria Cell Cultures. *Calcified Tissue International,* 65, 59-65.

BERND, S., ECKART, P., MATTHIAS, H., EVGENIJ, K., SUSANNE, B., DIETER, S., EBERHARD, K., UWE, E. & RONALD, M. 2008. Suitability of differently designed matrix-based implant surface coatings: An animal study on bone formation. *Journal of Biomedical Materials Research Part B: Applied Biomaterials,* 87B, 516-524.

BERTOLINI, D. R., NEDWIN, G. E., BRINGMAN, T. S., SMITH, D. D. & MUNDY, G. R. 1986. Stimulation of Bone-Resorption and Inhibition of Bone-Formation Invitro by Human-Tumor Necrosis Factors. *Nature,* 319, 516-518.

BEYER NARDI, N. & DA SILVA MEIRELLES, L. 2006. Mesenchymal stem cells: isolation, in vitro expansion and characterization. *Handb Exp Pharmacol,* 249-82.

BIGI, A., BRACCI, B., CUISINIER, F., ELKAIM, R., FINI, M., MAYER, I., MIHAILESCU, I. N., SOCOL, G., STURBA, L. & TORRICELLI, P. 2005. Human osteoblast response to pulsed laser deposited calcium phosphate coatings. *Biomaterials,* 26, 2381-9.

BOIVIN, G., MOREL, G., LIAN, J. B., ANTHOINE-TERRIER, C., DUBOIS, P. M. & MEUNIER, P. J. 1990. Localization of endogenous osteocalcin in neonatal rat bone and its absence in articular cartilage: effect of warfarin treatment. *Virchows Arch A Pathol Anat Histopathol,* 417, 505-12.

BOLANDER, M. E. 1992. Regulation of fracture repair by growth factors. *Proc Soc Exp Biol Med,* 200, 165-70.

BONEWALD, L. F. & JOHNSON, M. L. 2008. Osteocytes, mechanosensing and Wnt signaling. *Bone,* 42, 606-15.

BONEWALD, L. F. 2007. Osteocytes as Dynamic, Multifunctional Cells. *Ann NY Acad Sci,* annals.1402.018.

BORSARI, V., FINI, M., GIAVARESI, G., RIMONDINI, L., CHIESA, R., CHIUSOLI, L. & GIARDINO, R. 2007a. Sandblasted titanium osteointegration in young, aged and ovariectomized sheep. *Int J Artif Organs,* 30, 163-72.

BORSARI, V., FINI, M., GIAVARESI, G., RIMONDINI, L., CONSOLO, U., CHIUSOLI, L., SALITO, A., VOLPERT, A., CHIESA, R. & GIARDINO, R. 2007b. Osteointegration of titanium and hydroxyapatite rough surfaces in healthy and compromised cortical and trabecular bone: in vivo comparative study on young, aged, and estrogen-deficient sheep. *J Orthop Res.*

BOSKEY, A. L. 1992. Mineral-matrix interactions in bone and cartilage. *Clin Orthop Relat Res,* 244-74.

BOSKEY, A. L., GADALETA, S., GUNDBERG, C., DOTY, S. B., DUCY, P. & KARSENTY, G. 1998. Fourier transform infrared microspectroscopic

analysis of bones of osteocalcin-deficient mice provides insight into the function of osteocalcin. *Bone,* 23, 187-96.

BOULETREAU, P. J., WARREN, S. M., SPECTOR, J. A., PELED, Z. M., GERRETS, R. P., GREENWALD, J. A. & LONGAKER, M. T. 2002. Hypoxia and VEGF Up-Regulate BMP-2 mRNA and Protein Expression in Microvascular Endothelial Cells: Implications for Fracture Healing. *Plastic and Reconstructive Surgery,* 109, 2384-2397.

BOURRIN, S., PALLE, S., PUPIER, R., VICO, L. & ALEXANDRE, C. 1995. Effects of physical training on bone adaptation in three zones of the rat tibia. *Journal of Bone and Mineral Research,* 10, 1745-1752.

BOYCE, B. F., AUFDEMORTE, T. B., GARRETT, I. R., YATES, A. J. & MUNDY, G. R. 1989. Effects of interleukin-1 on bone turnover in normal mice. *Endocrinology,* 125, 1142-50.

BOYLE, W. J., SIMONET, W. S. & LACEY, D. L. 2003. Osteoclast differentiation and activation. *Nature,* 423, 337-342.

BRANDSTROM, H., JONSSON, K. B., VIDAL, O., LJUNGHALL, S., OHLSSON, C. & LJUNGGREN, O. 1998. Tumor necrosis factor-alpha and -beta upregulate the levels of osteoprotegerin mRNA in human osteosarcoma MG-63 cells. *Biochem Biophys Res Commun,* 248, 454-7.

BREKKEN, R. A. & SAGE, E. H. 2001. SPARC, a matricellular protein: at the crossroads of cell-matrix communication: [Matrix Biology (2000) 569-580]. *Matrix Biology,* 19, 815-827.

BROWNLEE, M. 2005. The pathobiology of diabetic complications: a unifying mechanism. *Diabetes,* 54, 1615-25.

BROWNLEE, M., CERAMI, A. & VLASSARA, H. 1988. Advanced glycosylation end products in tissue and the biochemical basis of diabetic complications. *N Engl J Med,* 318, 1315-21.

BUCCIARELLI, L. G., WENDT, T., RONG, L., LALLA, E., HOFMANN, M. A., GOOVA, M. T., TAGUCHI, A., YAN, S. F., YAN, S. D., STERN, D. M. & SCHMIDT, A. M. 2002. RAGE is a multiligand receptor of the immunoglobulin superfamily: implications for homeostasis and chronic disease. *Cell Mol Life Sci,* 59, 1117-28.

BUCKWALTER, J. A., GLIMCHER, M. J., COOPER, R. R. & RECKER, R. 1995. Bone Biology. *J Bone Joint Surg Am,* 77, 1276-1289.

BURGER, E. H., KLEIN-NULEND, J. & SMIT, T. H. 2003. Strain-derived canalicular fluid flow regulates osteoclast activity in a remodelling osteon--a proposal. *J Biomech,* 36, 1453-9.

BURGESS, T. L., QIAN, Y. X., KAUFMAN, S., RING, B. D., VAN, G., CAPPARELLI, C., KELLEY, M., HSU, H. L., BOYLE, W. J., DUNSTAN, C. R., HU, S. & LACEY, D. L. 1999. The ligand for osteoprotegerin (OPGL) directly activates mature osteoclasts. *Journal of Cell Biology,* 145, 527-538.

BUSER, D., BROGGINI, N., WIELAND, M., SCHENK, R. K., DENZER, A. J., COCHRAN, D. L., HOFFMANN, B., LUSSI, A. & STEINEMANN, S. G. 2004. Enhanced bone apposition to a chemically modified SLA titanium surface. *Journal of Dental Research,* 83, 529-533.

BUSER, D., NYDEGGER, T., HIRT, H. P., COCHRAN, D. L. & NOLTE, L. P. 1998. Removal torque values of titanium implants in the maxilla of miniature pigs. *Int J Oral Maxillofac Implants,* 13, 611-9.

BUSER, D., SCHENK, R. K., STEINEMANN, S., FIORELLINI, J. P., FOX, C. H. & STICH, H. 1991. Influence of surface characteristics on bone integration of titanium implants. A histomorphometric study in miniature pigs. *Journal of Biomedical Materials Research,* 25, 889-902.

CALVI, L. M., ADAMS, G. B., WEIBRECHT, K. W., WEBER, J. M., OLSON, D. P., KNIGHT, M. C., MARTIN, R. P., SCHIPANI, E., DIVIETI, P., BRINGHURST, F. R., MILNER, L. A., KRONENBERG, H. M. & SCADDEN, D. T. 2003. Osteoblastic cells regulate the haematopoietic stem cell niche. *Nature,* 425, 841-846.

CANALIS, E. & GABBITAS, B. 1994. Bone Morphogenetic Protein-2 Increases Insulin-Like Growth Factor-I and Factor-Ii Transcripts and Polypeptide Levels in Bone Cell-Cultures. *Journal of Bone and Mineral Research,* 9, 1999-2005.

CANALIS, E. 1986. Interleukin-1 has independent effects on deoxyribonucleic acid and collagen synthesis in cultures of rat calvariae. *Endocrinology,* 118, 74-81.

CANALIS, E., CENTRELLA, M. & MCCARTHY, T. 1988. Effects of Basic Fibroblast Growth-Factor on Bone-Formation Invitro. *Journal of Clinical Investigation,* 81, 1572-1577.

CARLSSON, L. V., ALBERKTSSON, T. & BERMAN, C. 1989. Bone response to plasma-cleaned titanium implants. *The International journal of oral & maxillofacial implants,* 4, 199-204.

CASSATELLA, M. A., MEDA, L., BONORA, S., CESKA, M. & CONSTANTIN, G. 1993. Interleukin 10 (IL-10) inhibits the release of proinflammatory cytokines from human polymorphonuclear leukocytes. Evidence for an autocrine role of tumor necrosis factor and IL-1 beta in mediating the production of IL-8 triggered by lipopolysaccharide. *The Journal of Experimental Medicine,* 178, 2207-2211.

CELIL, A. B. & CAMPBELL, P. G. 2005. BMP-2 and insulin-like growth factor-I mediate osterix (Osx) expression in human mesenchymal stem cells via the MAPK and protein kinase D signaling pathways. *Journal of Biological Chemistry,* 280, 31353-31359.

CENTRELLA, M., CASINGHINO, S., IGNOTZ, R. & MCCARTHY, T. L. 1992. Multiple regulatory effects by transforming growth factor-beta on type I collagen levels in osteoblast-enriched cultures from fetal rat bone. *Endocrinology,* 131, 2863-72.

CENTRELLA, M., HOROWITZ, M. C., WOZNEY, J. M. & MCCARTHY, T. L. 1994. Transforming Growth Factor-{beta} Gene Family Members and Bone. *Endocr Rev,* 15, 27-39.

CENTRELLA, M., MASSAGUE, J. & CANALIS, E. 1986. Human platelet-derived transforming growth factor-beta stimulates parameters of bone growth in fetal rat calvariae. *Endocrinology,* 119, 2306-12.

CHAMBERS, T. J. 2000. Regulation of the differentiation and function of osteoclasts. *The Journal of Pathology,* 192, 4-13.

CHAUDHARY, L. R., HOFMEISTER, A. M. & HRUSKA, K. A. 2004. Differential growth factor control of bone formation through osteoprogenitor differentiation. *Bone,* 34, 402-411.

CHENG, S.-L., SHAO, J.-S., CHARLTON-KACHIGIAN, N., LOEWY, A. P. & TOWLER, D. A. 2003. Msx2 Promotes Osteogenesis and Suppresses

Adipogenic Differentiation of Multipotent Mesenchymal Progenitors. *J. Biol. Chem.*, 278, 45969-45977.

CHO, S. A. & PARK, K. T. 2003. The removal torque of titanium screw inserted in rabbit tibia treated by dual acid etching. *Biomaterials,* 24, 3611-3617.

CHUNG, S. H., HEO, S. J., KOAK, J. Y., KIM, S. K., LEE, J. B., HAN, J. S., HAN, C. H., RHYU, I. C. & LEE, S. J. 2008. Effects of implant geometry and surface treatment on osseointegration after functional loading: a dog study. *Journal of Oral Rehabilitation,* 35, 229-236.

COCHRAN, D. L., BUSER, D., TEN BRUGGENKATE, C. M., WEINGART, D., TAYLOR, T. M., BERNARD, J. P., PETERS, F. & SIMPSON, J. P. 2002. The use of reduced healing times on ITI® implants with a sandblasted and acid-etched (SLA) surface: Early results from clinical trials on ITI® SLA implants. *Clinical Oral Implants Research,* 13, 144-153.

COCHRAN, D. L., SCHENK, R. K., LUSSI, A., HIGGINBOTTOM, F. L. & BUSER, D. 1998. Bone response to unloaded and loaded titanium implants with a sandblasted and acid-etched surface: A histometric study in the canine mandible. *Journal of Biomedical Materials Research,* 40, 1-11.

COOPER, L. F. 2000. A role for surface topography in creating and maintaining bone at titanium endosseous implants. *J Prosthet Dent,* 84, 522-34.

COOPER, L. F., MASUDA, T., WHITSON, S. W., YLIHEIKKILA, P. & FELTON, D. A. 1999. Formation of mineralizing osteoblast cultures on machined, titanium oxide grit-blasted, and plasma-sprayed titanium surfaces. *Int J Oral Maxillofac Implants,* 14, 37-47.

DACULSI, G., LABOUX, O., MALARD, O. & WEISS, P. 2003. Current state of the art of biphasic calcium phosphate bioceramics. *J Mater Sci Mater Med,* 14, 195-200.

DAI, J. C., HE, P., CHEN, X. & GREENFIELD, E. M. 2006. TNFalpha and PTH utilize distinct mechanisms to induce IL-6 and RANKL expression with markedly different kinetics. *Bone,* 38, 509-20.

D'ANDREA, L. D., DEL GATTO, A., DE ROSA, L., ROMANELLI, A. & PEDONE, C. 2009. Peptides targeting angiogenesis related growth factor receptors. *Curr Pharm Des,* 15, 2414-29.

DAVIES, J. E. 1996. In vitro modeling of the bone/implant interface. *Anat Rec,* 245, 426-45.

DAVIES, J. E. 2003. Understanding peri-implant endosseous healing. *J Dent Educ,* 67, 932-49.

DAY, T. F., GUO, X., GARRETT-BEAL, L. & YANG, Y. 2005. Wnt/[beta]-Catenin Signaling in Mesenchymal Progenitors Controls Osteoblast and Chondrocyte Differentiation during Vertebrate Skeletogenesis. *Developmental Cell,* 8, 739-750.

DE GROOT, K., WOLKE, J. G. & JANSEN, J. A. 1998. Calcium phosphate coatings for medical implants. *Proc Inst Mech Eng H,* 212, 137-47.

DE VRIES, J. E. 1995. Immunosuppressive and Anti-inflammatory Properties of Interleukin 10. *Annals of Medicine,* 27, 537-541.

DEBIAIS, F., HOTT, M., GRAULET, A. M. & MARIE, P. J. 1998. The effects of fibroblast growth factor-2 on human neonatal calvaria osteoblastic cells are differentiation stage specific. *Journal of Bone and Mineral Research,* 13, 645-654.

DELAFONTAINE, P., SONG, Y.-H. & LI, Y. 2004. Expression, Regulation, and Function of IGF-1, IGF-1R, and IGF-1 Binding Proteins in Blood Vessels. *Arterioscler Thromb Vasc Biol,* 24, 435-444.

DELANY, A. M., AMLING, M., PRIEMEL, M., HOWE, C., BARON, R. & CANALIS, E. 2000. Osteopenia and decreased bone formation in osteonectin-deficient mice. *J Clin Invest,* 105, 1325.

DELANY, A. M., KALAJZIC, I., BRADSHAW, A. D., SAGE, E. H. & CANALIS, E. 2003. Osteonectin-Null Mutation Compromises Osteoblast Formation, Maturation, and Survival. *Endocrinology,* 144, 2588-2596.

DELIGIANNI, D. D., KATSALA, N., LADAS, S., SOTIROPOULOU, D., AMEDEE, J. & MISSIRLIS, Y. F. 2001. Effect of surface roughness of the titanium alloy Ti-6Al-4V on human bone marrow cell response and on protein adsorption. *Biomaterials,* 22, 1241-51.

DENHARDT, D. T., NODA, M., OÂ€™REGAN, A. W., PAVLIN, D. & BERMAN, J. S. 2001. Osteopontin as a means to cope with environmental insults: regulation of inflammation, tissue remodeling, and cell survival. *The Journal of Clinical Investigation,* 107, 1055-1061.

DERYNCK, R., AKHURST, R. J. & BALMAIN, A. 2001. TGF-beta signaling in tumor suppression and cancer progression. *Nat Genet,* 29, 117-29.

DINARELLO, C. A. 2000. The role of the interleukin-1-receptor antagonist in blocking inflammation mediated by interleukin-1. *N Engl J Med,* 343, 732-4.

DING, J., GHALI, O., LENCEL, P., BROUX, O., CHAUVEAU, C., DEVEDJIAN, J. C., HARDOUIN, P. & MAGNE, D. 2009. TNF-[alpha] and IL-1[beta] inhibit RUNX2 and collagen expression but increase alkaline phosphatase activity and mineralization in human mesenchymal stem cells. *Life Sciences,* 84, 499-504.

DU, X., MATSUMURA, T., EDELSTEIN, D., ROSSETTI, L., ZSENGELLER, Z., SZABO, C. & BROWNLEE, M. 2003. Inhibition of GAPDH activity by poly(ADP-ribose) polymerase activates three major pathways of hyperglycemic damage in endothelial cells. *J Clin Invest,* 112, 1049-57.

DUCHESNE, L., TISSOT, B. R. R., RUDD, T. R., DELL, A. & FERNIG, D. G. 2006. N-Glycosylation of Fibroblast Growth Factor Receptor 1 Regulates Ligand and Heparan Sulfate Co-receptor Binding. *Journal of Biological Chemistry,* 281, 27178-27189.

DUCY, P., DESBOIS, C., BOYCE, B., PINERO, G., STORY, B., DUNSTAN, C., SMITH, E., BONADIO, J., GOLDSTEIN, S., GUNDBERG, C., BRADLEY, A. & KARSENTY, G. 1996. Increased bone formation in osteocalcin-deficient mice. *Nature,* 382, 448-452.

DUCY, P., ZHANG, R., GEOFFROY, V., RIDALL, A. L. & KARSENTY, G. 1997. Osf2/Cbfa1: A Transcriptional Activator of Osteoblast Differentiation. *Cell,* 89, 747-754.

EINHORN, T. A. 1998. The cell and molecular biology of fracture healing. *Clin Orthop Relat Res,* S7-21.

EINHORN, T. A., MAJESKA, R. J., RUSH, E. B., LEVINE, P. M. & HOROWITZ, M. C. 1995. The expression of cytokine activity by fracture callus. *J Bone Miner Res,* 10, 1272-81.

ELLIES, L. G. & AUBIN, J. E. 1990. Temporal sequence of interleukin 1[alpha]--mediated stimulation and inhibition of bone formation by isolated fetal rat calvaria cells in vitro. *Cytokine,* 2, 430-437.

ELLINGSEN, J. E., THOMSEN, P. & LYNGSTADAAS, S. P. 2006. Advances in dental implant materials and tissue regeneration. *Periodontology 2000,* 41, 136-156.

EMI, S. & YORIMASA, O. 2002. Activation of bone sialoprotein gene transcription by flavonoids is mediated through an inverted CCAAT box in ROS 17/2.8 cells. *Journal of Cellular Biochemistry,* 86, 35-44.

ERICES, A., CONGET, P., ROJAS, C. & MINGUELL, J. J. 2002. Gp130 activation by soluble interleukin-6 receptor/interleukin-6 enhances osteoblastic differentiation of human bone marrow-derived mesenchymal stem cells. *Exp Cell Res,* 280, 24-32.

ESPOSITO, M., MURRAY-CURTIS, L., GRUSOVIN, M., COULTHARD, P. & WORTHINGTON, H. 2007. Interventions for replacing missing teeth: different types of dental implants. *Cochrane Database Syst Rev,* CD003815.

FERRARI, D., PIZZIRANI, C., ADINOLFI, E., LEMOLI, R. M., CURTI, A., IDZKO, M., PANTHER, E. & DI VIRGILIO, F. 2006. The P2X7 receptor: a key player in IL-1 processing and release. *J Immunol,* 176, 3877-83.

FIORELLINI, J. P., CHEN, P. K., NEVINS, M. & NEVINS, M. L. 2000. A retrospective study of dental implants in diabetic patients. *Int J Periodontics Restorative Dent,* 20, 366-73.

FIORELLINI, J. P., NEVINS, M. L., NORKIN, A., WEBER, H. P. & KARIMBUX, N. Y. 1999. The effect of insulin therapy on osseointegration in a diabetic rat model. *Clin Oral Implants Res,* 10, 362-8.

FISHER, L. W., TORCHIA, D. A., FOHR, B., YOUNG, M. F. & FEDARKO, N. S. 2001. Flexible Structures of SIBLING Proteins, Bone Sialoprotein, and Osteopontin. *Biochemical and Biophysical Research Communications,* 280, 460-465.

FRANCESCHI, R. T., WANG, D., KREBSBACH, P. H. & RUTHERFORD, R. B. 2000. Gene therapy for bone formation: In vitro and in vivo osteogenic activity of an adenovirus expressing BMP7. *Journal of Cellular Biochemistry,* 78, 476-486.

FRANCHI, M., BACCHELLI, B., GIAVARESI, G., DE PASQUALE, V., MARTINI, D., FINI, M., GIARDINO, R. & RUGGERI, A. 2007. Influence of different implant surfaces on peri-implant osteogenesis: histomorphometric analysis in sheep. *J Periodontol,* 78, 879-88.

FRANCHIMONT, N., DURANT, D. & CANALIS, E. 1997. Interleukin-6 and its soluble receptor regulate the expression of insulin-like growth factor binding protein-5 in osteoblast cultures. *Endocrinology,* 138, 3380-3386.

FRANZ-ODENDAAL, T. A., HALL, B. K. & WITTEN, P. E. 2006. Buried alive: How osteoblasts become osteocytes. *Developmental Dynamics,* 235, 176-190.

FRIBERG, B., EKESTUBBE, A., MELLSTROM, D. & SENNERBY, L. 2001. Branemark implants and osteoporosis: a clinical exploratory study. *Clin Implant Dent Relat Res,* 3, 50-6.

FRIBERG, B., GRONDAHL, K., LEKHOLM, U. & BRANEMARK, P. I. 2000. Long-term follow-up of severely atrophic edentulous mandibles reconstructed with short Branemark implants. *Clin Implant Dent Relat Res,* 2, 184-9.

FRIEDENSTEIN, A. J. 1976. Precursor Cells of Mechanocytes. *International Review of Cytology-a Survey of Cell Biology,* 47, 327-359.

FU, L., TANG, T., MIAO, Y., ZHANG, S., QU, Z. & DAI, K. 2008. Stimulation of osteogenic differentiation and inhibition of adipogenic differentiation in bone

marrow stromal cells by alendronate via ERK and JNK activation. *Bone,* 43, 40-47.

GANGJI, V., RYDZIEL, S., GABBITAS, B. & CANALIS, E. 1998. Insulin-like growth factor II promoter expression in cultured rodent osteoblasts and adult rat bone. *Endocrinology,* 139, 2287-2292.

GATTO, M., DRUDI-METALLI, V., TORRICE, A., ALPINI, G., CANTAFORA, A., BLOTTA, I. & ALVARO, D. 2008. Insulin-like growth factor-1 isoforms in rat hepatocytes and cholangiocytes and their involvement in protection against cholestatic injury. *Lab Invest,* 88, 986-94.

GAUR, T., LENGNER, C. J., HOVHANNISYAN, H., BHAT, R. A., BODINE, P. V., KOMM, B. S., JAVED, A., VAN WIJNEN, A. J., STEIN, J. L., STEIN, G. S. & LIAN, J. B. 2005. Canonical WNT signaling promotes osteogenesis by directly stimulating Runx2 gene expression. *J Biol Chem,* 280, 33132-40.

GEBAUER, G. P., LIN, S. S., BEAM, H. A., VIEIRA, P. & PARSONS, J. R. 2002. Low-intensity pulsed ultrasound increases the fracture callus strength in diabetic BB Wistar rats but does not affect cellular proliferation. *J Orthop Res,* 20, 587-92.

GERSBACH, C. A., BYERS, B. A., PAVLATH, G. K. & GARCÍA, A. J. 2004. Runx2/Cbfa1 stimulates transdifferentiation of primary skeletal myoblasts into a mineralizing osteoblastic phenotype. *Experimental Cell Research,* 300, 406-417.

GERSTENFELD, L. C., CRUCETA, J., SHEA, C. M., SAMPATH, K., BARNES, G. L. & EINHORN, T. A. 2002. Chondrocytes Provide Morphogenic Signals That Selectively Induce Osteogenic Differentiation of Mesenchymal Stem Cells. *Journal of Bone and Mineral Research,* 17, 221-230.

GIACHELLI, C. M. & STEITZ, S. 2000. Osteopontin: a versatile regulator of inflammation and biomineralization. *Matrix Biology,* 19, 615-622.

GILBERT, L., HE, X., FARMER, P., RUBIN, J., DRISSI, H., VAN WIJNEN, A. J., LIAN, J. B., STEIN, G. S. & NANES, M. S. 2002. Expression of the Osteoblast Differentiation Factor RUNX2 (Cbfa1/AML3/Pebp2alpha A) Is Inhibited by Tumor Necrosis Factor-alpha. *J. Biol. Chem.,* 277, 2695-2701.

GOPALAKRISHNAN, V., VIGNESH, R. C., ARUNAKARAN, J., ARULDHAS, M. M. & SRINIVASAN, N. 2006. Effects of glucose and its modulation by insulin and estradiol on BMSC differentiation into osteoblastic lineages. *Biochem Cell Biol,* 84, 93-101.

GORSKI, J. P. 1998. Is all bone the same? Distinctive distributions and properties of non-collagenous matrix proteins in lamellar vs. woven bone imply the existence of different underlying osteogenic mechanisms. *Crit Rev Oral Biol Med,* 9, 201-223.

GOTFREDSEN, K., WENNERBERG, A., JOHANSSON, C., SKOVGAARD, L. T. & HJORTING-HANSEN, E. 1995. Anchorage of TiO2-blasted, HA-coated, and machined implants: An experimental study with rabbits. *Journal of Biomedical Materials Research,* 29, 1223-1231.

GOTO, Y., KAKIZAKI, M. & MASAKI, N. 1975. Spontaneous Diabetes Produced by Selective Breeding of Normal Wistar Rats. *Proceedings of the Japan Academy,* 51, 80-85.

GOWEN, M., MACDONALD, B. R. & RUSSELL, R. G. 1988. Actions of recombinant human gamma-interferon and tumor necrosis factor alpha on the

proliferation and osteoblastic characteristics of human trabecular bone cells in vitro. *Arthritis Rheum,* 31, 1500-7.

GRAVES, D. T., LIU, R., ALIKHANI, M., AL-MASHAT, H. & TRACKMAN, P. C. 2006. Diabetes-enhanced Inflammation and Apoptosis--Impact on Periodontal Pathology. *Journal of Dental Research,* 85, 15-21.

GROSS, T. S. & RUBIN, C. T. 1995. Uniformity of resorptive bone loss induced by disuse. *Journal of Orthopaedic Research,* 13, 708-714.

GU, G., MULARI, M., PENG, Z., HENTUNEN, T. A. & VAANANEN, H. K. 2005. Death of osteocytes turns off the inhibition of osteoclasts and triggers local bone resorption. *Biochem Biophys Res Commun,* 335, 1095-101.

GURANTZ, D., YNDESTAD, A., HALVORSEN, B., LUNDE, O. V., OMENS, J. H., UELAND, T., AUKRUST, P. L., MOORE, C. D., KJEKSHUS, J. & GREENBERG, B. H. 2005. Etanercept or intravenous immunoglobulin attenuates expression of genes involved in post-myocardial infarction remodeling. *Cardiovascular Research,* 67, 106-115.

HACK-YOUNG MAENG, D.-K. C. M. T. M. Y. M. T. T. T. M. T. T. I. Y. S. C. F. 2002. Appearance of Osteonectin-expressing Fibroblastic Cells in Early Rat Stomach Carcinogenesis and Stomach Tumors Induced with N-Methyl-N'-nitro-N-nitrosoguanidine. *Cancer Science,* 93, 960-967.

HAGA, M., FUJII, N., NOZAWA-INOUE, K., NOMURA, S., ODA, K., UOSHIMA, K. & MAEDA, T. 2008. Detailed Process of Bone Remodeling After Achievement of Osseointegration in a Rat Implantation Model. *Anat Rec (Hoboken).*

HANAZAWA, S., OHMORI, Y., AMANO, S., HIROSE, K., MIYOSHI, T., KUMEGAWA, M. & KITANO, S. 1986. Human Purified Interleukin-1 Inhibits DNA-Synthesis and Cell-Growth of Osteoblastic Cell-Line (Mc3t3-E1), but Enhances Alkaline-Phosphatase Activity in the Cells. *Febs Letters,* 203, 279-284.

HARADA, H., TAGASHIRA, S., FUJIWARA, M., OGAWA, S., KATSUMATA, T., YAMAGUCHI, A., KOMORI, T. & NAKATSUKA, M. 1999. Cbfa1 isoforms exert functional differences in osteoblast differentiation. *Journal of Biological Chemistry,* 274, 6972-6978.

HASEGAWA, H., OZAWA, S., HASHIMOTO, K., TAKEICHI, T. & OGAWA, T. 2008. Type 2 diabetes impairs implant osseointegration capacity in rats. *Int J Oral Maxillofac Implants,* 23, 237-46.

HATA, K., IKEBE, K., WADA, M. & NOKUBI, T. 2007. Osteoblast response to titanium regulates transcriptional activity of Runx2 through MAPK pathway. *Journal of Biomedical Materials Research Part A,* 81A, 446-452.

HE, H., LIU, R., DESTA, T., LEONE, C., GERSTENFELD, L. C. & GRAVES, D. T. 2004. Diabetes causes decreased osteoclastogenesis, reduced bone formation, and enhanced apoptosis of osteoblastic cells in bacteria stimulated bone loss. *Endocrinology,* 145, 447-52.

HEILIG, C. W., CONCEPCION, L. A., RISER, B. L., FREYTAG, S. O., ZHU, M. & CORTES, P. 1995. Overexpression of glucose transporters in rat mesangial cells cultured in a normal glucose milieu mimics the diabetic phenotype. *J Clin Invest,* 96, 1802-14.

HEINO, T. J., HENTUNEN, T. A. & VAANANEN, H. K. 2004. Conditioned medium from osteocytes stimulates the proliferation of bone marrow

mesenchymal stem cells and their differentiation into osteoblasts. *Exp Cell Res,* 294, 458-68.

HEINO, T. J., KURATA, K., HIGAKI, H. & VAANANEN, H. K. 2009. Evidence for the role of osteocytes in the initiation of targeted remodeling. *Technol Health Care,* 17, 49-56.

HELDIN, C.-H., MIYAZONO, K. & TEN DIJKE, P. 1997. TGF-[beta] signalling from cell membrane to nucleus through SMAD proteins. *Nature,* 390, 465-471.

HILL, T. P., SPÄTER, D., TAKETO, M. M., BIRCHMEIER, W. & HARTMANN, C. 2005. Canonical Wnt/[beta]-Catenin Signaling Prevents Osteoblasts from Differentiating into Chondrocytes. *Developmental Cell,* 8, 727-738.

HILLAM, R. A. & SKERRY, T. M. 1995. Inhibition of bone resorption and stimulation of formation by mechanical loading of the modeling rat ulna in vivo. *Journal of Bone and Mineral Research,* 10, 683-689.

HOANG, Q. Q., SICHERI, F., HOWARD, A. J. & YANG, D. S. C. 2003. Bone recognition mechanism of porcine osteocalcin from crystal structure. *Nature,* 425, 977-980.

HOFBAUER, L. C., LACEY, D. L., DUNSTAN, C. R., SPELSBERG, T. C., RIGGS, B. L. & KHOSLA, S. 1999. Interleukin-1 beta and tumor necrosis factor-alpha, but not interleukin-6, stimulate osteoprotegerin ligand gene expression in human osteoblastic cells. *Bone,* 25, 255-259.

HOLT, I., DAVIE, M. W. J. & MARSHALL, M. J. 1996. Osteoclasts are not the major source of interleukin-6 in mouse parietal bones. *Bone,* 18, 221-226.

HONG, J.-H., HWANG, E. S., MCMANUS, M. T., AMSTERDAM, A., TIAN, Y., KALMUKOVA, R., MUELLER, E., BENJAMIN, T., SPIEGELMAN, B. M., SHARP, P. A., HOPKINS, N. & YAFFE, M. B. 2005. TAZ, a Transcriptional Modulator of Mesenchymal Stem Cell Differentiation. *Science,* 309, 1074-1078.

HOOGEBOOM, D. & BURGERING, B. M. 2009. Should I stay or should I go: beta-catenin decides under stress. *Biochim Biophys Acta,* 1796, 63-74.

HSU, H., LACEY, D. L., DUNSTAN, C. R., SOLOVYEV, I., COLOMBERO, A., TIMMS, E., TAN, H.-L., ELLIOTT, G., KELLEY, M. J., SAROSI, I., WANG, L., XIA, X.-Z., ELLIOTT, R., CHIU, L., BLACK, T., SCULLY, S., CAPPARELLI, C., MORONY, S., SHIMAMOTO, G., BASS, M. B. & BOYLE, W. J. 1999. Tumor necrosis factor receptor family member RANK mediates osteoclast differentiation and activation induced by osteoprotegerin ligand. *PNAS,* 96, 3540-3545.

HUGHES, F. J., AUBIN, J. E. & HEERSCHE, J. N. M. 1992. Differential chemotactic responses of different populations of fetal rat calvaria cells to platelet-derived growth factor and transforming growth factor [beta]. *Bone and Mineral,* 19, 63-74.

HUGHES, F. J., BUTTERY, L. D. K., HUKKANEN, M. V. J., O'DONNELL, A., MACLOUF, J. & POLAK, J. M. 1999. Cytokine-induced prostaglandin E-2 synthesis and cyclooxygenase-2 activity are regulated both by a nitric oxide-dependent and -independent mechanism in rat osteoblasts in vitro. *Journal of Biological Chemistry,* 274, 1776-1782.

HUGHES, F. J., COLLYER, J., STANFIELD, M. & GOODMAN, S. A. 1995. The effects of bone morphogenetic protein-2, -4, and -6 on differentiation of rat osteoblast cells in vitro. *Endocrinology,* 136, 2671-2677.

HUGHES, F. J., TURNER, W., BELIBASAKIS, G. & MARTUSCELLI, G. 2006. Effects of growth factors and cytokines on osteoblast differentiation. *Periodontology 2000,* 41, 48-72.

HUKKANEN, M., HUGHES, F. J., BUTTERY, L. D. K., GROSS, S. S., EVANS, T. J., SEDDON, S., RIVEROSMORENO, V., MACINTYRE, I. & POLAK, J. M. 1995. Cytokine-Stimulated Expression of Inducible Nitric-Oxide Synthase by Mouse, Rat, and Human Osteoblast-Like Cells and Its Functional-Role in Osteoblast Metabolic-Activity. *Endocrinology,* 136, 5445-5453.

HULTENBY, K., REINHOLT, F. P., NORGARD, M., OLDBERG, A., WENDEL, M. & HEINEGARD, D. 1994. Distribution and synthesis of bone sialoprotein in metaphyseal bone of young rats show a distinctly different pattern from that of osteopontin. *Eur J Cell Biol,* 63, 230-9.

ISHIMI, Y., MIYAURA, C., JIN, C. H., AKATSU, T., ABE, E., NAKAMURA, Y., YAMAGUCHI, A., YOSHIKI, S., MATSUDA, T., HIRANO, T., KISHIMOTO, T. & SUDA, T. 1990. Il-6 Is Produced by Osteoblasts and Induces Bone-Resorption. *Journal of Immunology,* 145, 3297-3303.

IVANOFF, C.-J., WIDMARK, G., HALLGREN, C., SENNERBY, L. & WENNERBERG, A. 2001. Histologic evaluation of the bone integration of TiO2 blasted and turned titanium microimplants in humans. *Clinical Oral Implants Research,* 12, 128-134.

IWASAKI, K., KOMAKI, M., MIMORI, K., LEON, E., IZUMI, Y. & ISHIKAWA, I. 2008. IL-6 induces osteoblastic differentiation of periodontal ligament cells. *J Dent Res,* 87, 937-42.

JANSSENS, K., TEN DIJKE, P., JANSSENS, S. & VAN HUL, W. 2005. Transforming growth factor-beta 1 to the bone. *Endocrine Reviews,* 26, 743-774.

JOOS, U., WIESMANN, H. P., SZUWART, T. & MEYER, U. 2006. Mineralization at the interface of implants. *International Journal of Oral and Maxillofacial Surgery,* 35, 783-790.

KAISER, N., SASSON, S., FEENER, E. P., BOUKOBZA-VARDI, N., HIGASHI, S., MOLLER, D. E., DAVIDHEISER, S., PRZYBYLSKI, R. J. & KING, G. L. 1993. Differential regulation of glucose transport and transporters by glucose in vascular endothelial and smooth muscle cells. *Diabetes,* 42, 80-89.

KALFAS, I. H. 2001. Principles of bone healing. *Neurosurg Focus,* 10, E1.

KAMALIA, N., MCCULLOCH, C. A., TENEBAUM, H. C. & LIMEBACK, H. 1992. Dexamethasone recruitment of self-renewing osteoprogenitor cells in chick bone marrow stromal cell cultures. *Blood,* 79, 320-326.

KARTSOGIANNIS, V. & NG, K. W. 2004. Cell lines and primary cell cultures in the study of bone cell biology. *Mol Cell Endocrinol,* 228, 79-102.

KATAGIRI, T. & TAKAHASHI, N. 2002. Regulatory mechanisms of osteoblast and osteoclast differentiation. *Oral Diseases,* 8, 147-159.

KATAGIRI, T., YAMAGUCHI, A., IKEDA, T., YOSHIKI, S., WOZNEY, J. M., ROSEN, V., WANG, E. A., TANAKA, H., OMURA, S. & SUDA, T. 1990. The Nonosteogenic Mouse Pluripotent Cell-Line, C3h10t1/2, Is Induced to Differentiate into Osteoblastic Cells by Recombinant Human Bone Morphogenetic Protein-2. *Biochemical and Biophysical Research Communications,* 172, 295-299.

KAWAHARA, H., AOKI, H., KOIKE, H., SOEDA, Y., KAWAHARA, D. & MATSUDA, S. 2006. No evidence to indicate topographic dependency on bone formation around cp titanium implants under masticatory loading. *Journal of Materials Science: Materials in Medicine,* V17, 727-734.

KAWAI, S. & SUGIURA, T. 2001. Characterization of human bone morphogenetic protein (BMP)-4 and-7 gene promoters: Activation of BMP promoters by Gli, a sonic hedgehog mediator. *Bone,* 29, 54-61.

KELM, R. J., SWORDS, N. A., ORFEO, T. & MANN, K. G. 1994. Osteonectin in matrix remodeling. A plasminogen-osteonectin-collagen complex. *Journal of Biological Chemistry,* 269, 30147-30153.

KIESWETTER, K., SCHWARTZ, Z., DEAN, D. D. & BOYAN, B. D. 1996a. The role of implant surface characteristics in the healing of bone. *Crit Rev Oral Biol Med,* 7, 329-45.

KIESWETTER, K., SCHWARTZ, Z., HUMMERT, T. W., COCHRAN, D. L., SIMPSON, J., DEAN, D. D. & BOYAN, B. D. 1996b. Surface roughness modulates the local production of growth factors and cytokines by osteoblast-like MG-63 cells. *J Biomed Mater Res,* 32, 55-63.

KIM, B.-S., CHEN, J., WEINSTEIN, T., NOIRI, E. & GOLIGORSKY, M. S. 2002. VEGF Expression in Hypoxia and Hyperglycemia: Reciprocal Effect on Branching Angiogenesis in Epithelial-Endothelial Co-Cultures. *J Am Soc Nephrol,* 13, 2027-2036.

KIM, M.-J., KIM, C.-W., LIM, Y.-J. & HEO, S.-J. 2006. Microrough titanium surface affects biologic response in MG63 osteoblast-like cells. *Journal of Biomedical Materials Research Part A,* 79A, 1023-1032.

KINGSLEY, D. M., BLAND, A. E., GRUBBER, J. M., MARKER, P. C., RUSSELL, L. B., COPELAND, N. G. & JENKINS, N. A. 1992. The mouse short ear skeletal morphogenesis locus is associated with defects in a bone morphogenetic member of the TGF[beta] superfamily. *Cell,* 71, 399-410.

KINTO, N., IWAMOTO, M., ENOMOTOIWAMOTO, M., NOJI, S., OHUCHI, H., YOSHIOKA, H., KATAOKA, H., WADA, Y., YUHAO, G., TAKAHASHI, H. E., YOSHIKI, S. & YAMAGUCHI, A. 1997. Fibroblasts expressing Sonic hedgehog induce osteoblast differentiation and ectopic bone formation. *Febs Letters,* 404, 319-323.

KIRN, H. D. & VALENTINI, R. F. 1997. Human osteoblast response in vitro to platelet-derived growth factor and transforming growth factor-[beta] delivered from controlled-release polymer rods. *Biomaterials,* 18, 1175-1184.

KLOKKEVOLD, P. R. & HAN, T. J. 2007. How do smoking, diabetes, and periodontitis affect outcomes of implant treatment? *International Journal of Oral & Maxillofacial Implants,* 22, 173-198.

KOLLET, O., DAR, A. & LAPIDOT, T. 2007. The Multiple Roles of Osteoclasts in Host Defense: Bone Remodeling and Hematopoietic Stem Cell Mobilization. *Annual Review of Immunology,* 25.

KOMORI, T., YAGI, H., NOMURA, S., YAMAGUCHI, A., SASAKI, K., DEGUCHI, K., SHIMIZU, Y., BRONSON, R. T., GAO, Y. H., INADA, M., SATO, M., OKAMOTO, R., KITAMURA, Y., YOSHIKI, S. & KISHIMOTO, T. 1997. Targeted disruption of Cbfa1 results in a complete lack of bone formation owing to maturational arrest of osteoblasts. *Cell,* 89, 755-764.

KONO, S.-J., OSHIMA, Y., HOSHI, K., BONEWALD, L. F., ODA, H., NAKAMURA, K., KAWAGUCHI, H. & TANAKA, S. 2007. Erk pathways negatively regulate matrix mineralization. *Bone,* 40, 68-74.

KOUTOULAKI, A., LANGLEY, M., SLOAN, A. J., AESCHLIMANN, D. & WEI, X.-Q. TNF[alpha] and TGF-[beta]1 influence IL-18-induced IFN[gamma] production through regulation of IL-18 receptor and T-bet expression. *Cytokine,* 49, 177-184.

KUME, S., KATO, S., YAMAGISHI, S.-I., INAGAKI, Y., UEDA, S., ARIMA, N., OKAWA, T., KOJIRO, M. & NAGATA, K. 2005. Advanced Glycation End-Products Attenuate Human Mesenchymal Stem Cells and Prevent Cognate Differentiation Into Adipose Tissue, Cartilage, and Bone. *Journal of Bone and Mineral Research,* 20, 1647-1658.

KUSUNOKI, R., OKAZAKI, J. & KOMASA, Y. 2006. Bone Response after Tooth Extraction in Ovariectomized Rats. *Journal of Oral Tissue Engineering,* 4, 89-100.

KWON, P. T., RAHMAN, S. S., KIM, D. M., KOPMAN, J. A., KARIMBUX, N. Y. & FIORELLINI, J. P. 2005. Maintenance of osseointegration utilizing insulin therapy in a diabetic rat model. *J Periodontol,* 76, 621-6.

KYRIAKIDES, T. R., HARTZEL, T., HUYNH, G. & BORNSTEIN, P. 2001. Regulation of angiogenesis and matrix remodeling by localized, matrix-mediated antisense gene delivery. *Molecular Therapy,* 3, 842-849.

LACEFIELD, W. R. 1999. Materials characteristics of uncoated/ceramic-coated implant materials. *Adv Dent Res,* 13, 21-6.

LACEY, D. L., TIMMS, E., TAN, H. L., KELLEY, M. J., DUNSTAN, C. R., BURGESS, T., ELLIOTT, R., COLOMBERO, A., ELLIOTT, G., SCULLY, S., HSU, H., SULLIVAN, J., HAWKINS, N., DAVY, E., CAPPARELLI, C., ELI, A., QIAN, Y. X., KAUFMAN, S., SAROSI, I., SHALHOUB, V., SENALDI, G., GUO, J., DELANEY, J. & BOYLE, W. J. 1998. Osteoprotegerin ligand is a cytokine that regulates osteoclast differentiation and activation. *Cell,* 93, 165-176.

LAGASSE, E. & WEISSMAN, I. L. 1997. Enforced Expression of Bcl-2 in Monocytes Rescues Macrophages and Partially Reverses Osteopetrosis in op/op Mice. *Cell,* 89, 1021-1031.

LANE, T. & SAGE, E. 1994. The biology of SPARC, a protein that modulates cell-matrix interactions. *FASEB J.,* 8, 163-173.

LANGE, J., SAPOZHNIKOVA, A., LU, C., HU, D., LI, X., III, T. M. & MARCUCIO, R. S. 2009. Action of IL-1beta during fracture healing. *Journal of Orthopaedic Research,* 9999, n/a.

LARGER, E., MARRE, M., CORVOL, P. & GASC, J.-M. 2004. Hyperglycemia-Induced Defects in Angiogenesis in the Chicken Chorioallantoic Membrane Model. *Diabetes,* 53, 752-761.

LATEEF, M., BAIG, M. & AZHAR, A. 2009. Estimation of serum osteocalcin and telopeptide-C in postmenopausal osteoporotic females. *Osteoporosis International,* 21, 751-755.

LAWRENCE, T., WILLOUGHBY, D. A. & GILROY, D. W. 2002. Anti-inflammatory lipid mediators and insights into the resolution of inflammation. *Nat Rev Immunol,* 2, 787-795.

LAZZARA, R., SIDDIQUI, A. A., BINON, P., FELDMAN, S. A., WEINER, R., PHILLIPS, R. & GONSHOR, A. 1996. Retrospective multicenter analysis of

3i endosseous dental implants placed over a five year period. *Clinical Oral Implants Research,* 7, 73-83.
LE GUEHENNEC, L., LOPEZ-HEREDIA, M.-A., ENKEL, B., WEISS, P., AMOURIQ, Y. & LAYROLLE, P. 2008. Osteoblastic cell behaviour on different titanium implant surfaces. *Acta Biomaterialia,* 4, 535-543.
LE GUÉHENNEC, L., SOUEIDAN, A., LAYROLLE, P. & AMOURIQ, Y. 2007. Surface treatments of titanium dental implants for rapid osseointegration. *Dental Materials,* 23, 844-854.
LERNER, U. H. 2004. New Molecules in the Tumor Necrosis Factor Ligand and Receptor Superfamilies with Importance for Physiological and Pathological Bone Resorption. *Crit Rev Oral Biol Med,* 15, 64-81.
LERNER, U. H. 2006. Inflammation-induced Bone Remodeling in Periodontal Disease and the Influence of Post-menopausal Osteoporosis. *J Dent Res,* 85, 596-607.
LI, P., OHTSUKI, C., KOKUBO, T., NAKANISHI, K., SOGA, N. & DE GROOT, K. 1994. The role of hydrated silica, titania, and alumina in inducing apatite on implants. *J Biomed Mater Res,* 28, 7-15.
LIU, R., BAL, H. S., DESTA, T., KROTHAPALLI, N., ALYASSI, M., LUAN, Q. & GRAVES, D. T. 2006. Diabetes Enhances Periodontal Bone Loss through Enhanced Resorption and Diminished Bone Formation. *Journal of Dental Research,* 85, 510-514.
LIU, Y., ENGGIST, L., KUFFER, A. F., BUSER, D. & HUNZIKER, E. B. 2007a. The influence of BMP-2 and its mode of delivery on the osteoconductivity of implant surfaces during the early phase of osseointegration. *Biomaterials,* 28, 2677-2686.
LIU, Z., ARONSON, J., WAHL, E. C., LIU, L., PERRIEN, D. S., KERN, P. A., FOWLKES, J. L., THRAILKILL, K. M., BUNN, R. C., COCKRELL, G. E., SKINNER, R. A. & LUMPKIN, C. K., JR. 2007b. A novel rat model for the study of deficits in bone formation in type-2 diabetes. *Acta Orthop,* 78, 46-55.
LOE, H. 1993. Periodontal disease. The sixth complication of diabetes mellitus. *Diabetes Care,* 16, 329-34.
LORENZO, J. A., SOUSA, S. L., ALANDER, C., RAISZ, L. G. & DINARELLO, C. A. 1987. Comparison of the Bone-Resorbing Activity in the Supernatants from Phytohemagglutinin-Stimulated Human Peripheral-Blood Mononuclear-Cells with That of Cytokines through the Use of an Antiserum to Interleukin-1. *Endocrinology,* 121, 1164-1170.
LU, H., KRAUT, D., GERSTENFELD, L. C. & GRAVES, D. T. 2003. Diabetes Interferes with the Bone Formation by Affecting the Expression of Transcription Factors that Regulate Osteoblast Differentiation. *Endocrinology,* 144, 346-352.
LUC, M., LAURENT, M., THIERRY, F., LAURENT, P., REINE, B., SYLVAIN, M., ERIC, T., GERARD, R., JEAN-MICHEL, F., MARIE-HÃ©LÃ¨NE, L.-P., JANE, E. A., LAURENCE, V. & JOÃ«LLE, A. D. E. 2009. Absence of bone sialoprotein (BSP) impairs cortical defect repair in mouse long bone. *Bone,* 45, 853-861.
LUCAS, P. A., PRICE, P. A. & CAPLAN, A. I. 1988. Chemotactic response of mesenchymal cells, fibroblasts and osteoblast-like cells to bone Gla protein. *Bone,* 9, 319-23.

LUO, G., HOFMANN, C., BRONCKERS, A., SOHOCKI, M., BRADLEY, A. & KARSENTY, G. 1995. Bmp-7 Is an Inducer of Nephrogenesis, and Is Also Required for Eye Development and Skeletal Patterning. *Genes & Development,* 9, 2808-2820.

MACDONALD, B. R. & GOWEN, M. 1993. The cell biology of bone. *Baillieres Clin Rheumatol,* 7, 421-43.

MACKIE, E. J. 2003. Osteoblasts: novel roles in orchestration of skeletal architecture. *The International Journal of Biochemistry & Cell Biology,* 35, 1301-1305.

MADDOX, J. F., COLGAN, S. P., CLISH, C. B., PETASIS, N. A., FOKIN, V. V. & SERHAN, C. N. 1998. Lipoxin B4 regulates human monocyte/neutrophil adherence and motility: design of stable lipoxin B4 analogs with increased biologic activity. *FASEB J,* 12, 487-94.

MAEDA, S., HAYASHI, M., KOMIYA, S., IMAMURA, T. & MIYAZONO, K. 2004. Endogenous TGF-beta signaling suppresses maturation of osteoblastic mesenchymal cells. *Embo J,* 23, 552-63.

MALAVAL, L., WADE-GUÃ©YE, N. Y. M. M., BOUDIFFA, M., FEI, J., ZIRNGIBL, R., CHEN, F., LAROCHE, N., ROUX, J.-P., BURT-PICHAT, B., DUBOEUF, F. O., BOIVIN, G., JURDIC, P., LAFAGE-PROUST, M.-H. L. N., AMÃÇDÃÇE, J. L., VICO, L., ROSSANT, J. & AUBIN, J. E. 2008. Bone sialoprotein plays a functional role in bone formation and osteoclastogenesis. *The Journal of Experimental Medicine,* 205, 1145-1153.

MALLUCHE, H. H. 2002. Aluminium and bone disease in chronic renal failure. *Nephrol Dial Transplant,* 17 Suppl 2, 21-4.

MALONE, J. D., TEITELBAUM, S. L., GRIFFIN, G. L., SENIOR, R. M. & KAHN, A. J. 1982. Recruitment of osteoclast precursors by purified bone matrix constituents. *The Journal of Cell Biology,* 92, 227-230.

MANOLAGAS, S. C. 2000. Birth and death of bone cells: basic regulatory mechanisms and implications for the pathogenesis and treatment of osteoporosis. *Endocr Rev,* 21, 115-37.

MANSUKHANI, A., BELLOSTA, P., SAHNI, M. & BASILICO, C. 2000. Signaling by Fibroblast Growth Factors (FGF) and Fibroblast Growth Factor Receptor 2 (FGFR2)-activating Mutations Blocks Mineralization and Induces Apoptosis in Osteoblasts. *J. Cell Biol.,* 149, 1297-1308.

MARINUCCI, L., BALLONI, S., BECCHETTI, E., BELCASTRO, S., GUERRA, M., CALVITTI, M., LILLI, C., CALVI, E. M. & LOCCI, P. 2006. Effect of titanium surface roughness on human osteoblast proliferation and gene expression in vitro. *Int J Oral Maxillofac Implants,* 21, 719-25.

MARK, M. P., PRINCE, C. W., GAY, S., AUSTIN, R. L., BHOWN, M., FINKELMAN, R. D. & BUTLER, W. T. 1987. A comparative immunocytochemical study on the subcellular distributions of 44 kDa bone phosphoprotein and bone gamma-carboxyglutamic acid (Gla)-containing protein in osteoblasts. *J Bone Miner Res,* 2, 337-46.

MARTIN, A., KOMADA, M. R. & SANE, D. C. 2003. Abnormal angiogenesis in diabetes mellitus. *Medicinal Research Reviews,* 23, 117-145.

MARTIN, J. Y., DEAN, D. D., COCHRAN, D. L., SIMPSON, J., BOYAN, B. D. & SCHWARTZ, Z. 1996. Proliferation, differentiation, and protein synthesis of human osteoblast like cells (MG63) cultured on previously used titanium surfaces. *Clinical Oral Implants Research,* 7, 27-37.

MARTIN, J. Y., SCHWARTZ, Z., HUMMERT, T. W., SCHRAUB, D. M., SIMPSON, J., LANKFORD, J., JR., DEAN, D. D., COCHRAN, D. L. & BOYAN, B. D. 1995. Effect of titanium surface roughness on proliferation, differentiation, and protein synthesis of human osteoblast-like cells (MG63). *J Biomed Mater Res,* 29, 389-401.

MARTIN, T. J. & SEEMAN, E. 2008. Bone remodelling: its local regulation and the emergence of bone fragility. *Best Practice & Research Clinical Endocrinology & Metabolism,* 22, 701-722.

MASAKI, C., SCHNEIDER, G. B., ZAHARIAS, R., SEABOLD, D. & STANFORD, C. 2005. Effects of implant surface microtopography on osteoblast gene expression. *Clinical Oral Implants Research,* 16, 650-656.

MASSAGUE, J., SEOANE, J. & WOTTON, D. 2005. Smad transcription factors. *Genes Dev,* 19, 2783-810.

MCCRACKEN, M. S., APONTE-WESSON, R., CHAVALI, R. & LEMONS, J. E. 2006. Bone associated with implants in diabetic and insulin-treated rats. *Clinical Oral Implants Research,* 17, 495-500.

MCCRACKEN, M., LEMONS, J. E., RAHEMTULLA, F., PRINCE, C. W. & FELDMAN, D. 2000. Bone response to titanium alloy implants placed in diabetic rats. *Int J Oral Maxillofac Implants,* 15, 345-54.

MCPHERRON, A. C., LAWLER, A. M. & LEE, S. J. 1999. Regulation of anterior posterior patterning of the axial skeleton by growth differentiation factor 11. *Nature Genetics,* 22, 260-264.

MIYAZONO, A., YAMADA, A., MORIMURA, N., TAKAMI, M., SUZUKI, D., KOBAYASHI, M., TEZUKA, K.-I., YAMAMOTO, M. & KAMIJO, R. 2007. TGF-[beta] suppresses POEM expression through ERK1/2 and JNK in osteoblasts. *FEBS Letters,* 581, 5321-5326.

MIYAZONO, K., MAEDA, S. & IMAMURA, T. 2005. BMP receptor signaling: Transcriptional targets, regulation of signals, and signaling cross-talk. *Cytokine & Growth Factor Reviews,* 16, 251-263.

MODY, N., PARHAMI, F., SARAFIAN, T. A. & DEMER, L. L. 2001. Oxidative stress modulates osteoblastic differentiation of vascular and bone cells. *Free Radical Biology and Medicine,* 31, 509-519.

MOMBELLI, A. & CIONCA, N. 2006. Systemic diseases affecting osseointegration therapy. *Clin Oral Implants Res,* 17 Suppl 2, 97-103.

MONTANARO, L., ARCIOLA, C. R., CAMPOCCIA, D. & CERVELLATI, M. 2002. In vitro effects on MG63 osteoblast-like cells following contact with two roughness-differing fluorohydroxyapatite-coated titanium alloys. *Biomaterials,* 23, 3651-3659.

MORRIS, H. F., OCHI, S. & WINKLER, S. 2000. Implant survival in patients with type 2 diabetes: placement to 36 months. *Ann Periodontol,* 5, 157-65.

MORRIS, H. F., OCHI, S., SPRAY, J. R. & OLSON, J. W. 2000. Periodontal-Type Measurements Associated With Hydroxyapatite-Coated and Nonâ€"HA-Coated Implants: Uncovering to 36 Months. *Annals of Periodontology,* 5, 56-67.

MOSS, D. 1992. Perspectives in alkaline phosphatase research. *Clin Chem,* 38, 2486-2492.

MUELLER, W. D., GROSS, U., FRITZ, T., VOIGT, C., FRANKLIN, K. B., FISCHER, P., BERGER, G., ROGASCHEWSKI, S. & LANGE, K. P. 2003. Evaluation of the interface between bone and titanium surfaces being blasted

by aluminium oxide or bioceramic particles. *Clinical Oral Implants Research,* 14, 349-356.

MURPHY, M., GODSON, C., CANNON, S., KATO, S., MACKENZIE, H. S., MARTIN, F. & BRADY, H. R. 1999. Suppression Subtractive Hybridization Identifies High Glucose Levels as a Stimulus for Expression of Connective Tissue Growth Factor and Other Genes in Human Mesangial Cells. *J. Biol. Chem.,* 274, 5830-5834.

MUSTAFA, K., WROBLEWSKI, J., LOPEZ, B. S., WENNERBERG, A., HULTENBY, K. & ARVIDSON, K. 2001. Determining optimal surface roughness of TiO2 blasted titanium implant material for attachment, proliferation and differentiation of cells derived from human mandibular alveolar bone. *Clinical Oral Implants Research,* 12, 515-525.

MYERS, D. E., COLLIER, F. M., MINKIN, C., WANG, H., HOLLOWAY, W. R., MALAKELLIS, M. & NICHOLSON, G. C. 1999. Expression of functional RANK on mature rat and human osteoclasts. *FEBS Letters,* 463, 295-300.

NADEAU, K. C., AZUMA, H. & TILNEY, N. L. 1995. Sequential cytokine dynamics in chronic rejection of rat renal allografts: roles for cytokines RANTES and MCP-1. *Proc Natl Acad Sci U S A,* 92, 8729-33.

NAGANAWA, T., MAO, L., ABOGUNDE, E., SOBUE, T., KALAJZIC, I., SABBIETI, M., AGAS, D. & HURLEY, M. M. 2006. In vivo and in vitro comparison of the effects of FGF-2 null and haplo-insufficiency on bone formation in mice. *Biochemical and Biophysical Research Communications,* 339, 490-498.

NAGUIB, G., AL-MASHAT, H., DESTA, T. & GRAVES, D. T. 2003. Diabetes Prolongs the Inflammatory Response to a Bacterial Stimulus Through Cytokine Dysregulation. *J Investig Dermatol,* 123, 87-92.

NAKAGAWA, N., KINOSAKI, M., YAMAGUCHI, K., SHIMA, N., YASUDA, H., YANO, K., MORINAGA, T. & HIGASHIO, K. 1998. RANK Is the Essential Signaling Receptor for Osteoclast Differentiation Factor in Osteoclastogenesis. *Biochemical and Biophysical Research Communications,* 253, 395-400.

NAKASHIMA, K., ZHOU, X., KUNKEL, G., ZHANG, Z. P., DENG, J. M., BEHRINGER, R. R. & DE CROMBRUGGHE, B. 2002. The novel zinc finger-containing transcription factor Osterix is required for osteoblast differentiation and bone formation. *Cell,* 108, 17-29.

NANCI, A. 1999. Content and Distribution of Noncollagenous Matrix Proteins in Bone and Cementum: Relationship to Speed of Formation and Collagen Packing Density. *Journal of Structural Biology,* 126, 256-269.

NANES, M. S. 2003. Tumor necrosis factor-alpha: molecular and cellular mechanisms in skeletal pathology. *Gene,* 321, 1-15.

NEEPER, M., SCHMIDT, A. M., BRETT, J., YAN, S. D., WANG, F., PAN, Y. C., ELLISTON, K., STERN, D. & SHAW, A. 1992. Cloning and expression of a cell surface receptor for advanced glycosylation end products of proteins. *Journal of Biological Chemistry,* 267, 14998-15004.

NEVINS, M. L., KARIMBUX, N. Y., WEBER, H. P., GIANNOBILE, W. V. & FIORELLINI, J. P. 1998. Wound healing around endosseous implants in experimental diabetes. *Int J Oral Maxillofac Implants,* 13, 620-9.

NG, K. W., ROMAS, E., DONNAN, L. & FINDLAY, D. M. 1997. Bone biology. *Baillieres Clin Endocrinol Metab,* 11, 1-22.

NGUYEN, L., DEWHIRST, F. E., HAUSCHKA, P. V. & STASHENKO, P. 1991. Interleukin-1 beta stimulates bone resorption and inhibits bone formation in vivo. *Lymphokine Cytokine Res,* 10, 15-21.

NICOLELLA, D. P., MORAVITS, D. E., GALE, A. M., BONEWALD, L. F. & LANKFORD, J. 2006. Osteocyte lacunae tissue strain in cortical bone. *J Biomech,* 39, 1735-43.

NINOMIYA, J. T., TRACY, R. P., CALORE, J. D., GENDREAU, M. A., KELM, R. J. & MANN, K. G. 1990. Heterogeneity of human bone. *Journal of Bone and Mineral Research,* 5, 933-938.

O'BRIEN, C. A., LIN, S.-C., BELLIDO, T. & MANOLAGAS, S. C. 2000. Expression levels of gp130 in bone marrow stromal cells determine the magnitude of osteoclastogenic signals generated by IL-6-type cytokines. *Journal of Cellular Biochemistry,* 79, 532-541.

OHMORI, Y., HANAZAWA, S., AMANO, S., HIROSE, K., KUMEGAWA, M. & KITANO, S. 1988. Effects of recombinant human interleukin 1 alpha and interleukin 1 beta on cell growth and alkaline phosphatase of the mouse osteoblastic cell line MC3T3-E1. *Biochim Biophys Acta,* 970, 22-30.

OKAZAKI, R., DURHAM, S. K., RIGGS, B. L. & CONOVER, C. A. 1995. Transforming Growth-Factor-Beta and Forskolin Increase All Classes of Insulin-Like Growth-Factor-I Transcripts in Normal Human Osteoblast-Like Cells. *Biochemical and Biophysical Research Communications,* 207, 963-970.

OLDBERG, A., FRANZEN, A. & HEINEGARD, D. 1988. The primary structure of a cell-binding bone sialoprotein. *J Biol Chem,* 263, 19430-2.

OLSSON, I., GATANAGA, T., GULLBERG, U., LANTZ, M. & GRANGER, G. A. 1993. Tumour necrosis factor (TNF) binding proteins (soluble TNF receptor forms) with possible roles in inflammation and malignancy. *Eur Cytokine Netw,* 4, 169-80.

O'REGAN, A. W., CHUPP, G. L., LOWRY, J. A., GOETSCHKES, M., MULLIGAN, N. & BERMAN, J. S. 1999. Osteopontin Is Associated with T Cells in Sarcoid Granulomas and Has T Cell Adhesive and Cytokine-Like Properties In Vitro. *J Immunol,* 162, 1024-1031.

OWEN, M. 1967. Uptake of [3H]Uridine into Precursor Pools and RNA in Osteogenic Cells. *J Cell Sci,* 2, 39-56.

PALUMBO, C., PALAZZINI, S., ZAFFE, D. & MAROTTI, G. 1990. Osteocyte differentiation in the tibia of newborn rabbit: an ultrastructural study of the formation of cytoplasmic processes. *Acta Anat (Basel),* 137, 350-8.

PARFITT, A. M. 1994. Osteonal and hemi-osteonal remodeling: the spatial and temporal framework for signal traffic in adult human bone. *J Cell Biochem,* 55, 273-86.

PARK, J., Y. & DAVIES, J. E. 2000. Red blood cell and platelet interactions with titanium implant surfaces. *Clinical Oral Implants Research,* 11, 530-539.

PONADER, S., VAIRAKTARIS, E., HEINL, P., WILMOWSKY, C. V., ROTTMAIR, A., KÖRNER, C., SINGER, R. F., HOLST, S., SCHLEGEL, K. A., NEUKAM, F. W. & NKENKE, E. 2008. Effects of topographical surface modifications of electron beam melted Ti-6Al-4V titanium on human fetal osteoblasts. *Journal of Biomedical Materials Research Part A,* 84A, 1111-1119.

POSER, J. W. & PRICE, P. A. 1979. A method for decarboxylation of gamma-carboxyglutamic acid in proteins. Properties of the decarboxylated gamma-carboxyglutamic acid protein from calf bone. *Journal of Biological Chemistry,* 254, 431-436.

POSTIGLIONE, L., DI DOMENICO, G., RAMAGLIA, L., MONTAGNANI, S., SALZANO, S., DI MEGLIO, F., SBORDONE, L., VITALE, M. & ROSSI, G. 2003. Behavior of SaOS-2 Cells Cultured on Different Titanium Surfaces. *J Dent Res,* 82, 692-696.

PULEO & THOMAS 2006. Implant Surfaces. *Dental Clinics of North America,* 50, 323-338.

QU, Z., RAUSCH-FAN, X., WIELAND, M., MATEJKA, M. & SCHEDLE, A. 2007. The initial attachment and subsequent behavior regulation of osteoblasts by dental implant surface modification. *J Biomed Mater Res A,* 82, 658-68.

RAWADI, G., VAYSSIERE, B., DUNN, F., BARON, R. & ROMAN-ROMAN, S. 2003. BMP-2 Controls Alkaline Phosphatase Expression and Osteoblast Mineralization by a Wnt Autocrine Loop. *Journal of Bone and Mineral Research,* 18, 1842-1853.

RICKARD, D. J., GOWEN, M. & MACDONALD, B. R. 1993. Proliferative Responses to Estradiol, Il-1-Alpha and Tgf-Beta by Cells Expressing Alkaline-Phosphatase in Human Osteoblast-Like Cell-Cultures. *Calcified Tissue International,* 52, 227-233.

RITTLING, S. R., MATSUMOTO, H. N., MCKEE, M. D., NANCI, A., AN, X.-R., NOVICK, K. E., KOWALSKI, A. J., NODA, M. & DENHARDT, D. T. 1998. Mice Lacking Osteopontin Show Normal Development and Bone Structure but Display Altered Osteoclast Formation In Vitro. *Journal of Bone and Mineral Research,* 13, 1101-1111.

ROBERTS, W. E. & HARTSFIELD, J. K. 2004. Bone development and function: genetic and environmental mechanisms. *Seminars in Orthodontics,* 10, 100-122.

ROBEY, P. G., YOUNG, M. F., FLANDERS, K. C., ROCHE, N. S., KONDAIAH, P., REDDI, A. H., TERMINE, J. D., SPORN, M. B. & ROBERTS, A. B. 1987. Osteoblasts synthesize and respond to transforming growth factor-type beta (TGF-beta) in vitro. *J Cell Biol,* 105, 457-63.

ROBLING, A. G., CASTILLO, A. B. & TURNER, C. H. 2006. BIOMECHANICAL AND MOLECULAR REGULATION OF BONE REMODELING. *Annual Review of Biomedical Engineering,* 8, 455-498.

RODAN, G. A. 1997. Bone mass homeostasis and bisphosphonate action. *Bone,* 20, 1-4.

RONOLD, H. J. & ELLINGSEN, J. E. 2002. Effect of micro-roughness produced by TiO2 blasting - tensile testing of bone attachment by using coin-shaped implants. *Biomaterials,* 23, 4211-4219.

ROSEN, C. J., DIMAI, H. P., VEREAULT, D., DONAHUE, L. R., BEAMER, W. G., FARLEY, J., LINKHART, S., LINKHART, T., MOHAN, S. & BAYLINK, D. J. 1997. Circulating and skeletal insulin-like growth factor-I (IGF-i) concentrations in two inbred strains of mice with different bone mineral densities. *Bone,* 21, 217-223.

ROSEN, V., NOVE, J., SONG, J. J., THIES, R. S., COX, K. & WOZNEY, J. M. 1994. Responsiveness of Clonal Limb Bud Cell-Lines to Bone

Morphogenetic Protein-2 Reveals a Sequential Relationship between Cartilage and Bone Cell Phenotypes. *Journal of Bone and Mineral Research,* 9, 1759-1768.

ROSENQUIST, J. B., OHLIN, A. & LERNER, U. H. 1996. Cytokine-induced inhibition of bone matrix proteins is not mediated by prostaglandins. *Inflamm Res,* 45, 457-63.

RUPP, F., SCHEIDELER, L., OLSHANSKA, N., WILD, M. D., WIELAND, M. & GEIS-GERSTORFER, J. 2006. Enhancing surface free energy and hydrophilicity through chemical modification of microstructured titanium implant surfaces. *Journal of Biomedical Materials Research Part A,* 76A, 323-334.

RUSHING, G. D., GORETSKY, M. J., GUSTIN, T., MORALES, M., KELLY, J. R. E. & NUSS, D. 2007. When it is not an infection: metal allergy after the Nuss procedure for repair of pectus excavatum. *Journal of Pediatric Surgery,* 42, 93-97.

RYDZIEL, S., LADD, C., MCCARTHY, T. L., CENTRELLA, M. & CANALIS, E. 1992. Determination and expression of platelet-derived growth factor-AA in bone cell cultures. *Endocrinology,* 130, 1916-1922.

RYDZIEL, S., SHAIKH, S. & CANALIS, E. 1994. Platelet-Derived Growth Factor-Aa and Factor-Bb (Pdgf-Aa and Pdgf-Bb) Enhance the Synthesis of Pdgf-Aa in Bone Cell-Cultures. *Endocrinology,* 134, 2541-2546.

SAGE, E. H. & BORNSTEIN, P. 1991. Extracellular proteins that modulate cell-matrix interactions. SPARC, tenascin, and thrombospondin. *Journal of Biological Chemistry,* 266, 14831-14834.

SAKAI, D., OKAZAKI, J. & KOMASA, Y. 2008. Bone Healing of Tooth Extraction Socket in Type 2 Diabetes. *Journal of Oral Tissue Engineering,* 5, 134-144.

SALIDO, M., VILCHES, J. I., GUTIERREZ, J. L. & VILCHES, J. 2007. Actin cytoskeletal organization in human osteoblasts grown on different dental titanium implant surfaces. *Histol Histopathol,* 22, 1355-64.

SALVI, G. E., COLLINS, J. G., YALDA, B., ARNOLD, R. R., LANG, N. P. & OFFENBACHER, S. 1997a. Monocytic TNFα secretion patterns in IDDM patients with periodontal diseases*. *Journal of Clinical Periodontology,* 24, 8-16.

SALVI, G. E., YALDA, B., COLLINS, J. G., JONES, B. H., SMITH, F. W., ARNOLD, R. R. & OFFENBACHER, S. 1997b. Inflammatory mediator response as a potential risk marker for periodontal diseases in insulin-dependent diabetes mellitus patients. *J Periodontol,* 68, 127-35.

SANTANA, R. B., XU, L., CHASE, H. B., AMAR, S., GRAVES, D. T. & TRACKMAN, P. C. 2003. A role for advanced glycation end products in diminished bone healing in type 1 diabetes. *Diabetes,* 52, 1502-10.

SCHNEIDER, G. B., PERINPANAYAGAM, H., CLEGG, M., ZAHARIAS, R., SEABOLD, D., KELLER, J. & STANFORD, C. 2003. Implant Surface Roughness Affects Osteoblast Gene Expression. *J Dent Res,* 82, 372-376.

SCHOPPET, M., PREISSNER, K. T. & HOFBAUER, L. C. 2002. RANK ligand and osteoprotegerin - Paracrine regulators of bone metabolism and vascular function. *Arteriosclerosis Thrombosis and Vascular Biology,* 22, 549-553.

SCHUMACHER, BANU, G., LEENDERT, H. J. L., JAN ULRICH, B., KERSTIN, A., RAINER, E., JOERG, D., HANS, S., WOLFGANG, S. & BRIGITTE, R.-P. 2008. Characteristics of testicular dysgenesis syndrome and decreased

expression of *SRY* and *SOX9* in Frasier syndrome. *Molecular Reproduction and Development,* 75, 1484-1494.

SCHWARZ, F., HERTEN, M., SAGER, M., WIELAND, M., DARD, M. & BECKER, J. 2007. Bone regeneration in dehiscence-type defects at chemically modified (SLActive®) and conventional SLA titanium implants: a pilot study in dogs. *Journal of Clinical Periodontology,* 34, 78-86.

SCHWARZ, F., WIELAND, M., SCHWARTZ, Z., ZHAO, G., RUPP, F., GEIS-GERSTORFER, J., SCHEDLE, A., BROGGINI, N., BORNSTEIN, M. M., BUSER, D., FERGUSON, S. J., BECKER, J., BOYAN, B. D. & COCHRAN, D. L. 2009. Potential of chemically modified hydrophilic surface characteristics to support tissue integration of titanium dental implants. *Journal of Biomedical Materials Research Part B: Applied Biomaterials,* 88B, 544-557.

SEEMAN, E. 2009. Bone modeling and remodeling. *Crit Rev Eukaryot Gene Expr,* 19, 219-33.

SHARP, C. A. & MAGNUSSON, P. 2008. Isoforms of bone alkaline phosphatase, stem cells and osteoblast phenotypes. *Stem Cells and Development,* 17, 857-858.

SHIBLI, J. A., LUCIENE, S. G., DE FIGUEIREDO, C., FERES, M., MARCANTONIO JR, E., IEZZI, G. & PIATTELLI, A. 2007. Influence of implant surface topography on early osseointegration: A histological study in human jaws. *Journal of Biomedical Materials Research Part B: Applied Biomaterials,* 80B, 377-385.

SHYNG, Y. C., DEVLIN, H. & OU, K. L. 2006. Bone formation around immediately placed oral implants in diabetic rats. *Int J Prosthodont,* 19, 513-4.

SIMMONS, P. J. & TOROK-STORB, B. 1991. Identification of stromal cell precursors in human bone marrow by a novel monoclonal antibody, STRO-1. *Blood,* 78, 55-62.

SIMONET, W. S., LACEY, D. L., DUNSTAN, C. R., KELLEY, M., CHANG, M. S., LUTHY, R., NGUYEN, H. Q., WOODEN, S., BENNETT, L., BOONE, T., SHIMAMOTO, G., DEROSE, M., ELLIOTT, R., COLOMBERO, A., TAN, H. L., TRAIL, G., SULLIVAN, J., DAVY, E., BUCAY, N., RENSHAWGEGG, L., HUGHES, T. M., HILL, D., PATTISON, W., CAMPBELL, P., SANDER, S., VAN, G., TARPLEY, J., DERBY, P., LEE, R. & BOYLE, W. J. 1997. Osteoprotegerin: A novel secreted protein involved in the regulation of bone density. *Cell,* 89, 309-319.

SIQUEIRA, J. T., CAVALHER-MACHADO, S. C., ARANA-CHAVEZ, V. E. & SANNOMIYA, P. 2003. Bone formation around titanium implants in the rat tibia: role of insulin. *Implant Dent,* 12, 242-51.

SITTIG, C., TEXTOR, M., SPENCER, N. D., WIELAND, M. & VALLOTTON, P. H. 1999. Surface characterization. *Journal of Materials Science: Materials in Medicine,* 10, 35-46.

SODEK, J., GANSS, B. & MCKEE, M. D. 2000. Osteopontin. *Crit Rev Oral Biol Med,* 11, 279-303.

SOMERMAN, M. J., FISHER, L. W., FOSTER, R. A. & SAUK, J. J. 1988. Human bone sialoprotein I and II enhance fibroblast attachment in vitro. *Calcif Tissue Int,* 43, 50-3.

SOYOMBO, O., SPUR, B. W. & LEE, T. H. 1994. Effects of lipoxin A4 on chemotaxis and degranulation of human eosinophils stimulated by platelet-activating factor and N-formyl-L-methionyl-L-leucyl-L-phenylalanine. *Allergy,* 49, 230-4.

SPINELLA-JAEGLE, S., RAWADI, G., KAWAI, S., GALLEA, S., FAUCHEU, C., MOLLAT, P., COURTOIS, B., BERGAUD, B., RAMEZ, V., BLANCHET, A. M., ADELMAN, G., BARON, R. & ROMAN-ROMAN, S. 2001. Sonic hedgehog increases the commitment of pluripotent mesenchymal cells into the osteoblastic lineage and abolishes adipocytic differentiation. *Journal of Cell Science,* 114, 2085-2094.

STASHENKO, P., DEWHIRST, F. E., ROONEY, M. L., DESJARDINS, L. A. & HEELEY, J. D. 1987. Interleukin-1beta is a potent inhibitor of bone formation *in vitro*. *Journal of Bone and Mineral Research,* 2, 559-565.

STEINEMANN, S. G. 1998. Titanium - The material of choice? *Periodontology 2000,* 1998, 7-21.

STEWART, K., WALSH, S., SCREEN, J., JEFFERISS, C. M., CHAINEY, J., JORDAN, G. R. & BERESFORD, J. N. 1999. Further Characterization of Cells Expressing STRO-1 in Cultures of Adult Human Bone Marrow Stromal Cells. *Journal of Bone and Mineral Research,* 14, 1345-1356.

STOLZING, A., COLEMAN, N. & SCUTT, A. 2006. Glucose-Induced Replicative Senescence in Mesenchymal Stem Cells. *Rejuvenation Research,* 9, 31-35.

STREET, J., BAO, M., DEGUZMAN, L., BUNTING, S., PEALE, F. V., JR., FERRARA, N., STEINMETZ, H., HOEFFEL, J., CLELAND, J. L., DAUGHERTY, A., VAN BRUGGEN, N., REDMOND, H. P., CARANO, R. A. & FILVAROFF, E. H. 2002. Vascular endothelial growth factor stimulates bone repair by promoting angiogenesis and bone turnover. *Proc Natl Acad Sci U S A,* 99, 9656-61.

SUL, Y. T., JOHANSSON, C., WENNERBERG, A., CHO, L. R., CHANG, B. S. & ALBREKTSSON, T. 2005. Optimum surface properties of oxidized implants for reinforcement of osseointegration: Surface chemistry, oxide thickness, porosity, roughness, and crystal structure. *International Journal of Oral and Maxillofacial Implants,* 20, 349-359.

SUL, Y.-T., JEONG, Y., JOHANSSON, C. & ALBREKTSSON, T. 2006. Oxidized, bioactive implants are rapidly and strongly integrated in bone. Part 1 - experimental implants. *Clinical Oral Implants Research,* 17, 521-526.

SUL, Y.-T., JEONG, Y., JOHANSSON, C. & ALBREKTSSON, T. 2006. Oxidized, bioactive implants are rapidly and strongly integrated in bone. Part 1 - experimental implants. *Clinical Oral Implants Research,* 17, 521-526.

TABASSUM, A., WALBOOMERS, F., WOLKE, J. G., MEIJER, G. J. & JANSEN, J. A. 2009. The Influence of Surface Roughness on the Displacement of Osteogenic Bone Particles during Placement of Titanium Screw-Type Implants. *Clin Implant Dent Relat Res.*

TABASSUM, A., WALBOOMERS, X. F., WOLKE, J. G. C., MEIJER, G. J. & JANSEN, J. A. 2010. Bone Particles and the Undersized Surgical Technique. *Journal of Dental Research,* 89, 581-586.

TAICHMAN, R. S. 2005. Blood and bone: two tissues whose fates are intertwined to create the hematopoietic stem-cell niche. *Blood,* 105, 2631-9.

TAKAHASHI, N., YAMANA, H., YOSHIKI, S., ROODMAN, G. D., MUNDY, G. R., JONES, S. J., BOYDE, A. & SUDA, T. 1988. Osteoclast-Like Cell-

Formation and Its Regulation by Osteotropic Hormones in Mouse Bone-Marrow Cultures. *Endocrinology,* 122, 1373-1382.
TAUBMAN, M. A. & KAWAI, T. 2001. Involvement of T-lymphocytes in periodontal disease and in direct and indirect induction of bone resorption. *Crit Rev Oral Biol Med,* 12, 125-135.
TEITELBAUM, S. L. 2000. Bone Resorption by Osteoclasts. *Science,* 289, 1504-1508.
TENGVALL, P. & LUNDSTROM, I. 1992. Physico-chemical considerations of titanium as a biomaterial. *Clin Mater,* 9, 115-34.
THOLPADY, S. S., KATZ, A. J. & OGLE, R. C. 2003. Mesenchymal stem cells from rat visceral fat exhibit multipotential differentiation in vitro. *The Anatomical Record Part A: Discoveries in Molecular, Cellular, and Evolutionary Biology,* 272A, 398-402.
TOMKINSON, A., REEVE, J., SHAW, R. W. & NOBLE, B. S. 1997. The Death of Osteocytes via Apoptosis Accompanies Estrogen Withdrawal in Human Bone. *J Clin Endocrinol Metab,* 82, 3128-3135.
TRISI, P., LAZZARA, R., REBAUDI, A., RAO, W., TESTORI, T. & PORTER, S. S. 2003. Bone-implant contact on machined and dual acid-etched surfaces after 2 months of healing in the human maxilla. *J Periodontol,* 74, 945-56.
TSUKIMURA, N., KOJIMA, N., KUBO, K., ATT, W., TAKEUCHI, K., KAMEYAMA, Y., MAEDA, H. & OGAWA, T. 2008. The effect of superficial chemistry of titanium on osteoblastic function. *Journal of Biomedical Materials Research Part A,* 84A, 108-116.
TSURUOKA, N., YAMATO, R., SAKAI, Y., YOSHITAKE, Y. & YONEKURA, H. 2007. Promotion by collagen tripeptide of type I collagen gene expression in human osteoblastic cells and fracture healing of rat femur. *Biosci Biotechnol Biochem,* 71, 2680-7.
TURNER, R. T., EVANS, G. L. & WAKLEY, G. K. 1995. Spaceflight results in depressed cancellous bone formation in rat humeri. *Aviation Space and Environmental Medicine,* 66, 770-774.
TYNDALL, W. A., BEAM, H. A., ZARRO, C., O'CONNOR, J. P. & LIN, S. S. 2003. Decreased platelet derived growth factor expression during fracture healing in diabetic animals. *Clin Orthop Relat Res,* 319-30.
UDAGAWA, N., TAKAHASHI, N., YASUDA, H., MIZUNO, A., ITOH, K., UENO, Y., SHINKI, T., GILLESPIE, M. T., MARTIN, T. J., HIGASHIO, K. & SUDA, T. 2000. Osteoprotegerin produced by osteoblasts is an important regulator in osteoclast development and function. *Endocrinology,* 141, 3478-3484.
URIST, M. R. & STRATES, B. S. 1971. Bone Morphogenetic Protein. *Journal of Dental Research,* 50, 1392-&.
VALERO, A. M., GARCIA, J. C. F., BALLESTER, A. H. & RUEDA, C. L. 2007. Effects of diabetes on the osseointegration of dental implants. *Med Oral Patol Cir Bucal,* 12, E38-43.
VAN DEN DOLDER, J. & JANSEN, J. A. 2007. Enrichment of osteogenic cell populations from rat bone marrow stroma. *Biomaterials,* 28, 249-55.
VAN DER MEULEN, M. C. H., MOREY-HOLTON, E. R. & CARTER, D. R. 1995. Hindlimb suspension diminishes femoral cross-sectional growth in the rat. *Journal of Orthopaedic Research,* 13, 700-707.

VAN DER WIEL, H. E., LIPS, P., GRAAFMANS, W. C., DANIELSEN, C. C., NAUTA, J., VAN LINGEN, A. & MOSEKILDE, L. 1995. Additional weight-bearing during exercise is more important than duration of exercise for anabolic stimulus of bone: A study of running exercise in female rats. *Bone,* 16, 73-80.

VIDAL, O. N. A., SJÖGREN, K., ERIKSSON, B. I., LJUNGGREN, Ö. & OHLSSON, C. 1998. Osteoprotegerin mRNA Is Increased by Interleukin-1[alpha] in the Human Osteosarcoma Cell Line MG-63 and in Human Osteoblast-Like Cells. *Biochemical and Biophysical Research Communications,* 248, 696-700.

WADDINGTON, R. J. & LANGLEY, M. S. 1998. Structural analysis of proteoglycans synthesized by mineralizing bone cells in vitro in the presence of fluoride. *Matrix Biology,* 17, 255-268.

WADDINGTON, R. J. & LANGLEY, M. S. 2003. Altered expression of matrix metalloproteinases within mineralizing bone cells in vitro in the presence of fluoride. *Connect Tissue Res,* 44, 88-95.

WALSH, S., JEFFERISS, C., STEWART, K., JORDAN, G. R., SCREEN, J. & BERESFORD, J. N. 2000. Expression of the developmental markers STRO-1 and alkaline phosphatase in cultures of human marrow stromal cells: regulation by fibroblast growth factor (FGF)-2 and relationship to the expression of FGF receptors 1-4. *Bone,* 27, 185-195.

WANG, K. X. & DENHARDT, D. T. 2008. Osteopontin: Role in immune regulation and stress responses. *Cytokine & Growth Factor Reviews,* 19, 333-345.

WAUGH, A. & GRANT, A. 2002. The Skeleton. *In:* WOLFAARD, S. (ed.) *Anatomy and Physiology in Health and Illness.* Ninth ed.: Churchill Livingston.

WEBER, G. F., ASHKAR, S., GLIMCHER, M. J. & CANTOR, H. 1996. Receptor-ligand interaction between CD44 and osteopontin (Eta-1). *Science,* 271, 509-12.

WEI, S., KITAURA, H., ZHOU, P., ROSS, F. P. & TEITELBAUM, S. L. 2005. IL-1 mediates TNF-induced osteoclastogenesis. *Journal of Clinical Investigation,* 115, 282-290.

WEINBAUM, S., COWIN, S. C. & ZENG, Y. 1994. A model for the excitation of osteocytes by mechanical loading-induced bone fluid shear stresses. *J Biomech,* 27, 339-60.

WEINREB, M., SHINAR, D. & RODAN, G. A. 1990. Different Pattern of Alkaline-Phosphatase, Osteopontin, and Osteocalcin Expression in Developing Rat Bone Visualized by Insitu Hybridization. *Journal of Bone and Mineral Research,* 5, 831-842.

WEINSTEIN, R. S., JILKA, R. L., MICHAEL PARFITT, A. & MANOLAGAS, S. C. 1998. Inhibition of Osteoblastogenesis and Promotion of Apoptosis of Osteoblasts and Osteocytes by Glucocorticoids . Potential Mechanisms of Their Deleterious Effects on Bone. *J. Clin. Invest.,* 102, 274-282.

WENNERBERG, A., ALBREKTSSON, T. & ANDERSSON, B. 1996a. Bone tissue response to commercially pure titanium implants blasted with fine and coarse particles of aluminum oxide. *Int J Oral Maxillofac Implants,* 11, 38-45.

WENNERBERG, A., ALBREKTSSON, T. & LAUSMAA, J. 1996c. Torque and histomorphometric evaluation of c.p. titanium screws blasted with 25- and 75-microns-sized particles of Al2O3. *J Biomed Mater Res,* 30, 251-60.

WENNERBERG, A., ALBREKTSSON, T., ANDERSSON, B. & KROL, J. J. 1995. A histomorghometric study of screw shaped and removal torque titanium implants with three different surface topographies. *Clinical Oral Implants Research,* 6, 24-30.

WENNERBERG, A., ALBREKTSSON, T., JOHANSSON, C. & ANDERSSON, B. 1996b. Experimental study of turned and grit-blasted screw-shaped implants with special emphasis on effects of blasting material and surface topography. *Biomaterials,* 17, 15-22.

WENNERBERG, A., BOLIND, P. & ALBREKTSSON, T. 1991. Glow-discharge pretreated implants combined with temporary bone tissue ischemia. *Swedish dental journal,* 15, 95-101.

WENNERBERG, A., HALLGREN, C., JOHANSSON, C. & DANELLI, S. 1998. A histomorphometric evaluation of screw-shaped implants each prepared with two surface roughnesses. *Clinical Oral Implants Research,* 9, 11-19.

WERNER, F., JAIN, M. K., FEINBERG, M. W., SIBINGA, N. E. S., PELLACANI, A., WIESEL, P., CHIN, M. T., TOPPER, J. N., PERRELLA, M. A. & LEE, M.-E. 2000. Transforming Growth Factor-Î²1 Inhibition of Macrophage Activation Is Mediated via Smad3. *Journal of Biological Chemistry,* 275, 36653-36658.

WESTENDORF, J. J., KAHLER, R. A. & SCHROEDER, T. M. 2004. Wnt signaling in osteoblasts and bone diseases. *Gene,* 341, 19-39.

WHEELER, R. D., CULHANE, A. C., HALL, M. D., PICKERING-BROWN, S., ROTHWELL, N. J. & LUHESHI, G. N. 2000. Detection of the interleukin 18 family in rat brain by RT-PCR. *Molecular Brain Research,* 77, 290-293.

WHYTE, M. P. 1994. Hypophosphatasia and the Role of Alkaline Phosphatase in Skeletal Mineralization. *Endocr Rev,* 15, 439-461.

WIKTOR-JEDRZEJCZAK, W., BARTOCCI, A., FERRANTE, A. W., JR., AHMED-ANSARI, A., SELL, K. W., POLLARD, J. W. & STANLEY, E. R. 1990. Total Absence of Colony-Stimulating Factor 1 in the Macrophage-Deficient Osteopetrotic (op/op) Mouse. *PNAS,* 87, 4828-4832.

WINKLER, D. G., SUTHERLAND, M. S. K., OJALA, E., TURCOTT, E., GEOGHEGAN, J. C., SHPEKTOR, D., SKONIER, J. E., YU, C. & LATHAM, J. A. 2005. Sclerostin Inhibition of Wnt-3a-induced C3H10T1/2 Cell Differentiation Is Indirect and Mediated by Bone Morphogenetic Proteins. *Journal of Biological Chemistry,* 280, 2498-2502.

WUTTKE, M., MULLER, S., NITSCHE, D. P., PAULSSON, M., HANISCH, F. G. & MAURER, P. 2001. Structural characterization of human recombinant and bone-derived bone sialoprotein. Functional implications for cell attachment and hydroxyapatite binding. *J Biol Chem,* 276, 36839-48.

XIAO, G., WANG, D., BENSON, M. D., KARSENTY, G. & FRANCESCHI, R. T. 1998. Role of the Î±2-Integrin in Osteoblast-specific Gene Expression and Activation of the Osf2 Transcription Factor. *Journal of Biological Chemistry,* 273, 32988-32994.

XU, Z., HURCHLA, M. A., DENG, H., ULUÇKAN, Ö., BU, F., BERDY, A., EAGLETON, M. C., HELLER, E. A., FLOYD, D. H., DIRKSEN, W. P., SHU, S., TANAKA, Y., FERNANDEZ, S. A., ROSOL, T. J. & WEILBAECHER, K. N. 2009. Interferon-γ Targets Cancer Cells and Osteoclasts to Prevent Tumor-associated Bone Loss and Bone Metastases. *Journal of Biological Chemistry,* 284, 4658-4666.

YAMAGUCHI, A., KATAGIRI, T., IKEDA, T., WOZNEY, J. M., ROSEN, V., WANG, E. A., KAHN, A. J., SUDA, T. & YOSHIKI, S. 1991. Recombinant Human Bone Morphogenetic Protein-2 Stimulates Osteoblastic Maturation and Inhibits Myogenic Differentiation Invitro. *Journal of Cell Biology,* 113, 681-687.

YAMAGUCHI, A., KOMORI, T. & SUDA, T. 2000. Regulation of Osteoblast Differentiation Mediated by Bone Morphogenetic Proteins, Hedgehogs, and Cbfa1. *Endocr Rev,* 21, 393-411.

YASUDA, H., SHIMA, N., NAKAGAWA, N., YAMAGUCHI, K., KINOSAKI, M., MOCHIZUKI, S.-I., TOMOYASU, A., YANO, K., GOTO, M., MURAKAMI, A., TSUDA, E., MORINAGA, T., HIGASHIO, K., UDAGAWA, N., TAKAHASHI, N. & SUDA, T. 1998. Osteoclast differentiation factor is a ligand for osteoprotegerin/osteoclastogenesis-inhibitory factor and is identical to TRANCE/RANKL. *PNAS,* 95, 3597-3602.

YEH, L. C. C., ZAVALA, M. C. & LEE, J. C. 2002. Osteogenic protein-1 and interleukin-6 with its soluble receptor synergistically stimulate rat osteoblastic cell differentiation. *Journal of Cellular Physiology,* 190, 322-331.

YOKOYAMA, K., ICHIKAWA, T., MURAKAMI, H., MIYAMOTO, Y. & ASAOKA, K. 2002. Fracture mechanisms of retrieved titanium screw thread in dental implant. *Biomaterials,* 23, 2459-2465.

YOSHIDA, H., HAYASHI, S.-I., KUNISADA, T., OGAWA, M., NISHIKAWA, S., OKAMURA, H., SUDO, T., SHULTZ, L. D. & NISHIKAWA, S.-I. 1990. The murine mutation osteopetrosis is in the coding region of the macrophage colony stimulating factor gene. *Nature,* 345, 442-444.

YOSHITAKE, H., RITTLING, S. R., DENHARDT, D. T. & NODA, M. 1999. Osteopontin-deficient mice are resistant to ovariectomy-induced bone resorption. *Proceedings of the National Academy of Sciences of the United States of America,* 96, 8156-8160.

YOUNG, M. F., KERR, J. M., IBARAKI, K., HEEGAARD, A. M. & ROBEY, P. G. 1992. Structure, expression, and regulation of the major noncollagenous matrix proteins of bone. *Clin Orthop Relat Res,* 275-94.

YU, X., HSIEH, S. C., BAO, W. & GRAVES, D. T. 1997. Temporal expression of PDGF receptors and PDGF regulatory effects on osteoblastic cells in mineralizing cultures. *American Journal of Physiology - Cell Physiology,* 272.

YUASA, T., KATAOKA, H., KINTO, N., IWAMOTO, M., ENOMOTO-IWAMOTO, M., IEMURA, S. I., UENO, N., SHIBATA, Y., KUROSAWA, H. & YAMAGUCHI, A. 2002. Sonic hedgehog is involved in osteoblast differentiation by cooperating with BMP-2. *Journal of Cellular Physiology,* 193, 225-232.

ZECHNER, W., TRINKL, N., WATZAK, G., BUSENLECHNER, D., TEPPER, G., HAAS, R. & WATZEK, G. 2004. Radiologic follow-up of peri-implant bone loss around machine-surfaced and rough-surfaced interforaminal implants in the mandible functionally loaded for 3 to 7 years. *Int J Oral Maxillofac Implants,* 19, 216-21.

ZHAO, G., SCHWARTZ, Z., WIELAND, M., RUPP, F., GEIS-GERSTORFER, J., COCHRAN, D. L. & BOYAN, B. D. 2005. High surface energy enhances

cell response to titanium substrate microstructure. *Journal of Biomedical Materials Research - Part A,* 74, 49-58.
ZIMMET, P., SHAW, J. & ALBERTI, K. G. 2003. Preventing Type 2 diabetes and the dysmetabolic syndrome in the real world: a realistic view. *Diabet Med,* 20, 693-702.